SCHRIFTENREIHE ZUR
WASSERWIRTSCHAFT

TECHNISCHE UNIVERSITÄT GRAZ

Gabriele Harb

Numerical Modeling of Sediment Transport Processes in Alpine Reservoirs

73

Herausgeber:
Institut für Wasserbau und Wasserwirtschaft
Univ.-Prof. Dipl.-Ing. Dr.techn. Gerald Zenz

Technische Universität Graz, Stremayrgasse 10, A-8010 Graz
Tel. +43(0)316 / 873-8361, Fax +43(0)316 / 873-8357
Email: hydro@tugraz.at, Internet: www.hydro.tugraz.at

Verlag der Technischen Universität Graz **www.ub.tugraz.at/Verlag**
ISBN Print: 978-3-85125-451-8
ISBN E-Book: 978-3-85125-452-5
DOI: 10.3217/978-3-85125-451-8

Printed by TU Graz / Printservice

Foreword by the editor

Hydro power plants contribute substantially to the supply of electrical energy from renewable resources, particularly in alpine regions. Tapping this potential energy requires water retention by means of a reservoir or a channel from the original watercourse. These backwater areas experience a reduction in their flowrate and, in the case of sediment loaded rivers, result in deposition and gradual sedimentation within the retained volume. This negatively affects the storage capacity, the plant's efficiency and the situation downstream from the site. Reduced sediment transportation can in addition lead to riverbed erosion and groundwater depletion, thus negatively affecting vegetation.

Hydraulic plants are also constructed in order to protect the population and infrastructure from flooding. Their protective effect can be significantly reduced by sedimentation and the consequent reduction of the effective flowrate cross section.

Thus, after pre-determining appropriate volumes of water, desedimentation of the backwater and withdrawal areas, the – even partial – prevention or control of sedimentation processes is desirable in regard to the sustainable and long-term utilisation of plants. The necessary measures to be taken are based on objectified principles and vary according to the specifics of each plant and local situation.

The dissertation at hand supports the assessment of sedimentation and desedimentation in reservoirs and thus contributes to sustainable sediment management with regard to a long-term, reliable utilisation of river power plants. In her research, Dipl.-Ing. Dr.techn. Gabriele Harb investigates the sediment transport processes, sediment inflow and the occurrence of flood events to identify efficient desedimentation measures. Measures of sedimentation in cross sections of the reservoir prior to and after flood events serve as points of reference for her investigations. Based on these outcomes, strategies for desedimentation of reservoirs are developed and further measures are introduced.

Graz, June 2016
Univ.-Prof. Dipl.-Ing. Dr.techn. Gerald Zenz

Vorwort des Herausgebers

Wasserkraftanlagen tragen insbesondere im alpinen Raum maßgeblich zur Bereitstellung elektrischer Energie aus erneuerbarer Quelle bei. Zur energetischen Nutzung der Potentialdifferenz ist dazu ein Aufstau mit einem Speicher oder eine Ausleitung aus dem ursprünglichen Gerinne erforderlich. In diesen Staubereichen kommt es zu einer Reduktion der Fließgeschwindigkeit und im Falle von Feststoff führenden Flüssen zu einer Ablagerung und einer sukzessiven Verlandung von Stauraum. Dieser Umstand hat negative Auswirkungen auf die Speicherkapazität, den Wirkungsgrad der Anlage und die Situation im Bereich unterhalb der Sperrstelle. Es kann bei fehlendem Sedimenttransport unter anderem zu Eintiefungen der Flusssohle und Absinken des Grundwasserspiegels und damit zu negativen Auswirkung auf die Vegetation kommen.

Wasserbauliche Anlagen werden auch zum Schutz der Bevölkerung und der Infrastruktur vor Überschwemmungen errichtet. Deren Schutzwirkung kann durch Verlandung und damit Reduktion des durchflusswirksamen Querschnittes signifikant reduziert werden.

So ist sowohl in Hinblick auf die nachhaltige, dauerhafte Nutzung von Anlagen die – auch teilweise – Unterbindung bzw. Lenkung der Anlandung und bei Erkennen zuvor ermittelter, geeigneter Wassermengen eine Entlandung des Stau- und Entnahmebereiches zweckmäßig. Dazu werden unterschiedliche, spezifisch von der Anlage und der örtlichen Situation abhängige Maßnahmen zu ergreifen sein, die auf objektivierten Grundlagen basieren.

In Hinblick auf eine dauerhaft zuverlässige Nutzung von Laufkraftwerken stellt die vorliegende Dissertation einen Beitrag zur Beurteilung für An- und Entlandung in Speichern und damit der nachhaltigen Sedimentbewirtschaftung dar. Frau Dipl.-Ing. Dr.techn. Gabriele Harb untersucht in ihrer Arbeit Sedimenttransportprozesse, Feststoffeinträge und das Auftreten von Hochwasserereignissen zur Erarbeitung effizienter Entlandungsmaßnahmen. Messungen der Verlandung von Stauraumquerschnitten vor und nach Hochwasserereignissen dienen als Referenz für die Untersuchungen. Basierend auf diesen Ergebnissen werden Strategien zur Entlandung von Stauräumen erarbeitet und weiterführende Maßnahmen vorgestellt.

Graz, Juni 2016
Univ.-Prof. Dipl.-Ing. Dr.techn. Gerald Zenz

ABSTRACT

Sedimentation processes are in a “dynamic balance” in most natural rivers, but the construction of dams and reservoirs influences these natural conditions. The flow velocities, turbulences and bed shear stresses in reservoirs are reduced compared to free flow conditions, which lead to the deposition of the transported sediment particles. As a further consequence the sediment depositions reduce the storage volume by “filling up” the reservoir. This “reservoir sedimentation” is a problem in many Alpine reservoirs. However, the sediment transport processes in reservoirs are very complex and an appropriate knowledge is necessary to solve these problems.

This thesis focus on the sediment deposition problems and the sediment transport processes in reservoirs of river power plants with a small storage volume compared to the annual inflow. The aims of this thesis are the improvement of the sediment management in Alpine reservoirs and the analysis of the effect of sediment deposition in reservoirs on the operation of the reservoir and the flood protection of the surrounding area. This aim requires the knowledge of sedimentation, erosion and sediment transport processes together with field measurements and an adequate model to assess the impact of the selected sediment management method. Numerical modeling is already state-of-the-art for hydrodynamic calculations; whereas the modeling of sediment transport processes still needs further development and research. However, numerical models are able to reproduce the sediment transport processes. The enhancement of numerical modeling in Alpine reservoirs in case of flood and flushing events is thus also part of this thesis.

The thesis discusses first the processes of reservoir sedimentation and the reservoir sedimentation problems. The reservoir sedimentation and the storage loss worldwide and in Alpine reservoirs are connected with the sediment yield and the erosion in the catchment. Human impacts and climate change influences the sediment supply in the river systems. In the next step, the sedimentation processes are summarized. The understanding of the sediment transport processes in the rivers and reservoirs is necessary to limit the sedimentation in the reservoirs and enhance the erosion of deposited sediments for a sustainable sediment management to increase the usable lifetime of reservoirs.

In the literature, several sediment management methods can be found. These methods are discussed with respect to the application in Alpine reservoirs. Hydraulic removal like flushing is one of the most common ways to manage deposition problems in reservoirs. Reservoir flushing is normally conducted at higher discharges. The water level in the reservoir is lowered, which lead to increased flow velocities, bed shear stresses and erosion rates. The different types and stages of reservoir flushing are described including several parameters, which have an effect of the flushing efficiency. The sediment depositions in reservoirs often contain silt and clay fractions. The cohesive forces increase

the critical shear stress of the depositions. Additional flume tests were thus conducted to estimate the critical shear stress of cohesive sediments samples from different reservoirs.

In this thesis two different three-dimensional computational fluid dynamic programs were used to simulate the sediment transport processes and effects during flushing and flood events in two Alpine river reservoirs. The results of the simulations were calibrated and validated with measurements conducted in the prototype or in the physical model test. Several sediment transport algorithm were tested and validated with the measured bed changes. The simulated bed changes and sediment transport processes showed a good correlation with the measurements. The effects of sediment depositions and the remobilization of deposited sediment in reservoirs could be analyzed. Based on the results of the numerical modeling it is possible to recommend sediment management strategies for small Alpine reservoirs.

KURZFASSUNG

In den meisten natürlichen Flüssen sind die Sedimentations- und Erosionsprozesse in einem dynamischen Gleichgewicht. Die Konstruktion von Staudämmen und Stauräumen beeinflusst dieses natürliche Gleichgewicht, da die Fließgeschwindigkeiten, die Turbulenzen und die Sohlschubspannungen in Stauräumen geringer sind als in freien Fließstrecken. Dieser Effekt führt zu einer Anlandung der transportierten Sedimente. In Folge reduziert sich das Stauraumvolumen durch das „Auffüllen" des Stauraums. Diese „Stauraumverlandung" ist ein Problem in vielen alpinen Stauräumen. Aufgrund der Komplexität der Sedimenttransportprozesse ist ein umfassendes Verständnis notwendig, um dieses Problem lösen zu können.

Der Schwerpunkt dieser Arbeit liegt auf den Verlandungsproblemen und den Sedimenttransportprozessen von Flusskraftwerken mit einem relativ kleinen Verhältnis von Stauraumvolumen zum Jahresabfluss. Die Ziele der Arbeit sind die Verbesserung des Sedimentmanagements in alpinen Stauräumen und die Analyse der Auswirkungen der Stauraumverlandung auf den Betrieb der Kraftwerke und die Hochwassersicherheit der Umgebung. Diese Ziele setzten das Verständnis der Sedimentations-, Erosions- und Sedimenttransportprozesse voraus. Zusätzlich sind Naturmessungen und geeignete Modelle notwendig, um die Auswirkungen der gewählten Sedimentmanagementmethode evaluieren zu können.

Die Verwendung von nummerischer Modellierung ist bereits Stand der Technik im Bereich der Hydrodynamik. Bei der Modellierung von Sedimenttransportprozessen ist allerdings noch weiterer Forschungs- und Entwicklungsbedarf gegeben, obwohl einige numerische Modelle schon fähig sind, zahlreiche Sedimenttransportprozesse zu reproduzieren. Die Verbesserung der numerischen Modellierung von Hochwasserereignissen und Sedimenttransportprozessen in alpinen Stauräumen ist daher ebenfalls Teil dieser Arbeit.

In der Arbeit werden zuerst die Verlandungsprobleme und Verlandungsprozesse von Stauräumen analysiert. Die Stauraumverlandung und der weltweite Verlust von Stauraumvolumen sind eng mit der Sedimentfracht und der Erosion in den Einzugsgebieten verbunden. Menschliche Einflüsse und klimatische Veränderungen beeinflussen die Sedimentfracht in den Einzugsgebieten. Im nächsten Schritt werden die wesentlichen Sedimenttransportprozesse, die zur Verlandung von alpinen Stauräumen führen, zusammengefasst.

In der Literatur werden zahlreiche Sedimentmanagementmethoden erläutert. Diese werden in der Arbeit in Hinblick auf die Anwendbarkeit in Alpinen Stauräumen untersucht. Das hydraulische Entlanden von Stauräumen, z.B. durch die Nutzung von natürlichen Hochwässern ist dabei eine der meistgenutzten Möglichkeiten, um die Verlandung in Stauräumen zu reduzieren. Bei einer zusätzlichen Absenkung des Wasserspiegels am Wehr werden die Fließgeschwindigkeiten, die Turbulenzen und die Sohlschubspannungen

zusätzlich erhöht und die Erosion im Stauraum begünstigt.

Die Anlandungen in den Stauräumen enthalten oft auch Schluff- und Tonpartikel. Die kohäsiven Kräfte zwischen den Partikeln erhöhen dabei die kritische Sohlschubspannung dieser Sedimente. Die Größenordnung der Kohäsion ist aber von vielen Faktoren abhängig. Daher wurden im Rahmen der Arbeit Erosionsversuche in einem Glasgerinne zur Bestimmung der kritischen Sohlschubspannung von kohäsiven Sedimentproben aus unterschiedlichen Stauräumen durchgeführt.

In dieser Arbeit wurden zwei dreidimensionale nummerische Modelle verwendet, um die Sedimenttransportprozesse und deren Effekte bei Hochwasserereignissen und Stauraumentlandungen zu simulieren. Die nummerischen Ergebnisse wurden mit Naturmessungen und mit Messungen in einem hydraulischen Modell kalibriert und validiert. Sedimenttransportalgorithmen wurden getestet und die berechneten Sohländerungen mit den gemessenen Sohländerungen validiert. Die simulierten Ergebnisse zeigten eine gute übereinstimmung mit den Messungen. Auf Basis der Ergebnisse der nummerischen Modellierung werden Empfehlungen für Sedimentmanagementstrategien in hydrologisch kleinen, alpinen Stauräumen gegeben.

ACKNOWLEDGMENTS

This thesis was written during my time at the Institute of Hydraulic Engineering and Water Resources Management at the Graz University of Technology. Without the guidance and encouragement of several people this thesis would not have been possible.

First of all I would like to express my gratitude to my supervisor Professor Gerald Zenz. He gave me the opportunity to work on several projects concerning sediment management in the last years, for example Alp-S, SEE Hydropower, ClimCatch and the numerical modeling of the reservoirs Schönau, Leoben and Fisching. This was the main reason for me to focus my research on this topic. Thank you for the support of my PhD (including the visits at the NTNU in Trondheim) and the review of this thesis.

Then I would like to thank Professor Nils Reidar B. Olsen from the NTNU in Trondheim. He supported me during the last years and gave me the opportunity to visit Trondheim and work with his CFD group. I would like to thank him for the discussions of the case studies and the comments to this thesis, which improved my work significantly.

In the projects with the VERBUND Hydro Power I had the opportunity to improve my knowledge about sediment transport, reservoir flushing and numerical modeling of these processes. I would like to thank Hannes Badura for the support of my work and the fruitful discussions.

A huge thanks goes to my colleagues from Graz and Trondheim I met and worked with since my graduation. Josef Schneider, Cornelia Jöbstl, Wolfgang Richter, Clemens Dorfmann, Matthias Redtenbacher, Florian Asinger and Christopher Schreiber, thank you for your friendship and the often endless discussions. I also would like to thank my project leader, Josef Schneider, for the outstanding support during in the last years. Jochen Aberle, Nils Rüther and Stephan Spiller, thank you for the different point of view, which helped me to reflect my work. Thank you also to our technicians in the lab. The work on the model tests and in the flume wouldn't have been possible without their help.

A special thanks is addressed to my friends and most critical reviewers Christine Sindelar and Stefan Haun. They shared the last years with me, encouraged my ideas and discussed my work. Thank you for being there, when questions or doubts arouse.

I also would like to thank all my other friends, especially Birgit and Petra, for their emotional support in the last years.

Finally, I want to express my gratitude to my parents and my sister for their love and support. I also would like to say sorry to my sunshine Anna, because I spent a lot of time, especially in the last year, working and writing on this thesis.

Contents

NOMENCLATURE

$C/I - Ratio$	initial storage capacity to mean annual inflow ratio	–
C_1	constant in the logarithmic Law method, usually set equal to 8.5	–
C_f	dimensionless friction coefficient	–
C'_f	friction coefficient for the skin friction correction	–
C_h	Chèzy coefficient	$m^{1/2}/s$
D_*	sedimentological diameter	-
Fr	Froude number	–
Fr_*	dimensionless shear stress or Shields parameter Θ'	-
G	eroded amount of sediments	m^3
I	energy slope	–
K	correction factor by Brooks (1963)	–
N	number of sediment fractions	–
P	pressure	N/m^2
P_k	production of the turbulent kinetic energy	Joule/kg
R_h	hydraulic radius	m
Re_*	dimensionless diameter of the sediment also called grain Reynolds number or shear Reynolds number	–
Ri	Richardson number	–
S_c	Schmidt number	–
U, V, W	alternative indication of velocities in the x,y,z direction	m/s
U_m	mean or depth-averaged velocity	m/s
$U_{i,j}$	averaged velocity components in the numerical model	m/s
U_x, U_y, U_z	velocities in the x,y,z direction	m/s

Z_f	elevation of the river bed	m
Z_s	elevation of the water surface	m
Δ	bed form height	m
Φ_b	dimensionless bed-load transport rate	–
Φ_t	dimensionless total-load transport rate	–
Θ'	Shields parameter	–
Θ_c	critical Shields parameter	–
Θ_c	critical, dimensionless shear stress or critical Shields parameter	–
α	angle between the flow direction and the normal to the surface of the river bed	°
α_2	direction of the sediment transport in relation to the flow direction	°
α_1	angle of the slope perpendicular to the direction of the velocity vectors	°
β	empirical factor in the formula of Koch and Flokstra (1981)	m^2/s
δ	direction of the bottom shear stress in relation to the flow direction	°
δ_{ij}	Kronecker delta	–
ϵ	dissipation of the turbulent kinetic energy	m^2/s^3
η_i	correction factor for hiding/exposure	–
γ	specific weight	N/m^3
γ_s	specific weight of the sediment	N/m^3
γ_w	specific weight of the water	N/m^3
κ	Kármán constant (usually considered as $\kappa = 0.4$)	–
λ	bed form length	m
μ	dynamic fluid viscosity	N s $/m^2$
μ_g	skin friction parameter for the correction of the total bed shear stress	–
ν	kinematic fluid viscosity	m^2/s
ν_z	vertical turbulent eddy viscosity	m^2/s
ν_t	turbulent eddy viscosity	m^2/s
$\overrightarrow{r}$	direction vector pointing to the centre of the neighbor cell in SSIIM	–
$\overrightarrow{u}$	velocity vector of the cell in SSIIM	–
ϕ	angle of the slope of the river bed	°

ϕ_s	angle between the sediment transport vector and the velocity vector	$^\circ$
ρ	density of the fluid	kg /m^3
ρ_s	grain density of the sediment	kg/m^3
ρ_w	density of the water	kg/m^3
σ_k	constant empirical value in the standard $k-\epsilon$ model	-
σ_z	constant empirical value in the standard $k-\epsilon$ model	-
τ	shear stress	N/m^2
τ'	shear stress due to the grain roughness (skin friction)	N/m^2
τ''	shear stress due to the bed roughness	N/m^2
τ'''	shear stress due to suspended sediments	N/m^2
τ_0	calculated total bed shear stress in Telemac	–
τ_*	dimensionless shear stress	–
$\tau_{c,i}$	critical bed shear stress of the ith sediment fraction	N/m^2
$\tau_{l,w}$	shear stress at the wall for laminar flow	N/m^2
τ_{xy}	bed shear stress	N/m^2
θ	empirical factor derived by flume tests and related to the angle of response of the sediment	$^\circ$
a	reference level in the suspended load formula of Van Rijn	m
a_i	weighting coefficient for the neighbor cell in SSIIM	–
c	sediment concentration	–
$c_{1\epsilon}$	constant empirical value in the standard $k-\epsilon$ model	-
$c_{3\epsilon}$	constant empirical value in the standard $k-\epsilon$ model	-
c_μ	constant empirical value in the standard $k-\epsilon$ model	-
$c_{bed,i}$	concentration of the suspended sediments at the bed for the i^th sediment fraction	–
d	grain diameter	m
d_i	diameter of the ith sediment fraction	m
$d_{m,f}$	mean fall diameter of the sediment	N/m^3
d_m	mean diameter of the sediment	m

f'	friction parameter in the Engelund-Hansen formula	–
f_i	fraction size of the ith sediment fraction	–
g	acceleration due to gravity	m/s^2
h	flow depth	m
k	turbulent kinetic energy	Joule/kg
k'_{St}	Strickler coefficient due to grain roughness	m$^{(1/3)}$/s
k_{St}	Strickler coefficient of the channel bed	m$^{(1/3)}$/s
k_s	equivalent sand roughness	–
l_m	mixing length	m
m_1	constant set equal to 0.6 in the Hiding/Exposure Equation of Wu	–
n'_m	Manning coefficient due to grain roughness	s/m$^{(1/3)}$
n_m	Manning coefficient of the channel bed	s/m$^{(1/3)}$
p_{atm}	atmospheric pressure	N/m^2
p_i	pressure in the ith in SSIIM	N/m^2
p_p	pressure in the cell in SSIIM	N/m^2
$q_{b,i}$	volumetric transport rate of the fraction of the bed load	m^2/s
q_{b1}	modified sediment transport rate	m^2/s
q_b	volumetric sediment transport rate - bed load	m^2/s
$q_{s,b*}$	bed load transport rate per weight/time/unit widt	N/s m
$q_{s,c}$	volumetric depth-integrated suspended load transport	m^2/s
q_{t*}	volumetric sediment transport rate - total load	m^2/s
s	specific density ρ_s/ρ_w	–
t	time	s
u'	fluctuating velocity component in the longitudinal direction	m/s
u, v, w	local velocity components	m/s
u_*	shear velocity	m/s
u_{bed}	velocity in the bed cell	m/s
v'	fluctuating velocity component in the vertical direction	m/s
w_f	fall velocity of the particle	m/s

x	spatial geometrical scale	m
y	vertical distance from the river bed	m
z	water level elevation	m
z_i	water level elevation in the ith neighbor cell in SSIIM	m
z_p	water level elevation in the cell in SSIIM	m

1 INTRODUCTION

Sediment transport processes like erosion and deposition are in a “dynamic balance” in most natural rivers. The construction of dams and reservoirs influences this balance. In reservoirs the flow velocities, turbulences and bed shear stresses are reduced and this leads to sedimentation of the transported bed and suspended load. As a further consequence the bed levels raise and reduce the storage volume by “filling up” the reservoir (Harb et al., 2011). Decreased reservoir volume reduces and - in extreme cases - eliminates the capacity of hydro power production, water supply, irrigation and flood control benefits (e.g., Morris and Fan, 1998). The raise of the bed levels may also change the flow pattern in the reservoir.

Reservoirs in alpine areas can be divided in reservoirs of run-off river plants, diversion plants and reservoirs of storage and pump-storage hydro power plants. In case of reservoirs of storage and pump-storage hydro power plant the annual water inflow is small compared with the storage volume of the reservoir. Because of the large water depth and the resulting low flow velocities also the small sediment fractions settle in these reservoirs and the fine sediments, which are usually transported in suspension, presents the main part of the deposited sediments. However, due to the size of these reservoirs and the usually small catchment and therefore relatively small sediment yield, the deposition of sediments may not be a problem in these reservoirs for many years. High sediment yields with lots of fine sediments can create huge impacts, for example at the Margaritze reservoir in Austria.

The water depth of reservoirs of run-off river and diversion plants are usually lower than in reservoirs of storage and pump-storage hydro power plants. A larger part of the suspended sediments is thus transported through the reservoir and deposition of bed load fractions is the main problem. The deposition of coarse sediments at the head of the reservoir may cause problems regarding flood protection by raising the bed level and thus, raising the water level too. Furthermore massive sediment depositions in front of the turbine intakes, upstream or downstream of the weir or at the water intake can limit the operation and the electrical energy output of the hydro power plant.

Reservoir sedimentation reduces the sediment supply downstream of the dam additionally, which can cause erosion downstream of the reservoir or the coarsening and armoring of the river bed. This effect impacts also the habitat suitability and the spawning suitability for fishes.

1.1 Methodology and Methods

The methodologies and methods for the evaluation of a suitable sediment management strategy can be divided into the data acquisition, the preselection of a sediment management strategy, the simulation of the preselected sediment management method, the verification of the capability of the method and their results and the evaluation of the efficiency of the selected method. A further subdivision, applied in the thesis is given in the following part:

- *Observation and measurements:* The analysis of reservoir sedimentation is based on observations and measurements of the sediment inflow into the reservoir, the sediment deposition itself and the erosion processes in the reservoir. Different factors may influence this processes e.g., the operation plan of the power plant and have to taken into account accurately. The measured amount of transported and deposited sediment as well as the sedimentation pattern, is one of the key parameters for the selection of a sediment management method.

- *Selection sediment management method:* Based on the conditions in the reservoir, in the catchment and downstream of the reservoir a sediment management method or a combination of sediment management methods is chosen for a detailed analysis. In general, mechanical and hydraulic methods are available for the removal of deposited sediments from reservoirs. Every reservoir is unique regarding the purpose, the geometry, and other specifications like hydrological and hydraulic conditions. Consequently not every management method is suitable for every reservoir.

- *Numerical simulation:* Numerical modeling has become an important tool in fields of hydraulic engineering. There are various numerical models available, which are able to handle hydraulic problems. However, numerical models with with implemented sediment transport algorithm are relatively rare and often not validated. Two of these models are used in this thesis to simulate the sediment transport processes, including deposition and erosion, and their effects to evaluate the effect of the sediment management method.

- *Case studies - Numerical modeling of the sediment transport processes:* The geometry, hydrological and sedimentological conditions of the case studies are implemented in the numerical model. The numerical model is calibrated using field measurements in the prototype or measurements in a physical model.

- *Case studies - Verification and results:* The results of the numerical simulations are validated with a second independent flow dataset derived by Acoustic Doppler Current Profiler (ADCP) measurements conducted in the prototype or Acoustic Doppler Velocimeter (ADV) measurements in the physical model. Echo-soundings can be used for the validation of simulated erosion and deposition processes.

- *Conclusion and outlook:* The results are summarized and discussed. Recommendations for a sustainable sediment management and for further research are given.

The motivation and objectives are discussed in the next section.

1.2 Motivation and Objectives

Reservoir sedimentation is a problem in many Alpine reservoirs. Many rivers must deal with the consequences of reservoirs sedimentation like the coarsening or the armoring of the river bed. However, the sediment transport processes in reservoirs are very complex and appropriate knowledge is necessary to solve these problems.

Only a few documented flushing events can be found in literature. The reason may be that the documentation and the description of sediment transport processes and occurring bed forms during flushing events is difficult, because of the lack of appropriate measurement systems and techniques to acquire the spatial and temporal changes in the river bed and of the sedimentological parameters. Even the sediment balance derived from the echo soundings of the reservoir before and after the flushing events are often inconsistent, because of the frequently occurring time gap between the flushing event and the echo sounding. The eroded amount of sediment may thus be underestimated (Badura, 2007). Furthermore the sediment inflow during the flood or the flushing event is often unknown.

This thesis focus on the sediment deposition problems and the sediment transport processes in reservoirs of river power plants with a small storage volume compared to the annual inflow. The aim of this thesis is the improvement of the sediment management in Alpine reservoirs and the analysis of the effect of sediment deposition in reservoirs on the operation of the reservoir and the flood protection of the surrounding area. This aim requires the knowledge of sedimentation and sediment transport processes together with field measurements and an adequate model to assess the impact of the selected sediment management method. Numerical modeling is already used for hydrodynamic calculations; whereas the modeling of sediment transport processes still needs further development and research. However, numerical models are able to simulate the sediment transport processes. The enhancement of numerical modeling in Alpine reservoirs in case of flood and flushing events is thus also part of this thesis.

First the processes of reservoir sedimentation and the reservoir sedimentation problems are discussed. The reservoir sedimentation and the storage loss worldwide and in Alpine reservoirs are connected with the sediment yield and the erosion in the catchment. Human impacts and climate change influences the sediment supply in the river systems. In the next step, the sedimentation processes are summarized. The understanding of the sediment transport processes in the rivers and reservoirs is necessary to limit the sedimentation in the reservoirs and enhance the erosion of deposited sediments for a sustainable sediment management to increase the usable lifetime of reservoirs.

In the literature, several sediment management methods can be found. These methods are discussed and reviewed with respect to the application in Alpine reservoirs. Hydraulic removal like flushing is one of the most common ways to manage deposition problems in reservoirs. Reservoir flushing is normally conducted at higher discharges. The water level in the reservoir is lowered, which leads to increased bed shear stresses and erosion rates. The different types and stages of reservoir flushing are described including several parameters, which have an effect on the flushing efficiency. The sediment depositions in reservoirs often contain silt and clay fractions. The cohesive forces increase the critical shear stress of the depositions. To take this effect into account, additional flume tests were conducted to estimate the critical shear stress of cohesive sediments samples from different reservoirs, which still represents a gap in knowledge.

In this thesis the two three-dimensional computational fluid dynamic programs SSIIM and TELEMAC are used to simulate the sediment transport processes and effects during flushing and flood events in two Alpine river reservoirs. The results of the simulations are calibrated and validated with measurements conducted in the prototype or in the physical model test. Several sediment transport algorithm are tested and validated with the measured bed changes. The simulated bed changes and sediment transport processes show a good agreement with the measurements. The effects of sediment depositions and the remobilization of deposited sediment in reservoirs could be analyzed. Based on the results of the numerical modeling it is possible to recommend sediment management strategies for small reservoirs in the Alpine region.

2 RESERVOIR SEDIMENTATION

Several parameters concerning the sedimentation of reservoirs can be found in the literature. More than 50 percent of streams and rivers are dammed and the greater part of transported sediments, in fact some 80 percent, are trapped in reservoirs. This fact corresponds to a volume of about 8 to 16 km ^{3} (Lempérièr and Lafitte, 2006). Morris and Fan (1998) quantified the world's total sediment deposit between 15 and 40 Gt per year. White (2001) estimates that more than 0.5 percent of the total reservoir storage volume is lost worldwide due to reservoir sedimentation. Mahmood (1987), Yoon (1992) and Bruk (1996) estimated a worldwide loss of storage volume of about 1 percent of the initial reservoir volume per year.

The full extant of this problem becomes clear, if we consider the fact that around 20 percent of the cultivated areas are irrigated and that about 16 percent of the electrical energy is generated by hydro power (IEA, 2007). According to ICOLD (1998) more than 25,400 large reservoirs are used for multiple purposes and a large part of these reservoirs has to deal with sedimentation problems. The costs for restoring these losses and rebuilding the dams can be estimated at US$ 13 billion per year (Palmieri et al., 2003).

One of the most cited examples is the Camare irrigation reservoir in Venezuela, where it took only 15 years of operation until the storage volume was lost. This reservoir differs from other ones in only one aspect, the speed of the total sedimentation of the reservoir (Morris and Fan, 1998).

The average rate of sediment deposition in reservoirs is normally expressed in volume units such as cubic meters (m^3) per year. However, for comparing different reservoirs the deposition rate in percent of the original storage volume is used (Morris and Fan, 1998).

The loss of storage in a reservoir can be expressed with the *sediment release efficiency* of the reservoir. The sediment release efficiency is the mass ratio of the released sediment of the total sediment inflow over a specific time period (Morris and Fan, 1998). Churchill (1948) developed a relationship based on the sediment release efficiency.

The sediment trapping efficiency, which is the complement of the sediment release efficiency, was used by Brune (1953). This empirical relationships is based on the ratio of reservoir volume to mean annual inflow (C/I-ratio). Today, the sediment trapping efficiency is more commonly used. However, from the sediment management point of view, the sediment release efficiency is the more useful concept, because in cases where more sediment is released than entering the reservoir, the sediment release efficiency increases over 100 percent. Expressed in trapping efficiency the value would be negative.

Figure 2.1 shows the relationship between the release efficiency and the inflow ratio developed by Brune (1953). This function illustrates, that the sediment trapping efficiency

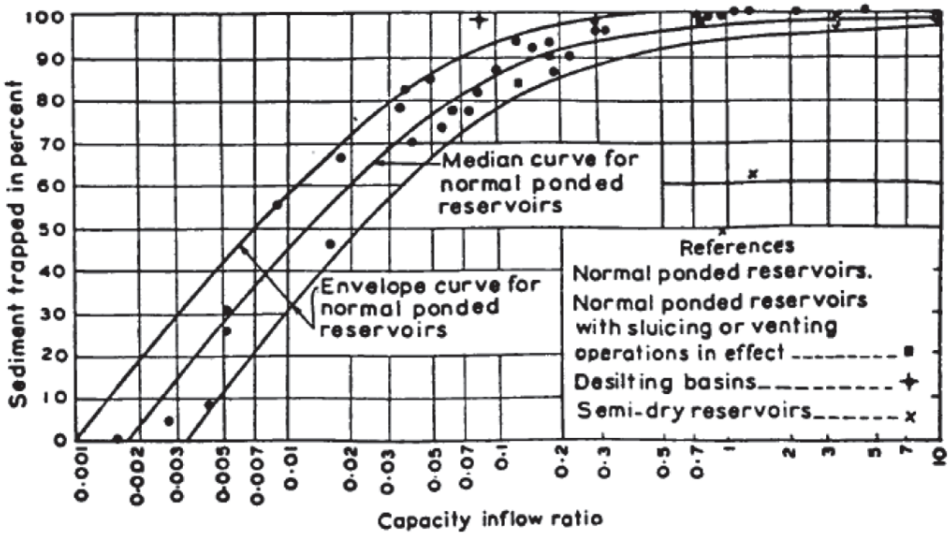

Figure 2.1: *Function for the estimation of sediment trapping or release efficiency in conventional impounding reservoirs in relation to ratio of reservoir volume to mean annual inflow (C/I-ratio) (Brune, 1953)*

of small reservoirs is nearly zero. However, in Alpine catchments, small reservoirs are mainly affected by sediment depositions. One explanation for this effect is the relationship derived by Brune (1953) does not take coarse sediment into account. This explanation was also found by Frenette and Julien (1986). Dendy et al. (1973) investigated the sedimentation rate in 1105 U.S. reservoirs and found a inverse relationship between the initial storage volume of the reservoir and the sedimentation rate (Table 2.1). This relationship is also quite interesting, because most of the Alpine river reservoirs have an initial storage volume smaller than 10 million m^3.

Table 2.1: *Relation of the initial storage volume and the sedimentation rate of U.S. reservoirs according to Dendy et al. (1973)*

Initial storage volume [million m^3]	Number of investigated reservoirs	Annual sedimentation rate mean [%]	Annual sedimentation rate medium [%]
0 – 0.012	190	3.56	2.00
0.012 – 0.123	257	2.00	1.20
0.123 – 1.23	283	1.02	0.62
1.23 – 12.3	176	0.81	0.55
12.3 – 123	107	0.43	0.27
123 – 1230	69	0.23	0.14
$>$ 1230	23	0.16	0.11

2.1 Storage Loss in Alpine Reservoirs

Alpine river reservoirs are usually small compared with storage reservoirs worldwide. In this thesis small and mediate river reservoirs are defined as reservoirs with a initial storage volume up to 10 million m^3 and a ratio between initial storage volume to annual mean inflow (C/I-ratio) of 10^{-2} to 10^{-5}. Unlike large reservoirs with a large ratio between initial storage volume to annual mean inflow, the main part of the suspended sediments is transported through the reservoir. Thus, the bed load is the decisive factor for reservoir sedimentation in Alpine river reservoirs.

Figure 2.2 shows the mean annual sedimentation rate of selected reservoirs.

The variation of the sedimentation rates can be explained by (e.g., Badura, 2007):

- Parameters of the catchment - geology, topography, vegetation cover, hydrology and climate
- Parameters of the reservoir - geometry, size, slope and sedimentological parameters
- Human impacts - land use in the catchment, trapping of sediments in the tributaries and in upstream reservoirs, desiltation of upstream reservoirs
- Volume errors caused by measurement and analysis failures

However, the storage loss is only one aspect of many sedimentation problems in reservoirs. The deposition of sediment in reservoirs may affect the operation of the reservoir,

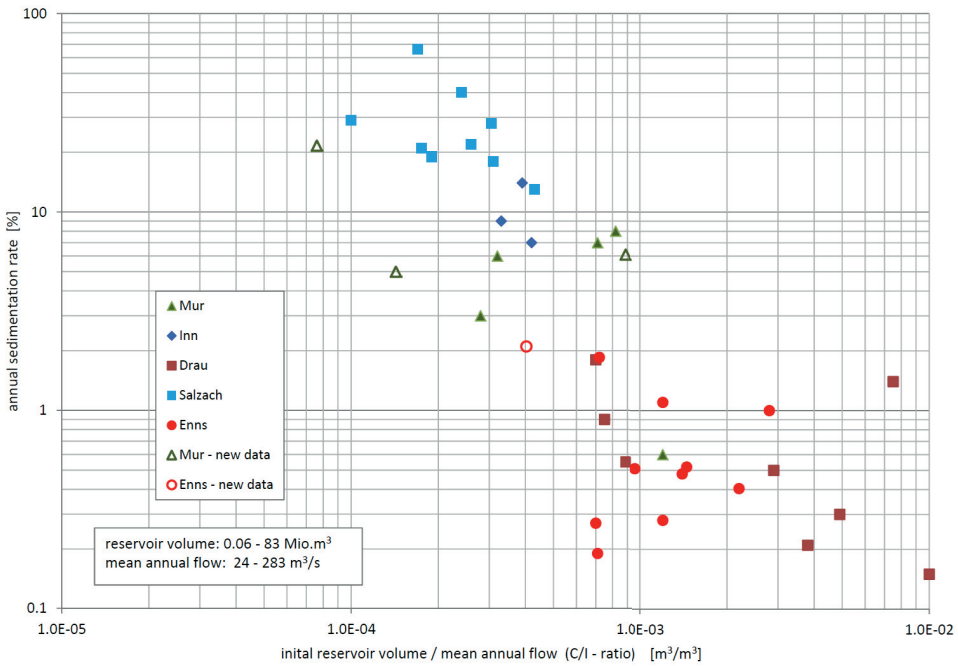

Figure 2.2: *Mean annual sedimentation rate of selected reservoirs of river power plants at Austrian rivers in relation to the C/I-ratio of the reservoirs (Badura, 2007, modified with additional data)*

increase the flood risk in certain areas near the reservoir or can block bottom outlets or turbine inlets. The sediment yield in the catchment is one of the main factors influencing the sedimentation rate in reservoirs.

2.2 Sediment Yield and Erosion in the Catchment

The land cover of an area is influenced by the topography, geology, soils and climate of the region. These factors also determine the land use by humans (White, 2001). The effect of cultivation or lack of land cover by vegetation on erosion rates is illustrated in Table 2.2.

Table 2.2: *Erosion rates for different land use categories according to Morris and Fan (1998)*

Land use	Erosion rate [t/km^2/yr]	Relative erosion rate forest = 1
Forest	8	1
Grassland	84	10
Abandoned surface mines	840	100
Croplands	1680	200
Harvest forest	4200	500
Active surface mines	16800	2,000
Construction sites	16800	2,000

In the WARMICE project ("Water resources management in a changing environment", funded in the FP4 of the European Union) erosion rates were measured in the Sölk valley located in Styria, Austria (Kohl et al., 2003). The erosion rates can be compared to the values given in Table 2.3. However, this measured erosion rates are calculated from seven field measurements and should therefore used as indicating values only. The measurements show that not only the land use, also other factors like e.g., the slope, the intensity of the land use, the soil structure, and the grain-size distribution may influence the erosion rates.

Table 2.3: *Measured erosion rates for different land use categories according to Kohl et al. (2003)*

Land use	Erosion rate [t/km^2/yr]	Relative erosion rate 8 t/km^2/yr = 1
Forest	0.02 - 25	0.0025 - 3.13
Grassland/meadow	3 - 8	0.375 - 1
Low vegetated alpine areas	90	11.25
Consolidated construction sites	10 - 800	1.25 - 100

The erosion in the catchment is one of the most important factors influencing reservoir sedimentation, but the loss of agricultural land and the erosion of soil in the catchment

may be much more important in the future. On a global scale, the growth in population is intensifying the change in land cover. In many parts of the world, increased population can also lead to expansion of commercial land use, land use changes and exploitation of native forests. These changes may cause increased erosion and sediment yield. Furthermore, increased population may be linked to increased industrial activity and exploitation of natural resources, for example through mining, building construction and infrastructure development, which again lead to changes in land use and the probability of increased sediment yields (Walling, 2006).

Syvitski et al. (2005) investigated the human impact on the global sediment balance using simulations and calibration measurements (suspended load measurements). *In addition to human impacts on global runoff, there are many anthropogenic influences on global sediment yield, including urbanization, deforestation, agricultural practices, mining, and the retention of sediment by reservoirs (Syvitski et al., 2005).* Figure 2.3 illustrates the human impact on the natural sediment load evaluated for 217 rivers with good observational data (before/after damming) according to Syvitski et al. (2005). The analysis indicates that rivers would move more sediment to the coasts, but lots of sediments are trapped in reservoirs. The red (with Yellow River) and the black line (without yellow river) exclude the impact of reservoirs. The green line demonstrates the basin-wide trapping of suspended sediment load by the large reservoirs (>0.5 km^3 maximum initial storage volume) that account for about 70% of the filled initial storage volume. The blue line highlights the impact of the smaller reservoirs (Syvitski et al., 2005).

Walling (2006) stated that the sediment yield in rivers should not be viewed as a static measure of the functioning of the system, but rather as providing a snapshot of the func-

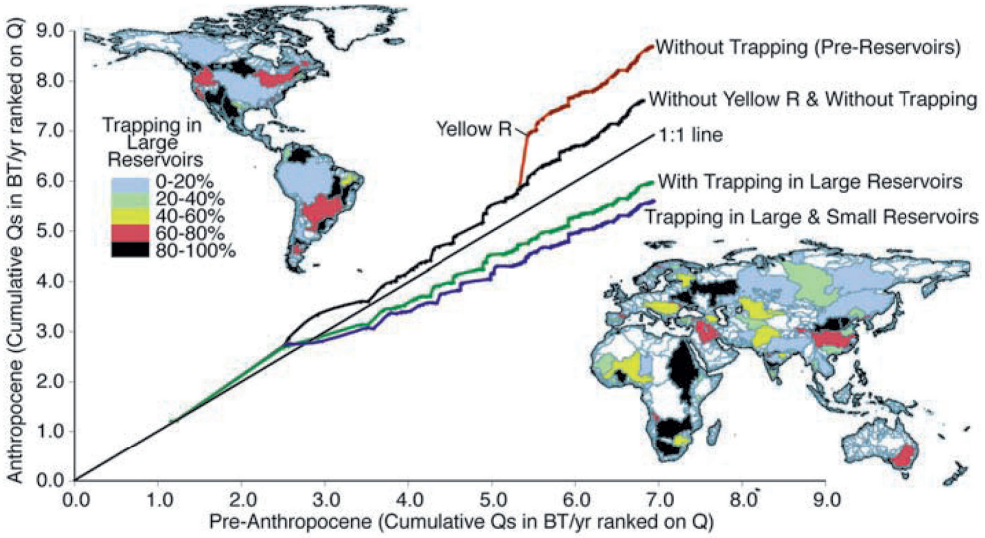

Figure 2.3: *Comparison between pre-anthropocene and modern sediment loads, using 217 global rivers with good observational before- and after-dam data. The red (with Yellow River) and the black line (without yellow river) had trapping by reservoirs removed and represent the increased sediment yield caused by human activities (e.g., deforestation). Two other curves show the impact of sediment trapping in large (green line) or small (blue line) reservoirs (Syvitski et al., 2005)*

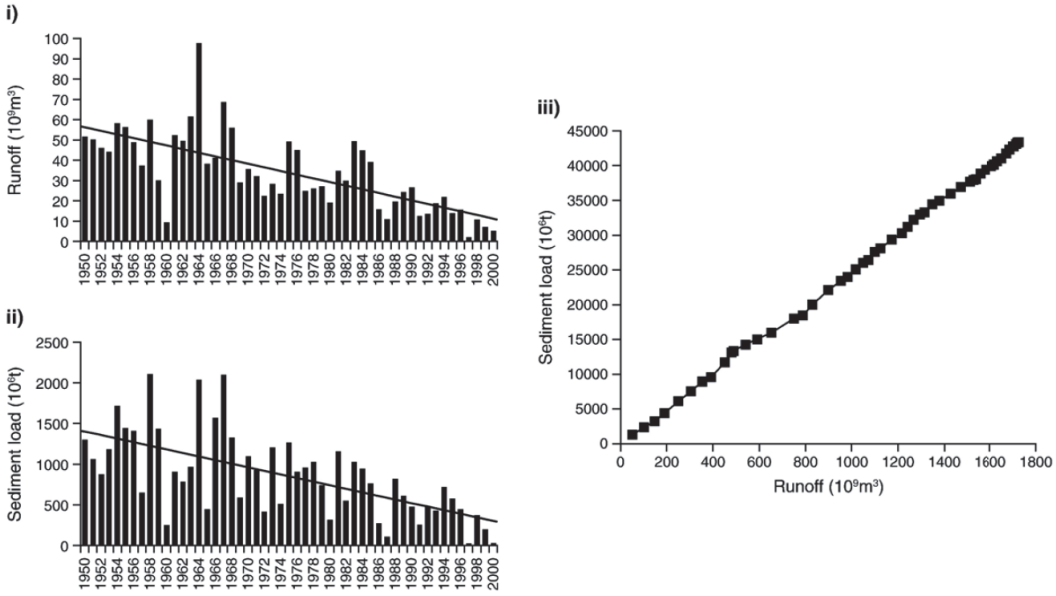

Figure 2.4: *Changes in the sediment load of the Yellow River, China; (i) time series of annual water discharge and (ii) annual sediment load and (iii) associated double mass plots(Walling, 2006)*

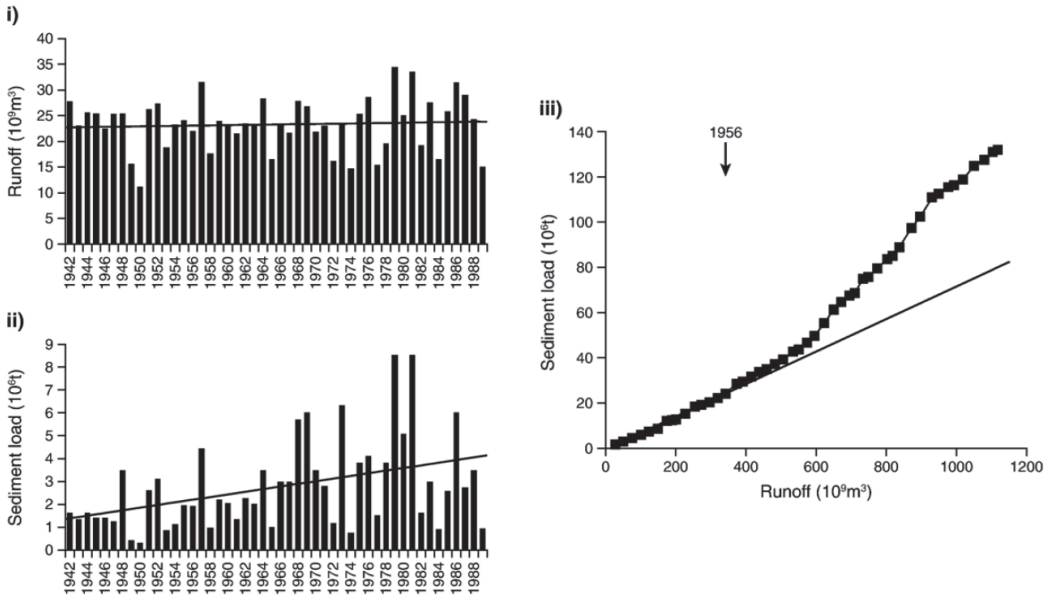

Figure 2.5: *Changes in the sediment load of the Kolyma River, W.Siberia; (i) time series of annual water discharge and (ii) annual sediment load and (iii) associated double mass plots (Walling, 2006)*

tioning of an ever-changing system. The River Nile, for example, has a near zero sediment load since the construction of the Aswan High Dam (e.g., Milliman and Meade, 1983; Milliman and Syvitski, 1992), whereas the pre-dam sediment load was likely about 100 million tons per year.

The human impact can increase or decrease the sediment yield in the rivers. The progres-

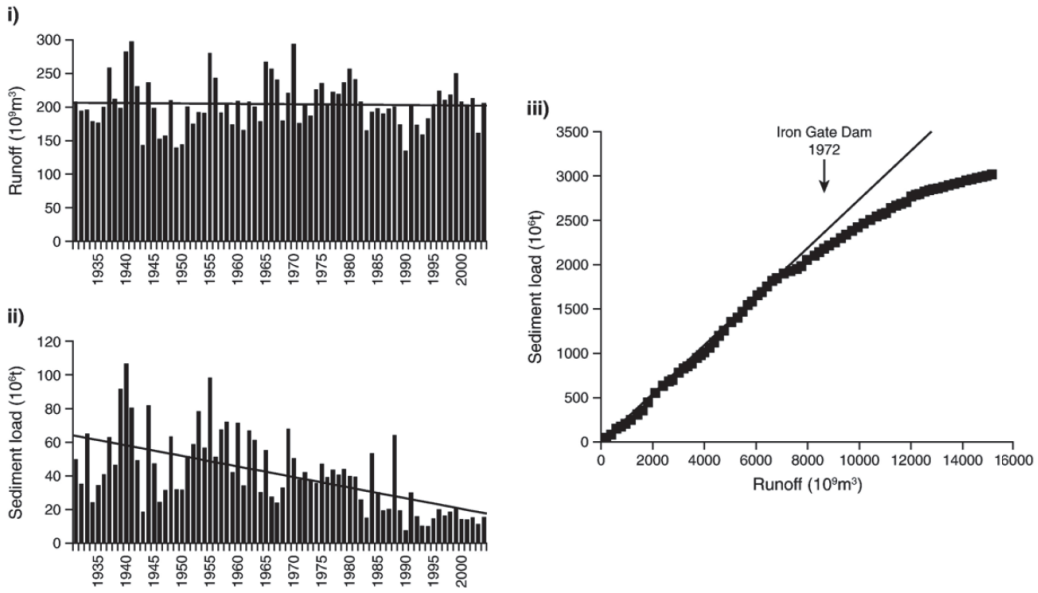

Figure 2.6: *Changes in the sediment load of the Danube, Europe; (i) time series of annual water discharge and (ii) annual sediment load and (iii) associated double mass plots (Walling, 2006)*

sive reduction in the water discharge and suspended sediment load of the Yellow River (Figure 2.4) is partly caused by climate change. However, it is mainly a reflection of human impact like increasing water abstraction, sediment trapping by an increased number of large and small reservoirs. An extensive program of soil and water conservation improves local agriculture and reduce sediment inputs to the river, where sediment deposition causes major problems for effective flood control and water use in the lower reaches of the basin (Walling, 2006). All these effects lead to a decreased runoff and a more or less proportional decreased sediment load.

Figure 2.5 shows the upper Kolyma River above Srednekansk in western Siberia with a catchment of 99,400 km^2. Over the years 1941 to 1988 exists a statistically significant trend of increasing sediment loads, but no significant change in runoff occurred. These effects can be affiliated to extensive gold mining activity within the catchment (Walling, 2006).

At the Danube the trend in sediment yield contrasts with that at the upper Kolyma River (Figure 2.6). Close to the delta at the Black Sea, at Cetail Izmail in Romania (Catchment Area 807,000 km^2), the Danube shows a declining trend in sediment load. Again, no significant trend exists in the annual runoff. A main reduction in the sediment load started in the mid-1960s and resulted in a reduction of about 70% by the 1990s. The Iron Gate Dam on the River Danube implemented a major sediment trap into the river in 1972, but the reduced sediment load also reflects the construction of a substantial number of other dams and reservoirs in the main river and the tributaries (Walling, 2006).

Schöberl et al. (2005) investigated the influence of hydro power plants and torrent control measures on the bed load yield of the Drau river near Lienz in Austria by using an one-dimensional numerical model. The study showed a significant reduction of the bed load yield due to the sedimentation in the reservoirs and sediment traps of the torrent control.

Reservoir sedimentation is a result of the erosion processes in the catchment and the sediment yield. Human impacts can influence the sediment yield in rivers and therefore one of the main factors of reservoir sedimentation.

3 SEDIMENT TRANSPORT

Sediment transport processes are one of the greatest issues in river engineering. Extensive literature is available concerning this topic. A short overview is given in this thesis. The sediment transport processes, which are relevant for the case studies, are described more detailed.

3.1 Introduction to Sediment Transport

Sediment transport is the general term used for the transport of solid particles (e.g., clay, silt, sand, gravel or boulders) in rivers and streams. The transported solid particles are called the sediment load.

Generally the total sediment load can be subdivided in

- Bed load
- Suspended sediment load

A special form of suspended sediment is wash load with a density close to the density of water. Wash load is washed through the fluvial system without significant interaction with the river bed. It is not possible to specify a clear threshold between bed load and suspended load. A wide range of definitions is given in the literature. Usually bed load is defined as the sediment particles which slide, roll or jump along the river bed, while suspended load refers to grains maintained in suspension by turbulence (Einstein et al., 1940; Van Rijn, 1984a). When the initiation of motion is reached, the sediment particles will first roll and slide in continuous contact to the river bed. With increasing force, the particles will be moved along the river bed by more or less regular jumps, which are called saltations. If the value of the bed shear velocity exceeds the fall velocity of the particle, the sediment particle can be lifted from the river bed. The particle may stay in suspension, if the turbulence forces are comparable or higher than the submerged weight of the particle (Van Rijn, 1984a). Graf (1971) gives indicating values, which uses the ratio of the shear velocity u_*, and the settling velocity of the particles w_f:

- $u_*/w_f > 0.10$ beginning of bed load transport
- $u_*/w_f > 0.40$ beginning of suspended load transport

Engelund (1965) and Bagnold (1966) gives a value near 1 for the beginning of significant suspension.

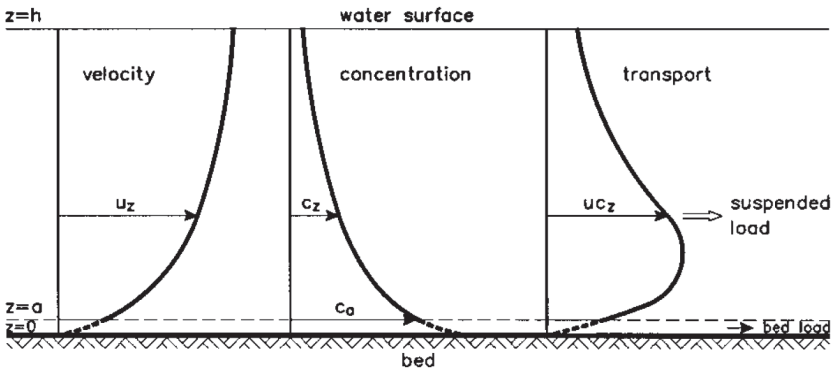

Figure 3.1: *Definition and sketch of suspended sediment transport (Van Rijn, 1993)*

According to Van Rijn (1993) the particle velocity in longitudinal direction is almost equal to the fluid velocity for suspended load (Figure 3.1). Usually, the behavior of the suspended sediment particles is described using the sediment concentration, which is normally given by the solid volume (m^3) per unit fluid volume (m^3) or by the solid mass (kg) per unit fluid volume (m^3). Observations showed that the suspended sediment concentrations decrease with increasing distance from the river bed. The rate of decrease depends also on the ratio of the shear velocity u_* and the settling velocity of the particles w_f. Thus, the depth-integrated suspended load transport ($q_{s,c}$) is defined as the integration of the product of velocity (u) and concentration (c) from the edge of the bed load layer ($z = a$) to the water surface ($z = h$).

Fine sediments like silt and clay particles are probably always transported in suspension, whereas gravel and cobbles are normally transported as bed load. However, depending on the turbulent energy, sand particles may stay in the river bed, move as bed load or be carried in suspension. Thus, the suspended sediment load in a river can consist of silt and clay particles at lower discharges, but include sand particles at higher discharges. In many rivers, the bed load constitutes only a small fraction of about 15 percent of the total sediment load (Morris and Fan, 1998).

3.2 Deposition and Erosion of Sediments

Erosion occurs, if the forces (turbulence, shear stress) responsible for the transportation of the sediment is sufficient to overcome the weight, fall velocity or the friction ($\tau > \tau_c$) of a sediment particle. If the force responsible for the transportation of the sediment is not longer sufficient to overcome the weight, fall velocity or the friction ($\tau < \tau_c$) of a sediment particle, the sediment particle deposits again (Yalin, 1977). Cohesive forces are important, if the sediment contains clay and silt particles. The driving forces are highly related to the local near-bed velocities. In cases of turbulent flow conditions the velocities fluctuate in time and space. Thus, with the randomness of particle size, shape and position of the sediment particle on the river bed, the initiation of motion is not merely a deterministic phenomenon but a stochastic process as well (Van Rijn, 1993).

One of the main factors concerning the deposition of suspended sediments is the settling velocity. A sediment particle can be transported in suspension only if its settling velocity is smaller than the vertical component of the hydraulic turbulence (Rouse, 1938). The

settling velocity of a sediment particle depends on the size, shape and the density of the particle, but also on the characteristics of the fluid, like temperature, salinity and suspended sediment concentration. The settling velocity of particles is given by Stoke's law or by using of empirical values.

Clay and silt particles have extremely low settling velocities, but short-distance van der Waals forces may cause the aggregation into flocs. The flocs are large enough to settle several orders of magnitude faster than individual clay particles. This effect is referred to as *flocculation*. The cohesion of very fine-grained sediments, i. e., silt and clay fractions, determines this flocculation processes (Hillebrand et al., 2012). Two different processes can be detected, either colliding particles bond and form larger particles, called flocs, or break up due to the collision-induced shear stress. If the shear stress, imposed by either a collision or by fluid forces, exceeds the particles strength, flocs disaggregate into smaller particles. Hence, both flow-induced shear stresses, causing flocs to break up into smaller particles, and collision-induced shear stresses, leading to aggregation or disaggregation processes, play an important role regarding the range of particle sizes and thus have a major impact on the settling velocity (Klassen et al., 2011). Therefore, these processes play an important rule for the deposition of fine suspended sediments.

3.2.1 Initiation of Motion of Sediment

In the literature, several parameters for the initiation of motion of sediment particles can be found. An overview over the different formulae describing the initiation of motion is given in Batuca and Jordaan (2000). Schoklitsch (1935) used the critical specific discharge depending on the bed slope and an characteristic grain diameter. This approach can also be found in the formula of Rickenmann (1991), who extended the tests made by Smart and Jäggi (1983) and modified the formula developed by Bathurst et al. (1987). Hjulström (1935) used the critical velocity to describe the initial sediment motion in Figure 3.2. The stream power was used by Yang (1984) as critical parameter. However, in most cases the shear stress is applied.

Shields (1936) developed a relation to describe the initiation of motion for sediment particles (Figure 3.3). This diagram is widely used to determine the condition of incipient motion based on the bed shear stress. The Shields curve in the diagram represents the critical conditions corresponding to the motion of sediment particles. Points below the curve correspond to no sediment motion and points above the curve correspond to motion of sediment.

This initiation of motion is related to the dimensionless diameter of the sediment Re_* (also referred to as grain Reynolds number or shear Reynolds number; Equation 3.1) and the dimensionless shear stress Fr_* (also referred to as Shields parameter Θ'; Equation 3.2). Therefore, the motion of sediment is a function of the size of the sediment particle and the hydraulic conditions (Shields, 1936):

$$Re_* = \frac{u_* d_i}{\nu} = \frac{d_i \sqrt{\frac{\tau}{\rho_s}}}{\nu} \tag{3.1}$$

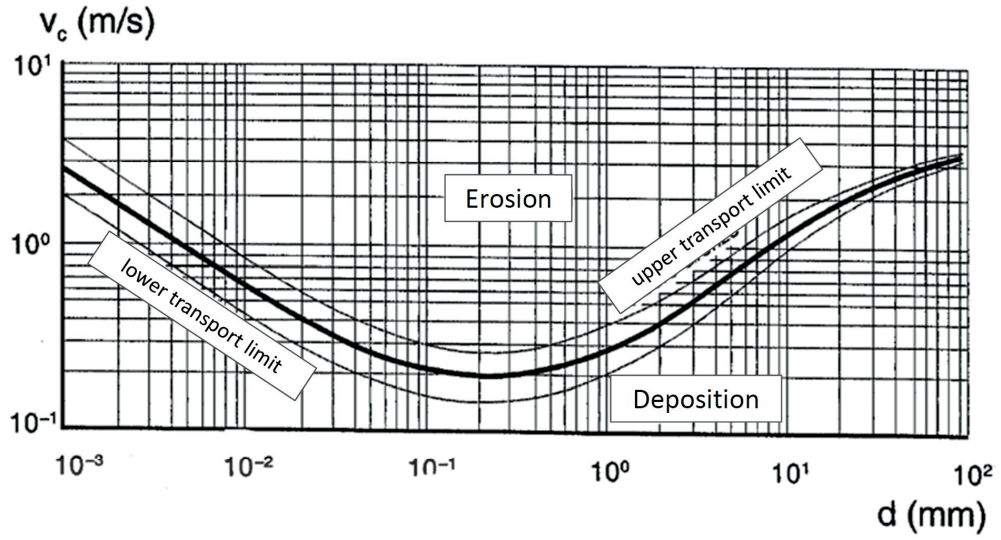

Figure 3.2: *Relation between critical velocity v_c and grain size d according to Hjulström (1935)*

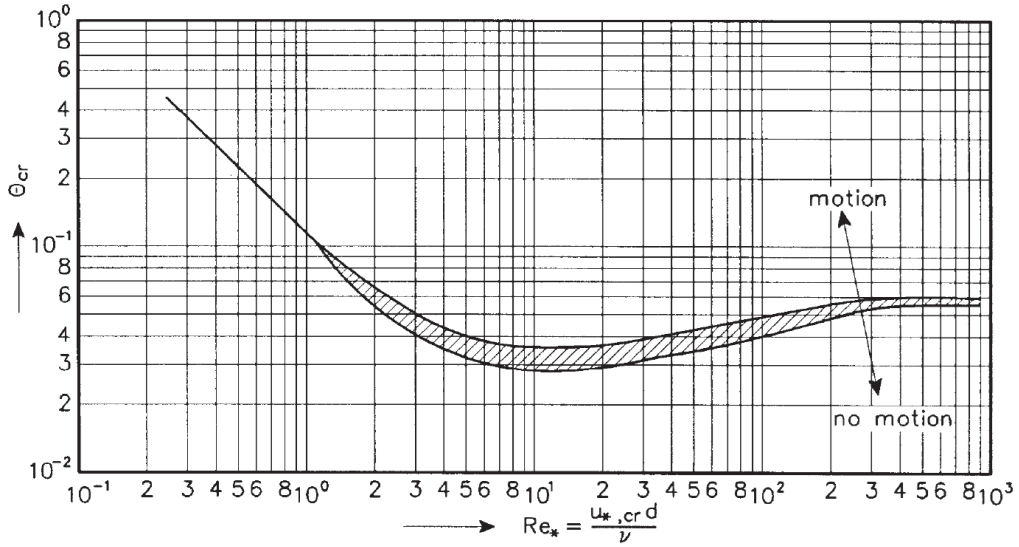

Figure 3.3: *Relation between the grain Reynolds number Re_* and critical dimensionless shear stress $\Theta' = \Theta_{cr}$ according to Shields (1936)*

$$Fr_* = \Theta' = \frac{\tau}{g(\rho_s - \rho_w)d_i} \tag{3.2}$$

where u_* is the shear velocity, d_i is the diameter of the ith sediment fraction, τ is the bed shear stress, ρ_s is the grain density of the sediment, ρ_w is the density of the water, g is the acceleration due to gravity and ν is the kinematic viscosity.

The grain Reynolds number and the dimensionless shear stress can be related to the sedimentological diameter D_* (Equation 3.3).

$$D_* = \left(\frac{Re_*^2}{Fr_*}\right)^{\frac{1}{3}} d_i = d_i \left[\frac{(\rho_s - \rho_w)g}{\nu^2}\right]^{\frac{1}{3}} \tag{3.3}$$

Zanke (1982) calculated the probability of motion (called R according to Zanke) of the sediment particles and added the probability curves to the Shields-diagram (3.4).

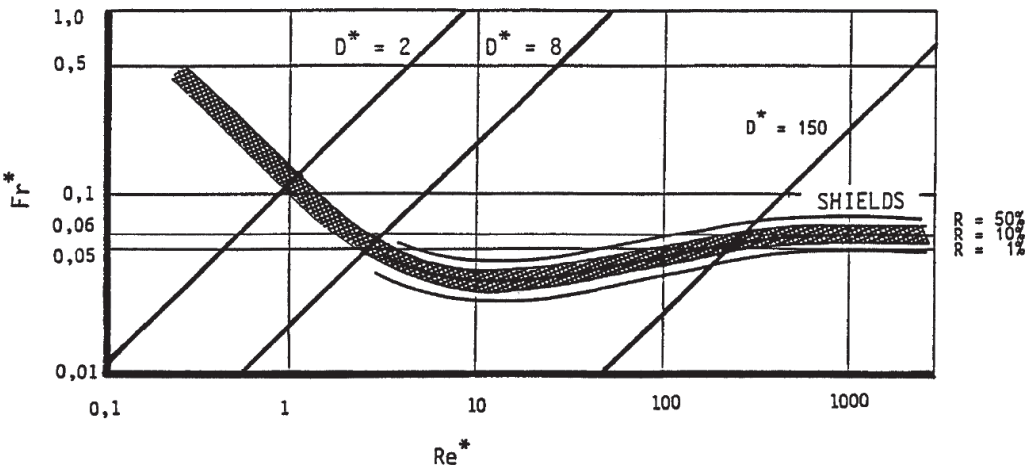

Figure 3.4: *Diagram after Shields including the probability of motion derived by Zanke (1982)*

The function derived by Zanke (1982) related the probability of motion (R) to the current and the critical shear stress.

$$R = \left[10 \times \left(\frac{\tau}{\tau_c}\right)^{-9} + 1\right]^{-1} \tag{3.4}$$

The critical bed shear stress is the main parameter for the initiation of motion for sediment particles. A large number of articles and books can be found in the literature discussing the relation of the bed shear stress to the sediment transport in hydraulic rough flow conditions (e.g., Shields, 1936; Zanke, 1982; Van Rijn, 1993).

The critical, dimensionless shear stress after Meyer-Peter and Müller (1948) is given by

$$\Theta_c = \frac{\tau_c}{(s-1)\ g\ d_m} = 0.047 \tag{3.5}$$

where s is ρ_s/ρ_w.

Depending on the author of the different sediment transport formulae and the definition of initiation of motion Θ_c varies from 0.03 to 0.06.

3.3 Evaluation of the Bed Shear Stress

This section is mainly cited from Harb et al. (2013c).

The bed shear stress is one of the key parameters for sediment transport processes. A large number of options can be found in the literature to predict the bed shear stress (Rowiński et al., 2005). The most widely used methods are the gravity/bed-slope method and the logarithmic wall law method. If measurements with time series of the fluctuating velocity components u' and w' near the bed are available, e.g., from ADV or PIV measurements in the laboratory or from a numerical model, the Reynolds Stress method may also be used (Harb et al., 2013c).

The shear stress at the wall for laminar flow is defined by

$$\tau_{l,w} = \mu \left.\frac{\partial u}{\partial y}\right|_w \tag{3.6}$$

where $\tau_{l,w}$ is the shear stress at the wall for laminar flow, μ is the dynamic fluid viscosity and $\left.\frac{\partial u}{\partial y}\right|_w$ is the velocity gradient at the wall (e.g., Yalin, 1977). Therefore, the shear stress depends on the velocity gradient at the wall, which is at the same time the difficulty in evaluating the shear stress in an appropriate way. For the evaluation of the shear stress both, direct and indirect methods can be used. These methods are based on the determination of the shear velocity u_*. The relation of the shear velocity to the shear stress is given by

$$\tau = \rho\ u_*^2 \tag{3.7}$$

where ρ is the density of the fluid.

The shear stress also depends on the roughness of the wall. The roughness of the wall is characterized by the shear Reynolds number Re* given in equation 3.1), where d_i, the diameter of the i^{th} sediment fraction, is substituted by k_s, which is the equivalent sand roughness.

$$Re_* = \frac{k_s \, u_*}{\nu} \tag{3.8}$$

Flow conditions with $Re_* < 5$ are referred to as hydraulic smooth, which means that all roughness elements are inside the viscous sub-layer. If $Re_* > 70$, the flow regime is hydraulic fully rough (e.g., Yalin, 1977). In this case the viscous sub-layer is so thin that the roughness elements penetrate the logarithmic layer (Yalin, 1977; Graf and Altinakar, 1998). Between $5 < Re_* < 70$ a hydraulic transitional flow occurs.

3.4 Methods for the Evaluation of Bed Shear Stresses

This section is mainly cited from Harb et al. (2013c).

3.4.1 Gravity or Bed-Slope Method

The gravity method determines the bed shear stress based on the control volume approach and reflects strongly one-dimensional flow conditions. In case of steady, uniform flow the shear velocity can be evaluated by:

$$\tau = \gamma \, R_h \, I \tag{3.9}$$

where γ is the specific weight, R_h is the hydraulic radius and I is the energy slope, which is in case of uniform flow equal to the channel slope.

3.4.2 Logarithmic Law Method

The logarithmic Law method is based on the Kármán-Prantl equation. The shear velocity u_* in the wall region $(y/h < 0.2)$ can be estimated in case of hydraulic rough conditions by fitting measured velocity profiles to the following equation:

$$u^+ = \frac{1}{\kappa} ln \frac{y}{k_s} + C_1 \tag{3.10}$$

with

$$u^+ = \frac{U_m}{u_*} \tag{3.11}$$

where U_m is the mean velocity, κ is the Kármán constant (usually considered as $\kappa = 0.4$), y is the vertical distance from the river bed and C_1 is a constant equal to 8.5 (Nezu and Nakagawa, 1993).

3.4.3 Reynolds Stress Method

The Reynolds Stress method can be used in a fully turbulent two-dimensional flow. For the calculation of the shear stress a time series of the fluctuating velocity components u' and w' near the bed is used. The bed shear stress is then given by

$$\tau = -\rho \, \overline{u'w'} \tag{3.12}$$

where u' is the velocity fluctuation in the longitudinal direction and w' is the velocity fluctuation in the vertical direction.

3.4.4 Turbulent Kinetic Energy Method

The bed shear stress can also calculated using the turbulent kinetic energy k close to the bed in cases, where it can be assumed that close to the wall the production and dissipation of turbulence is in equilibrium (Rodi, 1980).

$$\tau = \sqrt{c_\mu} \, \rho \, k = 300 \, k \tag{3.13}$$

where c_μ is a constant empirical values usually set equal to 0.09 given by Launder and Spalding (1972).

3.5 Sediment Transport Formulae

The different available sediment transport formulae were developed under different conditions by the analysis of flume and field experiments. Therefore, a wide range in the results can be expected by using different formulae. A detailed overview over different sediment transport formulae is given in Graf (1971). In this thesis, the following sediment transport formulae were used in the calculations and are therefore discussed in the following sections:

- Engelund-Hansen (1967)
- Meyer-Peter-Müller (1948)
- van Rijn (1984)

The parameters of the experimental setup used to develop the different sediment transport formulae are listed in Table 3.1. The listed parameters were taken from U.S. Army Corps of Engineers (1998) and Van Rijn (1984a).

The overall grain diameter d or the mean diameter d_m gives the range in the grain sizes of the sediment used in the experiments. The variable U_m denote the average velocity, I the energy gradient and h the flow depth.

The listed parameters are not limiting factors. Hence, several sediment transport formulae have been applied successfully outside of the range of the experimental setup.

Table 3.1: *Parameters of the sediment transport formulae*

Sediment transport formula	d [mm]	U_m [m/s]	h [m]	I [%]
Engelund-Hansen (d_m)	0.19 – 0.93	0.20 – 1.93	0.06 – 0.41	0.0055 – 1.9
Meyer-Peter-Müller	0.4 – 29	0.37 – 2.87	0.009 – 1.19	0.04 – 2.0
van Rijn	0.32 – 1.44	0.36 – 1.29	0.2 – 0.73	–

3.5.1 Sediment Transport Formula Derived by Engelund-Hansen

Engelund and Hansen (1967) established the following sediment transport formula, based on the stream power concept of Bagnold (1966):

$$f' \Phi_t = 0.1 \, \Theta'^{5/2} \tag{3.14}$$

with

$$f' = \frac{2g}{C_h^2} \tag{3.15}$$

and

$$\Phi_t = \frac{q_{t*}}{\gamma_s \sqrt{(\gamma_s/\gamma_w - 1) g d_{m,f}^3}} \tag{3.16}$$

where f' is a friction parameter, Φ_t is the total-load transport rate per weight/time/unit width, Θ' is the dimensionless Shields parameter, γ_s is the specific weight of the sediment, C_h is the Chézy-coefficient, γ_w is the specific weight of the water and $d_{m,f}$ is the mean fall diameter of the sediment.

3.5.2 Sediment Transport Formula Derived by Meyer-Peter-Müller

The sediment transport formula derived by Meyer-Peter and Müller (1948) is one of the most widely used sediment transport formulae for alpine rivers, because of the range of sediment size and slope. The Meyer-Peter-Müller formula is a bed load formula and uses the approach of the critical shear stress.

$$\Phi_b = 8(\Theta' - \Theta_c)^{\frac{3}{2}} \tag{3.17}$$

with

$$\Phi_b = \frac{q_b}{\sqrt{(s-1)gd_m^3}} \tag{3.18}$$

where Φ_b is the dimensionless bed-load transport rate, Θ' is the dimensionless Shields parameter, Θ_c is the critical Shields parameter, which is 0.047 according to Meyer-Peter and Müller (1948) given in Equation 3.5, q_b is the volumetric sediment transport rate, and s is the specific density (ρ_s/ρ_w).

The formula derived by Meyer-Peter and Müller (1948) can be also found in the following form (Wu, 2008):

$$\frac{q_{s,b*}}{\gamma_s\sqrt{(\gamma_s/\gamma_w - 1)gd_m^3}} = 8\left[\frac{(k_{St}/k'_{St})^{\frac{3}{2}}\gamma R_h I}{(\gamma_s - \gamma_w)d_m} - 0.047\right]^{\frac{3}{2}} \tag{3.19}$$

where $q_{s,b*}$ is the sediment transport rate per weight/time/unit width, d_m is the mean diameter of the sediment mixture, k_{St} is the reciprocal of the Manning coefficient n_m of the channel bed and k'_{St} is the reciprocal of the Manning coefficient n'_m due to the grain roughness. The value k'_{St} can be calculated with

$$k'_{St} = 26/d_{90}^{\frac{1}{6}} \tag{3.20}$$

The $(k_{St}/k'_{St})^{\frac{3}{2}}$ is a roughness parameter, which takes the roughness of the bed forms into account. In the absence of bed forms, it is recommended to take $(k_{St}/k'_{St})^{\frac{3}{2}} = 1$; but $1 > (k_{St}/k'_{St})^{\frac{3}{2}} > 0.35$, if bed forms are present (Graf and Altinakar, 1998).

3.5.3 Sediment Transport Formulae Derived by van Rijn

The empirical bed load formula derived by Van Rijn (1984a) was developed for sand particles originally.

$$\Phi_b = 0.053D_*^{-0.3}\left(\frac{\Theta' - \Theta_c}{\Theta_c}\right)^{2.1} \tag{3.21}$$

where Φ_b is the dimensionless bed-load transport rate, Θ' is the dimensionless Shields parameter and Θ_c is the critical Shields parameter and D_* is the sedimentological diameter given in Equation 3.3.

The formula of Van Rijn (1984a) can also be written in the following form:

$$\frac{q_b}{d_m^{1.5}\sqrt{\frac{(\rho_s-\rho)g}{\rho}}} = 0.053\,\frac{\left(\frac{\tau-\tau_c}{\tau_c}\right)^{2.1}}{d_m^{0.3}\left(\frac{(\rho_s-\rho)g}{\rho\,\nu^2}\right)^{0.1}} \tag{3.22}$$

where $q_{b,i}$ is the volumetric transport rate of the fraction of the bed load (per unit width), d_i is the particle diameter, τ is the bed shear stress, $\tau_{c,i}$ is the critical shear stress, ρ_s is the density of the sediment and ν is the kinematic viscosity.

Van Rijn (1984b) also developed a suspended load formula.

$$c_{bed,i} = 0.015\,\frac{d_i}{a}\,\frac{\left(\frac{\tau-\tau_{c,i}}{\tau_{c,i}}\right)^{1.5}}{\left(d_i\left(\frac{\rho_s/(\rho_w-1)\,g}{\nu^2}\right)^{\frac{1}{3}}\right)^{0.3}} \tag{3.23}$$

where $c_{bed,i}$ is the concentration of the suspended sediments at the bed for the i^{th} sediment fraction, d_i is the diameter of the i^{th} sediment fraction, a is equal to the height of the center of the bed cell, τ is the bed shear stress, $\tau_{c,i}$ is the critical shear stress for d_i, ρ_s is the grain density of the sediment, ρ_w is the density of the water, g is the acceleration due to gravity and ν is the kinematic viscosity.

3.6 Sediment Transport in Meandering Rivers

A meandering river consists of pool and riffle sequences (Figure 3.5). The sections C-C and B-B show the typical pattern of the river bed in river bends.

The water flow and the sediment transport in river bends are influenced by the helical flow of the water. This process occurs due to the centrifugal forces accelerating water particles on the water surface, which are transported to the outer part of the river bend (Figure 3.6). Therefore, the pressure difference between the outer and the inner streamlines are balanced by the spiral motion the water flow in the river bend. The lateral components of this helical flow are called *secondary currents*.

Caused by the secondary currents in the river bend the sediment particles are slightly moving to the inner side of the river bend, where they deposit due to lower velocities, forming a point bar. This process is also associated with a lateral grain sorting. The sediment depositions forming the point bar consist mainly of finer sediment eroded at the outer river bend or at the river bed upstream and transported to the inner part of the river bend. This effect causes erosion at the outer part of the river bend. Hence, the transversal slope increases with greater scour depth and higher point bars and the cross section in the river bend becomes strongly asymmetric. At a certain transversal slope the gravity

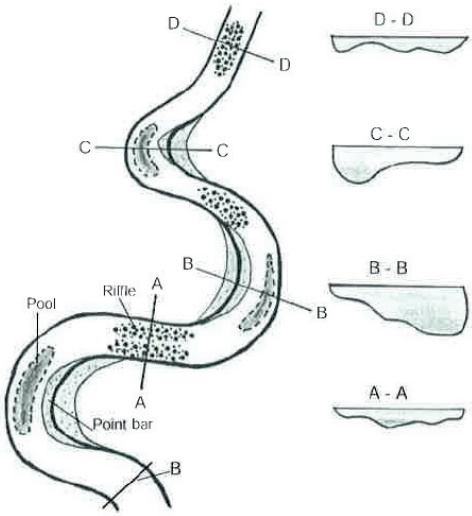

Figure 3.5: *Pool and riffle sequences in a meander system (Rüther, 2006)*

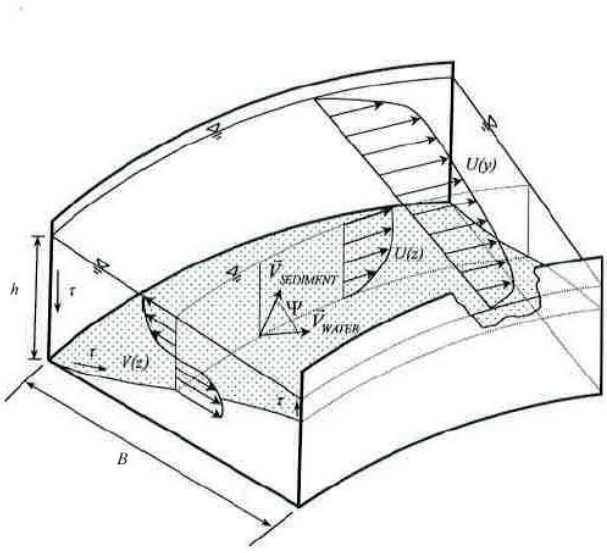

Figure 3.6: *Sketch of the flow direction $\overline{V}_{water}$ and of the direction of the sediment transport $\overline{V}_{sediment}$ in a river bend (Rüther, 2006)*

force acting on the sediment particle forces deflects the sediment particle. In this case the particle is no longer transported in the direction of the bed shear stress (compare Rüther, 2006). The deviation angle of the direction of the sediment particle to the direction of the bed shear stress is denoted with Ψ in Figure 3.6.

3.6.0.1 Influence of a Sloping Bed on Sediment Transport

The slope of the river bed and the river banks affect the sediment transport and the transported particle size in the river. Hence, the critical shear stress is modified in case of a sloping bed. A sloping river bed increase the sand transport rate in the downslope direction and reduce it in the upslope direction. Several formulas have been developed to take this effect into account.

In the formulae of Koch and Flokstra (1981) a correction factor for the magnitude is calculated to increase the downslope direction and reduce it in the upslope direction.

$$q_{b,1} = q_{b0}\left(1 - \beta\frac{\partial Z_f}{\partial s}\right) \tag{3.24}$$

where q_{b1} is the modified sediment transport rate, q_{b0} is the original sand transport rate, β is an empirical factor with a default value of 1.3, Z_f is the elevation of the river bed, and s is the coordinate in the current direction (EDF-R&D, 2010).

Brooks (1963) gives a formula for the correction of the critical shear stress in respect to a sloping bed. In this formula a correction factor K is applied to the critical shear stress (Equation 3.25). Figure 3.7 gives an overview over the parameters of the formula.

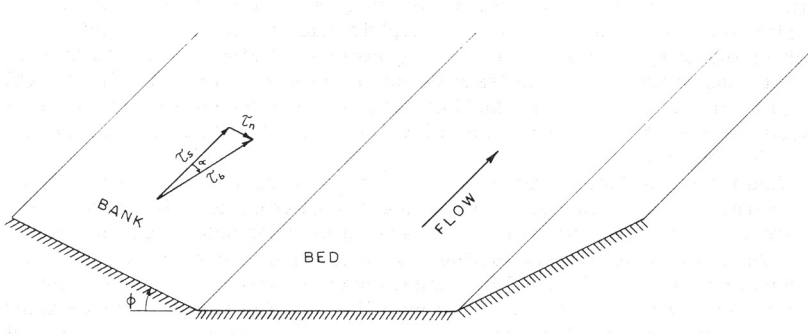

Figure 3.7: *Perspective view of the shear stress on a river bank (Brooks, 1963)*

$$K = -\frac{sin\phi\ sin\alpha}{tan\theta} + \sqrt{\left(\frac{sin\phi\ sin\alpha}{tan\theta}\right)^2 - cos^2\phi\left[1 - \left(\frac{tan\phi}{tan\theta}\right)^2\right]} \tag{3.25}$$

where α is the angle between the bed shear stress and the channel axis, ϕ is the angle of the side slope and θ is the natural angle of response of the sediment.

Sediment particles move in the direction of the bed velocity and the bed shear stress usually. However, if the river bed is sloping normal to the direction of the velocity vector (side slope), the sediment particle will also move in this direction caused by gravity.

Kikkawa et al. (1976) developed an approach to calculate the angle ϕ_s between the sediment transport vector and the velocity vector. In this approach ϕ_s is a function of the angle of the slope perpendicular to the direction of the velocity vectors (α_1) and the dimensionless shear stress τ_*.

$$\phi_s = \frac{0.6}{\sqrt{\tau_*}} tan\alpha_1 \tag{3.26}$$

The change in the direction of sediment transport can be also taken into account by using the formula of Koch and Flokstra (1981).

$$tan\alpha_2 = tan\delta - T\frac{\partial Z_f}{\partial n} \tag{3.27}$$

with the coefficient T, which according to Koch and Flokstra (1981), is depending on the Shields parameter Θ.

$$T = \frac{4}{6\Theta} \tag{3.28}$$

where α_2 is the direction of the sediment transport in relation to the flow direction, δ is the direction of the bottom shear stress in relation to the flow direction, n is the coordinate along the axis perpendicular to the flow and Θ is the Shields parameter (EDF-R&D, 2010).

3.7 Bed Forms

Bed forms are structures on the river bed, which are influencing the sediment transport. Bed forms in rivers results from complex sediment transport processes. The main parameters, which affect the bed form are the slope of the river bed, the flow depth, the flow velocity, and the grain size of the sediment. At low velocities, no motion of the bed occurs. With increasing flow velocities, the motion of the sediment particles is initiated and the sediment begins to move on the river bed and in suspension.

Bed forms are produced by the water flow over the river bed. They have an important feedback effect on the water flow and also influence the sediment transport. The bed forms can be classified in the bed forms of the lower flow regime, as with flat bed, ripples, bed load sheets and dunes, and the bed forms of the upper flow regime (Figure 3.8). In general the initial river bed develops with increasing flow velocities first ripples and then dunes. With further increasing flow velocities a transition phase with a plain river bed occurs, which is referred to as transitional bed. Finally standing waves and antidunes are formed.

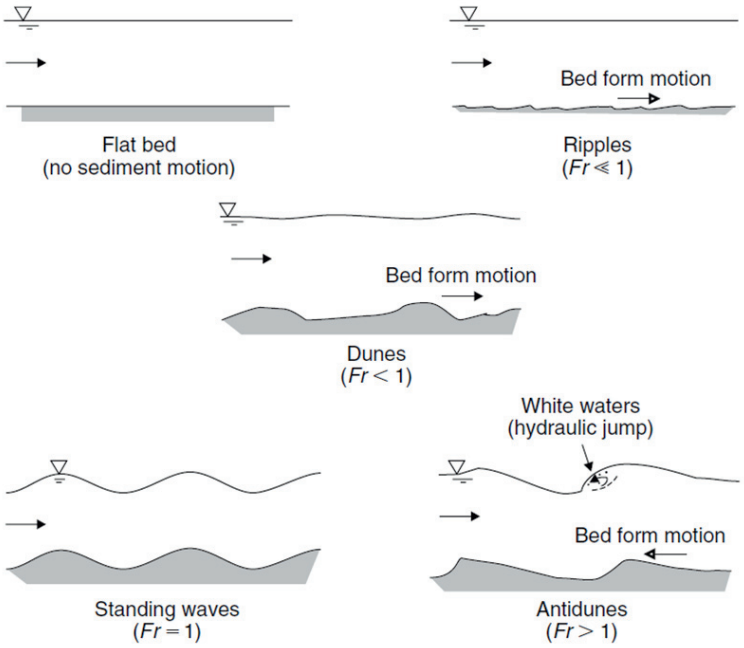

Figure 3.8: *Typical bed forms (Chanson, 2004)*

The development of bed forms depending on the sedimentological diameter D_* and the grain Reynolds number Re_* are summarized in Figure 3.9 (Vollmers and Giese, 1970). However, these diagrams are mostly based on laboratory data obtained in shallow flows over sand-size sediments. Consequently, a lack of experimental data for the transition from dunes to antidunes in sediments coarser than 5 mm exists (compare Carling, 1999). There is also a lack of experimental data concerning the development of bed forms in gravel bed rivers with wide grain-size distributions. The typology of the bed forms was developed for sandy sediments originally. These definitions are thus also applied here.

Carling (1999) extended the diagram after Allen (1984) with additional data from the literature (Figure 3.10). The diagram relates the non-dimensional mean shear stress Θ with the mean size diameter D. The effect of the relative depth and of the Froude number cannot be accommodated easily. This information is thus lacking in this diagram.

3.7.1 Bed Forms in Sediment Mixtures

The development of bed forms in sand beds has been widely studied in experimental flumes and rivers. In most experimental studies uniform sand grains were used. Carling (1999) found that the empirical diagrams developed for uniform sand grains can be extended up to coarse gravel. It has also been observed that the transitional bed might not develop in case of coarser sediment sizes. There is little information available concerning the effect of sediment mixtures on the bed forms at the transition or near to the transition between upper and lower flow regime.

Chang (1988) stated that the bed forms in gravel-bed rivers tend to be poorly developed and do not contribute significantly to the flow resistance. Núñez González and Martín-Vide (2010) found in flume experiments with sand, gravel and sand-gravel mixtures that bed form amplitudes *were higher the higher the sand content in the mixture was. In this*

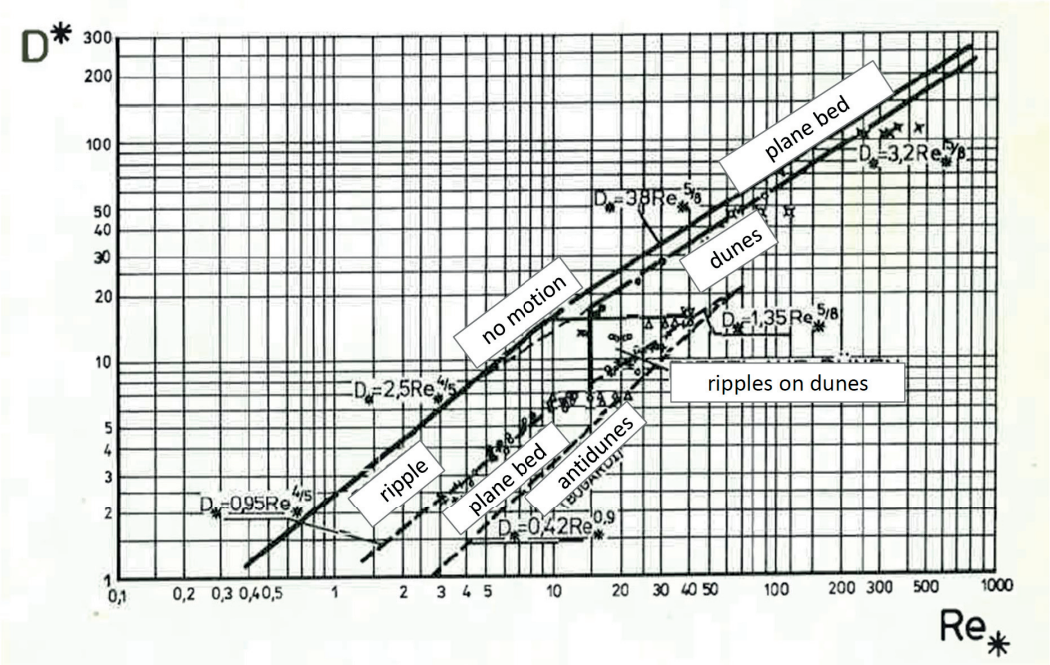

Figure 3.9: *Development of bed forms depending on the sedimentological diameter D_* and the grain Reynolds number Re_* (Vollmers and Giese, 1970, modified)*

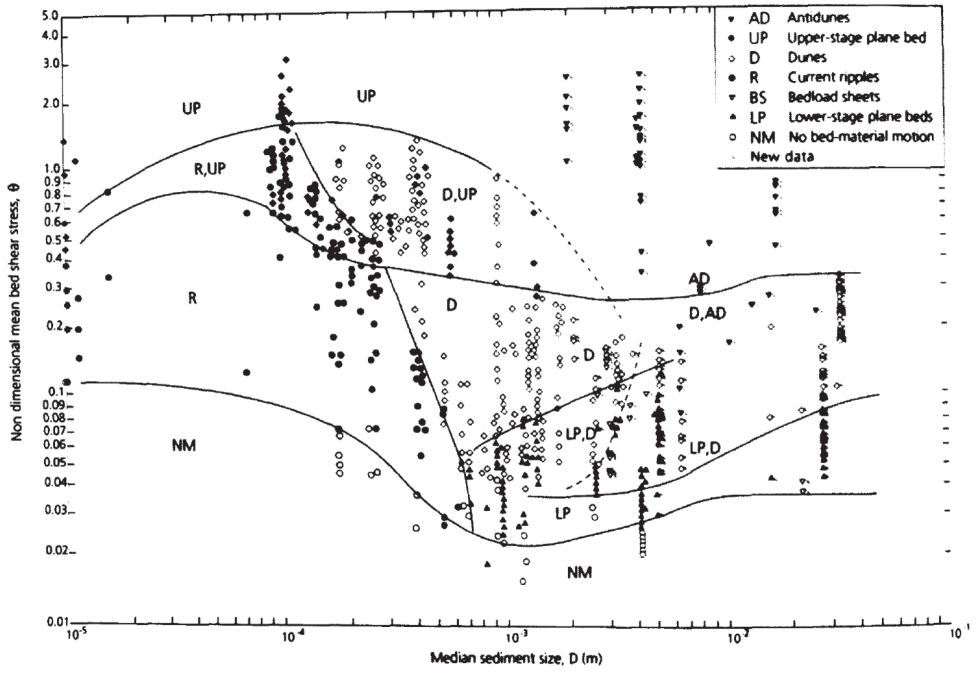

Figure 3.10: *Bed forms existence fields defined by the non-dimensional mean shear stress Θ and the mean diameter D (Carling, 1999)*

manner, amplitudes of sand bed forms were 3 to 5 times higher than in mixtures and gravel. Similar results were obtained by Tuijnder et al. (2010), who found that a small percentage of immobile gravel in the sediment mixture is able to limit the sediment supply. The bed forms, bed roughness and sediment transport are thus reduced. With increasing gravel content, the formed immobile layer becomes thicker and the limitation of sediment supply stronger. If the gravel content is higher than about 20 percent, the transport layer forms directly on top of the gravel layer (Tuijnder et al., 2010). Parker et al. (1982a) stated that in his experiments about the pavement of gravel bed rivers dunes and related smaller bed forms were entirely absent. He related this fact also with the bed shear stress conditions in gravel bed rivers. Even at bankfull conditions, the bed shear stress is rarely more than two or three times the critical value (Parker et al., 1982b).

According to Carling (1999) it is a common misconception that the bed forms in gravel, as with lower stage plane bed and upper stage plane bed respectively, these correspond simply with subcritical and supercritical flow. Theoretically, high Froude numbers exceeding 1.0 can be associated with the lower stage plane beds in gravel and shallow flows. As the relative depth increases the transition from dunes to the upper stage plane bed or antidunes can occur at Froude numbers progressively less than 1.0 (Carling, 1999).

As stated before, bigger bed forms such as dunes do not occur in case of grain sizes smaller than 0.2 mm (Zanke, 1982). Therefore, the shear stress due to bed forms is limited.

The range of the development of the bed forms and the influence of gravel is discussed in the following sections.

3.7.2 Lower Stage Plane Bed

When the critical shear stress of the sediment is reached, the sediment is first transported over the lower stage plane bed. Most of the available data used to define the lower stage plane bed are from experimental studies of fine gravel bed rivers with d_{50} less than 5 mm.

3.7.3 Ripples

Ripples occur in sand bed rivers with grain sizes up to 0.6 mm ($D_* \simeq 15$) (Zanke, 1982). Ripples migrate in downstream direction by erosion at the upstream face and deposition on the downstream side (Figure 3.11). The ripple length is proportional to the grain size or more precisely to the grain Reynolds number Re_* and less to of the water depth. The height Δ (up to a few centimeters) and the length λ (less than 0.6m) of the ripples are small related to the water depth (Carling, 1999). The water surface stays undisturbed in case of ripples.

3.7.4 Bed Load Sheets

Bed load sheets are low-relief bed forms and develop in sediment mixtures of coarse sand and gravel (d_{50} 2-5 mm). These bed forms may have a similar wavelength to dunes, but are poorly documented in well sorted gravels. Bed load sheets can grow in thickness resulting in asymmetric dune-like bed forms up to 0.10 m height. In pure gravel beds no sheets develop according to the flume experiments obtained by Iseya and Ikeda (1987) and Dietrich et al. (1989).

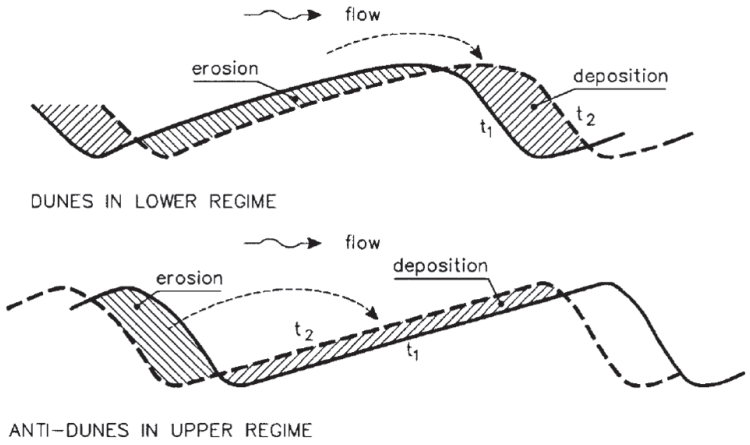

Figure 3.11: *Migration of bed forms in the lower and the upper regime (Van Rijn, 1993)*

3.7.5 Dunes

If the grain size is larger than 0.6 mm and the shear stress exceeds the critical shear stress, the sediment is transported over the flat river bed. With further increased shear stress, dunes are formed. According to Zanke (1982) dunes and other bigger bed forms do not occur in river beds with grain sizes smaller than 0.2 mm ($D_* \simeq 5$). The dimension of dunes are highly related to the water depth h. They are usually about 5-10 h (>0.6 m) long and 0.1-0.5 h (>0.1 m) high, but smaller dunes may also develop when dunes overlap with ripples. As dunes occur in the subcritical flows, the water surface is depressed above the dune crest and elevated over the dune trough (Carling, 1999). Dunes migrate like ripples in the downstream direction (Figure 3.11).

According to Carling (1999), who investigated data from the literature for sediments with a mean grain size larger than 2mm, dunes have been developed in flumes with median grain sizes up to 28.6 mm. In case of field conditions, data up to grain sizes of 60 mm are available. There is little data concerning the hydrodynamic development of gravel dunes available. Carling (1999) gives the Froude number with a range up to 0.75 and a non-dimensional mean bed shear stress (Θ) exceeding 0.1 as a guide for the development of gravel dunes. Dunes reach their maximum height at $\Theta = 0.25$. The dune height reduces again, if Θ exceeds 0.3. Froude numbers of 0.84 and higher lead to flattening of the dunes and dune diminution.

There are some formulas for the prediction of the bed form height available. In the formula of van Rijn (1987) the bed form height Δ is calculated.

$$\frac{\Delta}{h} = 0.11\left(\frac{d_{50}}{h}\right)^{0.3}\left[1 - e^{-\left(\frac{\tau-\tau_c}{2\tau_c}\right)}\right]\left[25 - \left(\frac{\tau-\tau_c}{\tau_c}\right)\right] \tag{3.29}$$

The van Rijn equation was developed for mainly uniform sediments. Hence, the bed forms will be smaller for non-uniform sediment mixtures.

3.7.6 Upper Stage Plane Bed

The upper stage plain bed may develop in the transition phase between the lower flow regime and the upper flow regime. After the flattening of the dunes in the lower flow regime in case of Froude numbers of 0.84 and higher, the upper stage plane bed can occur depending on the grain size distribution and other parameters. However, owing to lag effects described by Carling (1999), transitional bed forms have been recorded for Froude numbers near 1.

3.7.7 Antidunes

Antidunes develop mainly in supercritical flows. Antidunes may migrate short distances downstream, but they commonly migrate in the upstream direction (Figure 3.11). The antidune bed is normally separated from the dune bed by an upper stage plane bed. The transition state to an upper stage plane bed is narrow and well defined for relatively large flow depth, but little data exists for coarse sediments in shallow water. The critical Froude number for the development of antidunes in sandy river beds according to empirical data is 0.84. Antidunes may be replaced again by an upper stage plane bed in case of higher Froude numbers. However, again only little empirical data exists for this transitions in gravel beds (Carling, 1999).

3.8 Evaluation of the Effective Grain Shear Stress

Several formulae have been developed to describe the influence of the bed forms on the sediment transport. The most familiar ones are derived by Einstein and Barbossa (1952) and Engelund and Hansen (1972). Engelund and Hansen (1972) deduced the modification of the shear stress caused by bed forms by experiments. The total roughness can be divided into grain roughness and bed roughness (Equation 3.30).

$$\tau = \tau' + \tau''(+\tau''') \tag{3.30}$$

where τ is the total shear stress, τ' is the shear stress due to the grain roughness (skin friction) and τ'' is the shear stress due to the bed roughness and τ''' is the shear stress due to suspended sediments (Zanke, 1982). The shear stress due to the suspended sediments can be neglected in cases of lower suspended sediment concentrations.

Engelund and Fredsœ (1982) investigated the influence of bed forms on the distribution of the shear stress (Figure 3.12). In case of higher bed forms such as dunes, the shear stress due to the bed roughness increases and hence, the grain shear stress decreases.

Zanke (1982) stated that in his opinion not only τ' should be used in the sediment transport formula, because this value does not take the increased turbulence caused by the bed forms into account. These increased turbulences affect the sediment transport directly. According to Zanke (1982) the calculation of the sediment transport rates using the total bed shear stress τ gives more accurate results. Velocity measurements derived by Zanke (1982) also shows higher shear stresses over the bed forms.

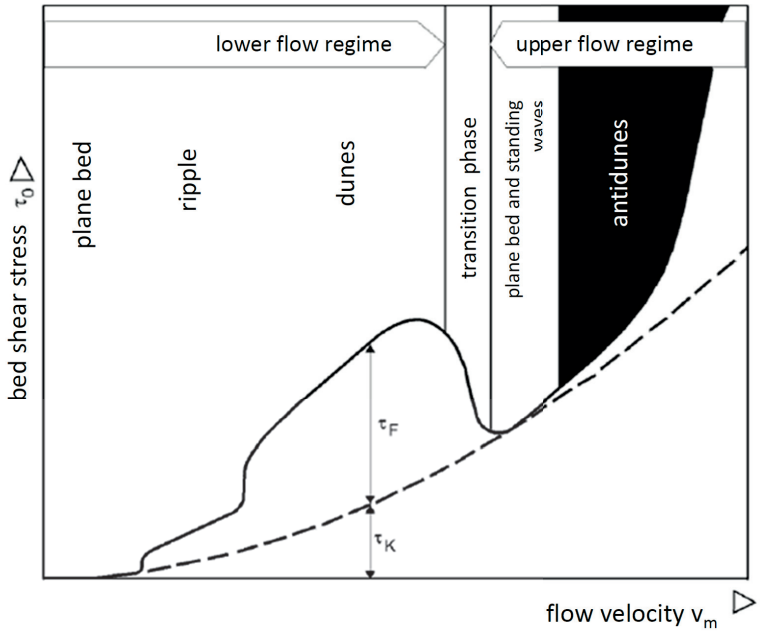

Figure 3.12: *Influence of the bed forms on the shear stress (Engelund and Fredsœ, 1982, modified)*

Van Rijn (1993) noted, *that a particle resting on the surface of a bed form will be set in motion by the friction force τ_c' or by the turbulent fluctuations in the eddy region downstream of the crest τ_c''. This means that the critical total shear stress τ_c is always larger when bed forms are present than when the bed is flat.*

The effective grain shear stress depend on the grain size distribution, the occurrence of cohesive sediments and bed forms. As a result it can be very difficult to determine the effective shear stress for the calculation of the sediment transport rates.

Van Rijn (1984c) developed an approach to calculate the total bed roughness:

$$k_s = 3.0\, d_{90} + 1.1\Delta\left(1.0 - e^{\left(\frac{-25\Delta}{\lambda}\right)}\right) \tag{3.31}$$

where d_{90} is a characteristic grain size, Δ is the bed form height and λ is the bedform lenght, calculated as $7.3h$.

3.9 Armoring of the River Bed

The armoring or the pavement of the river bed was investigated by many researchers. Both terms describe a thin, coarse surface layer with a large amount of finer sediment underneath. The main distinction between armor and pavement is that the former is associated with an immobile surface layer while the latter is associated with a mobile surface layer (Jain, 1990; Parker et al., 1982a).

The pavement of the river bed can often be found in graded rivers with poorly sorted gravel and is a result of a mobile bed response by which the river tends to equalize the relative mobility of the different grain sizes (Parker and Klingemann, 1982). In the pavement experiments of Parker et al. (1982a) the bed motion was almost entirely as bed load. At any time, only a small part of the surface grains were in motion, but the moving particles interchanged with the pavement constantly. However, grains in the subpavement layer were only rarely mobilized. In the experiments of Parker et al. (1982a) dunes and related smaller bed forms were entirely absent.

The armoring of the river bed is a natural process and occurs in gravel bed rivers with a wide range in the grain size distribution. The evolution of the armor and the pavement is shown in Figure 3.13. The eroded amount of sediments G increases with the shear velocity u_*. The critical shear velocity is too low to transport the larger grains in the river bed, but the fine sediment particles are carried away. Thus when the river bed is armored, the amount of eroded sediments decreases over time t and the grain size distribution in this top layer gets coarser than the river bed before the armoring occurred. The river bed stabilizes over time (Jain, 1990).

The armor evolution develops only in rivers with a wide range in the grain size distribution, which is typical for Alpine rivers. The bed load transport may decrease to zero at discharges, which are too low to destroy the armor layer. The coarse surface layer of the armored river bed will become mobile (pavement) and finally rip open when the critical shear stress of the coarser fractions is reached, e.g., in case of floods. After the rip open of the river bed, the sand fraction under the armor layer may be transported in suspension.

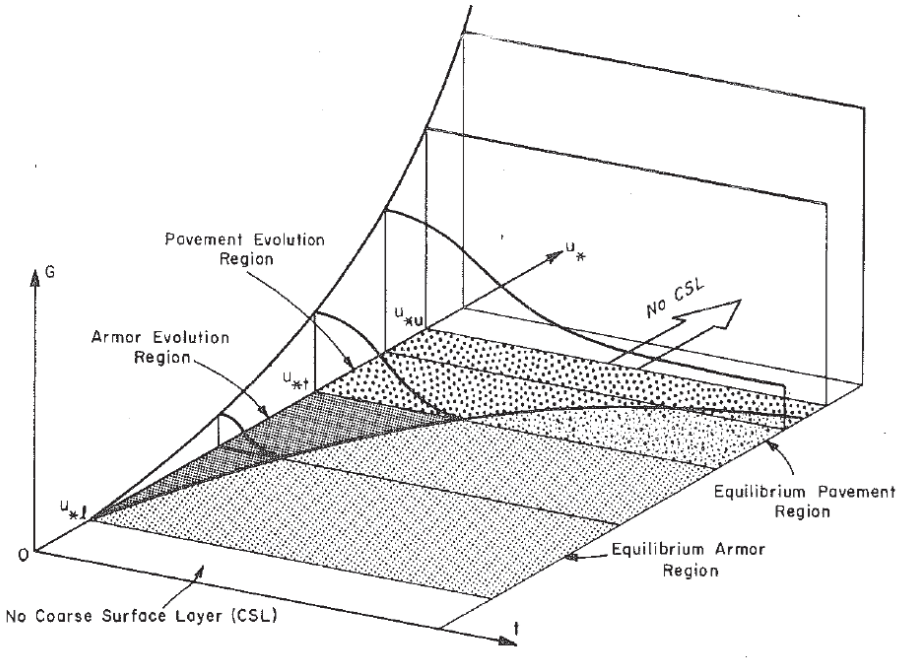

Figure 3.13: *Development of armor and pavement (Jain, 1990)*

A coarse surface layer can develop either by limiting the sediment inflow through the upstream section of the channel reach (e.g., Gessler, 1967) or due to varying bed shear

stress and a different relative mobility of the grain sizes, which lead to the evolution of the coarse surface layer (Parker and Klingemann, 1982). The processes of the armoring of the river bed in case of Alpine rivers were investigated by Badura et al. (2008) for the upper Mur river in Austria, who found similar results than Jain (1990).

3.10 Hiding and Exposure Effect

The initiation of motion of sediment particles depends on the current location of the sediment particle in the river bed. Smaller grains are often hidden by larger grains. Hence, these smaller particles will not move, although the shear stress of this particles is reached and the initiation of motion should occur theoretically. This effect is called "Hiding Effect". At the same time, larger grains are more exposed to the drag force of the water flow and peaks in the shear stress and will be transported over the river bed. Several formulae has been developed to take this effect into account.

Wu et al. (2000) developed a formula to calculate the effect of the hiding and exposure.

$$\eta_i = \left(\frac{P_{ei}}{P_{hi}} \right)_1^m \tag{3.32}$$

with

$$P_{ei} = \sum_{j=1}^{N} f_i \, \frac{d_i}{d_i + d_j} \tag{3.33}$$

and

$$P_{hi} = \sum_{j=1}^{N} f_i \, \frac{d_j}{d_i + d_j} \tag{3.34}$$

where η_i is the correction factor for hiding/exposure, N is the number of sediment fractions, f_i and d_i are the fraction and the grain size of the i^{th} sediment fraction and m is a constant equal to 0.6.

Egiazaroff (1965) developed a formula to determine the incipient motion of non-cohesive sediments by introducing a correction factor ζ_i as function of the non-dimensional grain size D_i/D_m.

$$\Theta_c = \eta_i \times 0.047 \tag{3.35}$$

with

$$\eta_i = \left[\frac{log(19)}{log(19 D_i/D_m)} \right]^2 \tag{3.36}$$

where Θ_c is the modified Shields parameter according to the hiding and exposure effect, Θ is the Shields parameter, η_i is the hiding/exposure factor, D_i is the grain size of the sediment class and D_m is the mean diameter.

Another formula was developed by Karim and Kennedy (1982), who used a correction factor to modify the sediment transport to take the hiding and exposure effect into account.

$$q_{s1} = \eta_i \times q_{s0} \tag{3.37}$$

with

$$\eta_i = \left(\frac{d_i}{d_m} \right)^{0.85} \tag{3.38}$$

where q_{s1} is the modified sediment transport rate according to the hiding and exposure effect, q_{s0} is the initial sediment transport rate, η_i is the hiding/exposure factor, D_i is the grain size of the sediment class and D_m is the mean diameter.

3.11 Initiation of Motion of Graded Sediment

Stelczer (1981) stated that the critical mean velocity of each sediment fraction in a graded river bed is almost identical to that for uniform sediment sizes. However, the initiation of motion of graded sediments can be affected by the hiding of smaller grains by the larger ones and the armoring of the river bed. These topics are discussed in Section 3.9 and 3.10. Graf (1971) stated that in case of graded sediments or river beds that contain cohesive sediments, the critical shear stress will be higher than predicted in the Shields diagram. Results from flume and field tests led Stelczer (1981) to the conclusion that the movement of graded sediments is controlled by the particle size around d_{80}. Smaller sediment fractions as well as the larger ones are set into motion almost simultaneously at the same critical shear stress than the d_{80}-fraction. Therefore, this fraction tends to shield the smaller fractions, whereas the large ones seams to get also in motion if the surrounding sediment fractions are moving.

3.12 Erosion of Cohesive Sediment

In the case of silt, clay or mud material in the river bed, cohesive forces between the sediment particles become important. Sediment mixtures with a fraction of clay particles larger than about 10 percent (Van Rijn, 1993) have cohesive properties because of electrostatic forces acting between the particles. Consequently, the sediment particles do not behave as single particles. They tend to stick together forming flocs. The size and the settling velocity of the flocs is much larger than the size or the settling velocity of the individual particles (Van Rijn, 1993). The cohesive forces cause an increase of the critical shear stress. Depending on the amount of silt or clay particles, this effect can be more or less important. Several researchers (e.g., Kamphuis and Hall, 1983; Mehta et al., 1989;

Berlamont et al., 1993; Kothyari and Jain, 2008, 2010) investigated the influence of silt and clay particles on the critical shear stress or the erosion rates of cohesive sediments.

An important factor governing the erodibility of cohesive sediments is the consolidation rate. Fresh cohesive depositions have a very loose texture of silt particles or clay flocs, which have a low density. In this stage the cohesive forces in the depositions are still very low. Erosion occurs readily as a result. When the sediment depositions are not eroded again, the consolidation increases the bulk density and the critical shear stress. Older, compacted sediments are highly resistant against erosion (Van Rijn, 1993).

The evaluation of the critical shear stress of the cohesive sediments in Alpine reservoirs are presented in Chapter 7.

4 SEDIMENT MANAGEMENT METHODS

Reservoir sedimentation is a common problem in dam engineering today. At any reservoir where a sustainable long-term use is required, it will be necessary to manage sediments as well as water (e.g., Morris and Fan, 1998).

Traditionally, reservoirs have been designed and operated with the assumption of a usable life of about 100 years, which will eventually be terminated by sediment deposition in the reservoir. The reservoirs have often been planned with a large volume of dead storage, which provided enough space for the sediment depositions of 20 - 40 years. Usually little thought was given to the fact that the reservoirs would have to be replaced, if the storage is lost. The assumption was always made that someone else in a future generation, will find a solution for the sedimentation problem. However, reservoir sedimentation is an increasing problem worldwide. Sediment management in reservoirs is not longer a problem that can put off to be dealt with in the future; it has become a contemporary problem. Traditional approaches of sediment management have not taken into account the need for a sustainable sediment management (Morris and Fan, 1998).

The implementation of a successful sediment management needs appropriate knowledge of the sedimentation and erosion processes in reservoirs. However, every reservoir is unique regarding the purpose, the geometry, and other boundary conditions like hydrological and hydraulic conditions. Consequently not every management method is suitable for every reservoir. An overview of reservoir management methods is given in this chapter. The success of the different management methods is often investigated using theoretical approaches and physical models. However, all theoretical approaches and physical models may contain uncertainties or scaling effects. Therefore it is important to include a sensitivity analysis in the investigations of the reservoir management methods. There is a large amount of literature available concerning sediment management methods, e.g., Morris and Fan (1998); Batuca and Jordaan (2000); White (2001) or Atkinson (1996), the focus here is on the principles behind the problems of reservoir sedimentation and on large storage reservoirs. The sedimentation problems in reservoirs of river power plants, which have often a small ratio between initial storage volume to annual mean inflow (C/I-ratio of 10^{-2} to 10^{-5}) are handled in the literature of lesser significance.

Several projects have been carried out to develop reservoir management tools. An example of a reservoir management tool is the Rescon model (Palmieri et al., 2003; Kawashima et al., 2003). This model was developed using the knowledge gained from several Chinese reservoirs. Hence the Rescon model should be used with caution for other reservoirs.

The use of physical models has been state-of-the-art for several decades for the modeling of reservoir sedimentation and flushing processes. However, in case of fine or cohesive sediments the application of physical models is limited by the model scale.

4.1 Purpose of Reservoirs

Reservoirs are often designed with more than one function. Multiple functions are the general rule, especially in the case of large dams. This multiple functions may create problems in the management of the reservoir, because the targets of these multiple functions may differ. The purposes of a reservoir may limit the usable strategies in terms of sediment management.

Some of the intended purposes of reservoirs are listed below:

- Flood protection and flood control
- Irrigation (agriculture)
- Drinking water supply
- Electric power generation including pumped-storage operation
- Water level increase during low flow periods (navigation, cooling water)
- Groundwater enrichment
- Sedimentation basins (suspended particles, bed load)
- Stabilization of the stream or river bed (gradient reduction)
- Leisure and recreation
- Fishing
- Tourism projects

Reservoirs are intended to store inflow for a certain period - on a daily, monthly, seasonal or year-to-year basis - to bring about a temporal and quantitative balance between water yield and water requirements as well as to control the flow regime. Resort is made to the stored water during periods of insufficient flow for the purposes of electricity generation, drinking water supply or supply to waterways. Retention of flood flows through storage may prevent inundations, and disastrous droughts may be avoided, or at least mitigated, through irrigation (Bechteler, 2006).

4.2 Choosing a Sediment Management Method in Reservoirs

Not all sediment management methods can be applied in all reservoirs or catchments. The measures should be designed and implemented according to the aspects of water resources management, ecology and economy as well as technical feasibility. Each reservoir has different specification and the sediment management methods have to be designed to suit each specific case. The natural sediment concentrations for example varies depending on the catchment and the hydrological conditions. Hence, a definition of standard limits (sediment concentration, oxygen concentration, chemistry, duration of a measure, flow etc.) is not appropriate, because the special conditions in the reservoir and downstream

has to be taken into account (e.g., ecosystem and fish habitat). As mentioned before, the multiple functions of a reservoir may also limit the sediment management methods that can be applied for it.

Atkinson (1996); Shen (1999) and White (2001) defined some main parameters, which influence the feasibility and the efficiency of sediment management methods in reservoirs. The design and assessment of a sediment management measure should be planned with respect to these main parameters.

An overview over these parameters is given below:

- Type, geometry and configuration of the hydro power plant, the reservoir and the tailwater section (flood protection of urban areas)
- Main purpose of the reservoir
- Legal aspects
- Ratio of maximum usable storage volume/inflow
- Maximum outlet discharge and minimum draw-down of the water level
- Forecasted duration of the flood and minimum flood forecast time
- Allowed water level lowering per hour
- Discharge
- Bed shear stresses in the reservoir
- Season of the event
- State of sedimentation - grain-size distribution of the sediment
- Possible duration of the measure/event
- Substances contained in the water and sediments (organic, anorganic, oxygen, toxic etc.)
- Solids concentration

Beside these parameters, additional parameters designed to suit the investigated plant may be needed, like morphology and type of land use in the catchment area, coordination with upstream and downstream riparian areas. In case of toxic contamination of the sediment depositions the allowed sediment management methods may be limited by the public authorities. In extreme cases, the toxic sediment has to be disposed of as hazardous waste.

4.3 Sedimentation in Reservoirs

There are three main processes in reservoir sedimentation:

- Reduced transport of coarse solids as bed load
- Transport of fine fractions in the form of a density current
- Transport of fine fractions in a stochastic distribution

The resulting sedimentation patterns mirror these topics. It is therefore essential to know the processes determining the sedimentation in order to choose the adequate measures.

Three sedimentation zones can be distinguished along the longitudinal section of a reservoir (Morris and Fan, 1998) (Figure 4.1):

- *Upstream portion ("topset bed")* - In the topset bed the coarser sediments are usually deposited. However, depending on the morphology of the delta, finer and very fine sediment depositions may be also found there.
- *Middle portion "foreset bed")* - The foreset bed is actually the head of the delta, which is characterized by an increasing longitudinal gradient along with decreasing grain sizes.
- *Downstream portion ("bottomset bed")* - The bottomset bed is the area next to the dam structure, where usually the finest particles are deposited. These sediment particles are carried by the density currents and stochastic transport processes in this area. The provision of additional dead storage can create additional volume and thus help to reduce the sedimentation problems in the reservoir.

4.4 Sediment Management Methods

Every reservoir has different specifications and different functions. The sediment management methods must thus be designed to suit each specific case. Flood management approaches and sedimentation problems vary widely from site to site. Due to the complexity of flood and sedimentation processes governed mainly by hydrological, geologic, topographic and geographic characteristics, neither an all-embracing description of the problem nor an analytical approach exits to predict or manage sedimentation processes accurately. The most promising way to face the occurring problems is to study specific sites with their conditions and best practice examples. One example of a combination of different sediment management methods for a river reach is given in Schöberl et al. (2005) for the river Drau near Lienz in Austria.

The measures against reservoir sedimentation can be divided into three groups, which are deposition control, removal of deposited sediments and compensation of reservoir silting (Batuca and Jordaan, 2000). These measures are schematically presented in Figure 4.2.

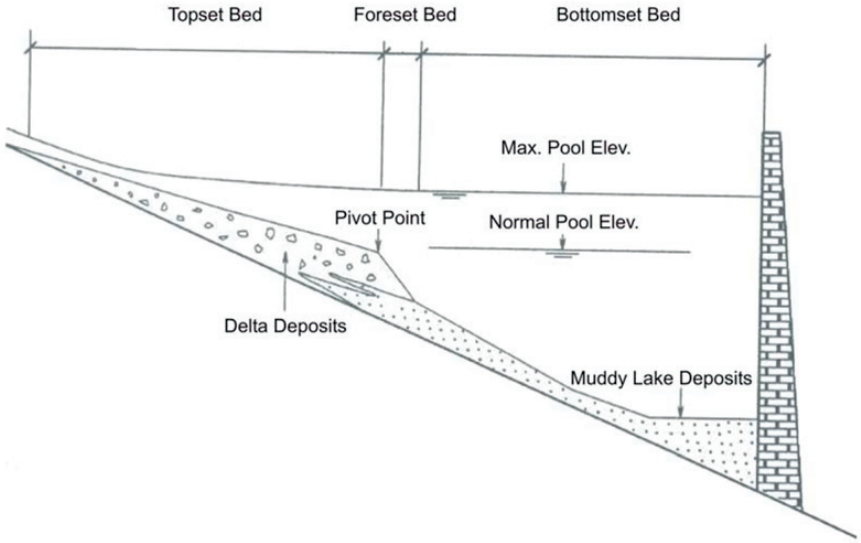

Figure 4.1: *Deposition zones in the longitudinal section through a reservoir (Morris and Fan, 1998)*

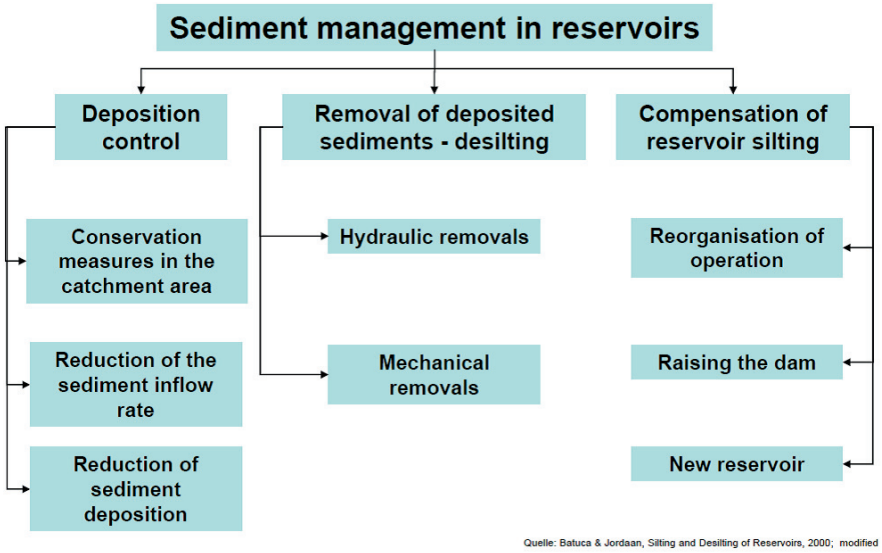

Figure 4.2: *Sediment management in reservoirs; modified after Batuca and Jordaan (2000)*

4.5 Deposition Control

Deposition control includes all methods to limit the erosion in the catchment and in the tributaries, the reduction of the sediment inflow rate into the reservoir and the reduction of the sediment depositions in the reservoir (Figure 4.3). These practices could be either independently or better jointly applied in the river catchment, in the reservoir basin and at the dam site.

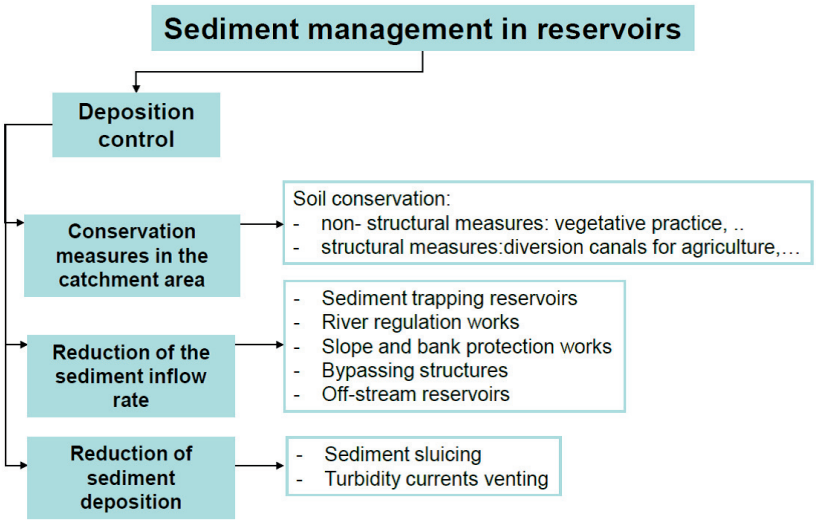

Figure 4.3: *Deposition control in reservoirs; modified after Batuca and Jordaan (2000)*

4.5.1 Conservation Measures in the Catchment Area

The sediment yield coming from the catchment of a reservoir is the main source of reservoir sedimentation. The key parameters of the soil erosion are water, wind, ice, and also human activities. At global scale, the growth in population intensify the change in land cover. In many parts of the world, increased population can also lead to expansion of commercial land use, land use changes and exploitation of native forests. The annual erosion rate in the main catchments of Europe is estimated with 50 t/km^2 (Batuca and Jordaan, 2000). The erosion rates in different countries and at different catchments may vary by several magnitudes. A detailed discussion on sediment yield is given in Section 2.2. Soil erosion is a critical subject around the world. Some figures may help to illustrate this fact (Walling and Webb, 1989):

- Loss in agricultural land since the beginning of organized agriculture: 530 million hectares
- Annual loss in agricultural land due to soil erosion: 3 million hectares
- Annual loss in soil: approx. 33 billion tones
- Annual loss in soil resources: 0.7 percent

Erosion protection is the most effective conservation measure against reservoir sedimentation in the catchment area. Depending on the climate conditions, surfaces should be protected by vegetation. Areas with vegetation have much lower erosion rates than areas without vegetation. Hence, grassing and afforestation works in catchment areas could be extremely effective in terms of soil stabilization and and soil erosion reduction (Batuca and Jordaan, 2000). *Unfortunately, these measures show their positive effect only in the long term. But they are also necessary to preserve valuable cultivated soils for agriculture and to provide protection against floods, mudslides and landslides. In vegetation-free catchment areas, such as the higher altitudes of Alpine catchment areas, erosion can only be prevented by technical means, such as stabilizing slopes, riverbeds and banks (Bechteler, 2006).*

Generally speaking, erosion protection in the catchment area should take priority over any other measures. Vegetation works are usually effective and inexpensive, but are not able to solve the sedimentation problem of reservoirs in its entirety. These non-structural soil conversation measures are recommended to be used combined with other reservoir management methods (e.g., Batuca and Jordaan, 2000; Morris and Fan, 1998).

4.5.2 Conservation Measures in and at Tributaries

Engineering structural works are frequently used to control steep tributaries in the catchment, like torrents or gullies. The following measures can be considered for this purpose; in many cases a combination of several approaches will prove most efficient and economic (Batuca and Jordaan, 2000; Bechteler, 2006):

- Stabilization of the banks
- Reduction of flow rate
- Training works / groynes
- Energy dissipation works
- Stabilization of the river bed
- Ramps
- Artificial riverbed widening

In most cases, the operator of a hydro power plant is not responsible for the catchment and the tributaries upstream of the hydro power plant. In this case the local or regional authorities may be responsible for the necessary conservation measures in the catchment area to reduce the sediment input in the rivers and to protect the soil in the agricultural or alpine area.

Some structural measures for the conservation and stabilization of the river bed are described in Section 4.8.

4.5.3 Reduction of the Sediment Inflow Rate

Measures to reduce the sediment inflow rate are usually sediment trapping reservoirs, river regulation works, slope and bank protection works, bypassing structures and off-stream reservoirs (Batuca and Jordaan, 2000).

Sediment Bypass - Flushing Tunnel - Sediment Routing Sediment bypasses are part of the sediment routing methods described by Morris and Fan (1998):*Sediment routing describes any method of influencing either the passage of the flow through the reservoir or its geometry or both, in order to make the sediment pass through, or bypass, the reservoir with minimum sedimentation*. Special importance should be given to the identification of the particularly sediment-rich inflow. Sediment routing should, however, not be confused with reservoir flushing, which remobilizes already deposited sediments by suitable methods, whereas sediment routing is intended to reduce or avoid sediment deposition in the reservoir from the start of the operation of the reservoir. Sediment routing largely maintains the natural solids flow in a body of water whereas flushing alters it significantly. However, these methods require a large inflow in relation to the reservoir volume in order to transport the sediment around or through the reservoir (e.g., Knoblauch, 2006).

Examples of sediment bypass tunnels are at the Nunobiki dam, the Asahi dam, the Miwa dam and the Matsukawa dam all located in Japan as well as the Palagnedra dam, the Pfaffensprung dam, the Rempen dam and the Runcahez dam located in Switzerland (Sumi, 2004).

For the design of a sediment bypass it is important to know, if bed load or suspended sediments cause reservoir sedimentation problems. Bed load bypasses certainly create the greater problems in design, because higher bed shear stresses are necessary to initiate the transport process and the abrasion of the bypass has to be taken into account. The This method will be chosen mainly in cases where the reservoir length is limited and provides a sufficient gradient to ensure transport along the entire length. A disadvantage is the often necessary steel lining of the tunnel, depending on the composition of the bed load (Vischer, 1987). Figure 4.4 is a schematic drawing showing the combination of an upstream debris dam with a bypass tunnel.

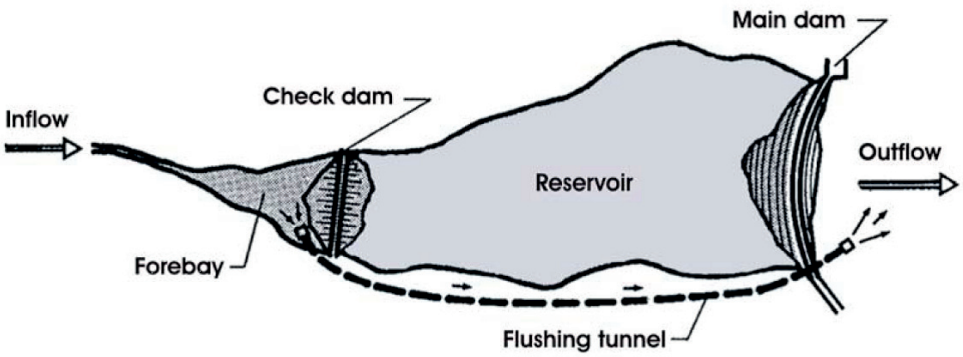

Figure 4.4: *Reservoir with upstream sedimentation basin that can be flushed through a tunnel ending in the river bed downstream from the dam (Vischer, 1981)*

Sediment traps - upstream debris dams Bed load retention basins, gravel traps as well as debris dams are used in torrents, gullies and mountain streams to prevent sedimentation in downstream sections in case of flood events. These basins practically intercept most of bed load material as soon as they fill with flood discharge. These basins have to be excavated periodically. Bed load retention basins have often only local impact on the transport capacity of a water body and retain only small amounts of suspended sediments usually. Sedimentation basins in the tributaries are similar to gravel traps in function. They may be pass-through or bypass basins, where the topography is conducive to a reduction in flow velocity. The maintenance requirements are the same as for gravel traps. They need to be continually evacuated in order to ensure their functionality (Bechteler, 2006).

Another possibility to reduce the sediment inflow rate is the provision of sand and gravel traps or sediment retention basins at the inflow or upstream of the reservoir. In these facilities, depending on the size, at least the coarse sediment fraction is deposited. The deposited sediments must be removed by mechanical means and may be re-introduced downstream of the dam. One example of a reservoir with a gravel trap at the inflow is the Sölk reservoir in Austria.

4.5.4 Reduction of the Sediment Deposition

The reduction of the sediment deposition in reservoir requires extensive knowledge about sedimentation processes in a certain reservoir. Measures to reduce the sediment deposition are mainly sediment sluicing and turbidity current venting (Batuca and Jordaan, 2000). It is also possible to build structures to reduce the sediment deposition in reservoirs. Most of these structures can be used to reduce the sediment deposition or enable the sediment transport through the reservoir in case of higher discharges.

Turbidity and density current venting Density currents are generally defined as stratified flows caused by differences in density. They develop if a fluid with higher density plunges in a fluid with lower density. A turbidity current is a special case of a density current and usually refer to stratified flows caused by differences in sediment concentration. Density currents can be observed in nature, e.g., at the inflow of the river Rhine in the Lake Constance in Austria. These turbidity currents in reservoirs can carry large amounts of sediments. Hence, they could be important for the sedimentation of reservoirs. Depending on the density conditions in the lake or reservoir, 3 different turbidity flow conditions can be observed (e.g., Morris and Fan, 1998):

- Top flow (overflow)
- Intermediate flow (interflow)
- Bottom flow (underflow)

The largest fraction of the sediments carried into a reservoir usually consists of suspended load (80 to 90 percent in the case of smaller and medium-sized reservoirs, 90 to nearly 100 percent in the case of larger reservoirs). Usually the bed load is of less significance for reservoir deposition, except in case of small Alpine reservoirs, where the flow velocities

are higher and a large part of the suspended load is transported through the reservoir also in case of normal flow conditions.

Large suspended sediment loads are transported in rivers during flood periods. The inflow from the catchment area is heavily loaded with fine sediments and has a higher unit density than the stored water in the reservoir. Normally, the entering sediment-laden water flow in the reservoir first pushes the clear lake water ahead until a state of impulse equilibrium is established. Then the denser and sediment-laden water flow dives under the less dense water in the reservoir. An underwater current develops, the so-called turbidity current, consisting of a mixture of water and suspended sediments. Physically, this turbidity flow could be compared to a loose-snow avalanche moving down the slope of a mountain. The turbidity current moves at considerable speed towards the dam within the former river bed, comes to a halt when reaching the dam and transforms into a so called submerged "muddy lake" (e.g., De Cesare, 2006; Schneider et al., 2012a). The barrier of the dam causes the suspended material to settle, which may influence the operation safety of the bottom outlets. *Depending on the gradient of the thalweg, turbidity currents may reach high velocities. This may remobilise already deposited sediments and carry them towards the dam. The introduction of additional fine sediments into the suspension increases the density of the turbidity current, which in turn increases its velocity. It slows down again in shallow sections so as to deposit sediments, which eventually leads to the disappearance of the turbidity flow (De Cesare, 2006).*

Turbidity flows are often the decisive process for the re-distribution of sediments within a reservoir. The probability of the occurrence of turbidity currents is a matter of correlation between hydrological and sedimentological conditions, as well of the topography of a reservoir, as e.g., its geometry. For the development of a turbidity current the reservoir has to be relatively short and straight with a substantial gradient and the valley should be V-shaped with steep slopes. The stability of turbidity currents also depend on the geometry, the slopes of the reservoir and on the difference gradient in the flow densities. Turbidity currents may be dissolved, either continuously or in an enforced and accelerated manner on their way down (Schneider et al., 2012b). The following conditions lead to the development of turbidity currents (e.g., Oehy et al., 2000; Schneider et al., 2012b):

- High concentrations of suspended particles in the inflow
- Lower temperature of the inflow than in the reservoir
- Greater water depths at the entrance of the inflow
- Nearly stagnant water in the reservoir
- Steep slope of the reservoir bed
- Pipe-shaped, straight reservoir geometry

These conditions are nearly always present in larger Alpine reservoirs (e.g., in storage or pump storage reservoirs) so that even minor annual floods may lead to the formation of turbidity currents. Figure 4.5 is a graph showing the maximum transportable grain diameter plotted against the flow velocity of the turbidity current (Morris and Fan, 1998).

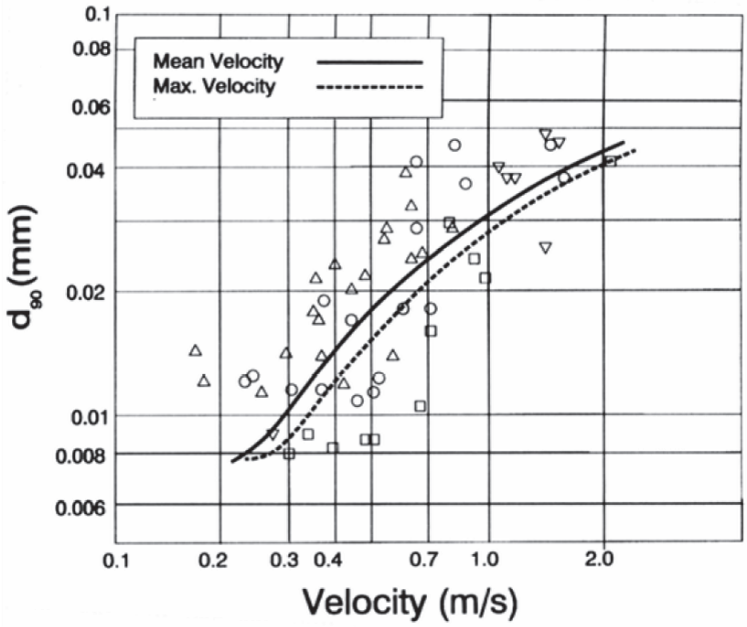

Figure 4.5: *Maximum transportable grain diameter versus flow velocity of the turbidity current (Morris and Fan, 1998)*

Typical turbidity currents may reach flow velocities of up to 0.5 to 0.8 m/s, with a maximum transported diameter between 0.01 and 0.03 mm (Figure 4.5). Turbidity currents normally occur during the annual flood events. Thus, they are the main cause for the transport of fine sediments along the thalweg of Alpine reservoirs to the dam. Whereas the sediment volume is small compared with the overall volume of the reservoir, the sediment deposition near the dam may affect the operation of the outlet works such as bottom outlet and power intake after a few years of operation (De Cesare, 2006).

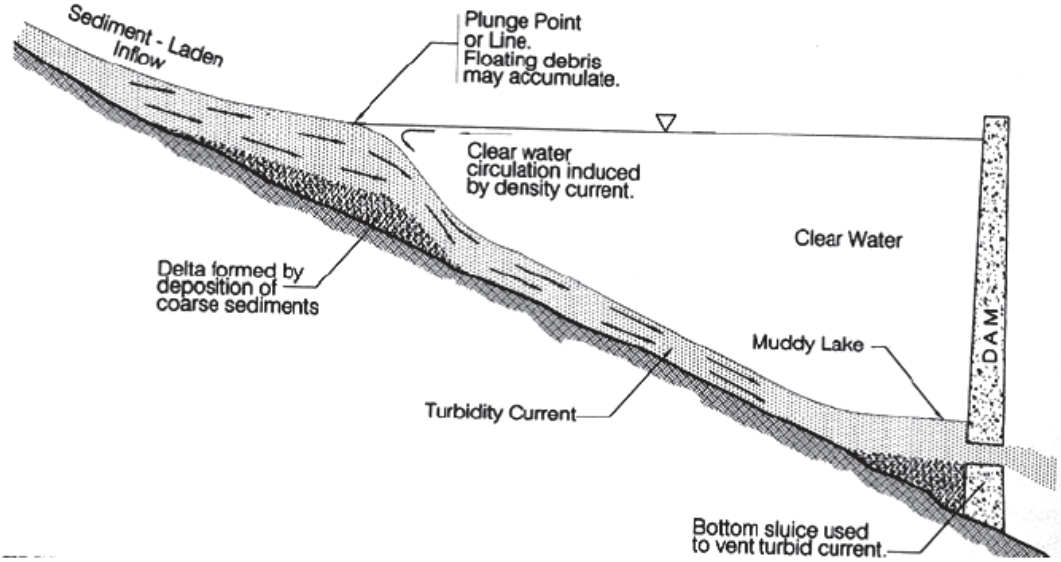

Figure 4.6: *Schematic representation of a turbidity current in a reservoir (Morris and Fan, 1998)*

In principle turbidity currents could be vented through a reservoir by opening the bottom outlets when the turbidity current reaches the dam (Figure 4.6). The advantage of the venting of turbidity currents is the desired reduction of sedimentation, the less frequent necessary variant of flushing, and the more ecological justifiable way to release sediments out of a reservoir (Schneider et al., 2012a). However, the location of the bottom outlets may limit the feasibility of turbidity current venting, if they are located to high at the dam.

Morris and Fan (1998) describe a successful venting e.g., at the Lost Creek reservoir in Oregon, USA, at the Steeg reservoir in Algeria, the Sefid-Rud reservoir in Iran as well as at the Sanmenxia reservoir in China. Further observations concerning density currents and turbidity currents are given in Batuca and Jordaan (2000); Cook and Richmond (2004); Bühler et al. (2004) and Molino et al. (2001), who did additional 2 dimensional numerical calculations. Firoozabadi et al. (2003) also used numerical models and compared the results with physical models. The venting of density currents resulted from temperature gradients at the Whiskeytown reservoir, California was observed by Knoblauch and Simões (2000). A lot of research in avoiding and scattering of turbidity currents was done by EPFL in Lausanne, Switzerland mainly at the Reservoir Luzzone and the Lake Lugano (e.g., Oehy et al., 2000; De Cesare and Schleiss, 2004). In the Sölk reservoir in Austria Schneider et al. (2007) used temperature, conductivity and turbidity as well as velocity measurements to detect inflowing and traversing turbidity currents even for very small “floods”. Schneider et al. (2007) also observed that the inflowing turbidity currents plunge at the head of the reservoir into deeper layers, flowing along the thalweg up to the dam and might be vented through the bottom outlet.

Finally, the venting and controlling of turbidity currents can reduce the sedimentation in reservoirs.

Sediment Pass-Through - Sediment Sluicing In the literature sediment pass-throughs are listed as part of the sediment routing methods (Morris and Fan, 1998) or as sediment sluicing (Batuca and Jordaan, 2000). According to Morris and Fan (1998) this term describes *any method of influencing either the passage of flow through the reservoir or its geometry or both, in order to make the sediment pass through, or bypass, the reservoir with minimum sedimentation.* This method should not be confused with reservoir flushing, which remobilizes already deposited sediments, whereas sediment sluicing is intended to reduce or avoid sediment deposition in the reservoir by sluicing high sediment laden flows through the reservoir. Sediment routing largely maintains the natural solids flow in a body of water, whereas flushing alters it significantly (Knoblauch, 2006).

Morris and Fan (1998) classify the following categories of sediment pass-throughs:

- Seasonal draw-down (partial or complete)
- Draw-down before floods through upstream gauge or hydrological forecast
- Density current venting

The seasonal partial draw-down is carried out during the flood periods, to use the high inflow rates necessary to reduce or avoid the retention of sediment in the reservoir. This

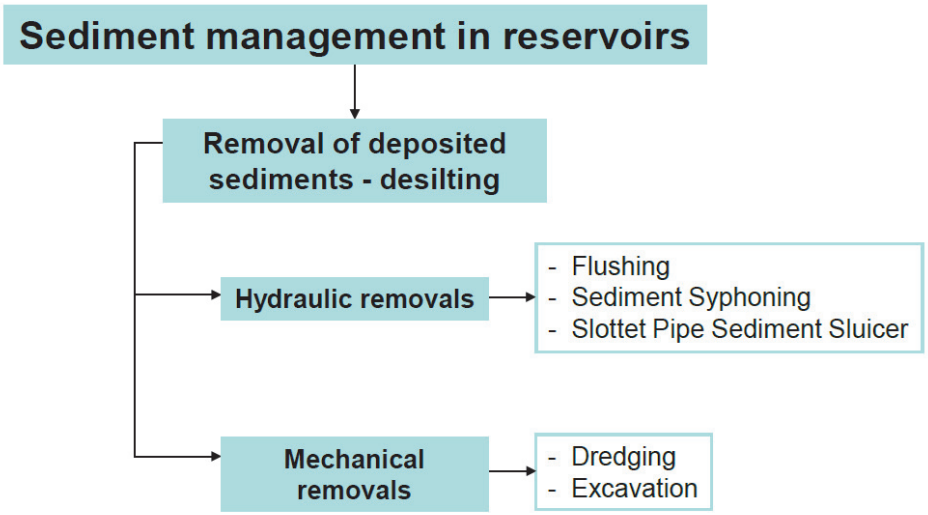

Figure 4.7: *Removal of deposited sediments; modified after Batuca and Jordaan (2000)*

method is practiced e.g., at many Chinese dams, Egyptian dams and dams located in India (Batuca and Jordaan, 2000). The largest part of the sediment load is carried into the reservoir during flood periods. The draw-down of the reservoir level increases the velocities, the turbulences and the shear stresses in the reservoir. The complete emptying of the reservoir produces effects similar to flushing. As a result a high percentage of the sediment load is sluiced through the reservoir. Short-term draw-down has the aim of passing through as much sediment as possible. The water-level draw-down can be controlled by upstream gauges for smaller reservoirs, and by hydrological forecasts based on precipitation-runoff models for large reservoirs. However, the coarsest sediment fractions will in most cases deposit in the reservoir (Knoblauch, 2006).

4.6 Removal of Deposited Sediments - Desilting

Once sediments are deposited in the reservoir, only retro-active or passive measures can be taken in order to remove them or to limit their negative effects. Sedimentation can be delayed or prevented by periodical removal of the deposited material. Figure 4.7 gives an overview of the different methods.

The removal of deposited sediments is one of the most challenging management tasks. Hydraulic removal of deposited sediments comprises sediment flushing and syphoning, whereas mechanical removal includes dredging and excavation of sediments. A very efficient measure is the flushing of the reservoir with the lowering of the water level until free flow conditions occur. However, flushing may cause ecological problems and sedimentation downstream from the dam.

The mechanical removals such as dredging or excavation, with a full reservoir or with the water level drawn down, from the banks or from boats can be applied in almost all reservoirs. Depending on the grain size of sediments and the depth to be dredged, suction dredgers or conventional, purely mechanical dredgers can be used.

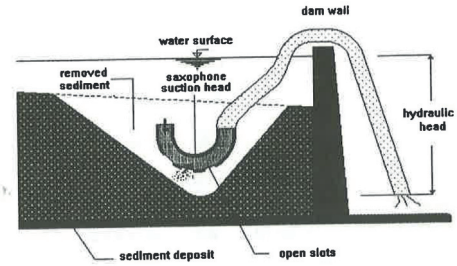

Figure 4.8: *Syphoning with a saxophone suction head (Lysne et al., 1995)*

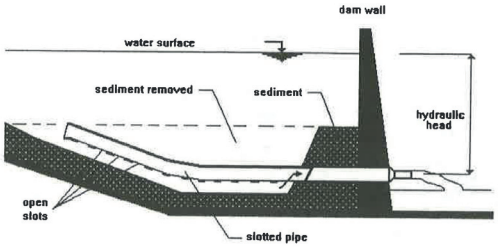

Figure 4.9: *Slotted pipe sediment sluicer (Lysne et al., 1995)*

4.6.1 Hydraulic Removals - Reservoir Flushing

Reservoir flushing is one of the most widely used approaches for the desilting of reservoirs (Scheuerlein, 1990; Atkinson, 1996). In case of reservoir flushing the sediment transport capacity in the reservoir is increased by lowering the water level at the weir. The gates or bottom outlets are opened to draw down the water level in the reservoir. The lowered water level leads to increased flow velocities, turbulence and bed shear stress in the reservoir. The increased shear stress facilitates erosion on the river bed in the reservoir and the turbulence keeps sediment particles in suspension (e.g., Morris and Fan, 1998).

Flushing can be distinguished from sediment routing by the fact, that flushing operations focus on the removal of deposited sediments, where as sediment routing focus on the pass-through of high sediment concentrations through the reservoir.

Reservoir flushing is discussed in detail in Chapter 5.

4.6.2 Syphoning of Sediments

Syphoning has a limited effectiveness and is usually practiced only for the local desilting of intakes or outlets (Batuca and Jordaan, 2000). Jacobsen (1997) investigated the syphoning and the sluicing of sediment. A special application of hydraulic removal is the suction of sediments by means of a piping system placed on the reservoir bottom. These pipes have special openings on the bottom side through, which the sediments are sucked in, when a valve is opened at the end of the pipe (SPSS - Slotted Pipe Sediment Sluicer). Due to the difference in height between the reservoir bed and the downstream river bed, no additional pump is required to suck the sediment slurry through the pipes (Jacobsen, 1997).

4.6.3 Mechanical Removals

Mechanical removal includes the removal of coarse and fine sediments by technical means without support from the drag of the flow. Mechanical removal measures are dredging or excavation. Dredging is an excavation activity carried out at least partly underwater. Dredging or excavation are among of the last methods resorted to when the conditions in the reservoir make other sediment management methods inefficient. Batuca and Jordaan (2000) stated, that dredging operations should be limited to small reservoirs or certain locations in a reservoir (e.g., at the intakes). Only in some cases dredging can be preferred to sluicing or flushing, because of its higher efficiency or the possibility provided for

dealing with overbank sediment depositions. The excavation or dredging of sediment depositions in reservoirs is usually the most expensive method. Normally it is also time consuming, involves transportation and disposal problems, including also environmental effects in the reservoir and downstream of the weir or dam.

The selection of the dredging method depends on factors like the volume of sediment deposition in the reservoir, the grain-size distribution and the location of the sediment depositions, the available disposal or reuse options, the water level in the reservoir, and environmental criteria. All these factors will influence the feasibility and the costs of the mechanical removal of the sediment depositions. All kinds of mechanical removal are costly because of the large sediment volumes involved and in most cases the difficulties involved in disposal. However, sometimes the excavation or the dredging of sediments is the only sediment management available (e.g., Morris and Fan, 1998). The dredging in reservoirs often focus on the removal of sediments near the intakes or the outlets. Morris and Fan (1998) mentioned that the dredging costs in the United States start at about \$2.50/m^3 and increase as a function of longer pumping distances, deeper dredging depth and increasing complexity of disposal.

Dry Excavation Dry excavation means that the sediments are removed from the sediment-filled reservoir area by use of conventional earthmoving equipment with a draw-down of the water-level and under low-flow conditions, while turbine operation is normally maintained. The advantages of this measure are the capacity and number of conventional equipment available enabling speedy and less expensive execution of the work. This measure allows the wide shallow-water areas to be drained temporarily; this can be done only during a low flow phase and may cause local high turbidity (Bechteler, 2006). Dry excavation is in most cases limited to the removal of coarse sediment deposited at the head of the hydro power plant.

Wet Dredging Wet dredging can be divided into suction dredging, which is also called hydraulic dredging, and any mechanical dredging using e.g., grab dredgers, scrapers, pontoon dredgers. In the case of suction dredging the removed sediments are pumped through pipes as slurry of water and sediments. Suction dredging can be carried out without the draw-down of the water level and not only at times of low flow, but also during medium flow conditions. In contrast to dry excavation, the area to be evacuated could be extend across the whole reservoir. The disadvantages compared with dry dredging are the lower efficiency and the limited choice of special equipment available. Also the grain size of the removable sediments is limited in case of hydraulic dredging. The additional transport equipment required to haul the sediments to the banks should also be mentioned (Batuca and Jordaan, 2000).

Re-Introduction of the Sediment in the Reservoir In case of large and wide reservoirs the sediment can be re-introduced in other parts of the reservoir (DWA, 2006). The sediment can be redeposited using special boats or pipelines. The artificial sediment depositions may be used to provide additional structures and shelters for aquatic life with protection against high flow velocities. However, the re-introduction of the sediment in the reservoir will not reduce the sedimentation rate.

Disposal The disposal of the dredged sediments can be a problem. In some cases the sediments can be used, e.g., for building material, final landfill or re-introduction down-

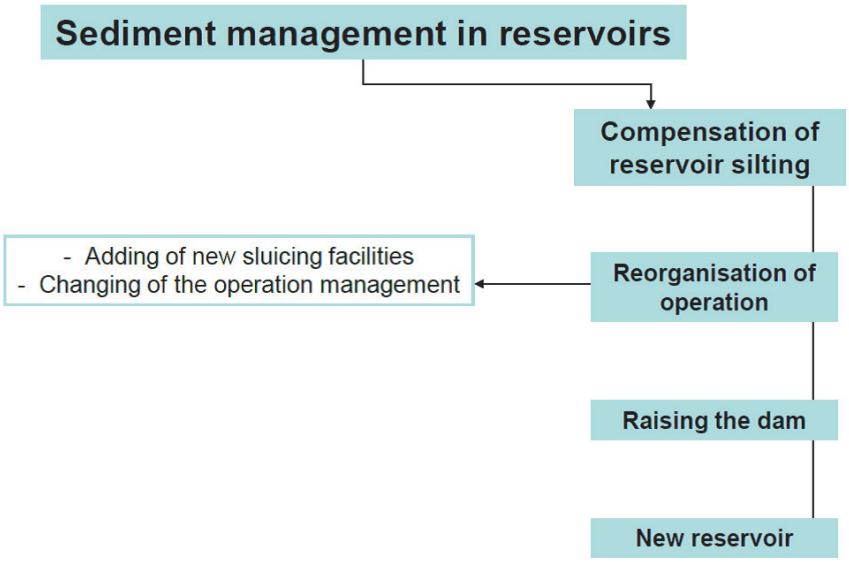

Figure 4.10: *Compensation of Reservoir Silting; modified after Batuca and Jordaan (2000)*

stream (Batuca and Jordaan, 2000). However, anthropogenic, chemical and organic fine fractions in the dredging can disqualify the material for the use as building material. Landfills cannot be seen as a long term solution due to the large volume of sediments, the lack of suitable sites and the unresolved problem of the bed load deficiency in downstream sections (Bechteler, 2006). The re-introduction of sediments further downstream should also be planned carefully to avoid increasing flood risk in these areas. The disposal of sediment can be complicated if the sediments are wet and need to be dried before transport, wood, root stocks or waste is contained in the sediments, some fractions of the sediment can not be used or if the sediment contains toxic substances (DWA, 2006). The processing of the sediment should be economically feasible.

4.7 Compensation of Reservoir Silting

A common measure used world-wide to maintain the usable storage capacity of a reservoir is to over-size its volume. This ensures sedimentation capacity for a certain period, typically about 50 years, where sediments can be deposited. Where not available for any other use, this space is termed dead storage (Figure 4.10).

4.7.1 Reorganization of Operation

The reservoir operation rules have a very significant influence on the sediment deposition pattern. A change in the operation rules can change the sediment deposition processes in the reservoir (e.g., Morris and Fan, 1998).

In some cases effective flushing is not possible because the outlet works of the dams are affected by sedimentation. Thus, the outlets have to be raised to a higher level in order to ensure effective operation. A recent project of this kind is the alteration of the bottom outlet and the water intake at the Mauvoisin dam (Hug et al., 2000; Schleiss et al., 1996). Pressure flushing normally creates a cone-shaped hollow whose slope corresponds to the friction angle of the deposited sediments only. If the outlet is already fully covered by

sediment depositions, the opening of the gates may cause the further consolidation of the sediment and prevent the erosion of the cone. This can be avoided by installing an injector shaft to introduce sufficient flushing water during the initial phase (Krumdieck and Chamot, 1981). Power intakes need to be combined with a flushing outlet placed immediately below to allow a cone to be washed out from the sediments (Hug et al., 2000; Schleiss et al., 1996).

In other cases the outlets may be too small for effective flushing operation. Additional outlets with sufficient design discharge must then be built.

4.7.2 Raising the Dam

If a large proportion of the usable storage volume has been lost to sedimentation, the heightening the dam may be a suitable solution. Such measures have been resorted at several dams in North Africa (Cornut, 1992). Raising the dam may also be a sensible alternative to the above measures in cases where reservoir sedimentation is beginning to jeopardize the flood safety of the surrounding areas (Bechteler, 2006). The raising of the dam to compensate for some lost storage capacity due to silting is in most cases one of the last options (Batuca and Jordaan, 2000).

4.7.3 New Reservoir

The abandonment (decommission) of a reservoir, which can no longer achieve its original designed functions, and constructing a new reservoir have similar functions to the above mentioned points (e.g., Batuca and Jordaan, 2000). But due to the high population density in Europe this approach is in most cases not viable. Also in other parts of the world the sedimented reservoirs cannot be replaced by new reservoirs at new sites indefinitely.

The decommission of dams is becoming more common in the United States as dams age and environmental concerns increase (USSD, 2012). The removal of a dam can be an alternatives to solve a specific problem at an existing facility, including dam safety concerns, high repair costs, high operation and maintenance costs, reservoir sedimentation or significant impacts on the aquatic ecosystem and water quality. The decommission and the full and partial removal of any type of dam requires the consideration of a variety of technical, environmental, social, and political issues (USSD, 2012). One example of the partial removal of a large dam in the United States is the Glines Canyon Dam. This dam was deconstructed between September 2011 and January 2012 (Figure 4.11 and 4.12).

Other examples of the decommission of dams are the Kernansquillec dam at the Léguer river, removed 1996, the Maisons-Rouges dam at the Vienne river, removed 1998, and the St-Etienne du Vigan dam at the Allier river, also removed 1998 (Aelbrecht, 2006).

The main arguments behind the removal and the decommissioning of dams are safety reasons, sedimentation problems and ecological aspects.

4.8 Optional Structures

Several optional structures can reduce the sediment supply from the catchment and the tributaries. Some structures like groynes or guide walls can also enhance the sediment transport through the reservoir during sediment sluicing or reservoir flushing.

Figure 4.11: *Glines Canyon Dam before deconstruction in September 2011 (USSD, 2012)*

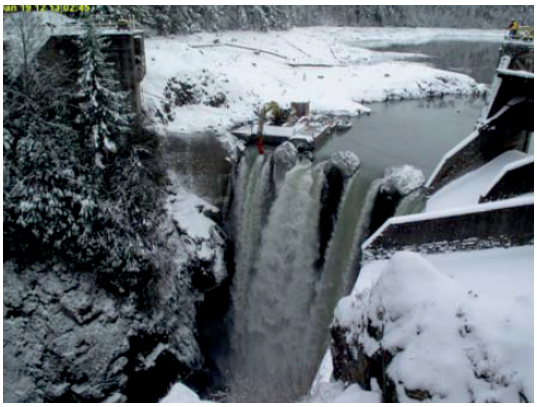

Figure 4.12: *Glines Canyon Dam after deconstruction in January 2012 (USSD, 2012)*

The following options are mainly cited from Bechteler (2006) and Batuca and Jordaan (2000).

4.8.1 Stabilization of the River Banks

The stabilization of the river banks is often required for flood protection and in most cases relatively economical. The stabilization also protects the land next to the river (e.g., agricultural area) from erosion. But it forces the stream in the river bed and the lack of the erodible sediment at the banks increases the erosion at the river bed.

4.8.2 Guide Walls

Guide walls are longitudinal structures usually introduced into wide flowing water bodies in order to concentrate sediment transport into defined main channel portions. They usually separate shallow zones from the line of maximum velocity in the reservoir and provide excellent shelters for aquatic life during floods. Subsequent installation in reservoirs already affected by sedimentation is difficult and expensive (Bechteler, 2006).

4.8.3 Training Works / Groynes

Groynes are lateral structures starting from the river banks and reaching into the river. They reduce the cross section of the river and increase the local bed shear stress and channel the water flow. Furthermore, groynes provide additional structures and shelters for aquatic life with protection against high flow velocities. Groynes can also be used to enhance reservoir flushing or sediment sluicing. In most cases groynes and training structures are relatively economical and may help to reduce the sedimentation at the head of the reservoir, in the tailwater or in free flow areas by increasing the drag forces. They can also be used to stabilize river banks in the upstream area of the reservoir. A stable construction is needed, especially of the head of the groyne, to avoid the destruction in case of medium to higher floods (DWA, 2006).

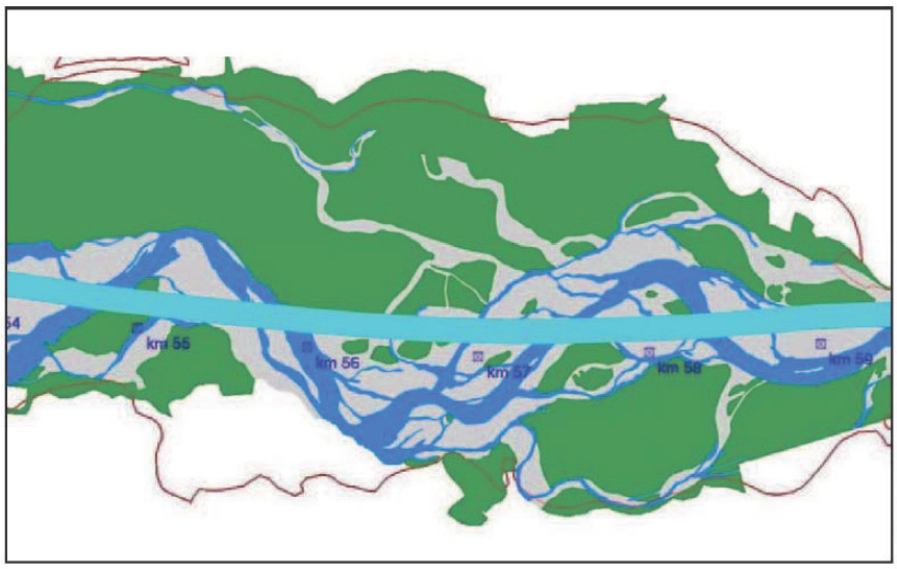

Figure 4.13: *River Salzach before the regulation works in1817 and nowadays (graphics by Wasserwirtschaftsamt Traunstein in Hopf (2006))*

4.8.4 Energy Dissipation Works / Ramps

Ramps and energy dissipation works may be required to stabilize the river bed in critical sections, for example near bridge piers. Ramps and energy dissipation works are also in most cases relatively economical. They can be constructed in a way, which enables the passage of aquatic life up- and downstream and facilitate sediment transport.

4.8.5 Stabilization of the River Bed

A balanced and stabilized river bed is sustainable, but the stabilization could be very difficult depending on the grain size and the sediment inflow.

4.8.6 Artificial River Bed Widening

An artificial river bed widening is sometimes required for flood protection, in most cases relatively economical, and at least the coarse sediment is deposited. However, the widening of a river bed requires area and space and it takes a longer time period to stabilize the river bed again.

One example for the application of optional structures are the rehabilitation works at the river Salzach in Austria. The degradation of the river bed at the “Untere Salzach” was caused by regulation works in the river reach at the beginning of the 19th century, which increased the bed slope and decrease the width of the river bed (Figure 4.13). The river bed of the “Untere Salzach” lays in a layer of quaternary gravels with fine grained lacustrine clay under it. Due to the degradation in the last centuries, the gravel layer has decreased and has even vanished in some areas. Now there is thus a huge risk of a sudden and unforeseeable severe further degradation of the riverbed, which consists of a fine clay layer with a very low critical shear stress (“Sohldurchschlag”). This “Sohldurchschlag” happened several times in the last decades, the last time during a flood event in August 2002 over a length of several kilometers with regional erosion rates of several meters.

To stop the erosion and to achieve a dynamic equilibrium of the system a rehabilitation concept has been developed, which also causes a significant ecological improvement. The main aspects of the the rehabilitation are the widening of the river bed and the installation of ramps and groynes (Spannring, 2012).

5 RESERVOIR FLUSHING

Reservoir flushing is one of the most widely used approaches for the desilting of reservoirs (Scheuerlein, 1990; Atkinson, 1996) as stated in Chapter 4.6. In general, reservoir flushing involves the lowering of the water level at the weir by opening the weir gates or low-level outlets. The lowered water level increases the bed shear stress in the reservoir and facilitates erosion on the river bed in the reservoir (compare Morris and Fan, 1998).

Flushing can be used to reduce or to limit the sediment depositions in a reservoir and has been successfully applied in several reservoirs. Batuca and Jordaan (2000) and White (2001) listed reservoirs all over the world with successful applied flushing strategies.

The periodical flushing of sediments from reservoirs has many advantages from a river-morphological as well as economic point of view. The connectivity of river systems is also in terms of sediment transport important for the ecosystem of the downstream area. This type of desedimentation is most effective in the case of sufficient discharge and free surface flow in the reservoir. Therefore, reservoir flushing is normally performed during natural floods or higher discharges.

Atkinson (1996); White (2001) and others describe successful flushing events. An extreme example is the Mangahao reservoir in New Zealand, where 57 percent of the original storage volume of the reservoir was lost in the first 34 years of operation. At the first flushing event approx. 75 percent of the deposited sediments were removed during one month. In this case, the sediment concentrations at the outflow can be very high and can create unacceptable impacts on the ecosystem downstream of the reservoir.

In the case of Alpine reservoirs of river power plants the storage volume is small compared to the mean annual inflow. Hence, the time interval between the flushing operations should be short enough to limit the sediment deposition in the reservoir. If there is a chain of power plants in the river, the coordination of the flushing operation of the different reservoirs is very important. The draw-down of the water levels and the refilling of the reservoirs has to be coordinated to prevent the deposition of sediment flushed out of one reservoir in the next downstream located reservoir. The problems occurring by flushing of chains of power plants are discussed in Badura (2007).

5.1 Kinds of Flushing

A main factor in reservoir flushing is the possible draw-down of the water level in the reservoir. Therefore, the water-level in the reservoir is often used to describe the different flushing methods:

- Without draw-down of the water level
- Partial draw-down of the water level (also referred to as “soft flushing”)
- Full draw-down of the water level

The efficiency of flushing processes depends on the ratio of the inflow to the reservoir volume and on the draw-down of the water level. Flushing can also be efficient without the draw-down of the water level, if the inflow is high compared to the reservoir volume. The lowering of the water level is often necessary to increase the success of the reservoir flushing. Generally flushing operations should be carried out under free-flow conditions (with full draw-down of the water level) rather than under pressure conditions (Batuca and Jordaan, 2000). The free flow conditions should be kept as long as possible to ensure the transport of sediment through the reservoir.

5.1.1 Flushing without Draw-Down of the Water Level

Flushing without draw-down of the water level is also called pressure flushing. Pressure flushing can be effective in two cases:

- A large inflow compared to reservoir volume can increase the bed shear stress in the reservoir and hence, remove the deposited sediments. Otherwise the sediment is removed only close to the outlets forming flushing cones.
- The approach of reservoir flushing without draw-down of the water level can be combined with the density current venting (Morris and Fan, 1998; Batuca and Jordaan, 2000).

Flushing without draw-down of the water level can occur at flood event if the lowering of the water level in the reservoir is not allowed due to regulations of local authorities or limited by the other purposes of the reservoir. A prevention of such a flushing operation is not possible generally (DWA, 2006).

5.1.2 Flushing with Partial Draw-Down of the Water Level

In the literature flushing with partial draw-down of the water level is also called “pressure flushing” and “soft flushing”. The partial draw-down of the water level move the head of the reservoir towards the weir. Thus, the velocities are increased mainly in the upper part of the reservoir, where the water depth is lower. This kind of flushing is performed if the bottom outlets are constructed as high level outlets, the capacity of the outlets is limited or if local regulations limit the draw-down of the water level (Haun, 2012). However, in the

literature flushing with partial draw-down of the water level is often stated as inefficient (Mahmood, 1987; Fan and Morris, 1992; Atkinson, 1996; Morris and Fan, 1998). In most cases quoted in the literature erosion occurred only close to the flushing gates (White and Bettess, 1984; Batuca and Jordaan, 2000). Most of these stated cases are reservoirs impounded by dams with 50 to more than 100 meters height, where the partial draw-down of the water level by several percent of the dam height is indeed inefficient. Soft flushing can be very efficient in reservoirs with high inflow in relation to the reservoir volume and relatively shallow water depths at flood events (Harb et al., 2011). This kind of flushing can be combined with sediment routing to increase the efficiency.

In Alpine reservoirs with larger fractions of coarse sediments flushing with partial draw-down involves another challenge. The mobilized coarser sediment from the head of the reservoir may start to settle in the middle part of the reservoir again, caused by the decreasing velocities, turbulences and shear stresses as a result of the partial draw-down of the water level (Scheuerlein, 1990). However, previous studies also showed that the success of reservoir flushing depends on the in-situ conditions, like the geometry of the reservoir. In some reservoirs flushing with partial draw-down can also reduce the depositions in reservoirs and remove deposited sediments (Harb et al., 2011, 2012).
The discharge and the water level in the reservoir control the bed shear stresses and therefore, the sediment transport capacity and the transportable grain sizes in the reservoir. Flushing processes with partial draw-down can be used to limit the suspended sediment concentrations in the downstream area.

5.1.3 Flushing with Full Draw-Down of the Water Level

In the case of flushing with full draw-down of the water level free flow conditions occur. Therefore, the velocities, turbulences and bed shear stresses in the whole reservoir are increased. In the literature flushing with full draw-down is often stated as the only effective kind of reservoir flushing (Mahmood, 1987; White and Bettess, 1984; Atkinson, 1996; Shen, 1999). Consequently this kind of flushing is mainly used for the flushing of all kinds of reservoirs.

In large reservoirs the lowering of the water level dries a part of the reservoir. The dried sediment banks can be eroded only by geotechnical failures of the banks.

It should be noted that in the event of higher floods the water level in river run-off reservoirs reaches the maximum operation level in the reservoir again. These reservoirs are usually designed with an outlet capacity in the range of the 100-year flood.

5.2 Parts of the Flushing Process

The flushing process can be divided into the following parts (Morris and Fan, 1998; Badura, 2007). These different parts of the flushing process are illustrated in Figure 5.1.

- *First stage* - draw-down of the water level to minimum operation level (electricity production is possible in this stage); the outflow of the reservoir is larger than the inflow into the reservoir
- *Second stage* - draw-down of the water level from minimum operation level to the

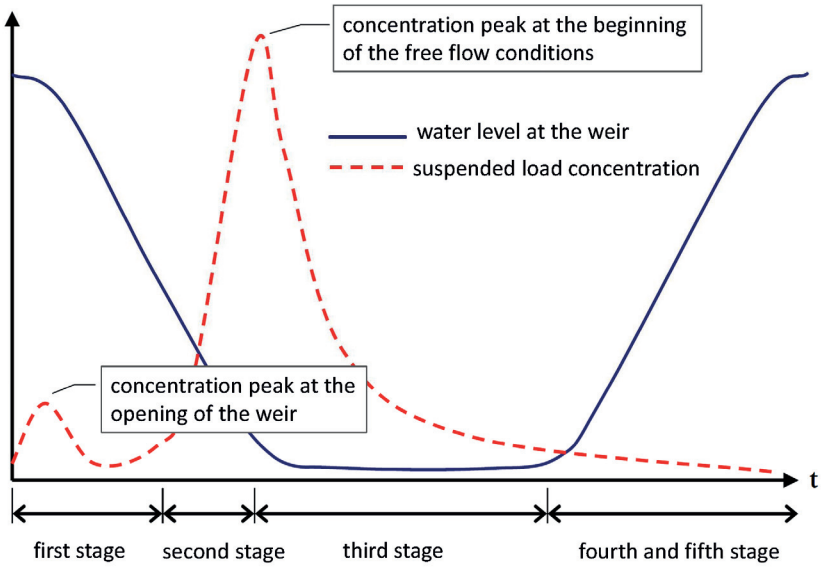

Figure 5.1: *Suspended load concentration and water level draw down during the flushing process, modified after Badura (2007) based on Morris and Fan (1998)*

level of dead storage or to free flow conditions; the outflow of the reservoir is also larger than the inflow into the reservoir

- *Third stage* - the so-called erosion phase with partial draw-down of the water level or free flow conditions; the outflow of the reservoir is equal to the inflow into the reservoir
- *Fourth stage* - post-flushing phase; the outflow of the reservoir is equal to the inflow into the reservoir
- *Fifth stage* - the so-called refill phase with rising water level for the refilling of the reservoir; the outflow of the reservoir is lower than the inflow into the reservoir

In Alpine reservoirs the draw-down of the water level (first and second stage) is usually initiated during the rising part of the flood wave is reaching the reservoir, to ensure free flow conditions when the peak of the flood wave arrives. Then the whole force of the flood wave can be used to remove deposited sediment in the reservoir. The absolute height of water draw-down and the maximum lowering of the water level per hour are the significant parameters for the duration of the draw-down (see also Badura, 2007).

In the third stage the erosion of the sediment depositions in the reservoir take place. In this stage the suspended sediment concentration is normally decreasing. But the formation of a flushing channel in the reservoir may cause instabilities at the river banks and geotechnical failures may increase the suspended sediment concentration abruptly. Figure 5.2 shows the water level draw down and the corresponding measured suspended load concentrations at the hydro power plant in Bodendorf at the river Mur in Austria in 2004 (Badura, 2007).

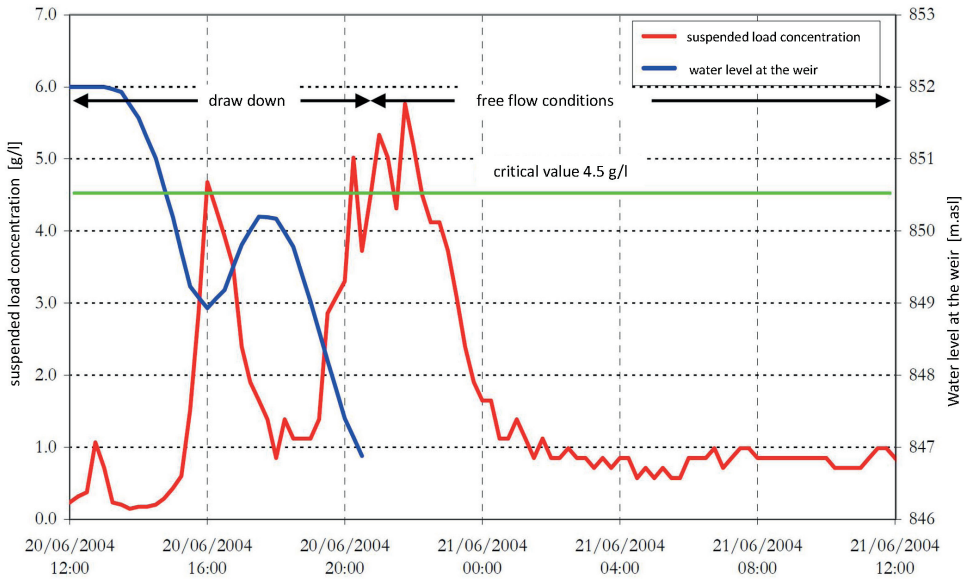

Figure 5.2: *Water level draw down and measured corresponding suspended load concentrations at the hydro power plant in Bodendorf at the river Mur in Austria, 2004 (Badura, 2007, modified)*

The post-flushing phase can be effective, if the discharge is sufficient to enable further sediment removal in the reservoir. Otherwise the post-flushing phase would be skipped for reasons of economy. From an ecological point of view a longer flushing of the reservoir can be reasonable to avoid the deposition of fine sediment in the downstream river section. In the refill phase a minimum outflow is usually defined by the public authorities. This minimum outflow is necessary to avoid negative surge waves and enable the suspended sediment transport in the downstream area.

5.3 Main Parameters for Reservoir Flushing

The main parameters for choosing sediment management methods were given in Chapter 4.2. Additional parameters beside the technical ones are defined to take the financial and the ecological effects of reservoir flushing into account:

- Type, geometry and configuration of the HPP, the reservoir and the tailwater section (flood protection of urban areas)
- Main purpose of the reservoir and legal aspects
- Ratio of inflow/maximum usable storage volume
- Maximum outlet capacity and minimum draw-down of the water level
- Discharge and possible duration of the flushing event
- Forecasted duration of the flood and minimum flood forecast time and allowed water level lowering per hour

- Season of the flood events and possible duration of the flushing event
- Status of sedimentation - grain-size distribution and the cohesion of the deposited sediments and the spatial variation in the reservoir
- Substances contained in the water and sediments (organic, anorganic, oxygen etc.)
- Suspended sediment concentration and ecological impact
- Costs of reservoir flushing

It is almost impossible to find universal flushing criteria which are valid for every reservoir in the world. White (2001) for example listed a collection of more than 200 reservoirs. Each reservoir is unique in geometry, purpose, annual inflow, storage volume and many other parameters.

The main flushing parameters will be discussed in detail in the following sections. All these parameters are linked and can not be discussed as a stand-alone topic.

5.3.1 Type and Geometry of the Reservoir

The type and the geometry of the reservoir are one of the most important parameters concerning reservoir flushing. Reservoirs with a large width to length ratio often show the formation of a flushing channel, which limits the lateral erosion in the reservoir during the flushing event. Additional erosion can occur due to instabilities at the banks of the flushing channel. But it is almost impossible to erode a large amount of sediment in shallow water areas or areas, which dry up because of the lowering of the water level. These facts are the reason for the greater efficiency of flushing events in narrow reservoirs with steep river banks. Flushing is most effective in reservoirs where the width of the flushing channel is almost identical with the total width of the reservoir (Atkinson, 1996; White, 2001; Badura, 2007; Harb et al., 2011). White (2001) also stated that long and relatively narrow reservoirs are better suited for flushing than short, wide and shallow reservoirs. The slope of the reservoir is also an important factor in terms of reservoir flushing (Batuca and Jordaan, 2000). Due to the deposition of sediments in the reservoir the slope may vary over time.

5.3.2 Main Purpose of the Reservoir and Legal Aspects

The main purpose of the reservoir and the associated legal aspects may limit the feasibility of flushing. The legal aspects can permit the full lowering of the water level in the reservoir.

5.3.3 Ratio of the Inflow/Maximum Usable Storage Volume

The feasibility of reservoir flushing is related to the ratio of storage volume to the mean annual inflow. If the ratio is large, e.g., the ratio is over 50 percent, the opportunity of periodical draw-down is limited, because the loss of water would be unacceptable. Morris and Fan (1998); White (2001) gives an initial storage capacity to mean annual inflow ratio (C/I-Ratio) of 0.3 as a limit for successful flushing operations. In the case of reservoirs with a reduced storage volume caused by sediment depositions flushing can also be an

option. The inflow should be sufficient for reservoir flushing, if the ratio is less than about 0.3. Reservoir flushing becomes more practicable with smaller C/I-ratios, because the probability of sufficient inflows is higher. Most hydrological small reservoirs (C/I-ratio < 0.05) have been flushed successfully. Examples are the Gmünd reservoir in Austria, the Palagnedra reservoir and the Gebidem reservoir in Switzerland, the Cachí reservoir in Costa Rica, the Santa Domingo reservoir in Venezuela and the Baira reservoir in India.

5.3.4 Maximum Outlet Capacity and Minimum Draw-Down of the Water Level

The lowering of the water level is one of the main factor for reservoir flushing. Without a lowering of the water level the velocity, the bed shear stresses and the turbulence will be insufficient in most cases. In general, a flushing process is most successful with full draw-down of the water level and free flow conditions in the reservoir.

Sometimes the bottom outlets are an additional limiting factor. If the design capacity of the bottom outlets is too small, the discharge for flushing is limited. If the bottom outlets are constructed as high level outlets, the full draw-down of the water level is not possible and thus the flushing efficiency is reduced. But this is not the case for river reservoirs in the Alpine area, because of the large design capacity of the weirs, which are usually designed with a capacity larger than the 100-year flood.

5.3.5 Discharge and Possible Duration of the Flushing Event

The hydrological conditions in the catchment influence the discharge, the duration, and thus, the efficiency of the flushing process. Reservoir flushing needs a sufficient discharge to enable erosion in the reservoir. The minimum required discharge for reservoir flushing depends on the slope of the reservoir, the draw-down of the water level, the deposited sediments in the reservoir and the duration of the discharge. Reservoirs with a clogged river bed need higher discharge rates for the initiation of the erosion process (Knoblauch et al., 2005). A high discharge rate also has the advantage of the reduction of the suspended sediment concentration, which may minimize the impacts on the ecosystem downstream of the weir.

Reservoirs with a large annual inflow compared with the storage volume of the reservoir are more suitable for higher annual flushing probabilities. Usually flood events or higher discharge rates (e.g., because of snow melt) can be used. The occurrence of flood events has a statistical character, so planned reservoir flushings with a longer intervall and higher flood events have a hydrological uncertainty. Additional in case of longer flushing intervals a relative high discharge is necessary to remove enough sediment for a sustainable flood management.

A common empirical value for the initiation of a flushing process in Alpine Reservoirs is a discharge of approximately 0.5 to 0.7 of the 1-year flood (threshold value) in order to achieve the required flushing effect while keeping a firm control about the essential parameters (sediment load, the content of chemical and organic matter, oxygen consumption rate, etc.). If the selected discharge for initiating a flushing process is too high, the probability of periodical reservoir flushing may decrease due to the variability of the discharge (Bechteler, 2006).

White (2001) mentioned that a successful reservoir flushing in large reservoirs often re-

quires a flushing discharge of about twice of the mean annual flow. In regions with wet and dry seasons flushing conditions can be achieved during the rainy season. An additional benefit of flushing during the wet season is that the high sediment laden inflows can be routed through the reservoir at the same time (Fan and Morris, 1992). Other advantages of a scheduled flushing in the wet season are the planning ability and the possible fast refill of the reservoir.

Badura (2007) stated that by flushing events in chains of power plants the water volume released by the draw-down of the water level in the upstream reservoirs can be used to enhance the flushing effect in the downstream reservoirs at hydrological small reservoirs with a small reservoir volume related to the annual inflow.

As already stated, a flood event or higher discharges are normally used for flushing processes. The necessary flushing interval depends on the sediment inflow in the reservoir, the amount of deposited sediment and the reservoir volume. The flushing interval should be short enough to enable a sustainable sediment management.

5.3.6 Forecasted Duration of the Flood and Minimum Flood Forecast Time and Maximum Allowed Water Level Lowering per Hour

The maximum lowering of the water level per hour should be defined with respect to the slope stability in the reservoir, the added water volume on the discharge in the downstream area and the coordination with other power plants. The rapid lowering of the water level in the reservoir may enhance bank failures due to the pore pressure in the river bank. In the case of constant lowering rate the probability of a positive surge wave in the downstream river section is high, since the volume of the upper "lamella" of the reservoir is larger than the lower ones. During the further lowering of the water level the added water volume decreases. If the added water volume should be constant, the lowering rate have to be varied. Hence, the lowering rate has to be increased according to the water level and the remaining water volume in the reservoir (Badura, 2007). Furthermore, the lowering rate of the water level can be used to control the concentration rate of the suspended sediments (Badura, 2007).

During the refilling phase of the reservoir the outflow should be decreased slowly to prevent negative surge waves in the downstream area. If there is a chain of power plants the harmonized interaction of the reservoirs during a flushing operation is one possibility to reduce the negative ecological effects on the river system (Badura et al., 2008).

The forecast duration of the flood is connected with the magnitude of the flood event. The flood forecast time depend on the size of the catchment. In the case of large catchments the flood forecast in based mainly on data provided by upstream gauges and additional data of hydrological models. If the size of the catchment decreases, a hydrological model is necessary to provide a appropriate flood forecast time. An appropriate flood forecast time is desired to enable the management of the flood operation at the power plant.

5.3.7 Status of Sedimentation - Grain-Size Distribution of the Sediment

The status of sedimentation in the reservoir and the grain-size distribution are also important parameters. Fine sediments like sand are relatively easy to erode. Coarser sediments like gravel or stones are more difficult to flush out of the reservoir. The coarser fractions

may be eroded in the upper part and the head of the reservoir but tend to settle again further downstream of the reservoir, especially in Alpine reservoirs with only partial draw-down of the water level.

Very fine sediment like silt and clay are due to the cohesive forces among the sediment particles another challenge in reservoir flushing. The cohesion of the sediment increases the critical shear stress and reduces the sediment erosion rate significantly.

An annual sedimentation rate of 1-2 percent probably represents the threshold value among reservoirs, where flushing should be planned and started early and reservoirs, where it may be delayed for perhaps 20 years (White, 2001). At sedimentation rates of 5 percent or higher, flushing operations should be planned in the design stage of the reservoir and implemented from the start of operation. Hydrological large reservoirs, except those which where located in areas of very high sediment yields, tend to have low mean annual sedimentation rates. Therefore, no active flushing operation may be needed during their economic life. However, most of the river reservoirs in the Alpine area are hydrological small and have sedimentation rates from 1-60 percent. In most of these cases, flushing would be the most effective sediment removal approach. Although several reservoirs have sedimentation rates below 1 percent, the sedimentation problem may increase in the next decades also in these reservoirs, because a large part of the sediment may be trapped in upstream reservoirs. If these reservoirs are flushed, the sediment inflow will be increased in the downstream reservoirs.

5.3.8 Substances Contained in the Water and Sediments

Toxic substances in the sediment, caused e.g., by industrial waste water or mining activities in the last decades, can limit the possibility of flushing. The risk of the reintroduction of these substances may be too big and hence, they have to be dredged and disposed of as hazardous waste.

5.3.9 Suspended Sediment Concentration and Ecological Impact

Flushing also creates problems from other perspectives, e.g., environmental issues or flood protection downstream of the reservoir. Due to the fact that the purpose of reservoir flushing is the remobilization of the sediments that were trapped during longer periods of time, flushing leads to a higher sediment concentration in the downstream section of the river. This concentration could be harmful to the downstream ecosystem (e.g., fish). If the suspended sediment concentration is over a certain threshold, it can damage fish and fish breeding areas, over strain the river fauna and clog the river bed in the downstream area (Knoblauch et al., 2005; Schneider et al., 2006).

The impact on the ecosystem can be reduced by limiting the suspended sediment concentration so that the upper natural concentration during natural floods is not reached (Scheuerlein, 1995). Therefore, reservoir flushing programs often require extensive regulations and monitoring. An example is the Bodendorf reservoir in Austria (Badura, 2007). In the ALPRESERV project (“ Sustainable Sediment Management of ALPine RESERVoirs considering ecological and economical aspects”, funded from the European Union in the Alpine Space Programme, 2004-2007) ecological investigations with special interest on the development of fish larvae and juvenile fish through the year. The results of

these investigations were compared with the monitoring of the fish stock from 1999 to 2006.

The analysis showed that flushing processes as well as natural flood events influence the juvenile fish stock. The negative effect on the juvenile fish depends on the time of the year and the stage of the development of the juvenile fish. Hence, the sediment management has to be planned for the specific river type with respect to the existing fish species (Eberstaller et al., 2008).

5.3.10 Costs of Reservoir Flushing

Reservoir flushing is most efficient when free flow conditions occur in the reservoir. Hence the total draw-down of the water level is required. The discharge used for the reservoir flushing is lost for the generation of electrical energy. Consequently, the total draw-down of the water level is a large economical loss in the case of large reservoirs. The reservoir flushing may thus be combined with maintenance works, which requires the emptying of the reservoir. A general rule is that the resulting costs of reservoir flushing should not exceed the benefits.

The ALPRESERV project investigated the flushing costs of the hydro power plant in the Bodendorf reservoir in Austria (Badura et al., 2008; Bischof, 2006). The costs of reservoir flushing can be divided into three categories:

- Preparation costs
  - Planning costs of the flushing process
  - Costs related to the flushing permission
  - Preparation costs
- Flushing costs
  - Loss of electricity energy generation
  - Costs for supervision in terms of the water act
  - Costs for rehabilitation works
- Costs related to ecology
  - Costs for ecological monitoring and preservation of evidence
  - Restitutions for the fishery

The preparation costs include the planning costs of the flushing process and the preparation costs like the development of operation instructions or meeting with stakeholders. The flushing costs consists of the costs obtained by the loss of electrical energy generation, the costs for the supervision in terms of the water act and the monitoring cost. The monitoring costs include the flood forecast system, the echo-soundings, and measurements of different parameters at various locations at the reservoir and upstream and downstream of the weir during the flushing event. The post-processing costs include the costs for rehabilitation works caused by the erosion of river banks or at the power plant.

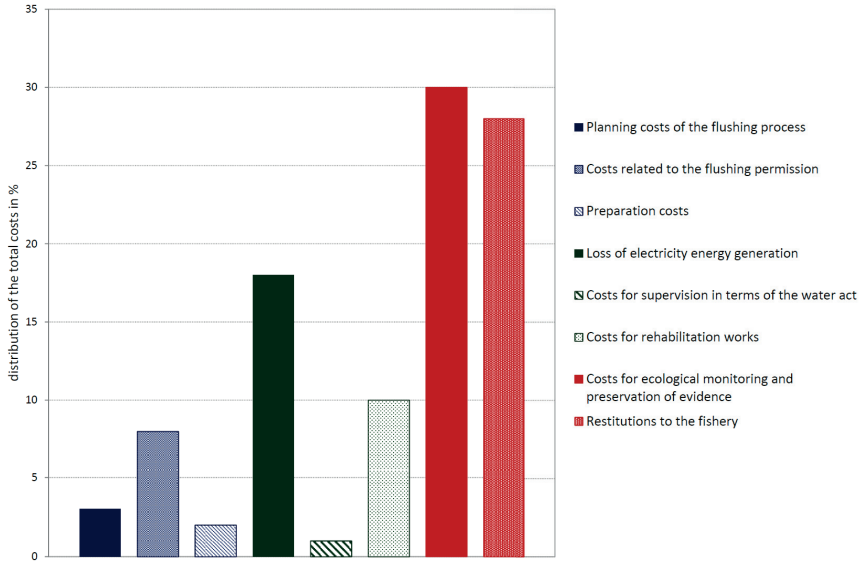

Figure 5.3: *Distribution of the flushing costs at the Bodendorf reservoir in Austria based on data from 1996 - 2006 (Badura et al., 2008, modified)*

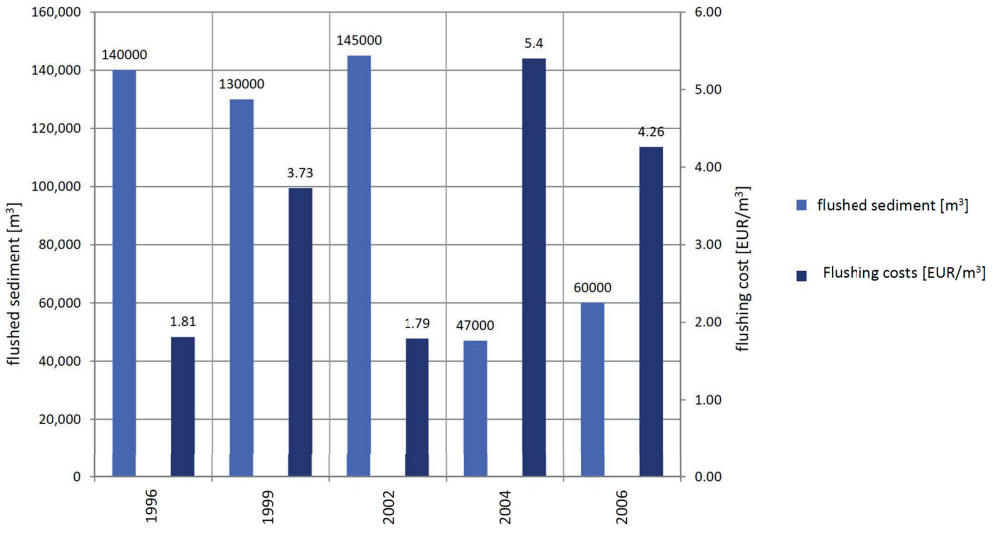

Figure 5.4: *Flushing costs in the Bodendorf reservoir based on data from 1996 - 2006 (Badura et al., 2008; Bischof, 2006, modified)*

The other categories are the costs for the ecological monitoring to assess the damage to fish and to find an agreement on the restitutions to the fishery (Badura et al., 2008).

Figure 5.3 illustrates the distribution of the flushing costs. The flushing operation including the loss of electrical energy generation and the monitoring costs during the flushing process and the rehabilitation works causes only 29 percent of the total costs. The preparation costs are about 13 percent. In Austria a large part of the costs refer to the cost for ecological monitoring and the restitutions to the fishery for the loss of fish. In the context of the case study in the ALPRESERV project the ecological monitoring and the restitutions to the fishery cover 58 percent of the total costs.

The costs per cubic meter of flushed sediment were also calculated by Badura et al. (2008) and Bischof (2006). The flushing costs are more or less constant, thus, the amount of flushed sediment determines the costs per cubic meter flushed sediments (Figure 5.4).

5.4 Increasing Flushing Efficiency

The flushing efficiency can be increased by optional structures in the reservoir. These optional structures can enable the sediment transport through the reservoir and reduce the sediment deposition at higher discharges and higher sediment inflow rates.

5.4.1 Initial Channels

An initial channel can be located near the weir or at the head of the reservoir. The flushing channel may enhance the sediment transport if cohesive sediments or clogged river beds occur. The deposited sediments are eroded not only retrogressive but also lateral to the initial channel. The width and depth of an initial channel depends on the local hydraulic situation and the available dredging capacity. Initial channels have been used at the reservoir Bodendorf (Austria) and in a reservoir in the River Isar (Germany), where the initial channel was filled with sediments after the first flushing events (Bechteler, 2006; Badura, 2007).

5.4.2 Groynes

Groynes are lateral structures starting from the river banks and reaching into the river. Groynes reduce the cross section of the river. Hence, groynes are used to increase the velocities and the bed shear stresses at flushing events to enhance the local erosion of sediments, for example at the head of the reservoir (Bechteler, 2006; DWA, 2006). In Austria there are several field sites where groynes are used to stabilize the river banks, structure the river or increase the sediment transport. One example of the installation of groynes in a reservoir is the Friesach reservoir at the river mur. There are shallow water groynes installed upstream of the weir to increase the sediment transport in the case of reservoir flushing. Unfortunately, the minimum discharge for flushing according to the operation permission is relatively high and therefore, flushing events are rare in this reservoir. Other examples of the installation of groynes are at St. Stefan at the river Mur, at the river Kainach near Dobl, and at the river Salza near Gusswerk, where micro groynes are used to stabilize and structure the river (Sindelar and Mende, 2009).

5.4.3 Guide Walls

Guide walls are longitudinal structures usually introduced into wide flowing water bodies in order to concentrate sediment transport into defined main channel portions. They usually separate shallow zones from the line of maximum velocity in the reservoir and provide excellent shelters for aquatic life during floods. Subsequent installation in reservoirs already affected by sedimentation is difficult and expensive (Bechteler, 2006; DWA, 2006). Guide walls are used in reservoirs at the river Drau in Austria.

5.5 Advantages and Disadvantages of Flushing

Flushing is often the most economic method to decrease the sedimentation in the reservoir. In river reservoirs normally a large part of the deposited sediment are sand and gravel fractions. The transport of coarser fractions in the downstream river sections at flushing events may also have a positive effect on the morphological and ecological system in the river. This transportation can provide new spawning areas for different fish species, avoid the lowering of the river bed caused by the lack of available sediments and can activate the sediment dynamics (Badura et al., 2008). A lack of sediment in the downstream areas can enhance the armoring effects of the river bed.

The negative effects of flushing are often related to the ecological system in the river. These negative effects may be the loss of aquatic invertebrates, the loss on fish caused by too high sediment concentrations, the bed clogging caused by the sedimentation of fine sediments like silt and clay at the river bed with the consequence of less spawning habitat for fish (Badura et al., 2008).

A monitoring program can observe the important parameters in terms of ecology and, therefore, limit the negative ecological effects caused by reservoir flushing.

5.6 Monitoring of the Flushing Process

In most cases a monitoring of the flushing process is necessary to evaluate the economic and ecological aspects. If negative impacts are expected, the flushing scenario should be changed to meet the requirements (Morris and Fan, 1998). Examples of flushing monitoring are e.g., given by Schneider et al. (2006), where the suspended sediment concentration and the oxygen concentration were measured downstream of the weir.

The preservation of evidence and the monitoring of the operations has to be carried out in most cases of flushings processes and other sediment management operations. The monitoring ensures that the operations comply with all technical and legal regulations and that the requested effect has been obtained. A preservation of evidence is generally required for all operations, which require a permit under the water act. The effort of the necessary preservation of evidence is directly related to the chosen sediment management method. Small measures (e.g., the installation of small groyne fields) require a smaller monitoring effort, operations with greater effect on the environment requires a larger monitoring effort. In this case certain investigations and measurements are needed to asses the potential effect of the desedimentation measures on the water body and the complex aquatic ecosystem. The extent of such investigations generally also depends on whether a first desedimentation operation is planned or a so-called follow-up operation or a periodically

repeated desedimentation operation will be performed (Hartmann, 2009). The amount and the grain-size of the deposited sediment in the reservoir must also be taken into account.

The preservation of evidence may be require the monitoring of the following parameters:

- Monitoring issues before flushing
  - Documentation of the morphology in the reservoir, in the tailwater and in the downstream area
  - Measurements of the suspended sediment concentration
  - Documentation of the fish population in the reservoir and downstream
  - Documentation of the fish population in a reference river stretch (upstream of the reservoir)
  - Documentation of the macrobenthos
  - Measurement of the water quality
  - Echo-sounding of the reservoir bed
  - Grain-size distribution of the reservoir
  - Measurements of the oxygen concentration
- Monitoring issues during flushing
  - Measurements of the suspended sediment concentration
  - Measurements of the oxygen concentration
- Monitoring issues after flushing
  - Documentation of the morphology in the reservoir, in the tailwater and in the downstream area
  - Documentation of the fish population in the reservoir and downstream
  - Documentation of the macrobenthos
  - Echo-sounding of the reservoir bed
  - Grain-size distribution of the reservoir

5.6.1 Monitoring Issues before Flushing

The planning of the flushing operation requires the calculation of the amount of deposited sediment, which should be removed. This is usually done by echo-soundings in the reservoir and the comparison of the measured profiles to previous measured profiles. Usually the distance between two profiles should not exceed 100 m to obtain a proper analysis of the data. Also the characteristic gravel banks and flow-controlling cross-sections downstream of the dam should be surveyed and mapped. Furthermore, a photo-documentation of the river is useful, starting from the head of the reservoir down to the downstream sections.

The suspended sediment concentration should be measured at different inflow rates including flood events to evaluate the natural suspended-sediment loads in the river section. In terms of ecology and fishery, it could be necessary to carry out an investigation to evaluate the stock of fish in the reservoir as well as downstream of the weir structure and down to the section where detrimental effects are not longer expected. In addition, an investigation of the stock of fish in a section of comparable ecological characteristics (a so-called reference site) upstream from the head of the reservoir is required. Additional investigations may be needed, such as e.g., macrobenthos surveys, water quality surveys, or reservoir-sediment investigations. The requirements of the monitoring process have to be adapted to each particular case. The determination of the content of oxygen-depleting substances in reservoir sediments (analysis of ignition residue) is also necessary (Knoblauch, 2006).

5.6.2 Monitoring Issues during Flushing

The monitoring during flushing operations should include the determination of suspended sediment concentrations at characteristic locations downstream from the reservoir, as well as a reference measurement upstream of the head of the reservoir. The number of monitoring points downstream of the dam may be reduced for the follow-up operations in the light of experience gained during former operations. Measurements of the oxygen content downstream of the dam can be required as well, especially in cases, where the deposited sediments in the reservoir show a substantial concentration of oxygen-depleting substances (Knoblauch, 2006). The water level and the inflow rates in the reservoir should also be documented for the planning of future events or the recalculation of the flushing events.

5.6.3 Monitoring Issues after Flushing

After the end of the flushing event, the characteristic gravel banks and flow-controlling cross-sections downstream of the dam should be surveyed and mapped again. The photo-documentation of the river should be repeated and the differences analyzed. The echo-soundings have also to be performed again in order to evaluate the volume of removed sediments. All the investigations carried out before the flushing operation as preservation of evidence for ecological and fishery purposes should be repeated after a suitable period. The results of these investigations should be compared and analyzed (Knoblauch, 2006).

6 Numerical Modeling

6.1 Current State-of-the-Art in Numerical Modeling

Over the past few decades physical models have been used to analyze processes and improve knowledge regarding water flow and sediment transport in rivers and reservoirs. Due to the rapid development of computational fluid dynamics (CFD), the increased computer power and the availability of clusters and parallel processing, numerical modeling has become an important tool in fields of hydraulics. There are various numerical models available which are able to handle hydraulic problems. However, numerical models with implemented and tested sediment transport algorithms are relatively rare.

In general, CFD models are classified by the calculated flow dimensions and the application range. There are a large number of one-dimensional, two-dimensional and three-dimensional numerical models available. One-dimensional models are well documented but the results are limited to the averaged water depth and the averaged flow velocity in the implemented cross sections. An alternative are two-dimensional numerical models, which are able to take floodplains or more complex river geometries into account. Two-dimensional models can be used if the three-dimensional nature of the flow processes is of minor importance, as in straight river reaches with a large width-to-depth ratio. Three-dimensional numerical models are able to model many processes in complex river geometries, such as meandering channels. The correct modeling of the secondary currents is of major importance there, due to the fact that the secondary currents play an important role in the evolution of the channel topography.

The benefits of the use of a numerical model compared with theoretical approaches, given by White (2001), are that the following factors could be taken into account:

- Reservoir geometry and topography
- Operation rules
- Sediment characteristics

Additional the long-term development can be investigated. White (2001) concluded that at the moment numerical models are able to give only approximative estimations of the reservoir sedimentation processes. However, since this statement the increased computer power has expanded the opportunities in numerical modeling. Additional several new algorithms has been implemented, numerous numerical models have been developed and improved.

The use of numerical models for the calculation of sediment transport processes in reservoirs started in the 1980s. White and Bettess (1984), Peng and Niu (1987), and Lai and Shen (1996) used a one-dimensional model for sediment transport calculations in reservoirs. Olsen (1999b) used in a previous study a two-dimensional numerical model for simulating the flushing process of the Kali Gandaki reservoir in Nepal. Badura et al. (2006) and Badura (2007) simulated flushing processes in Alpine run-off-river reservoirs with a two-dimensional model. However, most two-dimensional depth-averaged approaches are not able to model secondary currents in rivers and reservoirs appropriately. Three-dimensional models are thus used with increasing frequency, examples are the simulation of the sediment transport in the Three Gorges project (Fang and Rodi, 2003) or the simulation of the sediment transport in the Garita reservoir in Costa Rica (Olsen, 1999a). A detailed review of sediment transport simulations with CFD is given by Papanicolaou et al. (2008).

In this thesis the CFD codes SSIIM and Telemac were used to perform the numerical simulations of the case studies. The CFD code Telemac was used to model sediment transport processes by Huybrechts et al. (2010) and grain sorting effects by Merkel and Kopmann (2012). Goll and Kopmann (2012) simulated the influence of groynes on dunes. The two-dimensional model of Telemac was used to simulate flood events at the Danube (Kopmann, 2010).

The three-dimensional CFD code SSIIM was also used in previous studies. Olsen et al. (1999) and Bihs and Olsen (2008) modeled a scour hole. Olsen (2003) and Rüther and Olsen (2007) simulated the formation of a free forming meandering channel. The model was used by Fischer-Antze et al. (2008) to model the bed changes in the Danube during the flood event in 2002. Feurich and Olsen (2011) modeled the sediment transport in an S-shaped channel. Olsen and Haun (2010) and Haun and Olsen (2012b) improved the free surface algorithm for the modeling of a flushing event in the physical model of the Kali Gandaki reservoir in Nepal. SSIIM was also used for the modeling of sediment deposition and flushing processes in the Angustura reservoir in Costa Rica (Haun and Olsen, 2012a; Haun et al., 2012).

The two numerical models and their differences are described in the next sections.

6.2 Numerical Model SSIIM

The CFD code SSIIM was developed by Olsen (2012). It is a three-dimensional numerical model for free-surface flows and sediment transport in open channels.

6.2.1 Governing Equations and Discretisation

In SSIIM the three-dimensional flow and pressure field are described by the Navier-Stokes equations. The equations can be solved by using the Reynolds-averaging and a turbulence model together with the continuity equation with respect to the mass and momentum conservation in three dimensions (Versteeg and Malalasekera, 1995).

$$\frac{\partial U_i}{\partial x_i} = 0 \tag{6.1}$$

with i=1, 2, 3

$$\frac{\partial U_i}{\partial t} + U_j \frac{\partial U_i}{\partial x_j} = \frac{1}{\rho_w} \frac{\partial}{\partial x_j}(-P\delta_{ij} - \rho_w \overline{u_i u_j}) \tag{6.2}$$

where U_j is the averaged velocity, x is the spatial geometrical scale, ρ_w is the water density, P is the dynamic pressure, δ_{ij} is the Kronecker delta and $-\rho_w \overline{u_i u_j}$ are the turbulent Reynolds stresses.

In the Reynolds-averaged Navier-Stokes Equations (6.2) the transient term and the convection term are placed at the left side; the right side consists of the pressure term and the Reynolds stress term. The turbulent Reynolds Stress term is calculated using the Bussinesq approximation (6.3).

$$-\overline{u_i u_j} = \nu_t \left(\frac{\partial U_i}{\partial x_j} + \frac{\partial U_j}{\partial x_i}\right) - \frac{2}{3} k \delta_{ij} \tag{6.3}$$

where ν_t is the turbulent eddy viscosity and k is the turbulent kinetic energy. The turbulent kinetic energy k is calculated with

$$k = \frac{1}{2} \overline{u_i u_i} \tag{6.4}$$

In Equation 6.3 the turbulent eddy viscosity ν_t is unknown and has to be calculated using a turbulence model described in the next section.

The program applies the finite volume method as discretization scheme. The convective term in the RANS-equations can be modeled using the power law scheme, which is a first order upwind scheme, or the second order upwind scheme (Olsen, 2012).

The power law scheme is a weighted average of the six direct neighbor cells, whereas the second order upwind scheme uses the twelve neighbor cells. Usually the use of the power law scheme gives a more stable solution, but sometimes tends to give too diffusive results. The use of the second order upwind scheme reduces the false diffusion, but may overestimate eddies in the numerical model. An implicit time discretization is implemented in SSIIM and hence, the use of large time steps is possible. The largest time step used in the case studies is 60 seconds for the flushing cases. However, it is possible to use much larger time steps e.g., for the modeling of sediment depositions.

6.2.2 Turbulence and Pressure Model

The standard $k - \epsilon$ model, the $k - \omega$ model and the RNG two-equation model are implemented in SSIIM (Olsen, 2012). In general, the standard $k - \epsilon$ model gives the most accurate results for the simulation of flushing and deposition processes in reservoirs and river systems. The $k - \omega$ model is not quite standard in SSIIM, as it uses the wall laws from the $k - \epsilon$ model.

The standard $k-\epsilon$ model is a two equation model and the turbulent eddy viscosity ν_t, given in Equation 6.5, (Launder and Spalding, 1972) can be solved with

$$\nu_t = \frac{c_\mu k^2}{\epsilon} \tag{6.5}$$

where ν_t is the turbulent eddy viscosity and k is the turbulent kinetic energy and ϵ is the dissipation of the turbulent kinetic energy k.

The equations for k and ϵ are given below:

$$\frac{\partial k}{\partial t} + U_j \frac{\partial k}{\partial x_j} = \frac{\partial}{\partial x_j}\left[\left(\nu + \frac{\nu_t}{\sigma_k}\right)\frac{\partial k}{\partial x_j}\right] + P_k - \epsilon \tag{6.6}$$

$$\frac{\partial \epsilon}{\partial t} + U_j \frac{\partial \epsilon}{\partial x_j} = \frac{\partial}{\partial x_j}\left[\left(\nu + \frac{\nu_t}{\sigma_z}\right)\frac{\partial \epsilon}{\partial x_j}\right] + C_{1\epsilon}\,\frac{\epsilon}{k} P_k - C_{2\epsilon}\frac{\epsilon^2}{k} \tag{6.7}$$

$$P_k = \nu_t \frac{\partial U_i}{\partial x_j}\left(\frac{\partial U_j}{\partial x_i} + \frac{\partial U_i}{\partial x_j}\right) \tag{6.8}$$

where P_k is the production of the turbulent kinetic energy. The used constant empirical values given by Launder and Spalding (1972) are:

$$c_\mu = 0.09 \quad c_{1\epsilon} = 1.44 \quad c_{2\epsilon} = 1.92 \quad \sigma_k = 1.00 \quad \sigma_z = 1.26 \tag{6.9}$$

6.2.3 Grid Structure in SSIIM

SSIIM uses an unstructured, non-orthogonal and adaptive grid. Because of the adaptive grid, only the water body is modeled. The unstructured grid allows the use of a varying number of grid cells in all three spatial directions and moves according to the changes in the water levels and the bed levels (Olsen, 2012). The grid is made of tetrahedral and hexahedral cells and can be regenerated and updated after each time step.

The Rhie and Chow (1983) interpolation is used for the non-staggered grid to calculate the fluxes and velocities at the surface of the cell.

In the case of reservoir flushing the wet and dry areas in the grid may change very quickly. Consequently, an algorithm for wetting and drying is implemented in SSIIM to avoid distorted cells (Olsen, 2012). A decreased water depth due to the draw down of the water level will decrease the number of cells in the vertical direction of the grid, due to an implemented algorithm.

The algorithm used specifies how many cells are generated in the z-direction, depending on the water depth (h). Two limiting values are required as boundary conditions, where the first value (ζ_1) specifies if a cell is generated or if the water depth is too shallow and the domain dries up and disappears from the grid ($h < \zeta_1$). If the water depth is sufficient a second value (ζ_2) indicates if one cell is generated and a two-dimensional calculation is done ($\zeta_1 < h < \zeta_2$) or if the number of cells is calculated by equation 6.10 ($h > \zeta_1$) (Harb et al., 2013b).

$$n = n_{max} \times \left(\frac{h}{h_{max}} \right)^{p} \tag{6.10}$$

where n is the number of grid cells in the vertical direction, n_{max} is the maximum number of grid cells in the vertical direction and p is a parameter for the number of grid cells. In all studies presented in this work, the grid is updated after each time step so that changes in the bed and water levels during the computations are taken into account accurately. In SSIIM also a multiblock grid option and a nested grid option is possible. The grid is an important factor in numerical modeling regarding the accuracy and stability of the simulations. Hence in most cases a sensitivity analysis for the grid is necessary to find grid independent results.

6.2.4 Pressure and Water Level Calculation

SSIIM applies the Semi-Implicit Method for Pressure-Linked Equations (SIMPLE method) to find the unknown pressure term in the RANS-equations (Patankar, 1980). The principle of this method is to guess a pressure field and to use the following continuity defect to obtain a pressure correction. This pressure correction is then added in the next iteration until the continuity is satisfied.

The numerical program SSIIM was configured to take changes in the water level into account and enable large time steps to decrease the computation time of longer simulations. The used algorithm in SSIIM is implicit and changes in the water level were computed in accordance to the pressure gradient between the cell and the neighbor cell (Haun and Olsen, 2012b).

$$\frac{\partial P}{\partial x} = \rho \, g \, \frac{\partial z}{\partial x} \tag{6.11}$$

where P is the pressure, g is the acceleration of gravity, and z is the water level elevation.

A method used by Rüther and Olsen (2005) was based on a specified reference cell in the computation domain. In this method the water level in a cell was related to a specified reference cell with a known water level during the entire simulation time. This method was adapted for the reservoir flushing cases modeled by Olsen and Haun (2010) and Harb et al. (2013b) so that the water level in a cell is a function of the water levels of the neighboring cells. Depending on the location of the neighbor cell, the flow direction and the Froude number, a weighting coefficient is involved in the algorithm, which takes the location of the neighboring cell and the Froude number into account (Equation 6.12).

$$a_i = \begin{cases} min\,(2 - Fr; 1.0) \quad for \quad w > -0.1\ and\ Fr < 2.0 \\ w^2(Fr - 1.0) \quad for \quad w < -0.5\ and\ Fr > 2.0 \\ 0.0 \end{cases} \tag{6.12}$$

with

$$w = \frac{\overrightarrow{r} \times \overrightarrow{u}}{|\overrightarrow{r}| \times |\overrightarrow{u}|} \tag{6.13}$$

where a_i is the weighting coefficient for the neighbour cell, Fr is the Froude number, w is the dot product of $\overrightarrow{u}$ and $\overrightarrow{r}$, $\overrightarrow{u}$ is the velocity vector of the cell and $\overrightarrow{r}$ is the direction vector pointing to the center of the neighbor cell.

The coefficient a_i is used in the following discretized equation (Haun and Olsen, 2012a):

$$\sum_{i=1}^{8} a_i\ z_p = \sum_{i=1}^{8} a_i \left(z_i + \frac{1}{\rho\ g} \Big(p_p - p_i \Big) \right) \tag{6.14}$$

with z_p is the water level elevation in the cell, z_i is the water level elevation in the i^{th} neighbor cell, p_p is the pressure in the cell and p_i is the pressure in the i^{th} neighbor cell.

6.2.5 Boundary Conditions in SSIIM

In the case of hydraulic rough conditions - as in natural rivers - the boundary conditions at the walls and at the river bed are an important factor. The values in the boundary cells are computed according to the boundary conditions defined at the following locations in the computational domain (Rüther, 2006):

- Inflow
- Outflow
- Wall
- Surface

The following variables must be set at these locations:

- Velocities U_x, U_y, U_z
- Turbulence variables k and ϵ

The variables at the inflow boundary are defined by the Dirichlet boundary condition, which means the variables are set to a specific value. A zero gradient boundary condition is used for the outflow, i.e., they were set equal to the values of the next upstream cell. The variables U_x, U_y, P and ϵ have a zero boundary condition at the water surface, where as U_z is set to a certain value and k is equal to zero (Rüther, 2006).

SSIIM uses the wall laws by Schlichting (1979) to describe the velocity profiles near the wall and the center of the cell next to the bed (Equation 6.15).

$$\frac{U}{u_*} = \frac{1}{\kappa} ln \left(\frac{30\, y}{k_s} \right) \tag{6.15}$$

where u_* is the shear velocity, κ is the Karman constant equal to 0.4, k_s is the roughness coefficient and y is the distance between the center of the bed cell and the wall. Often k_s is specified by 3 times d_{90}. Another approach is the use of the Manning roughness value n_m (Equation 6.16).

$$k_s = \left(\frac{26}{k_{St}} \right)^6 \tag{6.16}$$

This approach is limited by the size of the bed cell. As long the roughness is small compared to the bed cell size, the use of the Manning-Strickler roughness works well. Otherwise another formula has to be used to reduce the velocity close to the bed and the walls (Olsen and Stokseth, 1995; Haun, 2012).

6.3 Sediment Transport in SSIIM

The computation of the sediment transport in SSIIM is subdivided into suspended and bed load transport (see Chapter 3).

6.3.1 Suspended Sediment Transport in SSIIM

The suspended sediment transport in SSIIM is calculated by solving the transient convection-diffusion equation. The convection-diffusion equation describes the two main transport processes: the convection and the turbulent diffusion for sediment flow.

$$\frac{\partial c}{\partial t} + U_j \frac{\partial c}{\partial x_j} + w_f \frac{\partial c}{\partial z} = \frac{\partial}{\partial x_j} \left(\Gamma \frac{\partial c}{\partial x_j} \right) \tag{6.17}$$

with

$$\nu_t = S_c\, \Gamma \tag{6.18}$$

where w_f is the fall velocity of the particle, Γ is the turbulent diffusivity, c is the sediment concentration over time t and over the spatial geometrical scales x and z, ν_t is the turbulent eddy viscosity and S_c is the Schmidt number.

The convection is the dominating transport process in rivers; mainly driven by the velocity of the water and the fall velocity of the sediment particle. In reservoirs the influence of the turbulent diffusion is increased due to the reduced velocities. In the case of multiple grain sizes the convection-diffusion equation is solved for each sediment size separately (Olsen, 2000).
An equilibrium sediment concentration is specified as boundary condition close to the bed. SSIIM uses the formula of Van Rijn (1984b) (Equation 3.23 in Section 3.5).

The critical shear stress $\tau_{c,i}$ is calculated according to the Shields curve. A specified sediment concentration in the bed cell was used as boundary condition for the computations (Van Rijn, 1984b).

6.3.2 Bed Load Transport in SSIIM

In SSIIM different sediment transport formulas are coded. The default sediment transport formula is the empirical formula derived by Van Rijn (1984a) (Equation 3.22 in Section 3.5). This formula was also used in Harb et al. (2011, 2013b). Previous studies showed also good results with this formula originally developed for sand particles (e.g Haun and Olsen, 2012a; Haun et al., 2012).

6.3.3 Bed Shear Stress in SSIIM

6.3.3.1 Calculation of the Bed Shear Stress

SSIIM calculates the bed shear stress using the wall law by Schlichting to derive the shear velocity.

$$\tau = \rho\, u_*^2 = \frac{U_{bed}\,\kappa}{ln\left(\frac{30y}{k_s}\right)} \tag{6.19}$$

where U_{bed} is the velocity in the bed cell, κ is the Karman constant equal to 0.4, k_s is the roughness coefficient and y is the distance between the center of the bed cell and the wall.

The bed shear stress τ is derived from the turbulent kinetic energy k close to the bed (Equation 3.13 in Section 3.4), if the $k-\epsilon$ turbulence model is used. The critical bed shear stress of a sediment particle is evaluated using the empirical approach derived by Shields (1936).

6.3.4 Other Sediment Transport Algorithms in SSIIM

6.3.4.1 Correction of the Critical Shear Stress - Sloping Bed

The slope of the river bed affects the sediment transport and the transported particle sizes in the river. Hence, the critical shear stress is modified for sloping river beds. SSIIM

uses the formula by Brooks (1963). In this formula a correction factor K is applied to the critical shear stress (Equation 3.25).

6.3.4.2 Correction of the Direction of Sediment Transport - Deviation of the Sediment Particle

Sediment particles usually move in the direction of the velocity vectors. However, if the river bed is sloping normal to the direction of the velocity vector, the sediment particle will also move in this direction caused by gravity. The formula of Kikkawa et al. (1976) is used to calculate this deviation in SSIIM.

6.3.4.3 Sand Slide Algorithm

The sand slide algorithm used in SSIIM is based on the angle of repose of the bed material. After each update of the mesh the angles of the river banks are checked if they are steeper as the pre-specified angle of repose. In such a case the angle of the river banks is corrected to the pre-specified angle of response to take the potential geotechnical failures into account (Olsen, 2001). This algorithm was first tested in Olsen and Kjellesvig (1998), but does not take cohesive forces into account.

6.3.4.4 Hiding and Exposure Effect

The sediment transport in rivers is unsteady and non-uniform with multiple grain sizes. Depending on the grain-size distribution the smaller sediment particles may hide behind the larger ones. This effect is called “hiding/exposure effect” (see Section 3.10) and results in the reduction of the eroded amount of smaller sediment particles. In SSIIM the formula derived by Wu et al. (2000) is implemented (Equation 3.32 in Section 3.10).

6.3.4.5 Roughness Caused by Bed Forms

Bed forms occur in many reservoirs and rivers during flushing operation or flood events. These bed forms are ripples, dunes or, in some cases, antidunes, depending on the grain-size distribution and the flow conditions (see Section 3.7). In SSIIM the increased roughness caused by the bed forms is added to the roughness caused by the grain-size distribution (Olsen, 2012). The approach derived by Van Rijn (1984c) is implemented in SSIIM (Equation 3.31 in Section 3.7).

6.4 Numerical Model Telemac

The TELEMAC suite consists of several parts of numerical models in the field of free-surface flow. In this study the three-dimensional model TELEMAC-3D and the sediment transport module SISYPHE have been used. TELEMAC was developed by Electricité de France R&D and distributed by Laboratoire d’Hydraulique de France (LHF). It is managed by a consortium of core organizations: Artelia (formerly Sogreah, France), BundesAnstalt für Wasserbau (BAW, Germany), Centre d’Etudes Techniques Maritimes et Fluviales (CETMEF, France), Daresbury Laboratory (United Kingdom), Electricité de France R&D (EDF, France), and HR Wallingford (United Kingdom).

The following sections are mainly based on Hervouet (2007), the manuals of Telemac-3D (EDF - R&D, 2012) and the manual of the sediment transport module Sisyphe (EDF-R&D, 2010).

6.4.1 Governing Equations and Discretisation

In TELEMAC-3D the three-dimensional flow field is determined by solving the continuity equation (Equation 6.1) and Reynolds-averaged Navier-Stokes equations (Equation 6.2).

In general the spatial discretization is linear, if the Finite Element method is used. Several advection schemes are available depending on the type of flow. The options include the method of characteristics, the streamline-upwind Petrov-Galerkin scheme (SUPG) and residual distributive schemes (such as the N-scheme and PSI-scheme) (Hervouet, 2007).

The time discretization is semi-implicit in TELEMAC-3D. The various implicitation coefficients can be varied. The defaults values are between 0.5 to 1 and generally adequate. In the case study Fisching the default implicitation coefficients with a time step of 1s was used to model the flushing events. This time step corresponds to a Courant number of approximately 1. The Courant criteria describes the relation of the time step to the velocity of a "water particle, which moves from one cell to another". A Courant number equal to 1 means, that the time step is equal to the cell size broken through the flow velocity.

6.4.2 Turbulence and Pressure Model

In TELEMAC-3D, several turbulence models are implemented: the constant viscosity model, the mixing-length model, the standard $k-\epsilon$ model, the Smargorinski mode and the k-ω model. The vertical and the horizontal turbulence model can be chosen independently. In the case study Fisching the constant viscosity model and the mixing-length model were used after a validation of the performance of the different turbulence models. In the final setup, the $k-\epsilon$ model gave almost identical results. The turbulence models are described on the next pages.

6.4.2.1 Constant Viscosity Model

In the constant viscosity model the molecular viscosity, turbulent viscosity and the dispersion is given by a coefficient. The value of this coefficient has a strong effect on the extent and shape of recirculation. By choosing a low value small eddies will tend to dissipate only, whereas by choosing a high value large recirculations will also tend to dissipate. The user must therefore handle this value with care (EDF - R&D, 2012). The calibration of this value using field measurements or a physical model test is recommended.

6.4.2.2 Mixing-length Model according to Prandtl

In mixing length models, the turbulent eddy viscosity v_t is calculated as a function of mean flow velocity gradients and mixing length l_m according to Prandtl (1925).

In Telemac a vertical mixing length model provides vertical turbulent eddy viscosities for velocities ν_z (Hervouet, 2007).

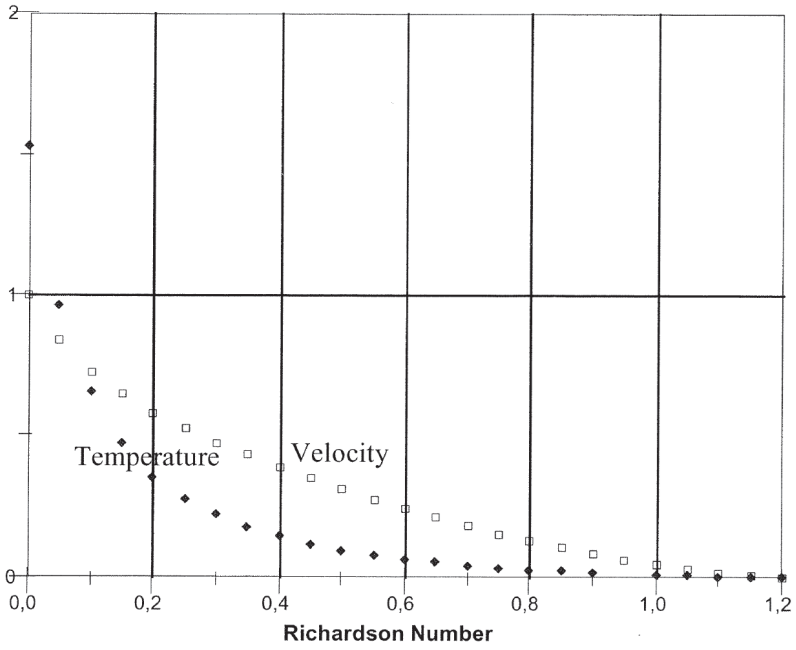

Figure 6.1: *Damping function for velocities and for tracers (Hervouet, 2007)*

$$\nu_z = f(Ri)\, l_m^2 \sqrt{\left(\frac{\partial U}{\partial z}\right)^2 + \left(\frac{\partial V}{\partial z}\right)^2} \tag{6.20}$$

with

$$Ri = -\frac{g}{\rho_0} \frac{\dfrac{\partial \rho}{\partial z}}{(\dfrac{\partial U}{\partial z})^2 (\dfrac{\partial V}{\partial z})^2} \tag{6.21}$$

Above, U and V are the averaged velocities, z is the spatial geometrical scale in the vertical direction, Ri is the Richardson number and f is a damping function of the velocity. In Telemac a damping function is according to Figure 6.1 was used.

The mixing length l_m can be modeled in different ways. In the case studies, the classical Prandtl model and the Nezu and Nakagawa model were used. The mixing length varies with the distance from the river bed z.

The mixing length according to Prandtl (1925) is calculated using the following formulae:

$$l_m = \begin{cases} \kappa\, z \quad if \quad z \leq 0.2h \\ 0.2\, \kappa\, z \quad if \quad z \geq 0.2h \end{cases} \tag{6.22}$$

According to Nezu and Nakagawa (1993), the mixing length vanishes at the free surface.

$$l_m = \kappa\, z\sqrt{(1 - z/h)} \tag{6.23}$$

where z= 0 is the bed level, h denotes the local water depth and κ = 0.4 is the Karman constant.

6.4.2.3 Modelling of Pressure in Telemac

The pressure in Telemac3D can be modeled using a hydrostatic or a non-hydrostatic pressure model. The hydrostatic pressure hypothesis simplifies the equation for the vertical velocity W, while neglecting the diffusion, the source terms and the acceleration, to obtain:

$$\frac{\partial p}{\partial z} = -\rho g \tag{6.24}$$

by substituting ρ with $\rho = \rho_0 + \Delta\rho$:

$$\frac{\partial p}{\partial z} = -\rho_0 g\Big(1 + \frac{\Delta\rho}{\rho_0}\Big) \tag{6.25}$$

from which the expression for pressure at the elevation z can be obtained:

$$p = p_{atm} + \rho_0 g(Z_s - z) + \rho_0 g \int_z^{Z_s} \frac{\Delta\rho}{\rho_0} dz' \tag{6.26}$$

The pressure p at one point depends then on the atmospheric pressure p_{atm} on the water surface Z_s and the hydrostatic pressure of the water column above it only.

In the case studies the hydrostatic model was used, because the results derived from the non-hydrostatic model were more of less the same. However, the hydrostatic model requires approx. 2 -5 times less computation time in the presented flushing cases. A detailed description of the non-hydrostatic model is given in Hervouet (2007).

6.4.3 Mesh Structure in Telemac

The mesh in TELEMAC-3D is obtained by dividing the two-dimensional domain in non-overlapping unstructured triangles. Then the mesh is extruded along the vertical direction and partitioned into a number of layers. Some examples of the used meshes and mesh sizes for the presented cases can be found in the description of the case studies in Chapter 8. The effect of the number of vertical layers was tested in the case study Fisching. The results by using two, five, eight and ten vertical layers were analyzed. The computed

water level in the two layer model was much higher than in the other models. The five, eight and ten layer models showed no significant differences in the computed flow vectors, water levels or bed shear stresses. Therefore, the five layer model was used for the further calculations.

In TELEMAC-3D an algorithm is implemented to take the drying and wetting of elements into account (Hervouet, 2007). The algorithm is called "Tidal flats" and can be processed in two different ways. In the first case, the elements are detected and the free surface gradient is corrected. In the second case, the elements are removed from the computation. In this case the dry elements are still part of the mesh but "frozen". However, in this case, mass-conservation may be slightly altered.

6.4.4 Boundary Conditions in Telemac

The values in the boundary cells in Telemac are computed according to the boundary conditions defined at the following locations in the computational domain:

- Inflow
- Outflow
- Wall
- Surface

The following variables must be set at these locations:

- Velocities U_x, U_y, U_z

The variables at the inflow boundary are prescribed by imposing the discharge and assuming a constant or a logarithmic velocity profile or imposed velocities with or without imposed water depth. A zero gradient boundary condition is used for the outflow, i.e., they were set equal to the values of the next upstream cell. At the side walls, the velocities tangential and normal to the boundary are set to zero (no-slip condition) (Huybrechts et al., 2012).

The variables U_x and U_y have a zero boundary condition at the water surface, whereas U_z is set to a certain value.

Telemac uses the wall laws to describe the velocity profiles near the wall (Equation 6.27). For the hydraulic rough flow the velocity profile takes the following form

$$\frac{U}{u_*} = \frac{1}{\kappa} ln\left(\frac{33\, y}{k_s}\right) \tag{6.27}$$

where u_* is the shear velocity, κ is the Karman constant equal to 0.4, k_s is the roughness coefficient and y is the distance between the cell and the wall.

6.5 Sediment Transport in Telemac

The sediment transport module in the TELEMAC suite is called SISYPHE. In the presented case studies, SISYPHE was internally coupled with TELEMAC. The sediment transport was modeled using different bed load and total load formulae. The suspended sediment option was not used for the numerical modeling of the sediment transport processes in the case study Fisching.

SISYPHE calculates the sediment transport rates as a function of the time-varying flow field and the sediment properties at each node of the triangular grid. The bed evolution is determined by solving the Exner equation (EDF-R&D, 2010). In the following sections the most important algorithms used in the case studies are presented. A detailed description of SISYPHE is given in EDF-R&D (2010).

6.5.1 Bed Load Transport in Telemac

Several sediment transport formulae are coded in SISYPHE, with respect to the literature. Examples are the formulae derived by Van Rijn (1984a), Meyer-Peter and Müller (1948) and Engelund and Hansen (1972). The formulae were discussed previous and can be found in Section 3.5.

6.5.2 Bed Shear Stress in Telemac

The bed shear stress τ_{xy} is calculated using the depth-averaged mean flow velocity and a dimensionless friction coefficient C_f (Hervouet, 2007).

$$\tau_{xz} = -\frac{1}{2}\rho_w C_f \, U^2 \tag{6.28}$$

where ρ_w is the density of water, C_f is a friction coefficient and U is the near bed velocity in the case of coupling with TELEMAC-3D to account for possible veering of the flow in the vertical direction.

The friction coefficient C_f is calculated based on the selected roughness option (Chézy, Strickler or Manning formulae). In the case study Fisching the Strickler formula was used:

$$C_f = \frac{2g}{h^{1/3} k_{ST}^2} \tag{6.29}$$

where h is the water depth and k_{ST} is the Strickler coefficient (Hervouet, 2007).

SISYPHE assumes that the direction of the bed shear stress and the direction of the depth-averaged velocity is the same for the internal coupling with TELEMAC-2D. In the case of coupling with TELEMAC-3D, the bed shear stress and thus the sediment transport are assumed to be in the direction of the near bed velocity.

The direction of the sediment transport can be changed using different algorithms, which are taking into account e.g., the effect of the sloping bed. These algorithm are discussed in Section 6.5.3.

The critical bed shear stress of a sediment particle is evaluated using the empirical approach derived by Shields (1936). The Shields parameter is calculated according to Van Rijn (1993).

6.5.3 Other Sediment Transport Algorithm in SISYPHE

6.5.3.1 Correction of the Critical Shear Stress - Sloping Bed

The slope of the river bed affect the sediment transport and the transported particle size in the river. Hence, the critical shear stress is modified for sloping river beds. A sloping river bed increase the sand transport rate in the downslope direction and reduce it in the upslope direction. In SISYPHE, a correction factor for the magnitude and direction of the solid transport rate, before the bed-evolution equation is solved.

In the case studies, the correction method based on the formula of Koch and Flokstra (1981) was used (Equation 3.24). The second available option is based on the formula of Soulsby (1997). The two different options gave similar results for the case studies.

6.5.3.2 Correction of the Direction of Sediment Transport - Deviation of the Sediment Particle

Sediment particles usually move in the direction of the velocity vectors. However, if the river bed is sloping normal to the direction of the velocity vector, the sediment particle will also move in this direction caused by gravity.

The change in the direction of sediment transport in taken into account by using the formula of Koch and Flokstra (1981) (Equation 3.27 and 3.28).

6.5.3.3 Sediment Slide Algorithm

The implemented sediment slide algorithm is coded for uniform sediments only. Therefore, this algorithm was not used in the case studies. The adaption of the sediment slide algorithm will be a topic for further work.

6.5.3.4 Hiding and Exposure Effect

The sediment transport rates of each sediment class are calculated using classical sediment transport formulae. Those formulae are initially valid for uniform particles and need to be modified to take sand grading effect into account. In a sediment mixture, big sediment particles are more exposed to the flow and smaller particles are protected by the larger ones.

Two different hiding and exposure formulae have been used in the case studies. The formula of Egiazaroff (1965) has been used in association with the Meyer-Peter and Müller formula (Meyer-Peter and Müller, 1948). The formula of Karim and Kennedy (1982) was used to take the hiding and exposure effect into account if the formulae derived by Engelund and Hansen (1972) or Van Rijn (1984a) was used.

6.5.3.5 Roughness Caused by Bed Forms

The influence of the bed forms on the roughness at the river bed is discussed in Section 3.7. The sediment transport rates in SISYPHE are calculated as a function of the local skin friction component τ'. The total bed shear stress τ_0 issued from the hydrodynamics model has to be corrected because of the bed forms.

$$\tau' = \mu_g \, \tau_0 \tag{6.30}$$

Physically, the skin roughness should be smaller than the total roughness ($\mu_g < 1$). Therefore, the skin friction subroutine has been modified to take this physical effect into account.

In Telemac are three options available: no skin friction correction, a skin friction correction proportional to the grain diameter and a skin friction correction based on a ripple predictor. The options no skin friction correction or the skin friction correction proportional to the grain diameter was used in the simulations of the different case studies, based on the grain sizes and the flow conditions in the reservoir. The skin friction correction proportional to the grain diameter is calculated using the following functions.

$$\mu_g = \frac{C'_f}{C_f} \tag{6.31}$$

with

$$C'_f = 2\left[\frac{\kappa}{log(\frac{12h}{k'_s})}\right]^2 \tag{6.32}$$

where C'_f is the friction coefficient for the skin friction correction, h is the water depth, k'_s is the grain diameter, which is equal to d_{50}, and κ, which is equal to 0.4. If the grain sizes are small (<0.5mm), the skin friction correction factor becomes very small (<0.2). Hence, the local skin friction component τ' is also very small and limit the sediment transport. This effect will be discussed in the case study Fisching in Section 8.2.

7 Cohesive Sediments – Flume and Field Tests

This chapter is mainly cited from Harb et al. (2013c).

The use of the Shields curve is the most used technique to determine the critical bed shear stress for cohesionless depositions. However, depositions in reservoirs often contain fine sediments like silt and clay. Even if it is possible to draw a clear threshold between fine and coarse particles (most times 60 μm is used as threshold), using a single number to describe the behavior of the sediments regarding cohesion (Mehta et al., 1989), as it is implemented in some numerical models, is not a straightforward procedure. The occurring cohesive forces increase the critical bed shear stress and the Shield curve is no longer valid. The critical shear stress of the cohesive sediment mixtures may be up to 50 times larger as for cohesionless sediments, having similar arithmetic mean sizes (Kothyari and Jain, 2008). Especially consolidation effects resulting in lower water content, higher shear strength and more stable structural configuration of the deposition layers influence the critical shear stress (Mehta et al., 1989). Kamphuis and Hall (1983) took e.g., the clay content and consolidation pressure in their experimentally studies into account. However, Berlamont et al. (1993) proposed a list of 28 parameters, which would be necessary to describe the behavior of natural cohesive sediments, as a result of physical, chemical and biological processes. Hence, additional data is required in such cases to estimate the cohesiveness and the valid critical shear stress. So far there is no standard procedure for the evaluation of the critical shear stresses of cohesive sediments available.

In this study the critical shear stress was developed from flume studies, where the discharge rate was increased stepwise until mass erosion took place. In addition field measurements with a miscellaneous device were conducted (Aberle, 2008). The vane strength measurements have been carried out in the reservoirs to determine the undrained shear strength of the sediments in situ. The results were used to test the transferability of the measured vane strength values from the field into usable values for estimating the erosion rates. In addition, a function, developed with the results of this study and with values from the literature, was established which may be used for a further studies in these reservoirs (Harb et al., 2013c).

7.1 Cohesive Sediments in Reservoirs

The sediment depositions in reservoirs often contains a high percentage of silt and clay fractions, especially at the weir. As stated above, the critical shear stress of cohesive sediments can be much higher than the critical shear stress of similar cohesionless sediments. There is a large difference in the threshold for erosion and deposition for these

Figure 7.1: *Sediment layers in the Zlatten reservoir*

fine sediments. If a particle is eroded, it need a substantial decrease in the flow velocity, turbulences and shear stress to cause the settlement of the particle again.

Several parameters are influencing the critical shear stress of cohesive sediments. The main parameters are (Kamphuis and Hall, 1983; Kothyari and Jain, 2010):

- Consolidation
- Grain-size distribution
- Amount of clay
- Type of clay
- Water content
- pH-value of the water
- Temperature of the water
- Thixotropy
- Bio-chemical processes

The practical application in reservoirs with cohesive sediments is complicated by the nonuniform nature of the depositions. These deposition patterns are caused by unsteady inflow processes and reservoir management tasks, which produce depositions of different thickness and grain size. Also the source of the sediment depositions may vary due to the hydrological conditions in the catchment responsible for the inflow in the reservoir. Coarse sediment fractions and organic depositions can also influence the mechanical behavior of the deposited sediments (compare Morris and Fan, 1998). The different settling velocities of different grain sizes causes a spatial distribution of sediment fractions, starting with the coarser fractions at the head of the reservoir and the finer fractions at the weir (compare Chapter 4.3). However, different discharge rates can create vertical deposition layers in reservoirs (Figure 7.1). This vertical layering can change depending on the position in the reservoir and is caused by the different flow conditions and bed shear stresses at normal operation and flood events.

Figure 7.2: *Weir and diversion channel of the Zlatten reservoir in Styria, Austria*

Additional, the consolidation of the cohesive sediments will increase the critical shear stress over time. Hence, the critical shear stress is not constant over the depth due to vertical layering of sediment depositions and consolidation effects.

7.2 Project Areas and Background

The sediment samples for the flume tests were collected in the Zlatten reservoir located in Austria. Additional sediment samples were taken from the Angostura reservoir located in Costa Rica to obtain a more general result concerning the shear stresses of cohesive sediments.

The Zlatten reservoir is located on the river Mur in Styria, Austria (Figure 7.2). The diversion power plant was built in the years 1925 to 1925. The reservoir has a maximum operation level of 467.35 m asl. and a initial water depth at the weir of approximately 11.5 m. The reservoir is 5.1 km long, has a width of 80 to 150 m and an initial reservoir volume of approximately 2.8 million m^3. The design capacity of the power plant is 19 MW with a design discharge of 147 m^3/s and a mean discharge of 108.1 m^3/s. The reservoir has a catchment area of about 6,250 km^2.

Figure 7.3 shows the sediment deposition at the weir in the reservoir Zlatten at the river Mur in Styria (Austria) during the complete draw-down of the water level. The sampling area is shown in Figure 7.4.

The Angostura hydro power plant is one of currently four power plants located at the river Reventazón in Costa Rica and has been in operation since October 2000. The dam is constructed as a rock-fill dam with a height of 38 m. The design capacity of the power plant is 177 MW with a mean discharge of 104 m^3/s. The reservoir was planned with a total size of 17 million m^3, where 2.5 million m^3 are required for the daily peaking purposes (Jiménez et al., 2004). The Angostura reservoir is filled from a catchment area of 1,463 km^2, mainly by the rivers Reventazón and Atirro.

Figure 7.3: *View from the weir of the Zlatten reservoir upstream with total lowering of the operation level due to rehabilitation works*

Figure 7.4: *View of the cohesive sediment banks in the middle of the reservoir with total lowering of the operation level*

Figure 7.5: *Angostura reservoir in Costa Rica with lowered operation level at a flushing event*

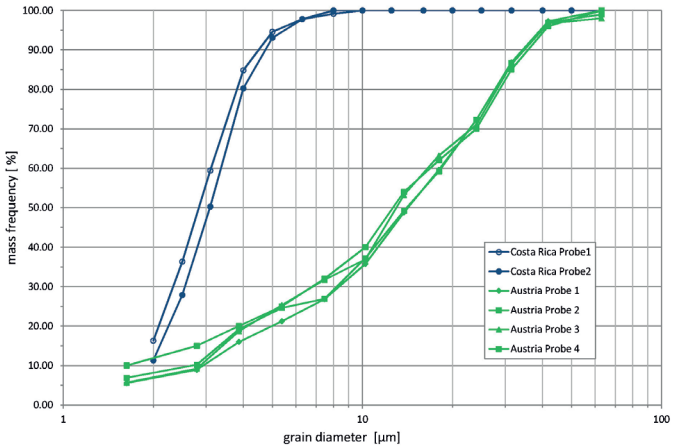

Figure 7.6: *Grain size distribution of the sediment samples gathered in reservoirs in Austria and Costa Rica (Harb et al., 2013c)*

7.3 Sediment Sampling

In August 2010 six representative sediment samples were taken at the Zlatten reservoir in Austria and analyzed according to the Austrian Standard ONORM B4412. An acrylic cutting cylinder with a diameter of 140 mm was used to obtain nearly undisturbed sediment samples. The cohesive sediment samples were collected at a sediment bank on the orographic left side of the reservoir. The water depth at the sediment bank was approx. 0.5 - 0.6 m. The grain size analysis of the sediment samples from the Zlatten reservoir showed a d_{90} of 35 μm and a d_m of 17 μm (Figure 7.6, green line). The water content of the samples varied between 30 and 35 percent.

The sediment samples from the Angostura reservoir were taken in July 2012 from a sediment bank, which has developed at the inflow area of the reservoir during the last years. The water depth at the bar was approx. 0.3 - 0.4 m. The acrylic cutting cylinder used had a diameter of 100 mm and the results were also analysed with respect to the same standards. The grain size analysis of the sediment samples showed a d_{90} of 5 μm and a d_m of 3 μm (Figure 7.6, blue line). The water content of the samples from Costa Rica also varied between 30 and 35 percent.

7.4 Experimental Setup

7.4.1 Flume Setup

The experimental program was carried out at the Hydraulic Laboratory of the Graz University of Technology. The flume is about 14 m long and has a constant rectangular section of 0.8 m width and 0.86 m height (Figure 7.7). The glass walls of the channel enable the installation of a Particle-Image-Velocimetry-System (PIV-System) and allow visual inspection of the test section. The water inflow into the flume is controlled by an upstream located valve in the feeding pipe and measured by an electromagnetic flow meter. The maximum discharge which could be reached with this setup was 150 l/s. The flow depth in the downstream area of the channel was controlled by a gate, located at the outflow area of the flume. For the experiments a 6 m long double bottom was installed with a dec-

lination of 1 percent and an open-bottomed test section. So the samples could be easily placed and fitted, with respect to the height, into bottom of the flume. The surface of the double bottom was a smooth acrylic glass plate.

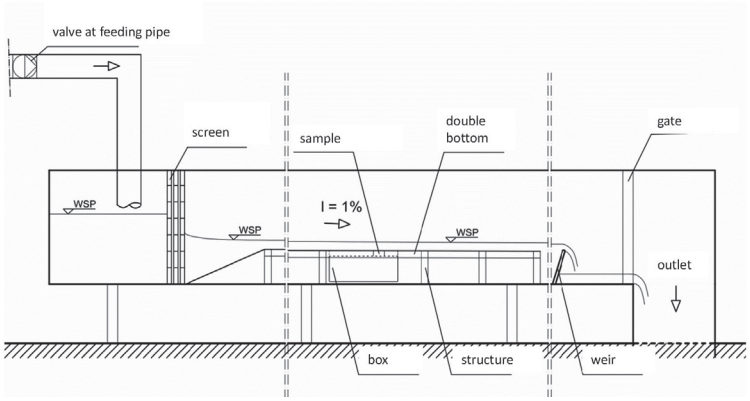

Figure 7.7: *Experimental setup in the flume (Harb et al., 2013c)*

7.4.2 Particle Image Velocimetry Measurements

A 2D Particle Image Velocimetry (PIV) system was used for the measurements of the velocity field around the soil sample. The laser used for the PIV-measurement is a Litron Laser – Model (LDY303-PIV) with a repetition rate of 0.2-20 kHz, an energy output up to 20 mJ and the defined wave length is 527 nm (green light) (LitronLasers, 2012). The camera is a Photron FASTCAM SA-1 with a frame rate of 5.4 kHz and a resolution of 1024 times 1024 pixel (Dantek, 2008). For the measurements the laser light sheet was located in the longitudinal axis of the flume directly above the sediment sample (Figure 7.8).

The camera was oriented normally to the 2D-Laser light sheet. The laser sheet lights the natural particles in the flume and the illuminated particles (seeding) are recorded (Figure

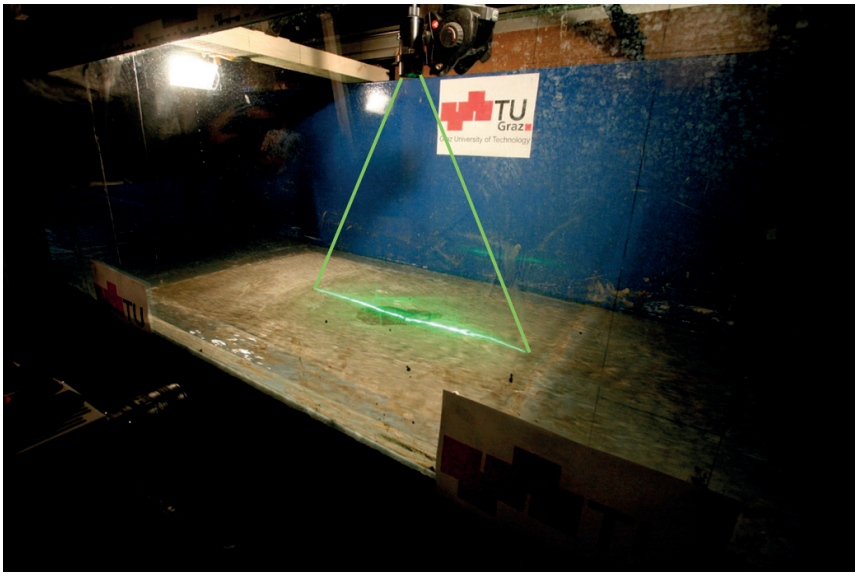

Figure 7.8: *Setup of the PIV measurements in the flume*

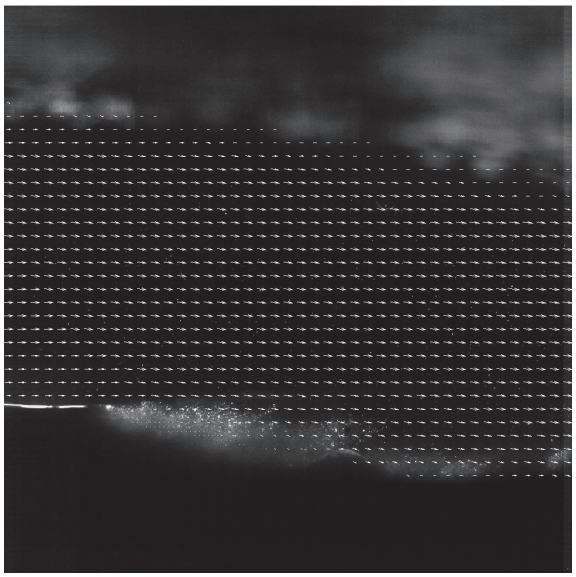

Figure 7.9: *Obtained picture from the PIV measurements (Harb et al., 2013c)*

7.9). Based on a sensitivity analysis the frame rate was set to 2 kHz (Harb et al., 2013c).

7.4.3 Experimental Conditions

Two sets of experiments were carried out for different flow conditions and different sediment samples. The slope of the flume was kept constant (with a declination of 1 percent). The flow was supercritical for all discharge rates. The tested flow conditions are summarized in Table 7.1.

The flow variables describing the different flow conditions are the flow rate Q, the mean velocity in longitudinal direction u_m, the flow depth h, the Reynolds number Re and the Froude number Fr. The sediment samples were fitted in the open-bottomed test section in the flume. To avoid an influence due to a sudden increase of the roughness (acrylic glass plate - soil sample) a working area of about 1.2 x 0.8 m around the undisturbed sediment sample was filled and uniformly pasted with naturally disturbed material (compare Kothyari and Jain, 2008; Roberts et al., 2003). The result was a similar roughness and surface structure to that in the reservoir. However, the use of field sediment samples in a laboratory flume has the disadvantage that the characteristics of these undisturbed samples may change during sampling and transportation (Aberle, 2008). The sediment samples were thus stored in the acrylic cutting cylinders in a water basin to retain the natural conditions in the reservoir. The surface of the disturbed material had to be enforced using cement slurry because of the lower critical shear stress. The experiments started usually with a discharge rate of 20 l/s, which was increased stepwise every 10-15 minutes. The sample was visually inspected at the same time. The discharge was held constant if erosion occurred. If no visible erosion was recognized the discharge was increased again (e.g., Aberle et al., 2003).

Table 7.1: *Flow conditions for the experiments (Harb et al., 2013c)*

Flow condition	Q [l/s]	u_m [m/s]	h [mm]	Re [-]	Fr [-]
V20	20	0.75	23	1.3x10-4	1.57
V25	25	0.84	28	1.7x10-4	1.60
V30	30	0.94	33	2.2x10-4	1.64
V35	35	1.02	38	2.7x10-4	1.67
V40	40	1.07	42	3.1x10-4	1.68
V50	50	1.18	49	3.9x10-4	1.71
V60	60	1.28	55	4.8x10-4	1.73
V70	70	1.36	62	5.6x10-4	1.75
V80	80	1.44	68	6.5x10-4	1.76
V90	90	1.50	73	7.3x10-4	1.77
V100	100	1.57	78	8.0x10-4	1.78
V120	120	1.67	89	9.5x10-4	1.80

where Q denotes the discharge, u_m is the mean velocity in the longitudinal flow direction, h is the measured water depth, Re is the Reynolds number and Fr is the occurring Froude number in the experiments.

7.5 Experimental Results and Discussion

7.5.1 Mean Velocity Profiles

The velocity profiles were measured for all flow conditions (Table 7.1) to evaluate the bed shear stress. The velocity in the longitudinal axis (u) are shown for the different flow conditions in Figure 7.10. The velocity values and vertical coordinates have been normalized using the maximum velocity component u_{max} and the corresponding coordinate y_{max}, respectively.

Six u-velocity component profiles are shown in Figure 7.11 for the flow condition V120, measured over different sediment samples. Figure 7.11 illustrates that the most significant difference among the velocity profiles occur next to the bed, probably due to the not perfectly flat surface of the different sediment samples. Depending on the exact height of the surface of the sediment sample and the resolution of the camera, the first measured velocity components are 0.1 mm above the bed.

7.5.2 Evaluation of the Bed Shear Stress

The bed shear stresses was evaluated using the gravity method and the Reynolds stress method, described in Section 3.3. In the case of the Reynolds stress method the measured shear stresses were time averaged and also spatial averaged over the sediment sample. This spatial averaging was necessary, because slight differences in the height of the probes

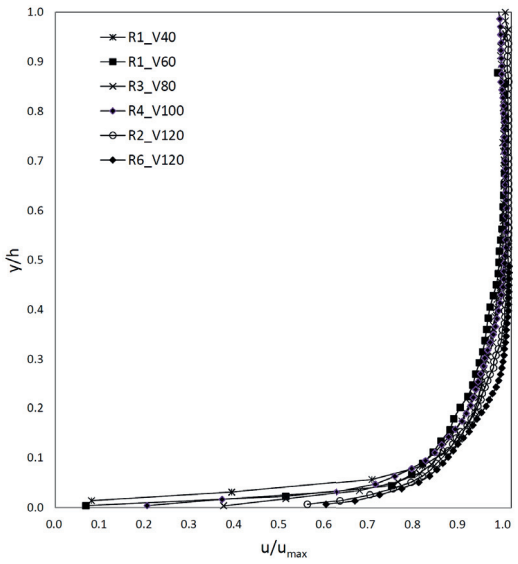

Figure 7.10: *Normalized u-velocity in the longitudinal direction (Harb et al., 2013c)*

caused peak values in the obtained shear stresses.

The shear stress values obtained are presented in Figure 7.12 to show the relationship of the values derived by the gravity method and the Reynolds stress method. The shear stresses derived by both methods agree well, which indicate that nearly uniform flow conditions occurred in the flume (Harb et al., 2013c). In this study six cohesive sediment samples from Austria and two cohesive sediment samples from Costa Rica were tested to evaluate the critical shear stresses. The erosion pattern was identified visually and characterized based on the erosion modes defined by Kothyari and Jain (2008). According to Kothyari and Jain (2008), the modes of incipient motion (namely: pothole erosion, line erosion and mass erosion) depend strongly on the clay content, the antecedent moisture

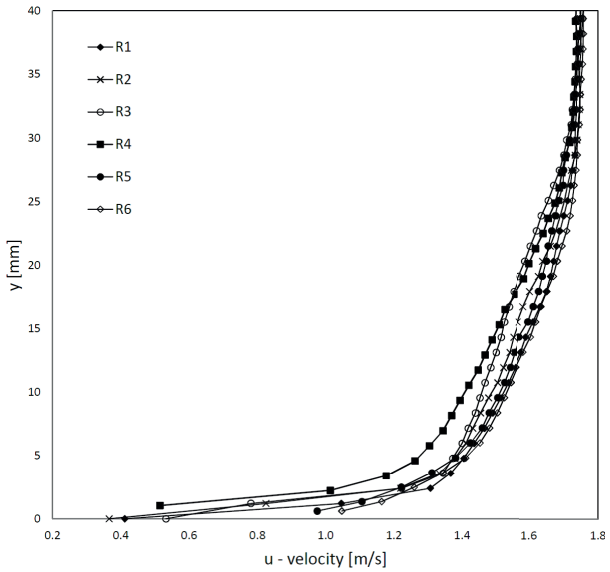

Figure 7.11: *Detail of the measured u-velocities for 6 different sediment samples (V120) close to the bed (Harb et al., 2013c)*

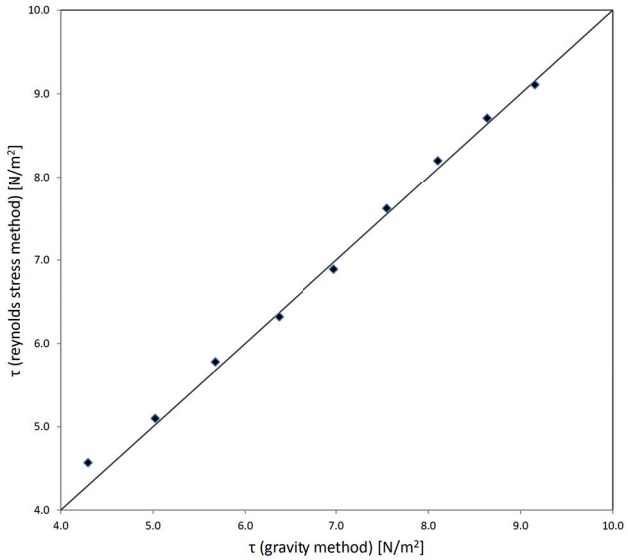

Figure 7.12: *Comparison of the shear stress values (time averaged and space averaged) derived by the gravity method and the Reynolds stress method for different flow conditions (Harb et al., 2013c)*

Table 7.2: *Evaluated critical shear stresses (Harb et al., 2013c)*

Sediment sample	Reservoir	Q_{crit} [l/s]	τ_{crit} [N/m^2]	Comment
R1	Austria	120	9.1	line erosion at 80 l/s
R2	Austria	70	6.4	–
R3	Austria	120	9.1	pothole erosion at 80 l/s
R4	Austria	120	9.1	mass erosion at 140 l/s
R5	Austria	60	5.7	–
R6	Austria	40	4.5	–
C1	Costa Rica	120	9.1	–
C2	Costa Rica	25	2.9	–

characteristics and the applied shear stress.

Table 7.2 presents an overview of the measured critical bed shear stresses and the observed erosion pattern. In the cases R2, R5, R6 and C2 the failure occured between two natural layers formed by sedimentation processes in the reservoirs. Figure 7.13 illustrates the erosion pattern of the sample C2. The structure of the sediment samples R1, R3, R4 and C1 was also not uniform because of inclusions of small clay lenses. In these cases mass erosion took place in the more or less compact sediment probe (see Figure 7.14). Layers or small lenses in the sediment depositions develop, if the characteristics of the inflowing sediments change during the deposition period (e.g., coarser sediments during flood events). However, it is possible to capture disturbances of this kind on a small scale, but an observation of these processes in a whole reservoir is almost impossible to conduct.

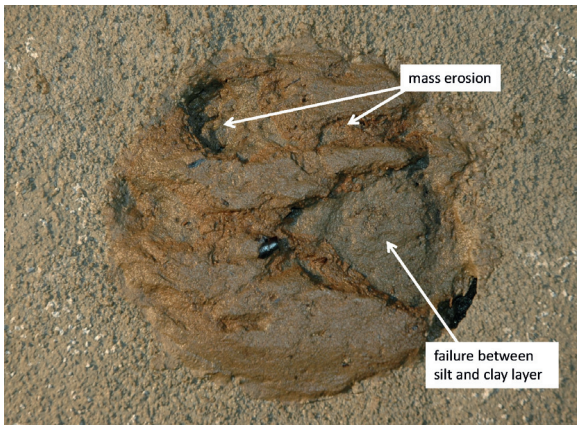

Figure 7.13: *Erosion pattern of the sample C2 after the final run (V 25) with a shear stress of 2.9 N/m^2 with failure between the silt and clay layer (Harb et al., 2013c)*

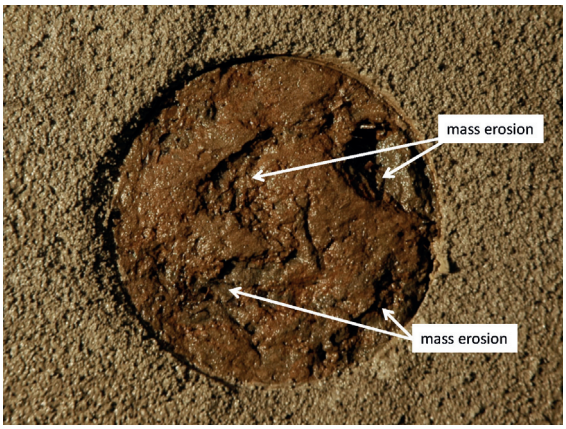

Figure 7.14: *Erosion pattern of the sample C2 after the final run (V 25) with a shear stress of 2.9 N/m^2 with failure between the silt and clay layer (Harb et al., 2013c)*

The critical bed shear stresses obtained in this study are relatively high compared with previous conducted studies, e.g., Aberle et al. (2006); Debnath et al. (2007); Kothyari and Jain (2008); Tolhurst et al. (2009) and Kothyari and Jain (2010). Only the critical shear stresses given by Kamphuis and Hall (1983) are in the same range as the values derived in this flume tests. The sediment characteristics and critical shear stresses given by Kothyari and Jain (2008, 2010) and Kamphuis and Hall (1983) are summarized in Table 7.3.

The reason for the mainly lower critical shear values found in the literature may be explained by the fact that no consolidation effects were taken into account in the laboratory produced sediment depositions. However, the sediment samples taken from reservoirs are influenced by consolidation, which leads to higher critical shear stresses.

7.5.3 Vane Strength Measurements

The field vane is one of the most used in situ measurement methods for the determination of the undrained shear strength of cohesive sediments (Chandler, 1988). Vane strength measurements have thus been carried out in the reservoirs chosen for this study to test the transferability of the measured vane strength values for the estimation of critical shear stresses of the depositions. A Geonor H-60 hand-held vane strength tester was used for measuring the undrained shear strength in the field (Geonor, 1995). The application range of this device spans from soft to stiff clays in a range of 0 kPa - 200 kPa. The benefits of a hand-held field vane are the easy handling, the repeatability of the results and economic aspects. The vane strength measurements were carried out in the same area where the sediment sampling for the flume test took place. The used vane size was 25.4 x 50.8 mm and the used rod had a length of 1 m for both reservoirs.

In the Zlatten reservoir the vane strength test was repeated ten times in an area of about 0.5 x 0.5 m. In the Angostura reservoir the test was repeated twelve times in the same areas size. Additional vane strength measurements were performed on the sediment samples placed in the flume after mass erosion took place. The vane strength measurements were compared with the obtained critical shear stresses from the laboratory study and with

Table 7.3: *Evaluated critical shear stresses compared with values found in the literature (Harb et al., 2013c)*

Sediment sample / Literature	d_m	Water content	Clay[a]	Silt[b]	Sand[c]	τ_{crit}	S_v
	[μm]	[%]	[%]	[%]	[%]	[N/m^2]	[kPa]
R1 Austria	17.8	30.4	10	89	1	9.1	14.2
R2 Austria	17.2	32.9	10	89	1	6.4	10.4
R3 Austria	16.9	31.4	10	89	1	9.1	15.8
R4 Austria	16.5	31.6	10	89	1	9.1	17.2
R5 Austria	17.2	30.9	10	89	1	5.7	9.6
R6 Austria	17.4	32.3	10	89	1	4.5	7.7
C1 Costa Rica	3.1	34.3	15	85	0	9.1	5.0
C2 Costa Rica	3.4	34.0	15	85	0	2.9	4
Kamphuis and Hall (1983)	–	24.2 - 37	60	35	5	8.6 -18.4	9.6 - 22.5
Kamphuis and Hall (1983)	–	35.6	60	38	2	12.2 - 13.4	17.1
Kamphuis and Hall (1983)	–	34.1	62	35	3	–	27.0
Kamphuis and Hall (1983)	–	37.8	60	39	1	9.9 - 10.7	12.2
Kamphuis and Hall (1983)	–	31.8	60	36	4	10.2 - 11.3	15.2
Kamphuis and Hall (1983)	–	35.7	58	40	2	11.3 - 12.5	13.3
Kamphuis and Hall (1983)	–	29.6 - 31.3	48	35	17	4.0 - 8.9	1.9 - 7.6
Kamphuis and Hall (1983)	–	22.6 - 25.8	36	35	29	1.0 - 5.4	3.6 - 11.0
Kamphuis and Hall (1983)	–	20.5	15	35	50	1.5 - 1.8	11.0
Kothyari and Jain (2008)	1500	7.2 - 13.4	10	0	90	0.9 - 1.3	–
Kothyari and Jain (2008)	1330	7.2 - 15.2	20	0	80	1.2 - 1.7	–
Kothyari and Jain (2008)	1170	9.5 - 21.	30	0	70	1.3 - 1.8	–
Kothyari and Jain (2008)	1000	10.3 - 19.2	40	0	60	1.0 - 1.6	–
Kothyari and Jain (2008)	840	10.0 - 20.4	50	0	50	0.9 - 1.5	–
Kothyari and Jain (2010)	1500	–	10	45	45	0.9 - 1.3	–
Kothyari and Jain (2010)	1000	–	40	30	30	0.9 - 1.5	–
Kothyari and Jain (2010)	850	–	50	25	25	0.8 - 1.4	–

where d_m denotes the mean sediment diameter, τ_{crit} is the critical bed shear stress and S_v is the measured vane shear strength

values found in the literature (Kamphuis and Hall, 1983; Kothyari and Jain, 2008, 2010, compare Table 7.3). Figure 7.15 presents the correlation of the data from the present study and the data from Kamphuis and Hall (1983). The new data was used to modify the original function of Kamphuis and Hall (1983). However, the critical shear stress of cohesive sediments depends on various parameters. Therefore, this diagram and this function may be used for a rough estimation of the critical shear stress based on measured vane strength values only.

7.6 Conclusion for the Flume and Field Tests

The results reflect that the behavior of natural cohesive sediments depend on a wide range of parameters. The effects of layer structures in depositions in particular could be observed as an important parameter. Even in the case of two layers with almost identical shear stress mass erosion can take place by lifting sheets from the upper layer or by sliding of the upper from the lower one. The failure or sliding zone is then often between the layers.

The results of the experiments showed that the average shear stress obtained is above most of the values found in previously conducted studies (e.g., Kothyari and Jain, 2008). This is most probably because of the natural consolidation effect of the samples taken from the reservoirs, compared to the artificially created depositions made of a mixture of clay, silt and sand, used in other studies. In addition vane strength measurements were performed in the reservoirs to evaluate the undrained shear strength of the depositions. The obtained vane strength values were related to the critical shear stresses derived by the experimental tests in the flume. These data was also correlated with data derived by Kamphuis and Hall (1983), who developed a correlation function between the vane shear strength and the bed shear stress:

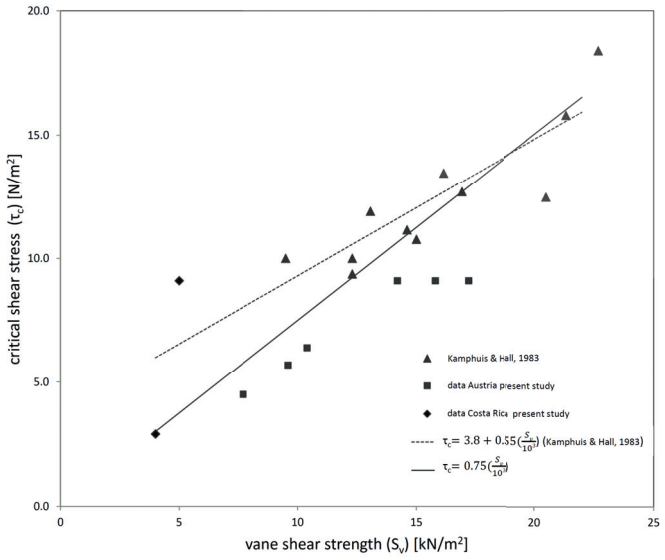

Figure 7.15: *Comparison of the critical shear stress values and the vane strength values based on data fromKamphuis and Hall (1983) modified with data of the present study (Harb et al., 2013c)*

$$\tau_c = 3.8 + 0.55\left(\frac{S_v}{10^3}\right) \tag{7.1}$$

The original function of the critical shear stress to the vane strength values obtained by Kamphuis and Hall (1983) was modified according to the additional data.

$$\tau_c = 0.75\left(\frac{S_v}{10^3}\right) \tag{7.2}$$

The new function may be used for a rough estimation of the critical shear stress, based on measured vane strength values in selected reservoirs. Especially for the Angostura reservoir, where only two sediment samples were available, this rough estimation should be handled with care in further studies. Further research is necessary to achieve accurate data for studies regarding sediment erosion. Future research tasks include basic research as well as the development of in-situ measurement devices, which are suitable to use in large reservoirs.

8 Case Studies

The case studies in this thesis focus on the numerical simulation of sediment deposition and the flushing of sediment. The presented work was published in form of scientific papers and can be found in the appendix.

The following reservoirs have been investigated:

- Schönau reservoir
- Fisching reservoir

The case studies are presented in the following sections.

The critical points in the numerical simulation of sediment transport processes during flushing or flood events are the accuracy of the numerical model and the quality of the input and validation data.

8.1 Case Study Schönau Reservoir

The first case study is the Schönau reservoir in Austria, located at the river Enns. The numerical simulations focused on the sediment deposition and on the removal of sediment during flood events. In this case study two different scenarios were investigated. These scenarios are presented in Harb et al. (2011) and Harb et al. (2013b).

In the first study (Harb et al., 2011) the sediment deposition in front of the turbines in the case of a 1-year flood was simulated and the influence of the draw-down of the water level investigated was in prototype scale.

The second study (Harb et al., 2013b) focuses on the prediction of morphological bed changes. The sediment deposition in a reservoir during a 10-year flood was investigated and the results of the simulation were validated with data derived from a physical model study. Because of the small grain sizes in the prototype, synthetic granulate was used in the physical model. The numerical computation domain was a reproduction of the physical model, including the grain sizes and the density of the particles, in order to ensure comparability.

8.1.1 Project Description and Background – Schönau Reservoir

The hydro power plant Schönau was built in 1973 in a river bend (Figure 8.1). The power house is located at the inner side of the river bend for infrastructural reasons. In the first

Figure 8.1: *Orthophoto of the Schönau reservoir at the river Enns (DORIS, 2013)*

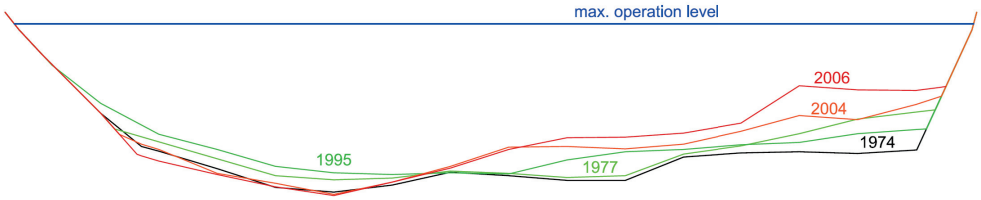

Figure 8.2: *Reservoir sedimentation in the Schönau reservoir since the start of operation in front of the weir (Section 10)*

years of operation the sediment deposition in the reservoir was not a problem, because most of the sediments were trapped in upstream reservoirs. In the last years the sediment load transported into the reservoir increased because of more frequently conducted flushing processes in the upstream located reservoirs. Legal restrictions prohibit the lowering of the water level of the Schönau reservoir under the minimum operation level and consequently, the flushing of the prototype itself is not possible. Therefore, in the event of higher discharges massive sediment depositions occur in the front of the turbine intakes of this hydro power plant, caused by flushing processes at the upstream located reservoirs. Several flood discharges were analyzed in the physical model to solve the sedimentation problem at the turbine inlets.

But not only the turbine inlets, the whole reservoir is affected by the deposition of sediments. Figure 8.2 illustrates the raise of the bed levels in the reservoir since the start of operation in 1973.

During the physical model tests a 10-year flood occurred at the prototype in July 2009. At this flood event the turbine inlets were blocked with wood stocks and fine sediments and no turbine operation was possible (Figure 8.3 and Figure 8.4). The removal of the deposited sediments in front of the turbine inlets was conducted by wet dredging and took eight weeks.

Figure 8.3: *Removed sediment from the turbine inlets in July 2009*

Figure 8.4: *Dredging at the turbine inlets in July 2009*

In this study the "soft flushing" approach (see Chapter 5) was investigated to reduce the sedimentation and to activate the erosion of the deposited sediments. A conventional flushing approach with free flow conditions in the reservoir is not possible in this case, because of legal restrictions concerning the downstream located city Steyr. Steyr is often flooded even in the occurrence of small flood events. The flushing of sediments to the city of Steyr may raise the bed levels and increase the flood risk. Consequently flushing operations are not allowed. Therefore, a soft flushing strategy is carried out in this study. In this scenario the water level is lowered from the maximum operation level (400.5 m asl) to the minimum operation level (398 m asl) during flood events to enhance the flow velocities, the bed shear stresses and thus the sediment transport in the reservoir.

8.1.2 Physical Model Study

The physical model study study was carried out at the Hydraulic Laboratory of the Institute of Hydraulic Engineering and Water Resources Management at the Graz University of Technology in the period between 2008 and 2010. The physical model was built in concrete with a fixed river bed at a scale of 1:40 based on the initial bed level in 1973 at the start of operation. The model was about 24 m long and 2.5 m wide and represented a natural river length of 950 m. The model was divided into a 570 m long part of the reservoir and a 380 m part downstream of the weir. Figure 8.5 shows an overview of the reservoir part of the physical model. Not only the initial conditions in 1973, but also the conditions in the sedimented reservoir were investigated. To do this, the bed levels measured in 2002 were installed in the physical model by filling up the cross sections with sand. The surface of the sand was enforced with cement slurry to obtain a fixed river bed again.

Figure 8.6 shows an overview of the reservoir in the physical model with bed levels from 1973. The Manning coefficient in the physical model for the bed roughness was n=0.01667 s/m$^{1/3}$, determined by similarity of the water levels. The grain-size distribution of the deposited sediments in the prototype is very fine (d_{90}=0.9 mm and d_{50}=0.25 mm) and has a grain density of 2.73-2.80 g/cm^3. In consequence of these small grain sizes, synthetic granulate was used to model the sediment transport and the sediment deposition in the physical model. The synthetic granulate had a cylindrical form with a grain size of 2 mm, a density of 1.29 g/cm^3 and a in the laboratory determined fall velocity of

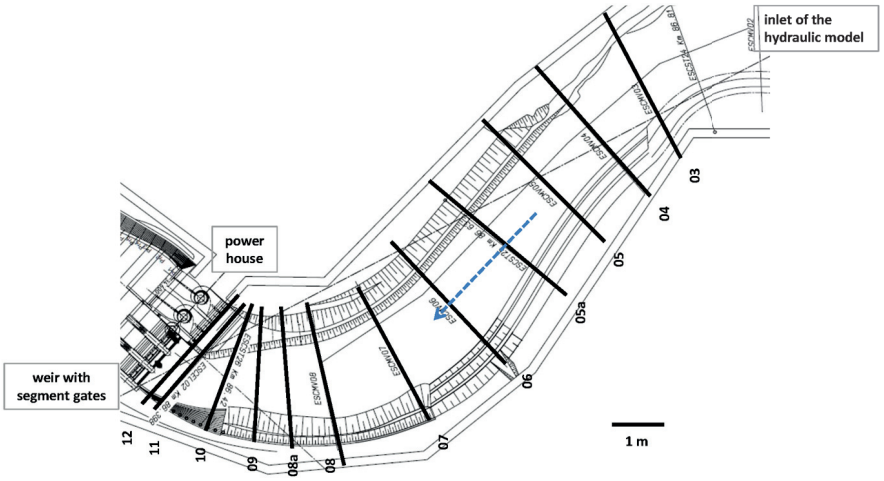

Figure 8.5: *Plan view of the reservoir part of the physical hydraulic model (Harb et al., 2013b)*

Figure 8.6: *A photograph illustration of the physical model with the initial bed level measured in 1973 (Harb et al., 2011)*

Figure 8.7: *Deposited sediment after the test run of a 1-year flood without turbine operation with the measured bed level in 2002 (Harb et al., 2011)*

0.07 m/s. The larger but lighter grains are typical for models designed by taking into account the grain Reynolds number (Yalin, 1971; Kobus, 1984). Figure 8.7 illustrates the deposited sediments near the turbine inlets after the test run of a 1-year flood without turbine operation for the bed level 2002.

8.1.3 Numerical Model

The three-dimensional numerical model SSIIM2 (Olsen, 2012) was used in this study. Because of the implemented wetting and drying algorithm the number of grid cells in the vertical direction changes according to the changes in the water level and the geometry of the river bed.

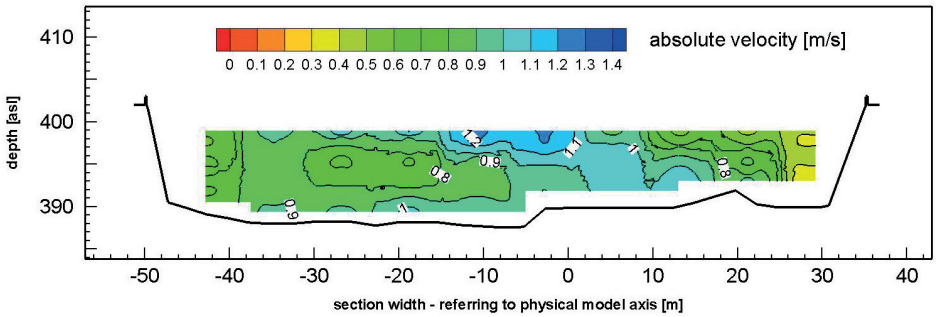

Figure 8.8: *Contour plot of the absolute velocities [m/s] for 1-year flood and turbine operation measured in the physical model in Section 10 (Harb et al., 2011, modified)*

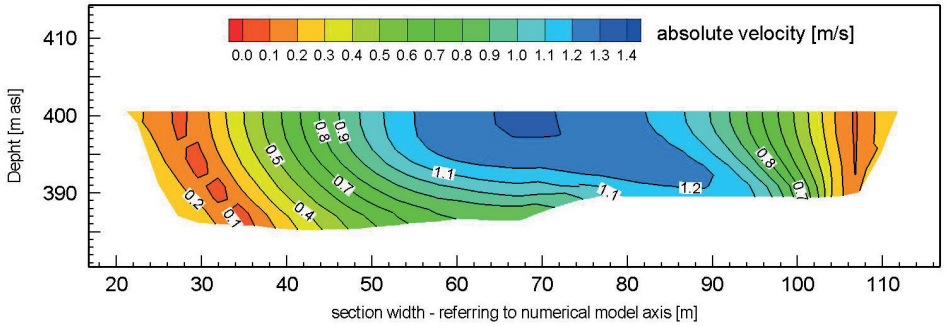

Figure 8.9: *Contour plot of the absolute velocities [m/s], 1-year flood and turbine operation computed in the numerical model in Section 10 (Harb et al., 2011, modified)*

8.1.3.1 Hydrodynamic Calibration of the Numerical Model

The velocity profiles derived of the numerical model were compared to the measured ADV profiles in the physical model. The bed roughness value was varied in the calibration process of the hydrodynamic calculations. Figure 8.8 shows the velocity profile measured in the physical model and Figure 8.9 illustrates the velocity profile of the numerical computation after the calibration process. After the hydrodynamic calibration a Strickler roughness of 60 $m^{1/3}/s$ was used for the further simulations.

The velocity distributions in the flow profiles show reasonable agreements. In this case the numerical model generally overestimates the high velocities in the middle of the section and underestimates the lower velocities near the river banks compared to the measured velocity profiles. The pattern of the flow field compares well, the location of the highest velocities can be reproduced in the numerical model.

8.1.4 Analysis Prototype Scale and Comparison with Physical Model and ADCP Measurements

As mentioned above, the first study was conducted in prototype scale. The model was calibrated using ADV measurements for the 1-year flood, taken at the physical model, and validated using ADCP measurements in the prototype. The bed shear stresses were analyzed and the sediment deposition for a 1-year flood simulated using the natural sediment sediment in the reservoir.

8.1.4.1 Numerical Model - Prototype Scale

In the first study (Harb et al., 2011) at the beginning of the calculation about 78,000 cells are used with a maximum cell size of approximately 5.0 x 5.0 m. At the end of the calculation between 50,951 and 48,520 cells are left, depending on the water level at the end of the simulation. The maximum number of cells in the vertical direction is 10. The numerical program SSIIM is described in Section 6.2.

The calibration of the numerical model was done by using measurements from the prototype. In the model the bed roughness was set to a constant value. The suspended sediment load capacity and the bed load were computed by using the empirical formulas of Van Rijn (1984a,b).

At the "soft-flushing" approach the reservoir level is drawn down linear to the minimum operation level of 398 m asl, if the discharge exceeds 750m^3/s (1-year flood). If the discharge increases further, the gates of the weir are opened according to the operation guidelines of the hydro power plant.

8.1.4.2 Validation of the Numerical Model Using ADCP Measurements

Additional field measurements with an ADCP (Acoustic Doppler Current Profiler) were used to validate the quality of the results in the numerical model. The field measurements were performed in June 2009 with approximate design discharge by the Hydrographic Institutes of the Styrian Government and the Upper Austrian Government. During the measurements the water level was constant (400.35 m asl). The maximum operation level of the reservoir is 400.5 m asl. A RDI ADCP WorkHorse RioGrande 1200 kHz was used to measure the flow field with the Section-by-Section method. The data collected in the reservoir were compared with the velocity profiles of the numerical model.

Figure 8.10 and 8.11 show the comparison of the flow fields derived from the ADCP measurements and the numerical simulation in Section 10.

Figure 8.12 and 8.13 show the comparison of the flow fields derived from the ADCP measurements and the numerical simulation in Section 8.

The flow field reproduced from the ADCP measurements and from the numerical model correlate very well. The ADCP measurements (Figure 8.12) show that, because of the complex geometry the highest velocities are at the inner site of the river bend. There is also an explicit separation zone and a backflow area at the left river bank in both measured ADCP profiles. All these characteristics are reproduced in the numerical flow profile (Figure 8.11 and 8.13). The bed levels of the measured cross section were derived from the ADCP measurements in 2009. The cross section implemented in the numerical model was measured using echo-sounding in 2002. Thus, the bed levels are slightly different, because of the sedimentation in the reservoir.

8.1.4.3 Comparison Flow Pattern 1973 and 2002

In the numerical model of the prototype the flow field with the bed levels of 1973 and 2002 were analyzed. The velocities at the river bed for the Figures 8.14 and 8.15 show clearly that the main flow in the river bend moved towards the outer side. This effect

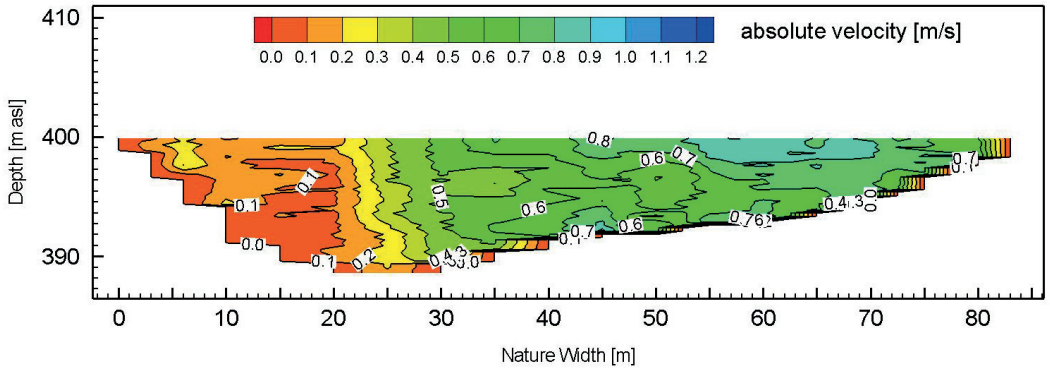

Figure 8.10: *Contour plot of the absolute velocities [m/s]for design discharge and turbine operation derived from ADCP measurements in the field in Section 10 with bed levels 2009 (Harb et al., 2011, modified)*

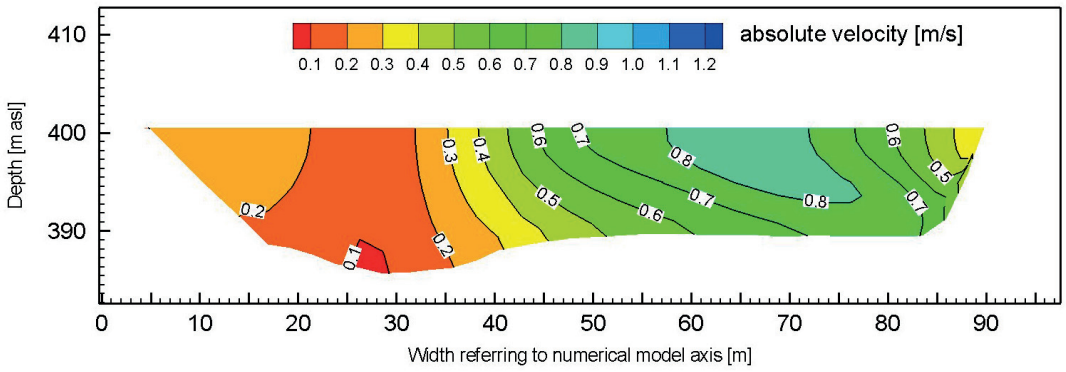

Figure 8.11: *Contour plot of the absolute velocities [m/s] for design discharge and turbine operation derived from the numerical model in Section 10 with bed levels 2002 (Harb et al., 2011, modified)*

may be caused by the sediment deposition in the reservoir and leads to a increased back flow zone at the turbine intakes. This increased backflow zone additionally enhances the sedimentation of suspended sediments in front of the turbine intakes.

8.1.4.4 Bed Shear Stresses

Figure 8.16 shows the "soft-flushing case" with a discharge of 1,000 m^3/s and a water level of 398 m asl and Figure 8.17 shows a discharge of 1,350 m^3/s (10-year flood event) with a water level of 400.5 m asl. The discharge of 1,000 m^3/s was chosen in context of the event probability to enable a frequently soft flushing of the reservoir. In both cases the turbines are not in operation.

The draw-down of the water level in the reservoir increases the flow velocities and the bed shear stresses at the river bed. Because of the low water depth in the middle part of the reservoir the bed shear stresses are also increased in this area. The shut-down of the turbines increases the large recirculation zones near the turbine inlets at the inner site of the river bend in the numerical model. These recirculation zones can also be observed in the physical model and in the prototype.

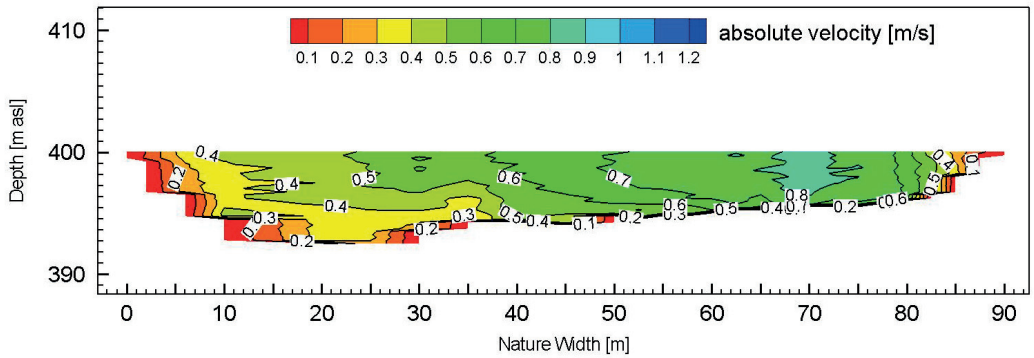

Figure 8.12: *Contour plot of the absolute velocities [m/s]for design discharge and turbine operation derived from ADCP measurements in the field in Section 8 with bed levels 2009 (Harb et al., 2011, modified)*

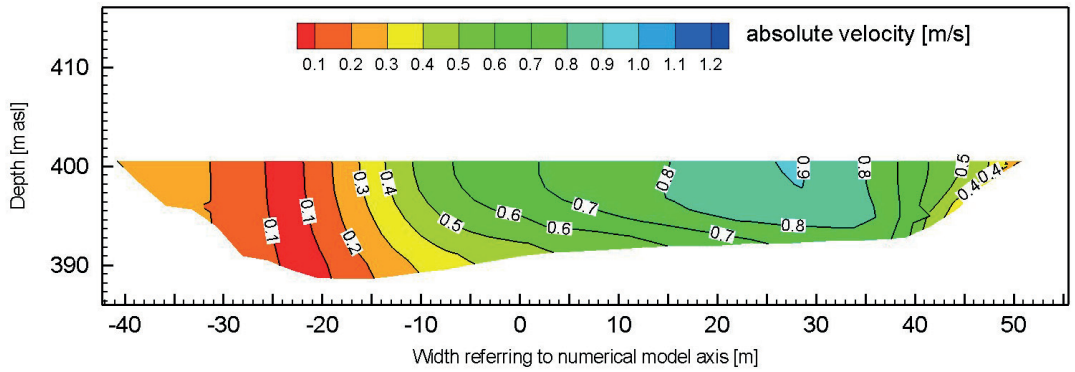

Figure 8.13: *Contour plot of the absolute velocities [m/s] for design discharge and turbine operation derived from the numerical model in Section 8 with bed levels 2002 (Harb et al., 2011, modified)*

8.1.4.5 Sediment Deposition – Investigations Prototype Scale

Figure 8.18 and 8.19 shows the comparison of the results obtained from the measured deposits in the physical and the numerical model. The digital elevation model of the sediment deposits in the physical model were measured by using the measurement data of a three-dimensional laser scanner.

In the physical model the flushing channel is much deeper than the simulated flushing channel in the numerical model. In addition, the numerical model shows more sediment depositions at the outer site of the river bend (Figure 8.19). This deviation can be explained by the fact that due to the very small grain sizes (d_{90}=0.9 mm and d_{50}=0.25 mm) of the deposited sediment in the reservoir, mineral granulates were used to model the sediment transport in the physical model. As a consequence the influence of the cohesive sediment behavior and of the flocculation processes in the prototype were neglected in the physical model. This could lead to higher erosion rates in the physical model. However, excluding this deviation, the deposition and the erosion of very fine and cohesive sediments is modeled well compared to the physical model (Harb et al., 2011).

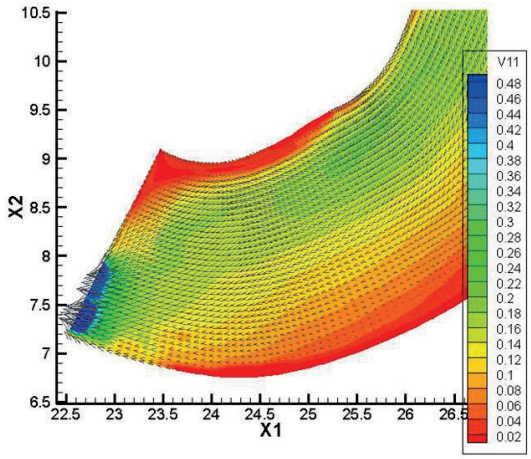

Figure 8.14: *Calculated flow velocities [m/s] and flow vectors at the river bed for the bed levels in 1973 in the event of a 1-year flood with maximum operation level*

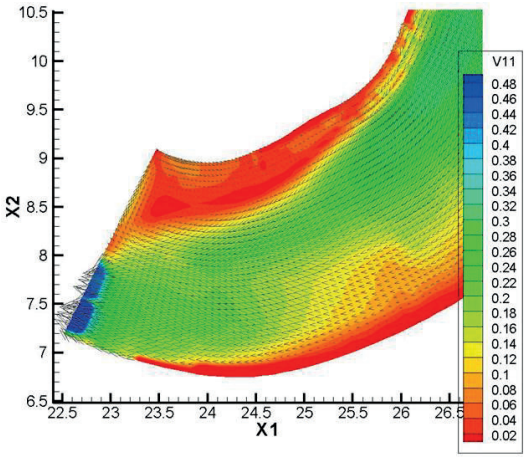

Figure 8.15: *Calculated flow velocities [m/s] and flow vectors at the river bed for the bed levels in 2002 in the event of a 1-year flood with maximum operation level*

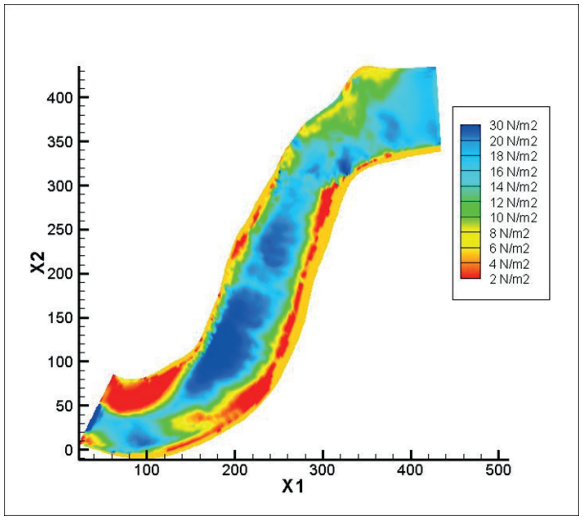

Figure 8.16: *Calculated bed shear stresses derived from the numerical model [N/m^2] for the "soft flushing" case with 1,000 m^3/s and water level in the reservoir of 398 m asl (Harb et al., 2011)*

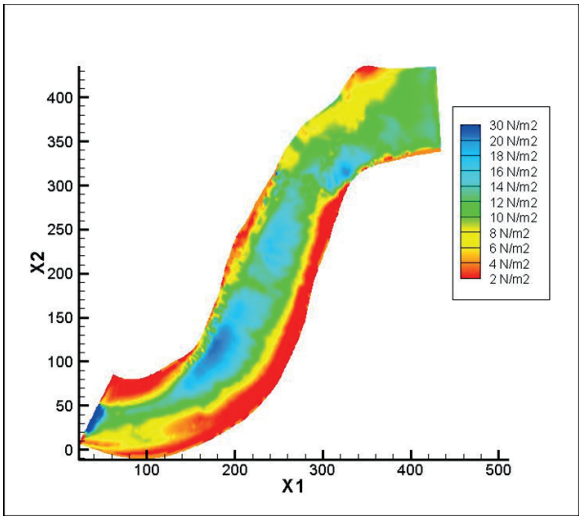

Figure 8.17: *Calculated bed shear stresses derived from the numerical model [N/m^2] for the 10-year flood event with 1,350 m^3/s and water level in the reservoir of 400.5 m asl (Harb et al., 2011)*

8.1.4.6 Conclusion Schönau Reservoir – Investigations Prototype Scale

In the first study (Harb et al., 2011) the characteristic flow pattern, bed shear stresses and the sediment transport were calculated with a three-dimensional numerical model. The results have been compared with ADCP field measurements and ADV measurements in the physical model. The comparisons of the flow velocities in different sections show good agreement. The numerical model predicts the flow characteristics in the river bend very well, but overestimates the high velocities and underestimates the low velocities in the backflow zones. This effect could be caused by slight differences of the reservoir bed geometry, the water level or the non-uniform distribution of the roughness in the reservoir. The turbulence model used may also cause these slight differences in the flow field.

The draw-down of the water level in the presented case also increases the bed shear stresses in the middle of the reservoir and not only close to the weir. The bed shear stresses in the soft flushing case are significantly higher than the bed shear stresses during flood events with higher discharges. Therefore, the regular draw-down of the water-level can reduce the sedimentation and facilitate the erosion of the sediment depositions in the reservoir compared to "normal flood-operation". Due to the fine and cohesive sediments in the prototype synthetic granulates were used to model the sediment transport in the physical model. The numerical model was a replication of the prototype, including the grain sizes of the natural sediment. The deposition and erosion pattern showed a good agreement with the results derived of the physical model, with slight deviations in the channel depth in consequence of the used granulates in the physical model. The model tests showed that in the case of very fine and cohesive sediments the application of physical models is limited. The deposition height could not be reproduced by the numerical model due to the flocculation processes of the fine sediments in the prototype. The description of flocculation processes is very complicated and depends on several parameters. An algorithm to take these processes into account is under development and will improve the results in future. More field data and sediment analysis is required to improve the

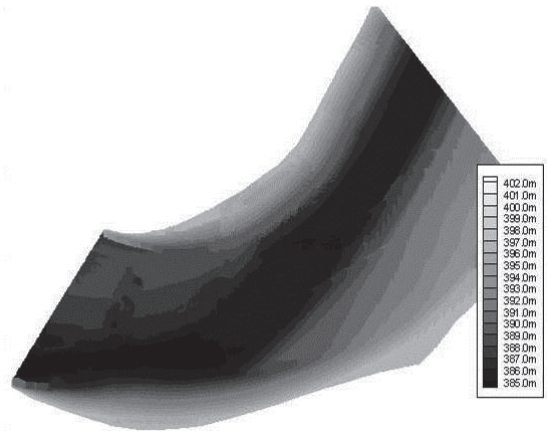

Figure 8.18: *Measured deposition pattern in the physical model in prototype scale [m asl] in the event of a 1-year flood with maximum operation level (Harb et al., 2011)*

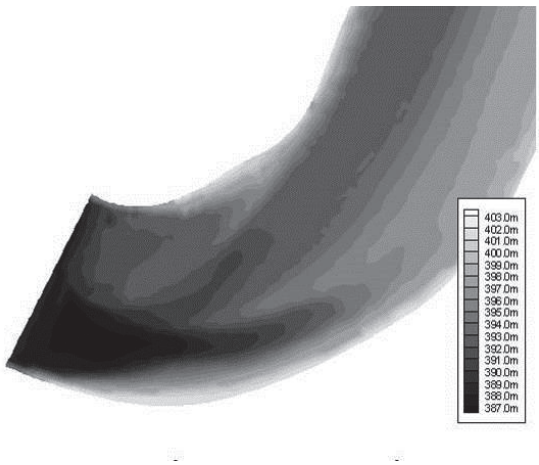

Figure 8.19: *Calculated deposition pattern in the numerical model in prototype scale [m asl] in the event of a 1-year flood with maximum operation level (Harb et al., 2011)*

results of the numerical model further.

8.1.5 Analysis Model Scale and Comparison with Physical Model

The simulations of the sediment depositions in the prototype scale showed that the numerical model was not able to handle the complex flocculation processes at that time. Therefore, a second study of the sediment deposition in model scale was conducted. In the second study, the synthetic granulate, which was used to model the sediment deposition in the physical model, was also implemented in the numerical model.

8.1.5.1 Setup Physical Model – 10-Year Flood

In the second analyzed scenario (Harb et al., 2013b) the flow field and the hydromorphological changes caused by the 10-year flood in the reservoir were analyzed. For the hydrodynamic investigation in the physical model a steady discharge rate of 133.4 l/s was applied with a duration of 6 hours, which represents 1,350 m^3/s and 12 hours in the prototype, respectively. The turbines were shut down during the flood event in accordance to the operation plan. The attached flap gates were fully opened. The left segment gate was shut, the middle and the right ones were opened approx. 30 percent. During the physical model simulation of the 10-year flood about 0.11 m^3 of synthetic granulate was added with a continuous rate of approx. 5 g/s by an upstream located sediment feeding equipment. A digital elevation model of the sediment deposition in the physical model was derived from a three-dimensional scan of the depositions.

8.1.5.2 Numerical Model – Analysis Model Scale

In this scenario the maximum number of cells in the vertical direction was limited to 11. The number of total cells at the beginning of the simulation was chosen with about 50,000, representing a cell size of 0.02 m x 0.02 m in the x-and the y-direction. Caused by changes of the bed and the water levels, 48,600 cells were left after the end of the simulation. The bed roughness was calibrated using the similarity of the water levels in the physical model and the numerical mode. In addition, ADV measurements in the physical model were used for the calibration of the numerical model. The computation was divided into two parts, the computation of the hydrodynamic flow field to obtain a steady flow situation of the flood scenario was made first. The second step was the simulation of the morphological bed changes. The hydrodynamic flow field was updated during the simulation of the morphological bed changes after each time step. The real-time computation times were 12 hours and 16 hours, respectively.

8.1.5.3 Validation of the Numerical Model Using Additional ADV Measurements

Additional ADV measurements for higher discharges were used to validate the numerical model. The comparison of the measured ADV profiles and the calculated velocity profiles can be found in Harb et al. (2013b).

Figure 8.20 and 8.21 show the velocity vectors in front of the intakes computed by the numerical model close to the bed and the surface, respectively. The velocity vectors at the surface cells are pointing to the open outlets at the outer side of the river bend (Figure 8.20). Due to the secondary currents at the bed, the bed vectors point directly to the

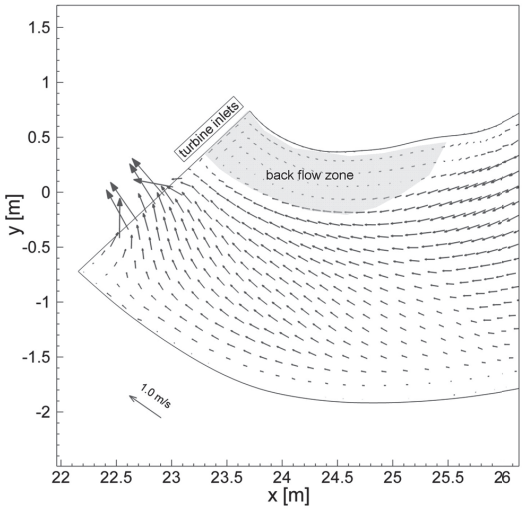

Figure 8.20: *Velocity vectors at the river bed in the area of the intakes for the 10-year flood scenario (plan view) (Harb et al., 2013b)*

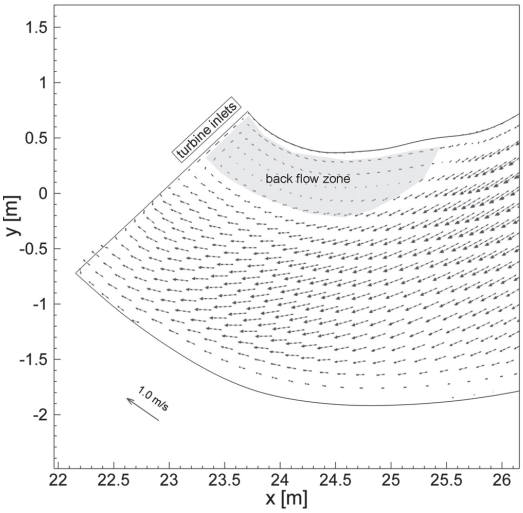

Figure 8.21: *Velocity vectors at the surface in the area of the intakes for the 10-year flood scenario (plan view) (Harb et al., 2013b)*

turbine inlets (Figure 8.21). This influences the sediment transport for the 10-year flood simulation in a massive way.

8.1.5.4 Sediment Deposition Using Synthetic Granulates

The power house is located at the inner side of the river bend in the prototype. Hence, the sediment is transported naturally towards the turbine inlets, which results in sediment deposition in front of the intakes. The results of the hydrodynamic simulation of the 10-year flood scenario show a distinctive back flow zone in front of the turbine inlets, which increases the sediment flow in this direction (see Figure 8.20 and 8.21). This leads to huge depositions in front of the intakes. Figure 8.22 illustrates the deposited synthetic granulates near the turbine inlets after the simulation without turbine operation in the physical model.

In the numerical simulation identical parameters for grain size, fall velocity and density of the synthetic granulate were used as in the physical model. The Shields coefficient was chosen with 0.05 following a sensitivity analysis. The sensitivity analysis conducted showed that the results are very sensitive to changes in this parameter. The Shields parameter was therefore a main calibration parameter for the sediment transport simulation beside the roughness, which was used to calibrate the hydrodynamic flow field.

Figure 8.23 compares the results of the physical and the numerical model. The deposition in the physical model was measured using a three-dimensional laser scanner with a minimum accuracy of +/- 2.0 mm. The data from the laser scan showed a large amount of sediments has deposited in front of the turbines on the orographic right side caused by the secondary currents.

Section 7 and 8 show clearly that the deposition in the physical model starts further upstream as in the numerical model. This difference is most likely caused by small dif-

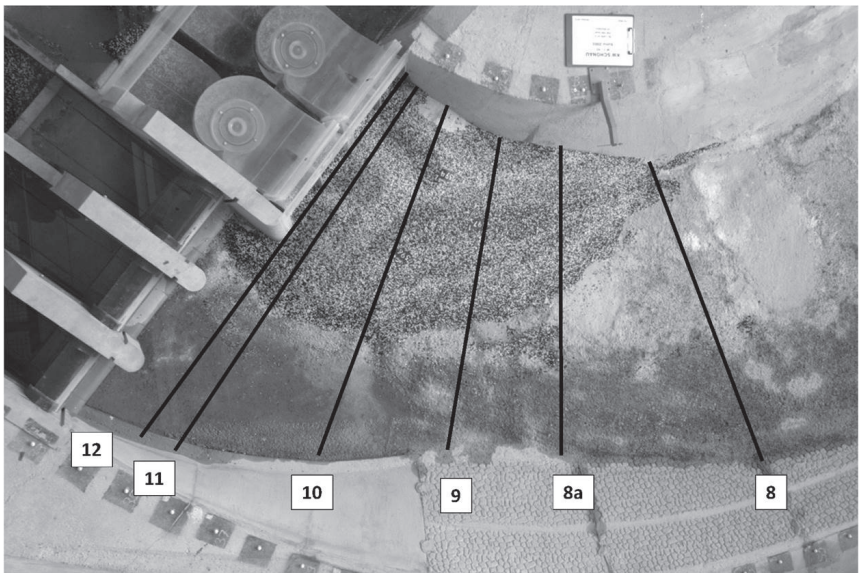

Figure 8.22: *Deposited synthetic granulates after the simulation of a 10-year flood in the physical model (plan view) (Harb et al., 2013b)*

ferences in the water level calculation and the used turbulence model. In the numerical model also a general drift to the inner side of the bend occurs in Section 8, which is most probably a result of an overestimation of the secondary currents in this area. Figure 8.24 shows the measured velocity vectors in the y-direction and the z-direction indicating the secondary currents in Section 9.

The deposition pattern in the physical model is wider than in the numerical model (Section 9, 10 and 11). The results showed also that the slopes of the deposited material have a steeper angle in the numerical simulation than in the physical study. This difference can be a result of the implemented sand slide algorithm, which does not take the properties, especially the plastic particles angle of repose completely into account. The result of Section 11 shows that the peak piles up in front of the closed intakes at the inner side of the bend in the numerical simulation. This agrees physically very well with the plotted velocity vectors in Figure 8.24. The numerical model, however, produces a compact deposition structure at the inner side of the bend and deposits too little sediments in the middle of the reservoir. An overestimation of the secondary currents could cause this displacement. A first order upwind scheme was used for the simulations, because the simulation with a second order upwind scheme would increase the overestimated eddies and secondary currents additionally.

8.1.5.5 Conclusion Schönau Reservoir – Investigations Model Scale

In the second analyses scenario (Harb et al., 2013b) presents the application of a three-dimensional numerical model for the prediction of morphological bed changes compared with a physical model. In both models the sediment depositions in a reservoir during a 10-year flood were simulated. Because of the small grain sizes in the prototype, synthetic granulate was used to model the deposition in the physical model. The numerical simulation was a replication of the physical model, including geometry, hydrodynamic boundaries and sediment properties. The hydrodynamic results of the three-dimensional

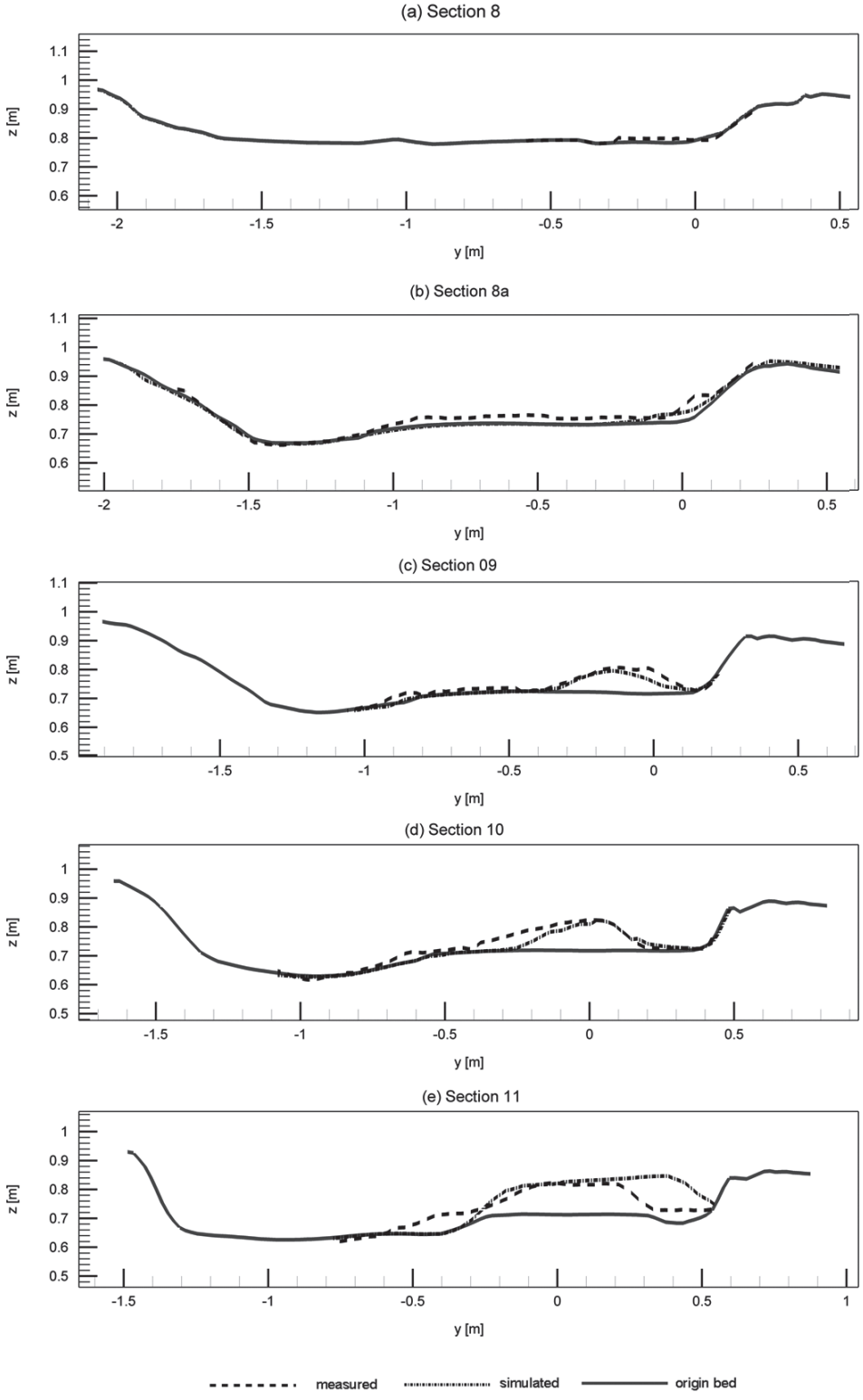

Figure 8.23: *Comparison of the measured and simulated depositions (Harb et al., 2013b)*

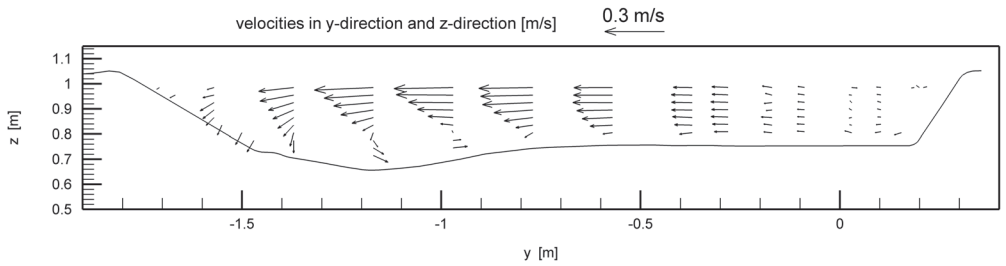

Figure 8.24: *Measured velocity vectors from the ADV measurements in Section 9 (Harb et al., 2013b)*

numerical model have been verified with ADV measurements conducted in the physical model. The comparisons of the flow velocities and the characteristic flow pattern show a good accuracy level. The maximum as well as the minimum flow velocities and the flow characteristics upstream of the intakes are predicted well. However, due to the approximations in the numerical model and small assumptions in the model setup (e.g., the complex partial opening of the gates at the weir, which could not be reproduced by the numerical model) small differences could be recognized. The bed load transport formula by van Rijn, developed for uniform and non-cohesive sediments, was used in this study to calculate the transport of the synthetic granulates.

It is demonstrated, that the computed bed elevation changes are in an overall agreement with the measured depositions. Although minor differences in the deposition pattern could be recognized, the results of the three-dimensional numerical model are consistent with the measured depositions in the physical model. The results support the application of the numerical model as part of a hybrid modeling approach in further sediment studies.

8.2 Case Study Fisching

The following analysis is partly cited from Harb et al. (2013a).

The second presented case study is the Fisching reservoir, which is located at the river Mur in Styria. In this case study a numerical analysis was carried out to investigate the sediment transport processes in the reservoir during two flushing events in 2009 and 2012. During the flood event 2009 the water level was partially lowered to enable the sediment transport in the reservoir. At the flood event in 2012 free flow conditions occurred and a large amount of sediments was removed from the reservoir. This two cases were analyzed and are presented in this study. The analysis focused on the hydrodynamic aspects and on the sediment transport processes during the flood events.

8.2.1 Project Description and Background – Fisching Reservoir

The reservoir is approximately 4.5 km long and had a average width of 80-100 m. The initial storage volume was about 1.4 million m^3. Previous conducted investigations showed that 85,000 m^3 of sediments deposit in the reservoir annually. A small amount of the deposited sediments has been eroded and transported through the reservoir during former flushing events. However, echo-soundings performed in 2009 showed that approximately 860,000 m^3 of sediments are already deposited in the reservoir. This represents an annual sedimentation rate of about 6.1 percent of the initial reservoir volume. Figure 8.25 shows an overview of the meandering reservoir with the sediment sampling points.

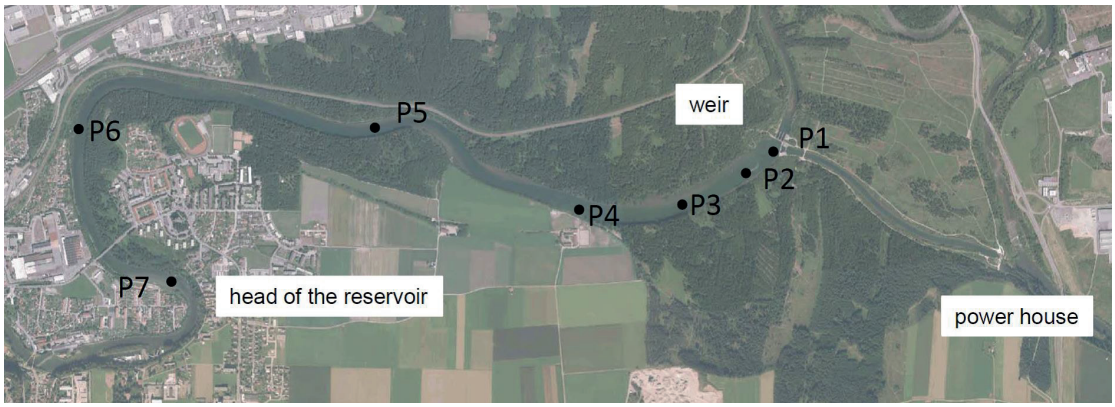

Figure 8.25: *Project area Fisching with sediment sampling points (Harb et al., 2013a)*

The head of the reservoir is located in an urban area. Hence, the rising of the bed levels in the reservoir and especially in this area creates a problem concerning flood safety for the surrounding areas. Figure 8.26 illustrates the rising of the bed levels since the start of operation. The deposition height in front of the weir is about 4-5 m, the deposition height at the head of the reservoir is about 0.5-1 m.

8.2.2 Sediment Sampling in the Fisching Reservoir

Seven representative sediment samples were taken from the reservoir and sieved according to the Austrian Standard in 2010. The freeze-core method was used for taking the sediment samples, starting from the weir (Sample 1) to the head of the reservoir (Sample 7). The locations of the sediment sampling points can be found in Figure 8.25. Large

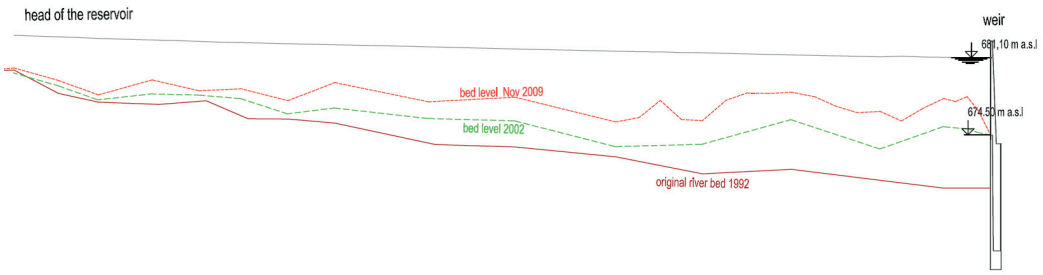

Figure 8.26: *Rising of the bed levels caused by sedimentation in the reservoir, longitudinal section from the head of the reservoir to the weir (Harb et al., 2013a)*

variations in the grain sizes between Sample 1 and Sample 7 can be observed. The mean diameter d_m of Sample 1 is below 0.1 mm, whereas the d_m of Sample 7 at the head of the reservoir is about 20 mm, which is still relatively small for a reservoir in an Alpine river. Figure 8.27 illustrates the grain-size distribution of all samples.

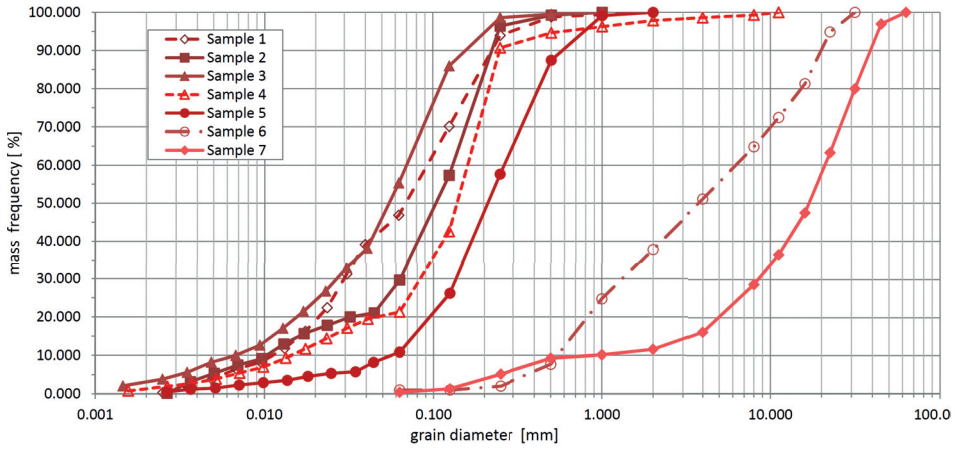

Figure 8.27: *Grain size distributions of the sediment samples taken in the Fisching reservoir (Harb et al., 2013a)*

8.2.3 Numerical Simulations – Fisching Reservoir

The hydrodynamic simulations of the presented cases were performed with TELEMAC-3D. A short description of the TELEMAC suite is given in Chapter 6. More detailed information can be found in Hervouet (2007).
The simulations in the presented cases were performed with a hydrostatic pressure assumption, because a conduced sensitivity analysis showed that the use of the non-hydrostatic pressure assumption did not change the results in this kind of applications significantly. In TELEMAC-3D the two-dimensional triangular mesh is extended to the vertical dimension by the implementation of a number of planes or levels. In the Fisching cases a homogeneous distribution in the vertical direction with five levels was used. The sensitivity analysis using ten levels for the vertical discretization proved that no differences occurred in the computed water surface or in the velocity field compared to the use of five levels. The method of characteristics was chosen, but also several other schemes are

available for the computation of the advection terms. The solver offers a semi-implicit scheme for the time integration. TELEMAC-3D is able to separate the vertical and horizontal turbulence scales for modeling of the turbulence. In the investigations a constant eddy viscosity was applied for the horizontal turbulence and the Prandtl mixing length model was used for the vertical turbulence. The Prandtl mixing length model expresses the turbulent viscosity as a function of the mean velocity gradient and the mixing length (Section 6.4.2.2). The Strickler friction law was applied to compute the energy losses caused by bottom friction with a constant Strickler value of 35 $m^{1/3}/s$ for the whole domain. A time step of 1.0 second was chosen for the numerical simulation. For the sediment transport simulations TELEMAC-3D was internally coupled with the morphological module SISYPHE. For the calculation of the sediment transport the formulae of Meyer-Peter-Müller, Engelund-Hansen and Van Rijn were used. The evaluation of the sediment transport functions compared with the measured erosion and deposition pattern in the reservoir is presented later. The active layer thickness was set to 0.05 m, the slope correction function for the bed shear stress, the skin friction correction algorithm, the hiding/exposure algorithm and the deviation formula were used. Based on the existing bathymetry data, two three-dimensional digital elevation models were generated for each case; one before and one after the flushing event. The mesh with approximately 211,500 prismatic cells and an average edge length of 4 m was mapped on the digital elevation model using the free software BlueKenue (CHC, 2011).

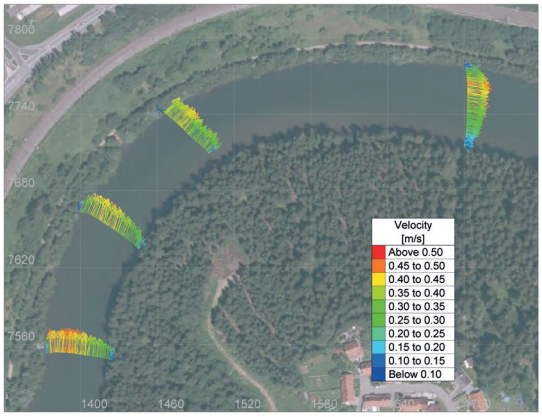

Figure 8.28: *Measured depth-averaged velocities vectors derived from the ADCP measurements at turbine operation (Harb et al., 2013a)*

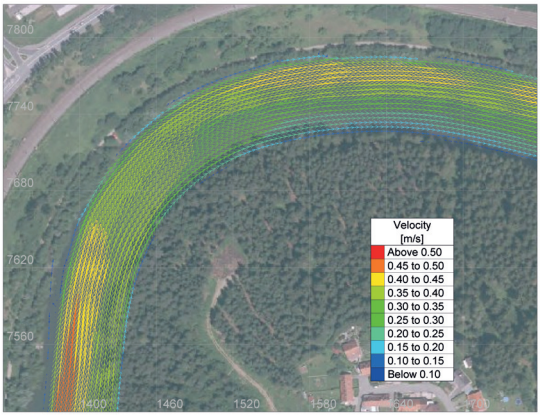

Figure 8.29: *Calculated depth-averaged velocities vectors at turbine operation (Harb et al., 2013a)*

8.2.4 Validation of the Numerical Model using Field Measurements

The hydrodynamic model was validated using ADCP measurements performed at the prototype. The ADCP measurements were performed during normal turbine operation. The velocity fields from the measurements were analyzed using the Open Source post-processing software ADCPtool (Dorfmann and Steidl, 2013). With this ADCP tool two-dimensional depth averaged flow velocities were calculated and georeferenced. Figure 8.28 and 8.29 compare the measured ADCP flow velocities and the computed depth averaged velocities resulting from the 3-D hydrodynamic model. The figures illustrate that

the magnitude and the direction magnitude and the direction of the calculated velocity vectors compare well with the measured velocity vectors.

8.2.5 Analysis of the Flushing Event in 2009

In May 2009 a small flood event was used to lower the water level in the reservoir to initiate the erosion of the deposited sediments in the reservoir. The flood event had a maximum discharge of approximately 205 m^3/s (nearly 1-year flood). The water level was partially lowered about 1.6 m from the maximum operation level at 681.1 m asl to 679.5 m asl. Therefore, this flushing event was conducted as pressure flushing without full draw down at the weir. The water level at the weir and the inflow hydrograph are shown in Figure 8.30.

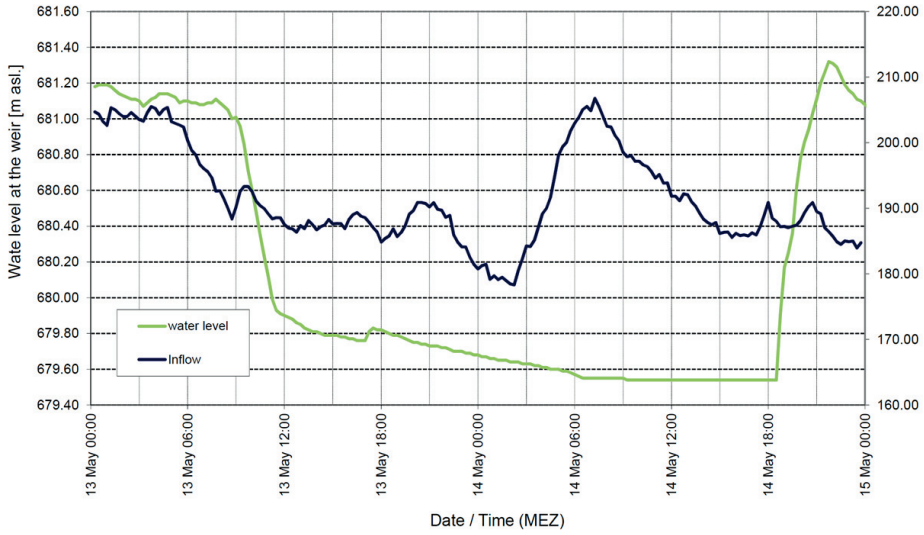

Figure 8.30: *Hydrograph of the flood event in May 2009, provided by the Hydrographic Institute of the Government of Styria*

8.2.5.1 Evaluation of the Bed Changes Caused by the Flushing Event 2009

Echo-soundings performed before and after the flushing event were used to evaluate the morphological changes calculated by the numerical model. The measured bed levels before (Figure 8.31) and after the flushing event (Figure 8.32) were used to calculate the differences in the bed levels and the erosion pattern caused by the flushing operation. The differences in the bed levels (Figure 8.33) were used for validation of the numerical model. The measurements are unusual and hence very interesting, because in this case most of the erosion occurred at the inner site of the river bends and not on the outer side as expected. This effect may be caused by the complex meandering geometry of the reservoir and the flushing operation itself. The massive depositions at the inner site of the river bend are eroded in the event of higher discharges. Additional sand slides and instabilities at the river banks lead to the erosion on the inner site and deposition on the outer site of the river bend. The flushing was performed with a maximum discharge of about 205 m^3/s (nearly 1-year flood). The lowering of the water level during at the weir during the flushing event was only 1.6 m. The water level in the reservoir was thus

relatively high and the bed shear stress at the outer bends was apparently not high enough to deepen the flushing channel. Erosion of the sediment depositions at the inner side of the river bank was caused due to bank failures and sand slides. A part of these eroded sediments were again deposited in the outer river bends.

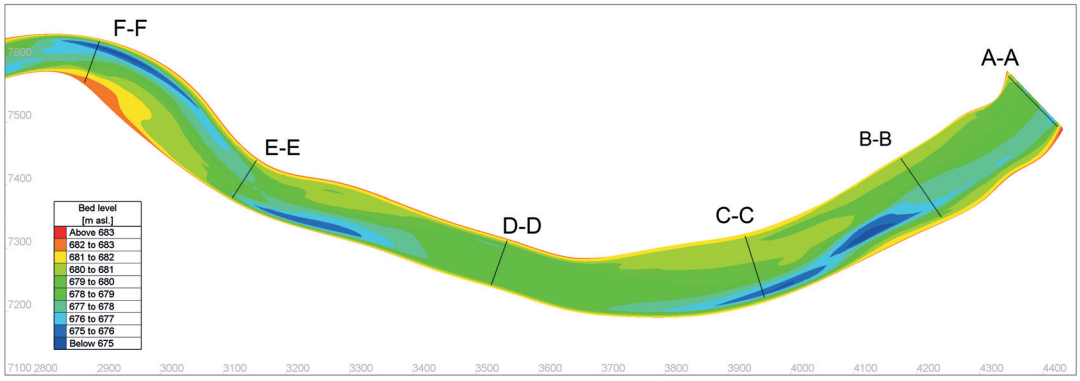

Figure 8.31: *Digital elevation model of the reservoir bed in Fisching before the flood event 2009*

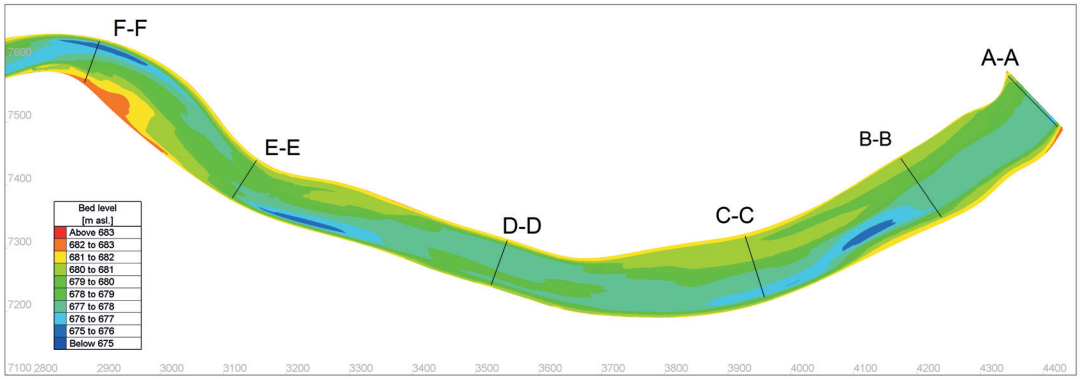

Figure 8.32: *Digital elevation model of the reservoir bed in Fisching after the flood event 2009*

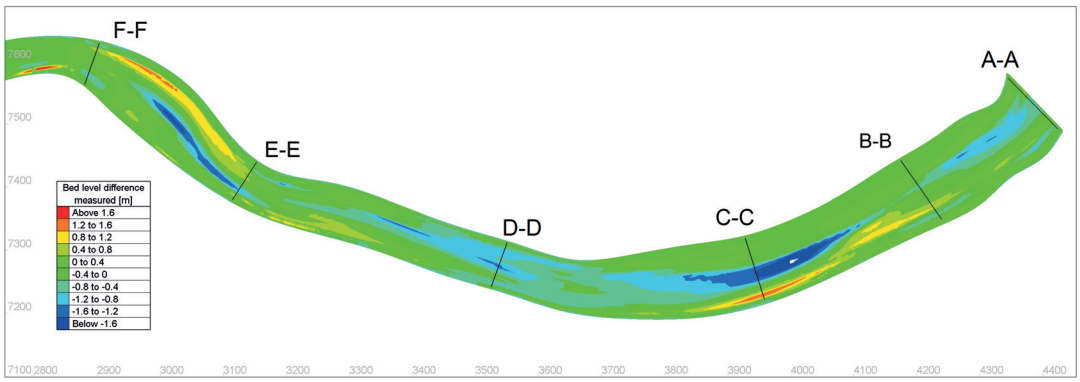

Figure 8.33: *Measured bed level changes obtained by subtracting the digital elevation models before and after the flushing event in May 2009*

8.2.5.2 Numerical Simulation of the Sediment Transport Caused by the Flushing Event 2009

The simulation of the sediment transport caused by the flood event 2009 was not trivial because of the complex erosion pattern in the reservoir. A sensitivity analysis was thus carried out to evaluate the most important parameters for this event. The following parameters were varied:

- Sediment transport formulae (Meyer-Peter-Müller, Engelund-Hansen, Van Rijn)
- Skin friction correction due to bed forms
- Slope effect formula and deviation formula
- Different hiding and exposure functions

The different sediment transport functions influenced the calculated sediment transport rates and the calculated bed changes. The variation of the different implemented hiding and exposure formulas (Egiazaroff, Ashida & Michiue, Karim, Holly & Yang) showed only marginal differences. The use of a slope effect formula improved the results. However, the slope effect formulas of Koch et Flokstra and Soulsby gave similar results. The sensitivity analysis showed that the skin friction correction and the deviation formula affect the results significantly. Without the deviation formula the erosion pattern is inverted due to the secondary currents effect and the direction of the shear stress vectors. In the sections C-C, D-D and E-E so called "furrows" occurred in the first numerical simulations. Figure 8.34 shows a typical pattern with these furrows. This erosion pattern was a result of small differences in the water level from one node of the mesh to the other. Therefore, the free surface gradient was varied and a value below 0.5 gave slightly better results (the default value is set equal to 0.9). But it was not possible to get rid of these "furrow-pattern" totally.

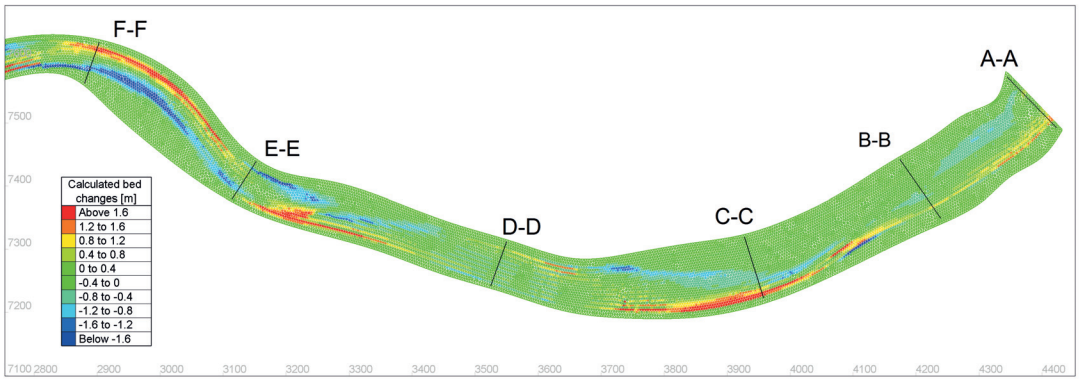

Figure 8.34: *Calculated bed changes using the Van Rijn formula with derived "furrow-pattern" in the sections C-C, D-D and E-E*

Figure 8.35 shows the measured and the calculated bed changes in different sections. In the sections C-C, D-D and E-E, the calculated bed levels have been averaged to eliminate the furrow pattern. The implemented skin friction correction algorithm reduces the

calculated sediment transport rates are in the areas with very fine sediment very to approximately 20 percent of the total shear stresses. Therefore, the calculated bed changes were too low in most areas (Figure 8.35). The calculated bed changes show only in section B-B and E-E a very good agreement with the measured bed changes. Otherwise, without skin friction correction, the calculated sediment transport rates would be much too high.

The calculated bed changes derived using the Engelund-Hansen formula showed the highest deviations to the measured bed changes. Although the three-dimensional model is able to take the secondary currents into account and the use of the slope effect and the deviation algorithm, the measured erosion pattern could not be reproduced using the Engelund-Hansen formula. The calculated bed changes obtained by the Meyer-Peter-Müller formula and the formula of van Rijn show good agreement with the measured bed changes, but the calculated bed levels tend to be too high. This difference may be caused by the skin friction algorithm, which is apparently not able to take the grain sizes in these areas in combination with the occurring bed forms correct into account.

8.2.5.3 Conclusion for the Sediment Transport Simulations of the Flushing Event 2009

This study focus on the simulation of the sediment transport processes during a flushing event in an Alpine reservoir. The open source numerical model TELEMAC-3D combined with the morphological module SISYPHE was used to simulate the sediment transport processes. The results of the numerical model were compared with the measured bed changes. These measurements are unusual and hence interesting, because in this special case most of the erosion occurred at the inner site of the river bends. This effect may be caused by the complex meandering geometry of the reservoir, the relatively high water level, sand slides and instabilities at the river banks. The sediment transport formulae of Engelund-Hansen, Meyer-Peter-Müller and Van Rijn were used to model the sediment transport. The calculated bed changes derived from Meyer-Peter-Müller and Van Rijn formula showed the best agreement with the measured bed changes. An adaptation of the skin friction correction could thus also improve the results of the simulations.

However, the simulation results showed a “furrow” pattern in the computed bed changes. These “furrows” are caused by small differences in the computed water level from one node to the other node of the mesh, lead to higher shear stresses in some nodes and result in this erosion pattern. The occurrence of these “furrows” could be limited with the adaption of the free surface coefficient and the adaption of the positive depth algorithm, but it was not possible to eliminate them totally.

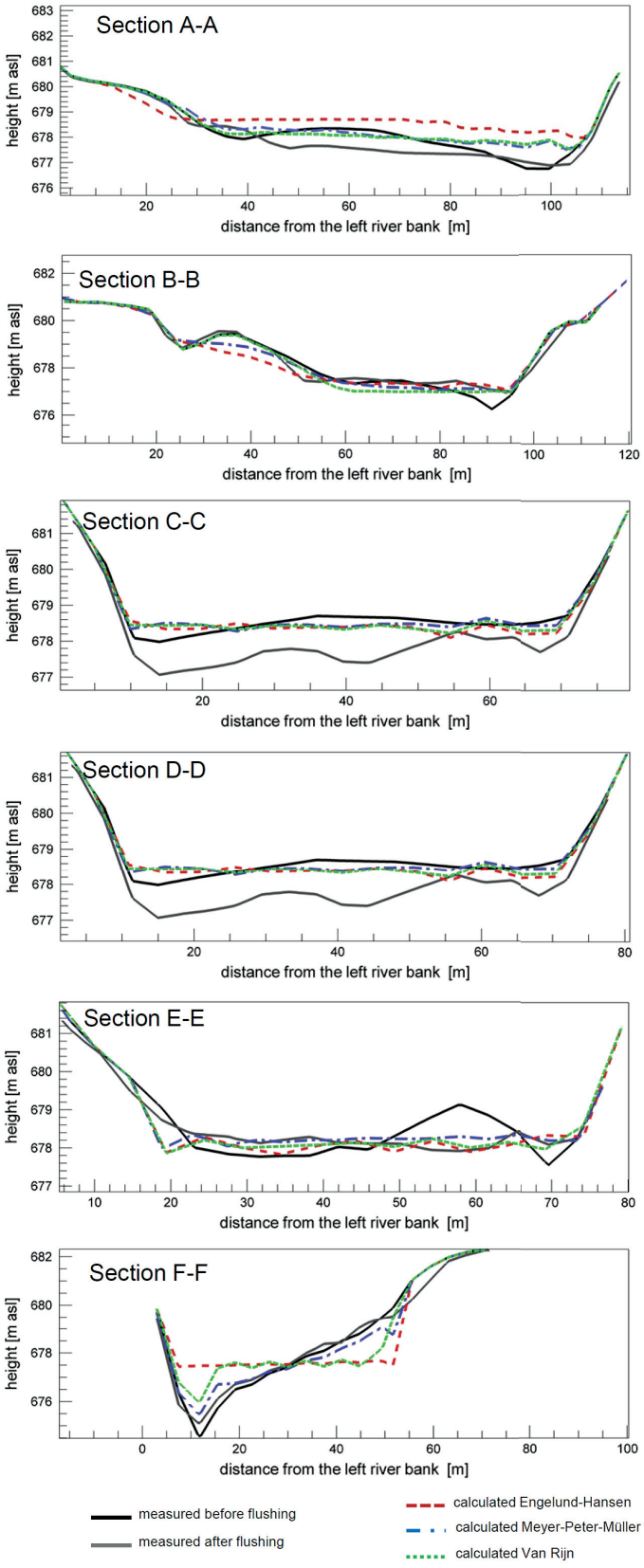

Figure 8.35: *Measured and calculated bed level changes*

8.2.6 Analysis of the Flushing Event in 2012

In July 2012, two flood events with a probability of approximately 0.2 and 0.05 (5-year flood and 20-year flood) occurred within 10 days. The water level in the reservoir was lowered according to the operation rules of the hydro power plant and a large amount of sediment was eroded in the reservoir. Figure 8.36 shows the hydrograph of the flood events in July 2012.

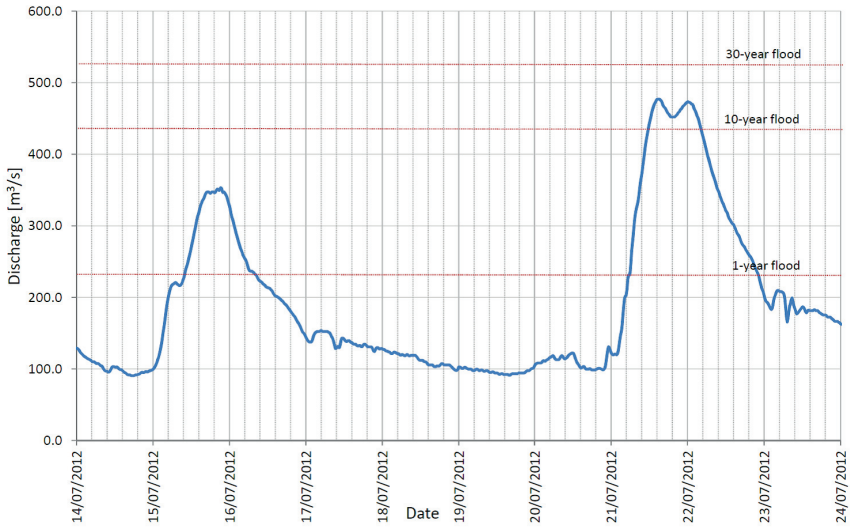

Figure 8.36: *Hydrograph of the flood events in July 2012, provided by the Hydrographic Institute of the Government of Styria (Harb et al., 2013a)*

8.2.6.1 Evaluation of the Bed Changes caused by the Flushing Event 2012

Echo-soundings before and after the flushing event were used to analyze the morphological changes. Based on the measurements two digital elevation models were developed. The digital elevation model before (Figure 8.37) and after the flushing event (Figure 8.38) were used to calculate the differences in the bed levels and the resulting erosion pattern caused by the flushing operation. The measured differences in the bed levels are shown in Figure 8.39. The erosion at the head of the reservoir and in the upper part of the reservoir was limited due to the larger grain sizes and the armored river bed at the head of the reservoir. Massive erosion occurred in the first half of the reservoir upstream of the weir with a lowering of the bed levels in the range of up to 2 m. At the flushing event in July 2012 approximately 240,000 m^3 of sediment depositions were removed from the reservoir.

The erosion pattern of the flushing event in 2012 differs significantly from the erosion pattern in 2009. These differences may be caused by the much higher discharge and the free flow conditions in 2012. Therefore, the deposited sediment in front of the weir was eroded after several hours. Hence, the water level in the reservoir also lowered due to lowering of the bed levels at the weir and this effect increased the slope in the reservoir. The increased slope in the reservoir enhanced the sediment transport and lead to higher erosion rates. In consequence, the water levels lowered again.

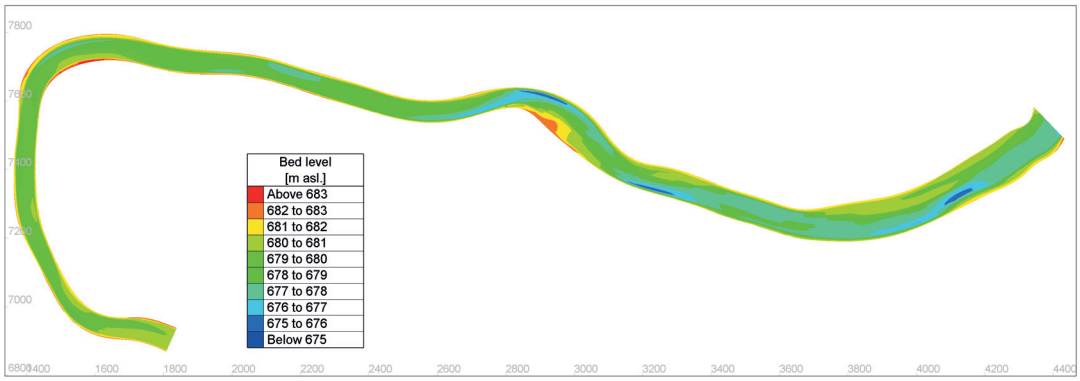

Figure 8.37: *Digital elevation model of the reservoir bed in Fisching before the flushing event in July 2012 (Harb et al., 2013a)*

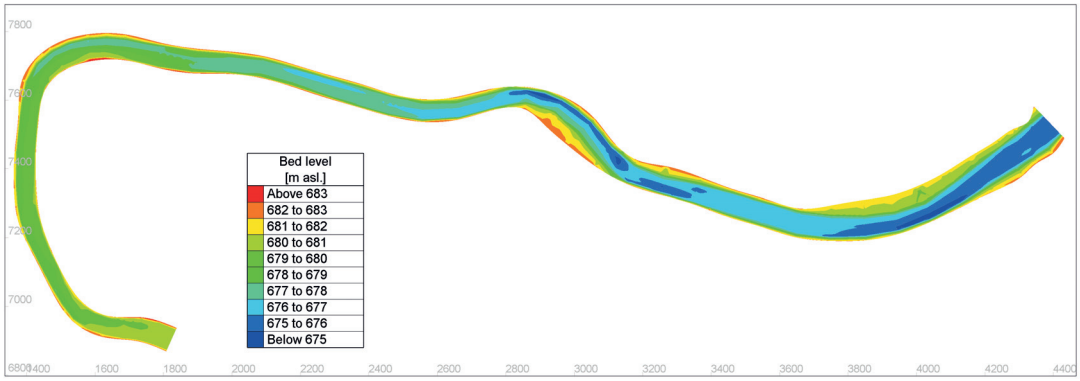

Figure 8.38: *Digital elevation model of the reservoir bed in Fisching after the flushing event in July 2012 (Harb et al., 2013a)*

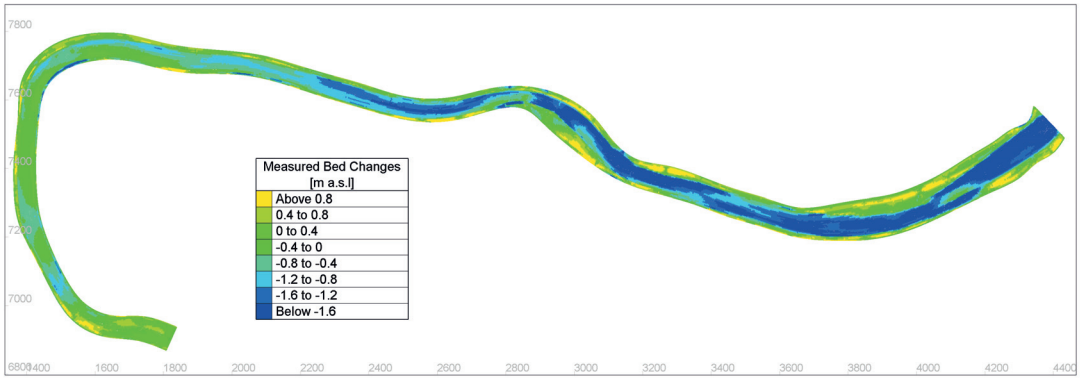

Figure 8.39: *Measured bed changes obtained by subtracting the digital elevation models before and after the flushing event in July 2012 (Harb et al., 2013a)*

8.2.6.2 Numerical Analysis of the Changes of the Water Level Caused by the Flushing Event in 2012

The massive sediment depositions in the reservoir increased the flood risk due to the rising bed levels before the flushing event 2012. During the flushing event in July 2012 a large amount of sediment depositions were removed from the reservoir. The average bed slope in the reservoir increased, because of the erosion of these sediment depositions. Hence, in

the case of free flow conditions the water level during flood events decreases and the bed shear stress increases. The differences in the water levels are shown in Figure 8.40. The water level decreased in the whole reservoir. The highest differences in the water level are in the first half of the reservoir upstream of the weir. These higher differences are caused by the massive sediment erosion which indicates a good flushing efficiency in the zone upstream of the weir.

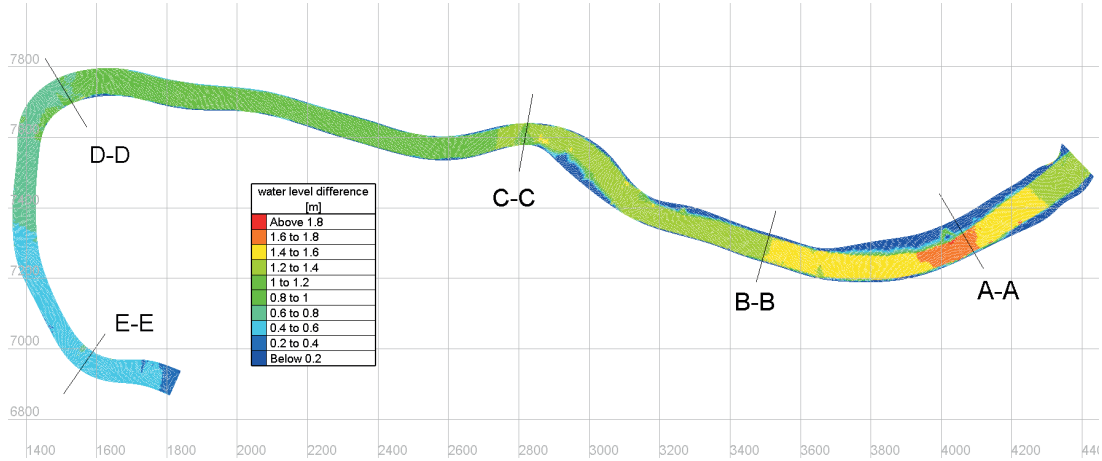

Figure 8.40: *Differences in the water level as a consequence of the flushing event in 2012 and the desilting of the reservoir (Harb et al., 2013a)*

Figure 8.41 illustrates the changes in the bed levels and the caused differences in the water level for the cross sections A-A to E-E. The erosion of the sediment depositions decreases from the weir (cross section A-A) to the head of the reservoir (cross section E-E). Thus, also the lowering of the water level is higher at cross sections A-A and B-B than at cross sections D-D and E-E. The analysis of the water levels showed that the flushing of the reservoir lowered the flood probability of the urban areas at the head of the reservoir significantly.

8.2.6.3 Numerical Analysis of the Bed Shear Stresses in the Fisching Reservoir - Flushing Event 2012

The bed shear stresses in the reservoir were modeled to provide a better understanding of the sediment transport processes in the reservoir during a flushing event. Figure 8.42 illustrates the calculated total bed shear stresses for the bed levels before the flushing event in July 2012 in the event of a 20-year flood. The highest bed shear stresses occur at the weir. The bed shear stresses at the upper part of the reservoir and at the head of the reservoir are relatively low. This low bed shear stresses and the reduced slope in the reservoir caused by the massive sediment depositions reduces the sediment transport capacity in the reservoir during flushing events. This effect decreases the possible erosion in the reservoir with continuous progression of the reservoir sedimentation. In the Alpine area flushing events are linked to hydrological boundaries such as flood events. Therefore, large flushing events like the flushing event in July 2012 cannot be planned in advance, but can be used to remove sediment depositions from reservoirs. A large quantity of deposited sediments caused by the previously mentioned high discharge and the long duration of the flushing event could be eroded from the reservoir. Therefore, the bed shear stresses for the

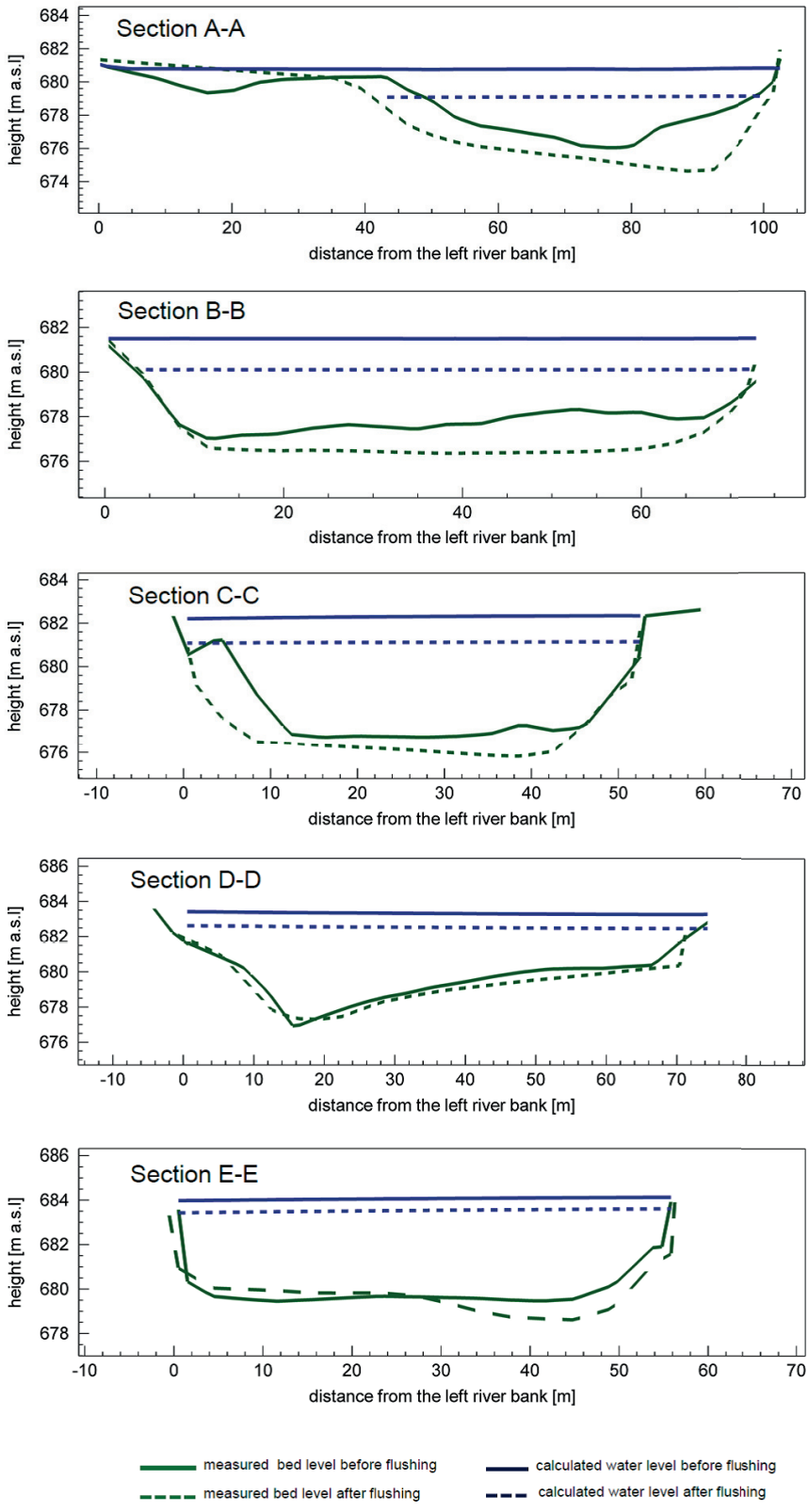

Figure 8.41: *Changes in the bed level and in the water level caused by the flushing event 2012 in the sections A-A to E-E (Harb et al., 2013a)*

bed levels after the flushing event in July 2012 are much higher due to the increased bed slope in the reservoir (Figure 8.43). The higher bed shear stresses will lead to enhanced sediment erosion during future flushing events even during smaller flood events.

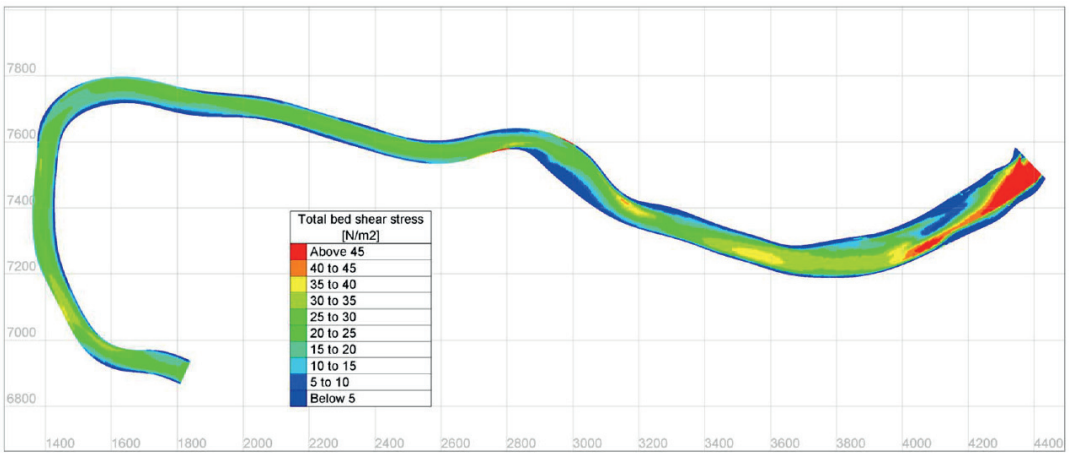

Figure 8.42: *Calculated total bed shear stress before the flushing event in July 2012 for a 20-year flood (Harb et al., 2013a)*

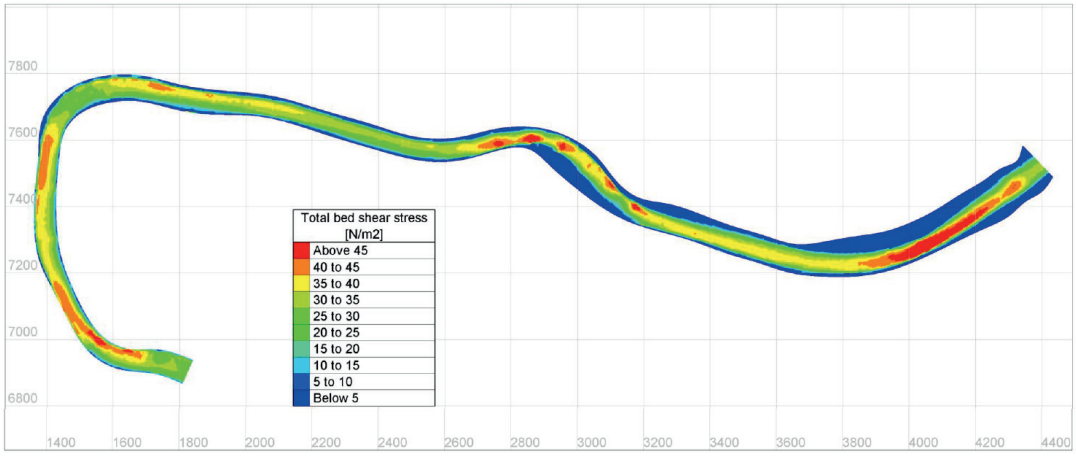

Figure 8.43: *Calculated total bed shear stress after the flushing event in July 2012 for a 20-year flood (Harb et al., 2013a)*

8.2.6.4 Conclusion and Next Steps - Flushing Event 2012

The study presented discussed the simulation of a flushing event in an Alpine reservoir. The bed levels in the reservoir were analyzed using echo-soundings of the reservoir before and after the flushing event. It is shown that a large part of the massive sediment depositions in the reservoir were eroded due to the flushing event. During the flushing event in 2012 the highest erosion rates occurred in the first half of the reservoir upstream of the weir with a lowering of the bed level in the reservoir of up to 2 m. In this area the mean grain size of the sediment depositions was below 0.1 mm. The erosion at the head of the reservoir and in the upper part of the reservoir was limited due to the larger grain sizes (about 20 mm) and the armored river bed. The numerical analysis showed that the removal of the sediment depositions increased the bed slope in the reservoir and led to the lowering of the water level in the reservoir. Hence, the probability of flooding decreased

for the urban areas near the head of the reservoir. The increased bed slope in the reservoir and the lower water level also enhances the bed shear stresses in the reservoir. These changed conditions could increase the flushing efficiency for performing flushing during smaller flood events. However, the possibility of flushing is strictly linked to the hydrological conditions and and the flood events associated with them in the Alpine area. The next steps in this study will be the numerical modeling of the sediment transport processes during the flushing event in July 2012.

9 CONCLUSION AND OUTLOOK

Reservoir sedimentation is a problem in many Alpine reservoirs. Many rivers must deal with the consequences of reservoir sedimentation, such as the coarsening and armoring of the river bed downstream. However, the sediment transport processes in reservoirs are very complex and appropriate knowledge is necessary to solve these problems. In the case of reservoirs of run-off river and diversion plants the water depth is usually lower than in reservoirs of storage and pump-storage hydro power plants. Therefore, a larger part of the suspended sediments is transported through the reservoir and the deposition of bed load fractions is the main problem. The deposition of coarse sediments at the head of the reservoir may cause problems regarding flood protection by raising the bed level and thus, raising the water level too. Furthermore massive sediment depositions in front of the turbine intakes, upstream or downstream of the weir or at the water intake can limit the operation and the electrical energy output of the hydro power plant.

The implementation of a successful sediment management needs appropriate knowledge of the sedimentation and erosion processes in reservoirs. However, every reservoir is unique in terms of its purpose, geometry and other factors such as hydrological and hydraulic conditions. Consequently, not every sediment management method is suitable for every reservoir. Reservoir flushing is one of many possible approaches to remove deposited sediment, but often a combination of sediment management methods will be necessary to limit the sedimentation in a reservoir. In general, reservoir flushing involves the lowering of the water level at the weir by opening the weir gates or low-level outlets. The lowered water level increases the bed shear stress in the reservoir and facilitates erosion on the river bed in the reservoir. The periodical flushing of sediments from reservoirs has many advantages from a river-morphological as well as economic point of view. The connectivity of river systems is also in terms of sediment transport important for the ecosystem of the downstream area. Reservoir flushing is most effective in the case of sufficient discharge and free surface flow in the reservoir. Therefore, reservoir flushing in Alpine reservoirs is normally performed during natural floods or higher discharges.

The critical shear stress is one of the most important parameters concerning sediment transport processes with fine sediments. Hence, a series of flume experiments and basic tests were conducted to evaluate the critical shears stress of cohesive sediments. The flume tests showed that the estimation of the critical shear stress of cohesive sediments can be difficult. Cohesion, consolidation, vertical sediment layers and many other factors influence the critical shear stress. However, the critical shear stress influences the possible erosion rates in the reservoir and is therefore a key factor for reservoir flushing. In the experiments the Reynolds shear stress and the gravity method were used to calculate the critical shear stress of the cohesive sediments. The results of the two methods are in agreement, which confirms that nearly uniform flow conditions occurred in the flume.

The average critical shear stresses obtained are above most of the values found in previous conducted studies. This effect can be explained by the fact that in this case consolidated sediment samples taken from a reservoir were used in the experiments, whereas in many other studies artificial sediment mixtures were analyzed.

In addition vane strength measurements were performed in the reservoirs to evaluate the undrained shear strength of the sediment depositions. The vane strength values obtained were related to the critical shear stresses derived from the experiments in the flume. The function obtained by Kamphuis and Hall (1983) was adapted with the new measurement data and may be used for a rough estimation of the critical shear stress, based on measured vane strength values in selected reservoirs. However, this rough estimation should be handled with care in further studies and additional field data to validate the function will be necessary.

The assessment and the selection of the possible sediment management methods is an important task and can be improved by numerical analysis. Therefore, two different three-dimensional CFD programs were used to investigate the sediment transport processes in two Alpine reservoirs in Austria. The aim of the study was to evaluate the success of flushing operations in the reservoir and to assess the effect of the reservoir flushing on the flood risk of the surrounding areas. The CFD program SSIIM was used for the simulations of flushing and flood events at the reservoir Schönau and compared to the results derived from physical model test. The CFD program TELEMAC-3D was validated with data from field measurements in the reservoir Fisching.

The two investigated reservoirs have a complex geometry and hence a complex flow pattern. Accurate input data is a major factor influencing the quality of the simulations. An appropriate simulation is not possible without data about the water level at the weir, the discharge, the sediment parameters in the reservoir and the sediment inflow in the reservoir. The calibration and validation of numerical models is also an important point to ensure the quality of the simulation results. In the case studies ADV measurements in the physical model or ADCP field measurements in the prototype were used to calibrate the flow field. In the case of the Schönau reservoir the ADV measurements of flood events in the physical model could be used for the validation of the flow field. The hydrodynamic simulations showed that both three-dimensional models are able to reproduce the complex flow fields very well, but overestimates the high velocities and underestimates the low velocities in some areas, e.g., in the backflow zones. This effect could be caused by slight differences of the implemented reservoir bed geometry, the water level or the non-uniform distribution of the roughness in the prototype and in the physical model, respectively. Also the used turbulence models may cause these slight differences in the flow fields. Additional measurements of the water levels in the middle or at the head of the reservoir may help to improve the results of flood or flushing simulations.

The sediment transport was validated with measurement data of the bed level changes in the prototype and in the physical model. In general, the deposition and erosion pattern showed a good agreement with the validation data, but the two case studies showed some problems in the simulation of sediment transport processes as well.

In the first study of the Schönau reservoir the numerical model was a replication of the prototype, including the grain sizes of the natural sediment. However, in the physical model study, which was used for the validation, granulates were used to model the sed-

iment transport due to the fine and cohesive sediments in the prototype. Therefore, the cohesive behavior of the sediments was neglected in the physical model, but is taken into account in the numerical model. Neither the physical model nor the numerical model were able to take the flocculation processes of the fine sediments into account. Because of these effects, the deposition height and the depth of the flushing channel could not be reproduced by the numerical model compared with the physical model. However, the application of the physical models is limited in the case of very fine and cohesive sediments. In contrast to the numerical model, the consideration of cohesive forces and flocculation processes will not be possible in the case of scale models. The implementation of flocculation processes in numerical models is not straightforward as well. The description of flocculation processes is very complicated and depend on several parameters. A flocculation algorithm is under development and will improve the results in future. Additional field data and sediment analysis are required to improve the results of such simulations further.

The second numerical study of the Schönau reservoir focused on the sediment deposition in the physical model including the synthetic granulate. In this case the computed bed elevation changes are in an overall agreement with the measured depositions. Although minor differences in the deposition pattern could be recognized, the results support the application of the numerical model as part of a hybrid modeling approach in further sediment studies.

The simulation of the flushing events of the reservoir Fisching in 2009 and 2012 were also challenging test cases. The flushing event in 2009 resulted in an unusual and hence very interesting erosion pattern, because in this case most of the erosion occurred at the inner site of the river bends and not on the outer site as expected. Because of this erosion pattern, the calibration of the numerical model was very complex and several sediment transport algorithm were tested and validated to obtain this pattern. The algorithm, which takes the deviation of a sediment grain by gravity on a sloping bed normal to the direction of the velocity into account, was the most important algorithm in this case. The calculated bed changes derived from Meyer-Peter-Müller and Van Rijn formula showed the best agreement with the measured bed changes of the flushing event 2009. However, the simulation results showed a “furrow” pattern in the computed bed changes. As discussed before, the occurrence of these “furrows” could be limited, but it was not possible to eliminate them totally. Further improvement and adaption of the related algorithm will be necessary in future.

In contrast to the flushing event 2009 the flushing event 2012 gave the typical erosion pattern. In this study the effect of the reservoir flushing on the flood risk of the surrounding areas are investigated. The numerical analysis showed that the reservoir flushing lead to a lowering of the water level in the whole reservoir. Hence, the probability of flooding decreased in the urban areas near the head of the reservoir too. The flushing 2012 increased bed slope and the bed shear stresses in the reservoir as well. These changed conditions could increase the flushing efficiency during minor flood events. However, the possibility of flushing is strictly connected to the hydrological conditions and in the Alpine area consequently linked to flood events. The simulation of the sediment transport of the flushing event 2012 would be part of future work too.

In the presented case studies the draw-down of the water level at the weir additionally

increases the bed shear stresses in the middle of the reservoir and not only close to the weir. The bed shear stresses in this cases are significantly higher than without draw-down of the water level. Therefore, the draw-down of the water-level at higher discharges can reduce the sedimentation and facilitate the erosion the sediment depositions in the reservoir.

The size of the reservoirs that were studied make it almost impossible to obtain an exact knowledge about all input parameters. One of the most important and often missing parameters is the water level at the middle or at the head of the reservoir. The measurement of the water levels at the head of the reservoir would enhance the calibration of the numerical model and thus, also improve the results of the numerical model. However, it will not be possible to measure all parameters in the next few years, for example the grain-size distribution in the whole reservoir including the vertical layering of the sediment depositions. Also the distribution of cohesive sediments in the reservoir and the critical shear stress of these cohesive sediments cannot be taken into account reliably. This facts may explain the differences in the erosion pattern in the case studies. Another uncertainty is that the used numerical models cannot take sand slides, retrogressive erosion or other geotechnical effects (e.g., caused by the lowering of the water level at flushing events) fully into account. The numerical models use the Shields curve (Shields, 1936), which was developed for non-cohesive sediments, or empirical values to estimate the critical shear stress of sediment particles. The cohesion can be taken into account by increasing the critical shear stress. Hence, the critical shear stress of the cohesive sediments in the reservoir has to be known, but it is very difficult to measure the cohesion or the critical shear stress of the sediment in situ in the reservoir.

The further development of numerical models is also an important point, but it must be admitted that our knowledge of the complex processes, which govern sediment/turbulent flow/bed forms interactions is still limited. Other issues like the influence of the suspended sediment on the damping of the turbulence level are still subject of continual development and research.

The numerical studies showed that reservoir flushing can mobilize sediment depositions in Alpine reservoirs. The interval between two flushing events should not be too long to limit the sediment deposition in the reservoir. In the Alpine area flushing events are linked to hydrological aspects such as flood events. Therefore, the threshold for a flushing event should not be to high. The value should be selected with respect to the hydrological conditions in the reservoir. The hydrological conditions in the catchment influence the discharge, the duration, and thus, the efficiency of the flushing process. Reservoir flushing needs a sufficient discharge to enable erosion in the reservoir. The minimum required discharge for reservoir flushing depends on the slope of the reservoir, the draw-down of the water level, the deposited sediments in the reservoir and the duration of the discharge. Reservoirs with a clogged river bed need higher discharge rates for the initiation of the erosion process. A high discharge rate has also the advantage of the reduction of the suspended sediment concentration, which may minimize the impacts on the ecosystem downstream of the weir. Reservoirs with a large annual inflow compared with the storage volume of the reservoir are more suitable for higher annual flushing probabilities. Usually flood events or higher discharge rates (e.g., because of snow melt) can be used. The occurrence of flood events has a statistical character, so planned reservoir flushing events with a longer interval and higher flood events have a hydrological uncertainty. At longer

flushing intervals a relative high discharge is thus necessary to remove enough sediment for a sustainable flood management. A common empirical value for the initiation of a flushing process in Alpine Reservoirs is a discharge of approximately 0.5 to 0.7 of the 1-year flood (threshold value) in order to achieve the required flushing effect while keeping a firm control about the essential parameters (sediment load, the content of chemical and organic matter, oxygen consumption rate, etc.). If the selected discharge for initiating a flushing process is too high, the probability of periodical reservoir flushing may decrease due to the variability of the discharge.

9.1 Outlook and Recommendations for Further Work

The modeling of sediment transport processes requires further work to improve the quality of the simulation results. The most important part of this work should be fundamental research to gather more data about sediment transport in laboratory flumes and in the field. The improvement or adaption of sediment transport formulae will be necessary in the future as well. Many of the algorithms implemented in numerical models are based on empirical formulae from flume of field studies and are developed for specific sediment characteristics and water flow conditions only. The development of bed-forms influence the flow field and the bed roughness. As a consequence the total amount of transported sediments is changed and the erosion and deposition pattern may not be modeled correctly in this area. The improvement or implementation of numerical algorithms to take geotechnical and soils mechanical issues like bank failures or cohesion better into account would also improve the numerical simulations.

However, the improvement of numerical modeling is only a part of the further work. The collection of monitoring data of flushing events and their long term effects are necessary, to obtain a better knowledge about this complex topic. Field measurements for calibration and validation of numerical models have to be extended and improved additionally. An example for the additional required field data are water level measurements in the middle or at the head of the reservoir for the calibration of the water level. Usually, the interval between two flushing events in Alpine reservoirs is about three to five years, depending on the hydrological conditions and on the selected threshold for the flushing discharge. Therefore, field measurements and monitoring data of flushing events are very important and can improve the understanding as well as the numerical modeling of reservoir flushing processes.

All these improvements can help to enhance the numerical simulation of reservoir flushing and increase the flushing efficiency based on a better management of flushing events. Sediment management in reservoirs will nevertheless continue to represent a challenge for the future and is required for a sustainable reservoir management.

BIBLIOGRAPHY

Aberle, J. (2008). Measurement Techniques for the Estimation of Cohesive Sediment Erosion. In *Hydraulic Methods for Catastrophes: Floods, Droughts, Environmental Disasters, P. Rowinski (ed.), Publs. Inst. Geophys. Pol. Acad. Sc., E-10 (406), 5 -20.*

Aberle, J., Nikora, V., McLean, S., Doscher, C., McEwan, I., Green, M., Goring, D., and Walsh, J. (2003). Straight benthic flow-through flume for insitu measurements of cohesive sediment dynamics. *Journal of Hydraulic Engineering, Vol. 129, No. 1, 63-67.*

Aberle, J., Nikora, V., and Walters, R. (2006). Data Interpretation for In Situ Measurements of Cohesive Sediment Erosion. *Journal of Hydraulic Engineering, Vol. 132, No. 6, 581-588.*

Aelbrecht, B. (2006). Lessons learned from dam removal experiences in France. Hydrovision conference - Portland (OR), USA - Aug 3, 2006.

Allen, J. (1984). *Sediment Structures: Their Character and Physical Basis*. Elsevier, Amsterdam.

Atkinson, E. (1996). *The Feasibility of Flushing Sediment from Reservoirs*. TDR Project R5839, Report OD 137, HR Wallingford.

Badura, H. (2007). Feststofftransportprozesse während Spülungen von Flussstauräumen am Beispiel der oberen Mur. Dissertation, Schriftenreihe zur Wasserwirtschaft der Technischen Universität Graz, 51.

Badura, H., Knoblauch, H., and Schneider, J. (2008). Pilot Action Bodendorf Reservoir (Austria). In *ALPRESERV - Pilot Actions and Database*. Universität der Bundeswehr München, Volume 5/2008, ISSN 1862-9636.

Badura, H., Schneider, J., Knoblauch, H., Larsen, O., and Heigerth, G. (2006). Numerische Simulation des Abstauvorganges während Stauraumspülungen am Beispiel des KW Bodendorf / Mur. Schriftenreihe zur Wasserwirtschaft der Technischen Universität Graz, 46.

Bagnold, R. (1966). An approach to the sediment tranport problem from general physics. *Professional Paper 422-j, USGS, Washington D.C., USA*.

Bathurst, J. C., Graf, W., and Cao, H. (1987). *Bed load discharge equations for steep mountain rivers*. John Wiley and Sons, New York, 453-477.

Batuca, D. and Jordaan, J. (2000). *Silting and Desilting of Reservoirs*. A.A. Balkema, Rotterdam.

Bechteler, W. (2006). The purposes of impounding facilities. In *ALPRESERV - Sediment Management Methods - Technical and legal aspects*. Universität der Bundeswehr München, Volume 4/2006, ISSN 1862-9636.

Berlamont, J., Ockenden, M., Toorman, E., and Winterwerp, J. (1993). The characterisation of cohesive sediment properties. *Coastal Engineering, 21(1-3), 105-128*.

Bühler, J., C., S., Simitovic, R., A., W., and Zeh, M. (2004). Trübeströme im Grimselsee. *Wasser, Energie, Luft, Heft 5/6, Baden, Switzerland*.

Bihs, H. and Olsen, N. (2008). Three dimensional numerical modeling of pier scour. In *4th International Conference on Scour and Erosion, Tokyo, Japan*.

Bischof, I. (2006). Rechtliche und Wasserwirtschaftliche Aspekte der Entlandung von Stauräumen. Master's thesis, Diplomarbeit am Institut für Wasserbau und Wasserwirtschaft der Technischen Universität Graz.

Brooks, N. (1963). Discussion of "Boundary Shear Stresses in Curved Trapezoidal Channels" by A.T Ippen and P.A. Drinker. *Journal of Hydraulics Division, ASCE, 89(3), 327-333*.

Bruk, S. (1996). Reservoir sedimentation and sustainable management of water resources-the international perspective. In *International Conference on Reservoir Sedimentation, Fort Collins, USA, 9th -13th September 1996*.

Brune, G. N. (1953). Trap Efficiency of Reservoir. *Transaction of the American Geophysical Union, Vol. 34, No. 3*.

Carling, P. (1999). Subaqueous gravel dunes. *Journal of Sediment Research*, 69 (3):534–545.

Chandler, R. (1988). *The In-Situ Measurement of the Undrained Shear Strength of Clay Using the Field Vane. Vane Shear Strength Testing in Soils: Field and Laboratory Studies, ASTM STP 1014*. American Society for Testing And Materials, Philadelphia.

Chang, H. H. (1988). *Fluvial Processes in River Engineering*. John Wiley and Sons, New York.

Chanson, H. (2004). *The Hydraulics of Open Channel Flow: An Introduction*. Elsevier Butterworth-Heinemann, Second Edition.

CHC, C. H. C. (2011). Blue Kenue - Reference Manual. Homepage of the National Research Council Canada.

Churchill, M. A. (1948). Discussion of Analysis and Use of Reservoir Sedimentation Data. In *Proceedings of the Federal Interagency Sedimentation Conference, Denver, Colorado, 139-140*.

Cook, C. and Richmond, M. (2004). Monitoring and Simulating 3-D Density Currents at the Confluence of the Snake and Clearwater Rivers. *http://www.pubs.asce.org/*.

Cornut, R. (1992). Surélévation du barrage de Lalla Takerkoust (Maroc). *wasser, energie, luft, Heft 7/8, pp. 155-160*.

De Cesare, G. (2006). *In: ALPRESERV - Sediment Management Methods - Technical and legal aspects*, chapter Density currents. Universität der Bundeswehr München, Volume 4/2006, ISSN 1862-9636.

De Cesare, G. and Schleiss, A. (2004). Physical and Numerical Modelling of Turbidity Currents. EPFL.

Debnath, K., Nikora, V., Aberle, J., Westrich, B., and Muste, M. (2007). Erosion of Cohesive Sediments: Resuspension, Bed Load, and Erosion Pattern from Field Experiments. *Journal of Hydraulic Engineering, Vol. 133, No. 5, 508-520*.

Dendy, F. E., Champion, W., and Wilson, R. (1973). Reservoir Sedimentation Surveys in the United States. In Ackermann, W. C., White, G. F., and Worthington, E., editors, *Man-made Lakes: Their Problems and Environmental Effects*. Geophysical Monograph No. 17. American Geophysical Union, Washington, D.C.

Dietrich, W. E., Kirchner, J. W., and Ikeda, H.and Iseya, F. (1989). Sediment supply and the delvelopment of the coarse surface layer in gravel-bedded rivers. *Nature*, 340:215–217.

Dorfmann, C. and Steidl, J. (2013). ADCPtool - A postprocessing framework for ADCP measurements, Reference Manual.

DORIS (2013). Digitales Oberösterreichisches Raum-Informationssystem [DORIS]. http://dorisooe.gv.at.

DWA (2006). *Entlandung von Stauräumen*. DWA Deutsche Vereinigung für Wasserwirtschaft, Hennef.

Eberstaller, J., Pinka, P., Unfer, G., Jungwirth, M., Wiesner, C., and Renner, R. (2008). Water ecologic aspects - a research project on sediment management based on the example of the River Mur power plant Bodendorf. In *ALPRESERV - Pilot Actions and Database*. Universität der Bundeswehr München, Volume 5/2008, ISSN 1862-9636.

EDF - R&D (2012). TELEMAC modelling system - 3D hydrodynamics TELEMAC-2D software, Version 6.1, User Manual. www.opentelemac.org/.

EDF-R&D (2010). SISYPHE 6.0 Manual, TELEMAC modelling system. www.opentelemac.org/.

Egiazaroff, I. (1965). Calculation of non-uniform sediment concentrations. *Journal of Hydr. Div. ASCE, Vol. 91, N°4, pp. 225-248*.

Einstein, H., Anderson, A., and Johnson, J. (1940). A distinction between bed-load and suspended load in natural streams. In *Transactions of the American Geophysical Union's annual meeting, 22, 628 - 633*.

Einstein, H. A. and Barbossa, N. L. (1952). River channel roughness. *Transaction, ASCE, Vol. 117, 1121 - 1146*.

Engelund, F. (1965). Turbulent energy and suspended load. *Basic Research Progress Report 10, Hydraulic Lab., Tech. Univ. of Denmark, Lyngby, Denmark*.

Engelund, F. and Fredsœ, J. (1982). Sediment Ripples and Dunes. *Annual Review Fluid Mechanic, No 14, 13 - 37*.

Engelund, F. and Hansen, E. (1967). A Monograph on Sediment Transport in Alluvial Stream. *1-63. Teknisk Forlag, Copenhagen V, Denmark*.

Engelund, F. and Hansen, E. (1972). *A monograph on sediment transport*. Technisk Forlag, Copenhagen, Denmark.

Fan, J. and Morris, G. (1992). Reservoir Sedimentation. II: Reservoir Desiltation and Long-Term Storage Capacity. *Journal of Hydraulic Engineering, ASCE, 118(3)*.

Fang, H. and Rodi, W. (2003). Three-dimensional calculations of flow and suspended sediment transport in the neighbourhood of the dam for the Three Gorges Project (TGP) reservoir in the Yangtze River. *IAHR Journal of Hydraulic Research, 41(4), 379-394*.

Feurich, R. and Olsen, N. (2011). Three-Dimensional Modeling of Nonuniform Sediment Transport in an S-shaped Channel. *Journal of Hydraulic Engineering, ASCE, 137(4), 469-480*.

Firoozabadi, B., Farhanieh, B., and Rad, M. (2003). Hydrodynamics of two-dimensional, laminar turbid density currents. *Journal of Hydraulic Research Vol. 41, No.6, S.623-630*.

Fischer-Antze, T., Olsen, N., and Gutknecht, D. (2008). Three-dimensional CFD modeling of morphological bed changes in the Danube River. *Water Resources Research, 44(9), 1-15*.

Frenette, M. and Julien, P. (1986). Advances in Predicting Reservoir Sedimentation. In *Proc. 3rd Int. Symp. River Sedimentation, U. Missisippi, Oxford*.

Geonor (1995). Instructions for use - Inspection Vane Tester, H-60. User Manual. Geonor AS, Oslo, Norway.

Gessler, J. (1967). *The beginning of bed-load movement of mixture investigated as natural armoring in channels*. Report No. T-5, W. M. Keck Lab. of Hydraulics and Water Res., California Inst, of Tech., Pasadena, Calif.

Goll, A. and Kopmann, R. (2012). Numerical simulations of groyne influenced dunes. In *Proceedings of the 6th International Conference on Fluvial Hydraulics, River Flow 2012, San José, Costa Rica*.

Graf, W. (1971). *Hydraulics of Sediment Transport*. McGraw-Hill Book Co., New York.

Graf, W. and Altinakar, M. (1998). *Fluvial Hydraulics*. Wiley.

Harb, G., Dorfman, C., Schneider, J., Haun, S., and Badura, H. (2012). Numerical analysis of sediment transport processes in a reservoir. In *Proceedings of the 6th International Conference on Fluvial Hydraulics, River Flow 2012, San José, Costa Rica*.

Harb, G., Dorfmann, C., Badura, H., and Schneider (2013a). Numerical Analysis of the Flushing Efficiency of an Alpine Reservoir. In *Proceedings of the 35th IAHR World Congress, September 2013, Chengdu, accepted*.

Harb, G., Haun, S., Olsen, N., and Schneider, J. (2013b). Numerical analysis of synthetic granulate deposition in a physical model study. *International Journal of Sediment Research, accepted on the 18th of March 2013*.

Harb, G., Haun, S., Ortner, S., Dorfmann, C., and Schneider, J. (2011). The influence of secondary currents on reservoir sedimentation - experimental and numerical studies. In *Proceedings of the 34th IAHR World Congress, Engineers Australia, July 2011, Brisbane*.

Harb, G., Haun, S., and Schneider, J. (2013c). Evaluation of critical shear stresses of cohesive sediments by using PIV compared with vane strength measurements. In *Proceedings of the 12th International Symposium on River Sedimentation (ISRS2013), September 2-5, Kyoto, JAPAN*.

Hartmann, S. (2009). *ALPRESERV - Sediment Management in Alpine Reservoirs - Recommendations and Best Practice Guide*. Universität der Bundeswehr München, Volume 7/2009, ISSN 1862-9636.

Haun (2012). *Three-Dimensional Numerical Modelling of Sediment Transport During the Flushing of Hydropower Reservoirs*. PhD thesis, Dissertation submitted to the Faculty of Engineering Science and Technology at the Norwegian University of Science and Technology.

Haun, S., Kjærås, H., Løvfall, S., and Olsen, N. (2012). Three-dimensional measurements and numerical modelling of suspended sediments in a hydropower reservoir. *Journal of Hydrology*.

Haun, S. and Olsen, N. (2012a). Three-dimensional numerical modelling of reservoir flushing in a prototype scale. *International Journal of River Basin Management. 10(4) 341-349*.

Haun, S. and Olsen, N. R. B. (2012b). Three-dimensional numerical modelling of the flushing process of the kali gandaki hydropower reservoir. *Lakes & Reservoirs: Research and Management*, 17:25–33.

Hervouet, J.-M. (2007). *Hydrodynamics of Free Surface Flows: modelling with the finite element method*. Wiley.

Hillebrand, G., Klassen, I., Olsen, N., and Vollmer, S. (2012). Modelling fractionated sediment transport and deposition in the Iffezheim reservoir. In *Proceddings of the 10th International Conference on Hydroinformatics, Hamburg, Germany*.

Hjulström, F. (1935). The morphological activity of rivers as illustrated by river Fyris. *Bull. Geolog. Institution, Univ. Uppsala, Vol. 25*.

Hopf, G. (2006). Die sanierung der unteren salzach. Berichte der Bayrischen Landesanstalt für Wald und Forstwirtschaft.

Hug, C., Boillat, J.-L., and Schleiss, A. (2000). Hydraulische Modellversuche für die neue Wasserfassung der Stauanlage Mauvoisin. In *Proceedings Wasserbau Symposium "Betrieb und Überwachung wasserbaulicher Anlagen", 19.- 21. Oktober 2000, Graz,*

Austria, Mitteilung des Instituts für Wasserbau und Wasserwirtschaft Nr. 34, pp. 367-376.

Huybrechts, N., Tassi, P., and Villaret, C. (2012). Application of TELEMAC-3D to sediment-laden flow on flat bed configuration. In Bourban, S., Durand, N., and Hervouet, J.-M., editors, *Proceedings of the XIXth TELEMAC-MASCARET User Conference, 18 to 19 October 2012, St Hugh's College, Oxford*.

Huybrechts, N., Villaret, C., and Hervouet, J.-M. (2010). Comparison between 2D and 3D modelling of sediment transport: application to the dune evolution. In *Proceedings of the 5th International Conference on Fluvial Hydraulics, River Flow 2010, Braunschweig, Germany*.

ICOLD (1998). World register of large dams. International Commission on Large Dams, CD ROM.

IEA (2007). *Renewables in Global Energy Supply: An IEA Fact Sheet*.

Iseya, S. and Ikeda, H. (1987). Pulsation in bedload transport rates induced by a longitudinal sediment sorting: a flume study of sand and gravel mixtures. *Geografiska Annaler*, 69A:15–27.

Jacobsen, T. (1997). *Sediment problems in reservoirs - Control of sediment deposits*. PhD thesis, Doctoral Thesis. Department of Hydraulic and Environmental Engineering, NTNU, Trondheim, Norway.

Jain, S. C. (1990). Armor or Pavement. *Journal of Hydraulic Engineering, ASCE, 116(3), 436-440*.

Jiménez, O., Rodriguez, C., and Olsen, N. (2004). Sedimentation in the Angostura Reservoir, Studies and Experiences. In *Proceedings of the 9th International Symphosium on River Sedimentation, Yichang, China*.

Kamphuis, J. and Hall, K. (1983). Cohesive material erosion by unidirectoral current. *Journal of Hydraulic Engineering, Vol. 109, No. 1, January, 1983*.

Karim, M. and Kennedy, J. (1982). A computer based flow and sediment routing. In *IIH Report N°250 Modelling for streams and its application to the Missouri River, University of Iowa, Iowa City, IA*.

Kawashima, S., Butler Johndrow, T., Annandale, G., and Shah, F. (2003). *Reservoir Conservation Volume II: RESCON Model and User Manual, Economic and engineering evaluation of alternative strategies for managing sedimentation in storage reservoirs*. The International Bank for Reconstruction and Development, The World Bank, Washington D.C., June 2003.

Kikkawa, H., Ikeda, J., and Kitagawa, A. (1976). Flow and bed topography in curved open channels. *Journal of Hydraulic Engineering, ASCE, 102(9), 1327-1342*.

Klassen, I., Hillebrand, G., Olsen, N., Vollmer, S., Lehmann, B., and Nestmann, F. (2011). Modeling fine sediment aggregation processes considering varying fractal dimensions. In *The 7th IAHR Symposium on River, Coastal and Estuarine Morphodynamics, 6.-8. Sept. 2011, Peking, China. Beitrag im Tagungsband*.

Knoblauch, H. (2006). *ALPRESERV - Sediment Management Methods - Technical and legal aspects*. Universität der Bundeswehr München, Volume 4/2006, ISSN 1862-9636.

Knoblauch, H., Badura, H., Schneider, J., Pichler, W., and Heigerth, G. (2005). Geschiebetransportmodell zur Festlegung der Mindestwassermenge bei Stauraumspülungen. In *Wasserbaukolloquium 2005: Strömungssimulation im Wasserbau, Dresdener Wasserbauliche Mitteilungen Heft 32*.

Knoblauch, H. and Simões, F. (2000). Calculation of the Plunge Point at Whiskeytown Reservoir, California. In *Proceedings of the 5th International Symposium on Stratified Flows, University of British Columbia, Vancouver, 10.-13.7.2000*.

Kobus, H. (1984). *Wasserbauliches Versuchswesen*. Schriftenreihe des deutschen Verbandes für Wasser-wirtschaft und Kulturbau, 2nd Edition. Parey Verlag, Hamburg.

Koch, F. and Flokstra, C. (1981). Bed level computations for curved alluvial channels. In *Proceedings of the XIXth Congress of the International Association for Hydraulic Research, New Delhi India*.

Kohl, B., Markart, G., and Bauer, W. (2003). Abflußmenge und Sedimentfracht unterschiedlich genutzter Boden-/Vegetationskomplexe bei Starkregen im Sölktal/Steiermark. Institut für Lawinen- und Wildbachforschung, Forstliche Bundesversuchsanstalt, Abteilung für Bewirtschaftung von Lawinen- und Wildbacheinzugsgebieten, unpublished.

Kopmann, R.and Schmidt, A. (2010). Comparison of different reliability analysis methods for a 2D morphologic numerical model of the River Danube. In *Proceedings of the 5th International Conference on Fluvial Hydraulics, River Flow 2010, Braunschweig, Germany*.

Kothyari, U. and Jain, R. (2008). Influence of cohesion on the incipient motion conditions of sediment mixtures. *Water Resources Research, Vol. 44, W04410*.

Kothyari, U. and Jain, R. (2010). Erosion characteristics of cohesive sediment mixtures. In *Proceedings of the International Conference on Fluvial Hydraulics, Braunschweig, Germany*.

Krumdieck, A. and Chamot, P. (1981). Spülung von Sedimenten in kleinen und mittleren Staubecken. In *Mitteilung Nr. 53 der Versuchsanstalt für Wasserbau, Hydrologie und Glaziologie der ETH Zürich, pp. 257-270*.

Lai, J. and Shen, H. (1996). Flushing sediments through reservoirs. *IAHR Journal of Hydraulic Research, 34(2), 237-255*.

Launder, B. and Spalding, D. (1972). *Lectures in mathematical models of turbulence*. Academic Press, London.

Lempérièr, F. and Lafitte, R. (2006). The role of dams in the XXI Century to achieve a sustainable development target. In *Dams and Reservoirs, Societies and Environment in the 21st Century, ICOLD-SPANCOLD, 18 June 2006, Barcelona, Spain*.

Lysne, D., Olsen, N.R.B.and Stole, H., and Jacobsen, T. (1995). Sediment control: recent developments for headworks. *Hydropower and Dams*, March.

Mahmood, K. (1987). *Reservoir sedimentation: impact, extent and mitigation.* World Bank Technical Paper 71, Washington D.C.

Mehta, A., Hayter, E., Parker, W., Krone, R., and Teeter, A. (1989). Cohesive Sediment Transport. I: Process Description. *Journal of Hydraulic Engineering, Vol. 115, No. 8, 1076-1093*.

Merkel, U. H. and Kopmann, R. (2012). A continuous vertical grain sorting model for Telemac & Sisyphe. In *Proceedings of the 6th International Conference on Fluvial Hydraulics, River Flow 2012, San José, Costa Rica*.

Meyer-Peter, E. and Müller, R. (1948). Formulas for bed-load transport. In *Proceedings of the 2nd Meeting of the International Association for Hydraulic Structures Research, 39-64, Int. Assoc. Hydraul. Res., Delft, Netherlands*.

Milliman, J. and Meade, R. (1983). World-wide delivery of river sediment to the oceans. *Journal of Geology 91, 1-21*.

Milliman, J. and Syvitski, J. (1992). Geomorphic/tectonic control of sediment discharge to the ocean: the importance of small mountainous rivers. *Journal of Geology 100, 325-344*.

Molino, B., Greco, M., and Rowan, J. (2001). A 2-D Reservoir Routing Model: Sedimentation History of Abbeystead Reservoir U.K. *Water Resources Management 15: pp. 109-122*.

Morris, G. and Fan, J. (1998). *Reservoir Sedimentation Handbook*. McGraw-Hill Book Co., New York.

Nezu, I. and Nakagawa, H. (1993). *Turbulence in open-channel flows*. A.A. Balkema, Rotterdam, Netherlands.

Núñez González, F. and Martín-Vide, J. P. (2010). Downstream-migrating antidunes in sand, gravel and sand-gravel mixtures. In *Proceedings of the River Flow Conference 2010, Bundesanstalt für Wasserbau.*

Oehy, C., De Cesare, G., and Schleiss, A. (2000). Einfluss von Trübeströmen auf die Verlandung von Staubecken. In *Symposium "Betrieb und Überwachung wasserbaulicher Anlagen", 19. - 21. Oktober 2000, Graz, Österreich, Mitteilung des Instituts für Wasserbau und Wasserwirtschaft Nr. 34, pp. 413-422*.

Olsen, N. (1999a). 3D CFD modelling of water and sediment flow in a hydropower reservoir. *International Journal of Sediment Research 14 (1)*, pages 16–24.

Olsen, N. (1999b). Two-dimensional numerical modelling of flushing processes in water reservoirs. *IAHR Journal of Hydraulic Research, 37(1)*, pages 3–16.

Olsen, N. (2000). *CFD Algorithms for Hydraulic Engineering*. Department of Hydraulic and Environmental Engineering, The Norwegian University of Science and technology.

Olsen, N. (2001). *CFD modelling for hydraulic structures*. Department of Hydraulic and Environmental Engineering, The Norwegian University of Science and technology.

Olsen, N. (2003). Three-Dimensional CFD Modeling of Self-Forming Meandering Channel. *Journal of Hydraulic Engineering, ASCE, 129(5)*, pages 366–372.

Olsen, N. (2012). *A Three-Dimensional Numerical Model for Simulate of Sediment Movements in Water Intakes with Multiblock Option, User's Manual*. Department of Hydraulic and Environmental Engineering, The Norwegian University of Science and Technology, Trondheim.

Olsen, N. and Haun, S. (2010). Free surface algorithms for 3D numerical modelling of reservoir flushing. In et al., D., editor, *Proceedings of the River Flow Conference 2010, Bundesanstalt für Wasserbau*.

Olsen, N., Kjellberg, G., Bakken, T., and Alfredsen, K. (1999). Numerical modelling of water quality in Lake Mjøsa, Norway, during the flood of 1995. In *Proceedings of the 3th conference on Ecohydraulics 1999, Salt Lake City, USA*.

Olsen, N. and Kjellesvig, H. (1998). Three-dimensional numerical flow modelling for estimation of maximum local scour depth. In *IAHR Journal of Hydraulic Research, 36(4), 579-590*.

Olsen, N. and Stokseth, S. (1995). Three-dimensional numerical modelling of water flow in a river with large bed roughness. *IAHR Journal of Hydraulic Research, 33(4), 571-581*.

Palmieri, A., Shah, F., Annandale, G., and A., D. (2003). *Reservoir Conservation Volume I: The RESCON Approach Economic and engineering evaluation of alternative strategies for managing sedimentation in storage reservoirs*. The International Bank for Reconstruction and Development, The World Bank, Washington, June 2003.

Papanicolaou, A., Elhakeem, M., Krallis, G., and Edinger, J. (2008). Sediment Transport Modelling Review - Current and Future Developments. *Journal of Hydraulic Engineering, ASCE, 134(1), 1-14*.

Parker, G., Dhamotharan, S., and Stefan, H. (1982a). Model experiments on mobile, paved gravel bed streams. *Water Resour. Res., 18(5), 1395-1408*.

Parker, G. and Klingemann, P. (1982). On Why Gravel Bed Stream Are Paved. *Water Resour. Res., 18(5), 1409-1423*.

Parker, G., Klingemann, P., and McLean, D. (1982b). Bedload and Size Distribution in Paved Gravel-Bed Streams. *J. Hydraulic Division Am. Soc. Civ. Eng., 108(HY4)*, pages 544–571.

Patankar, S. (1980). *Numerical Heat Transfer and Fluid Flow*. McGraw-Hill Book Company, New York.

Peng, R. and Niu, J. (1987). Numerical model of headwater erosion on bed load. *Journal of Sediment Research, (3), (in Chinese)*.

Prandtl, L. (1925). Bericht über Untersuchungen zur ausgebildeten Turbulenz. *ZAMM. Z. angew. Math. Mech.*, 5:136–139.

Rhie, C. and Chow, W. (1983). Numerical study of the turbulent flow past an airfoil with trailing edge separation. *AIAA Journal 21(11), 1525-1532*.

Rickenmann, D. (1991). Hyperconcentrated Flow and Sediment Transport at Steep Slopes. *Journal on Hydraulic Engineering, Volume 117, No. 11, 1419-1439*.

Roberts, J., Jepsen, R., and James, S. (2003). Measurements of sediment erosion and transport with the adjustable shear stress erosion and transport flume. *Journal of Hydraulic Engineering, Vol. 129, No. 11, 862-871*.

Rodi, W. (1980). *Turbulence Models and Their Application in Hydraulics*. A. A. Balkema, Rotterdam.

Rouse, H. (1938). *Fluid Mechanics for Hydraulic Engineers*. Dover, New York.

Rowiński, P., Aberle, J., and Mazurczyk, A. (2005). Shear velocity estimation in hydraulic research. *Acta Geophysica Polonica, Vol. 53, No. 4, 567-583*.

Rüther, N. (2006). *Computational fluid dynamics in fluvial sedimentation engineering*. PhD thesis, Dissertation submitted to the Faculty of Engineering Science and Technology at the Norwegian University of Science and Technology.

Rüther, N. and Olsen, N. (2005). Three dimensional modelling of sediment transport in a narrow 90° channel bend. *Journal of Hydraulic Engineering, ASCE, 131(10), 917-920*.

Rüther, N. and Olsen, N. (2007). Modelling free-forming meander evolution in a laboratory channel using three-dimensional computational fluid dynamics. *Geomorphology, 89, 308-319*.

Scheuerlein, H. (1990). Removal of sediment deposits in reservoirs by means of flushing. In *Proceedings International Conference on Water Resources in Mountainous Regions, Symp. 3: Impact of Artificial Reservoirs on Hydrological Equilibrium, Lausanne, Switzerland*.

Scheuerlein, H. (1995). Downstream effects of dam construction and reservoir operation. *6th International Symposium on River Sedimentation, New Delhi, India*.

Schleiss, A., Feuz, B., Aemmer, M., and Zünd, B. (1996). Verlandungsprobleme im Stausee Mauvoisin. Ausmass, Auswirkungen und mögliche Massnahmen. In *Proceedings of Internationales Symposium "Verlandung von Stauseen und Stauhaltungen, Sedimentprobleme in Leitungen und Kanälen", Mitteilungen der VAW Nr. 142, Teil 1, Zürich, Switzerland, pp. 37-58.*

Schlichting, H. (1979). *Boundary layer theory*. McGraw-Hill Book Company, New York.

Schneider, J., Badura, H., and Harb, G. (2012a). *Encyclopedia of Lakes & Reservoirs*, chapter Venting Turbidity Currents in Reservoirs, pages 841 – 842. Springer Verlag.

Schneider, J., Badura, H., and Harb, G. (2012b). *Encyclopedia of Lakes & Reservoirs*, chapter Turbidity Currents in Reservoirs, pages 820 – 826. Springer Verlag.

Schneider, J., Badura, H., Knoblauch, H., Frei, R., and Eberstaller, J. (2006). Flushing of the run-of river plant Bodendorf in Styria/Austria in respect of technical and ecological impacts. In *The 7th International Conference on Hydroscience and Engineering (ICHE-2006), Sep 10-Sep 13, Philadelphia, USA*.

Schneider, J., Badura, H., Troy, W., and Knoblauch, H. (2007). Determination of Parameters for Venting Turbidity Currents through a Reservoir. In *Proceedings of the 32nd Congress of IAHR, Venice, Italy*.

Schöberl, F., Reindl, R., and Feurich, R. (2005). Improved bed load management for the alpine upper drau river/austria. In *In: Byong-Ho, Jun et al.: Water engineering for the future. Abstracts of 31 IAHR Congress, Coex, Seoul, September 11 - 16, 2005. Seoul: Korea Water Resources Association.*

Schoklitsch, A. (1935). *Stauraumverlandung und Kolkabwehr*. Springer Verlag, Wien.

Shen, H. (1999). Flushing sediment through reservoirs. *IAHR Journal of Hydraulic Research, 37(6), 743-757*.

Shields, A. (1936). *Use of dimensional analysis and turbulence research for sediment transport*. Preussen Research Laboratory for Water and Marine Constructions, Publication no. 26, Berlin.

Sindelar, C. and Mende, M. (2009). Lenkbuhnen zur Strukturierung und Stabilisierung von Fließgewässern. *Wasserwirtschaft, Heft 1-2, 70-75*.

Smart, G. and Jäggi, M. (1983). Sediment transport on steep slops. *Mitteilungen der Versuchsanstalt für Wasserbau, No. 64, Hydrologie und Glaziologie, ETH Zürich*.

Soulsby, R. (1997). *Dynamics of marine sands*. Thomas Thelford Edition.

Spannring, M. (2012). Hydropower and nature conservation: Salzach summary. 4th International Conference "Water in the Alps" Sustainable Hydropower - Strategies for the Alpine Region - Munich, Germany, 22-23 October 2012,.

Stelczer, K. (1981). *Bed-load Transport Theory and Practice*. Water Resources PublicatioMc, Littleton, Colerado.

Sumi, T. (2004). Reservoir sedimentation management with bypass tunnels in Japan. In *Proceedings of the Nineth International Symposium on River Sedimentation, October 18 - 21, 2004, Yichang, China*.

Syvitski, J. P. M., Vörösmarty, C. J., Kettner, A. J., and Green, P. (2005). Impact of Humans on the Flux of Terrestrial Sediment to the Global Coastal Ocean. *Science 308, 376-380*.

Tolhurst, T., Black, K., and Paterson, D. (2009). Muddy Sediment Erosion: Insights from Field Studies. *Journal of Hydraulic Engineering, Vol. 134, No. 1, 73-87*.

Tuijnder, A. P., Spekkers, M. H., and Ribberink, J. S. (2010). Development of supply-limited transport due to vertical sorting of a sand-gravel mixture. In *Proceedings of the River Flow Conference 2010, Bundesanstalt für Wasserbau*.

U.S. Army Corps of Engineers, W. E. S. (1998). SAM Hydraulic Design Package for Channels User's Manual. Vicksburg, MS.

USSD, U. S. S. o. D. (2012). Guidelines for Dam Decommissioning Projects. http://ussdams.com.

Van Rijn, L. (1984a). Sediment Transport. Part I: Bed load transport. *Journal of Hydraulic Engineering, ASCE, 110(10), 1431-1456*.

Van Rijn, L. (1984b). Sediment Transport. Part II: Suspended load transport. *Journal of Hydraulic Engineering, ASCE, 110(11), 1613-1641*.

Van Rijn, L. (1984c). Sediment Transport. Part III: Bed forms and alluvial roughness. *Journal of Hydraulic Engineering, ASCE, 110(12), 1733-1754*.

van Rijn, L. (1987). *Mathematical modeling of morphological processes in case of suspended sediment transport*. PhD thesis, PhD-Thesis, Delft University of Technology.

Van Rijn, L. (1993). *Principles of Sediment Transport in Rivers, Estuaries and Coastal Seas*. Aqua Publications.

Versteeg, H. and Malalasekera, W. (1995). *An introduction to Computational Fluid Dynamics, The Finite Volume Method*. Pearson Education Limited, Edinburgh.

Vischer, D. (1981). Internationale Fachtagung "Verlandung von Stauhaltungen und Speicherseen im Alpenraum". In *Mitt. Nr. 53, VAW, ETH Zürich, 9-25*.

Vollmers, M. and Giese, E. (1970). Instability of flat bed in alluvial channels. *Discussion, ASCE, Journal of Hydraulic Engineering, No. 6*.

Walling, D. (2006). Human impact on land - ocean sediment transfer by the world's rivers. *Geomorphology 79 (2006) 192-216*.

Walling, D. and Webb, B. (1989). Erosion and sediment yield: a global overview. In *Erosion and Sediment Yield: Global and Regional Perspectives, Proceedings of an international symposium held at Exeter, UK*.

White, R. (2001). *Evacuation of sediments from reservoirs*. Thomas Telford Publishing.

White, W. and Bettess, R. (1984). The feasibility of flushing sediments through reservoirs. In *Challenges in African Hydrology and Water Resources, Proceedings of the Harare Symposium, July 1984*.

Wu, W. (2008). *Computational River Dynamics*. Taylor & Francis Group, London, UK.

Wu, W., Wang, S., and Jia, Y. (2000). Nonuniform sediment transport in alluvial rivers. *IAHR Journal of Hydraulic Research, 38(6), 427-434*.

Yalin, M. (1971). *Theory of Hydraulic Models*. The Macmillan Press LTD, London.

Yalin, S. (1977). *Mechanics of Sediment Transport*. Second Edition, Pergamon Press, New York, USA.

Yang, C. (1984). Unit Stream Power Equation for Gravel. *Journal of Hydraulic Division. ASCE, No. 110, 1783-1798*.

Yoon, Y. (1992). The state and the perspective of the direct sediment removal methods from reservoirs. *International Journal of Sediment Research*, 7(2):99–116.

Zanke (1982). *Grundlagen der Sedimentbewegung*. Springer Verlag.

List of Figures

List of Tables

APPENDIX - SCIENTIFIC PAPERS

10.1 Schönau - IAHR 2011

The Influence of Secondary Currents on Reservoir Sedimentation - Experimental and Numerical Studies
Harb, G.; Haun, S.; Ortner, S.; Dorfmann, C. & Schneider, J.
Proceedings of the 34th IAHR World Congress, Engineers Australia, July 2011, Brisbane, 2011

10.2 Schönau - International Journal of Sediment Research

Numerical Analysis of Synthetic Granulate Deposition in a Physical Model Study
Harb G.; Haun, S.; Olsen, N. R. B.& Schneider, J.
International Journal of Sediment Research, accepted on the 18th of March 2013

10.3 Leoben - Riverflow 2012

Numerical Analysis of Sediment Transport Processes in a Reservoir
Harb, G.; Dorfman, C.; Schneider, J.; Haun, S. & Badura, H.
Proceedings of the 6th International Conference on Fluvial Hydraulics, River Flow 2012, San José, Costa Rica, 2012

10.4 Bodendorf - IAHR Europe 2012

3D Numerical Modelling of the Reservoir Flushing of the Bodendorf Reservoir, Austria
Haun, S.; Dorfman, C.; Harb, G.; & Olsen N. R. B.
Proceedings of the 2nd IAHR Europe Congress, Munich, 2012

10.5 Fisching - IAHR 2013

Numerical Analysis of the Flushing Efficiency of an Alpine Reservoir
Harb, G.; Dorfman, C.; Badura, H.; & Schneider, J.
Proceedings of the 35th IAHR World Congress, Chengdu, China, September 2013

10.6 Flume Tests - ISRS2013

Evaluation of Critical Shear Stresses of Cohesive Sediments by Using PIV Compared with Vane Strength Measurements
Harb, G.; Haun, S. & Schneider, J.
Proceedings of the 12th International Symposium on River Sedimentation (ISRS2013), September 2-5, Kyoto, Japan, 2013

SCHÖNAU - IAHR 2011

The influence of secondary currents on reservoir sedimentation – experimental and numerical studies

G. Harb[1], S. Haun[2], S. Ortner[1], C. Dorfmann[1] and J. Schneider[1]
[1]Institute of Hydraulic Engineering and Water Resources Management
Graz University of Technology
Stremayrgasse 10, 8010 Graz
AUSTRIA
[2] Department of Hydraulic and Environmental Engineering
The Norwegian University of Science and Technology
S. P. Andersens veg 5, 7491 Trondheim
NORWAY
E-mail: gabriele.harb@tugraz.at

Abstract: *In the current paper the sedimentation problems in a reservoir of a run-of-river power plant will be discussed. The hydropower plant is located at the river Enns in Austria. The reservoir is affected by massive deposits of suspended sediment load near the turbines, which are located at the inner site of the river bend. In case of floods, the secondary currents in the river bend further increase the transport of suspended load to the turbine inlets. To reduce the sedimentation, to facilitate transportation of suspended load and to activate the transportation of the deposited sediments an operation method called "soft flushing" has to be carried out. In a three-dimensional numerical model the sedimentation processes and the secondary currents were investigated. The results were compared to ADCP field measurements and supplemental measurements in the physical model of the reservoir.*

Keywords: *reservoir sedimentation, secondary currents, river flow, numerical studies, field measurements*

1. INTRODUCTION

Sedimentation processes are balanced in the most natural rivers. The construction of dams and reservoirs influence this balance. In reservoirs the flow velocities, turbulences and bed shear stresses are reduced and this leads to settlements of the transported bed and suspended sediment load. As a consequence, the bed levels rise and reduce the storage volume by "filling up" the reservoir. Decreased reservoir volume reduces, and in extreme cases eliminates, the capacity of hydropower, water supply, irrigation and flood control benefits (Morris & Fan, 1998). In complex geometries secondary currents may increase the sedimentation problems, because of the transportation of sediments from the outer to the inner site of the river bend (Charlton, 2008).
Flushing is one of the most common ways to reduce this problem. In case of natural floods or higher discharges the water level is lowered to increase the flow velocities, turbulences and bed shear stresses in the reservoir. The increased shear stress causes erosion on the bed of the reservoir and the turbulence keeps the sediment particles in suspension. But flushing creates also problems from other point of views, e.g. environmental issues or flood protection in the downstream areas of the river. Due to the fact that the purpose of reservoir flushing is the remobilization of the sediments that were trapped during longer periods, flushing leads to a higher sediment concentration in the downstream section of the river. This concentration could be harmful to the downstream ecosystem (e.g. fish). Therefore reservoir flushing programs often require extensive regulations and monitoring. An example is the Bodendorf reservoir in Austria (Badura, 2007). In other cases flushing can increase the flood risk downstream of the reservoir, if the flushed sediments deposit in a specific river section. These constraints may limit the allowable drawdown or the opening of the flushing outlets, requiring that flushing be undertaken with only partial drawdown of the water level (Morris & Fan, 1998). One example of this strategy is the so-called "soft flushing". Soft flushing is a kind of pressure flushing, which can be performed in instream-reservoirs of run-of-river power plants or in diversion plants with high inflow in relation to the storage volume and relatively shallow reservoirs. During a soft flushing the reservoir level is drawn down for some meters on the minimum operating level and then the spillway gates are opened slowly. Caused by the lower water level the velocities and the bead shear stresses in the reservoir are higher than in normal flood situations and therefore erosion takes place.

ISBN 978-0-85825-868-6

2. PROJECT BACKGROUND

The reservoir of the hydropower plant Schoenau in Austria is affected by huge deposits of suspended sediment load near the turbines, which are located at the inner side of the river bend. In case of floods, the secondary currents in the river bend additionally increase the transport of suspended load towards the turbine inlets. To reduce the sedimentation, to facilitate transportation of suspended load and to activate the transportation of the deposited sediments, operation arrangements like “soft flushing” have been carried out. A conventional flushing approach is not possible in this case, because of the downstream located city Steyr. Steyr is flooded even in case of small flood events. The flushing of sediments into the area of the river which flows through the city of Steyr would raise the bed levels and would increase the flood risk, consequently this is not allowed. Therefore a soft flushing strategy is carried out in this study. If the discharge exceeds 750m^3/s (1-year-flood) the reservoir level is drawn down linear as shown in Figure 1. After reaching a water level of 398 m asl the gates of the weir are opened according to the operation guidelines of the hydropower plant.

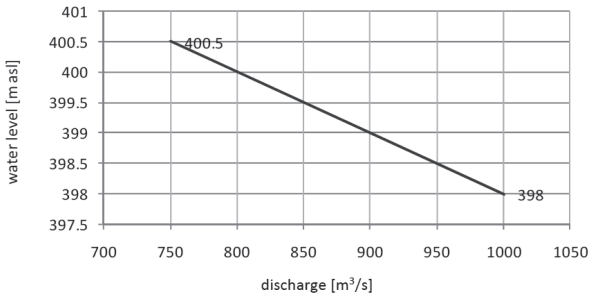

Figure 1 discharge – water level correlation of the soft flushing strategy

The physical model study of the project was carried out at the Hydraulic Laboratory of the Graz University of Technology in the period between 2008 and 2010. The physical model was built in concrete with a fixed river bed at a scale of 1:40. It was about 24 m long and 2.5 m wide and represented a natural river length of 950 m. The model was divided into a 570 m long part of the reservoir and a 380 m part downstream of the weir. Figure 2 shows on the left an overview of the reservoir in the physical model and on the right the deposited sediments near the turbine inlets after the simulation of a 1-year-flood without turbine operation.

Figure 2 left: overview of the upstream part of the reservoir in the physical model (view from the weir upstream); right: deposited sediments near the turbine inlets in the physical model (view in flow direction)

The deposited sediments in the reservoir have very small grain sizes (d_{90}=0.9 mm and d_{50}=0.25 mm) and a density of 2.73-2.80 g/cm^3. In consequence of this small grain sizes different synthetic and

mineral granulates, based on Kobus (1984), were used to model the sediment transport and the sediment deposition in the physical model.

3. NUMERICAL MODEL

The three-dimensional numerical model SSIIM 2 (Olsen, 2009) is used in this study. SSIIM 2 uses a non-orthogonal, adaptive and unstructured grid. The unstructured and adaptive grid allows a variation of the size and the shape of the grid during the computation. Through the implemented wetting and drying algorithm the number of grid cells in the vertical direction changes according to the changes in the water level and the geometry of the river bed. In this case at the beginning of the calculation about 78,000 cells are used with a maximum cell size of approximately 5.0 x 5.0 m. At the end of the calculation, through the adaptive grid, between 50,951 and 48,520 cells were left, depending on the water level at the end of the simulation. The maximum number of cells in the vertical direction was 10 in the simulation. The numerical program solves the continuity equation and the RANS-equations for determining the flow velocities in three directions. The turbulence is predicted by the standard k–ε turbulence model (Rodi, 1980). As boundary condition wall laws by Schlichting (1979) are used. The control volume method is applied for the discretization, together with the power-law scheme (Olsen, 2009). The CFD code uses the SIMPLE method for the computation of the pressure field (Patankar, 1980). The calibration of the numerical model was done by using measurements from the prototype. In the model the bed roughness was set to a constant value.
The suspended sediment transport was calculated by solving the transient convection-diffusion equation. The suspended sediment load capacity and the bed load were computed by using the empirical formulas of Van Rijn (1984a,b).

4. CALIBRATION OF THE NUMERICAL MODEL

The velocity profiles derived of the numerical model were compared to the measured ADV-Profiles in the physical model (Figure 3). Several parameters, e.g. the bed roughness value were varied in the calibration process. Figure 4 shows the velocity profile of the numerical computation after the calibration process.

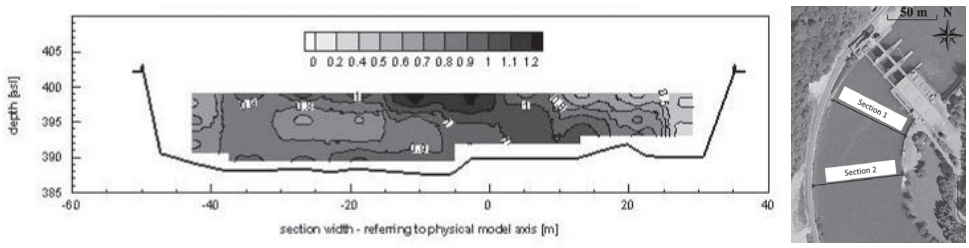

Figure 3 Contour plot of the absolute velocities [m/s], 1-year flood and turbine operation measured in the physical model in Section 1

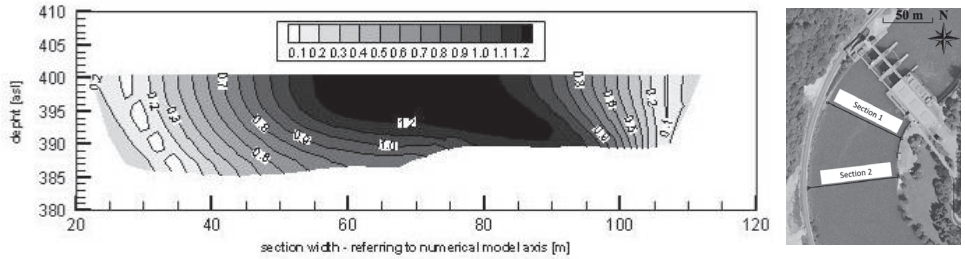

Figure 4 Contour plot of the absolute velocities [m/s], 1-year flood and turbine operation computed in the numerical model in Section 1

The velocity distributions in the flow profiles show reasonable agreements. In this case the numerical model generally overestimates the high velocities in the middle of the section and underestimates the lower velocities near the river banks compared to the measured velocity profiles. The pattern of the flow field compares well.

5. NUMERICAL MODELLING OF THE SECONDARY CURRENTS

Additional field measurements with an ADCP were carried out to ensure the quality of the results in the numerical and physical model. The field measurements were realised in June 2009 during a moderate flow near design discharge by the Hydrographic Institutes of the Styrian Government and the Upper Austrian Government. During the measurements the water level was kept on a constant level (400.35 m asl). The design reservoir level is 400.5 m asl. A RDI ADCP (Acoustic Doppler Current Profiler) WorkHorse RioGrande© 1200 kHz was used to collect the data with the Section-by-Section method. Three transects (Section 1-3) were measured in the reservoir and compared with the velocity profiles in the numerical model. Figure 5 and 6 show the comparison of the flow fields derived by the ADCP measurements and the numerical simulation in Section 2.

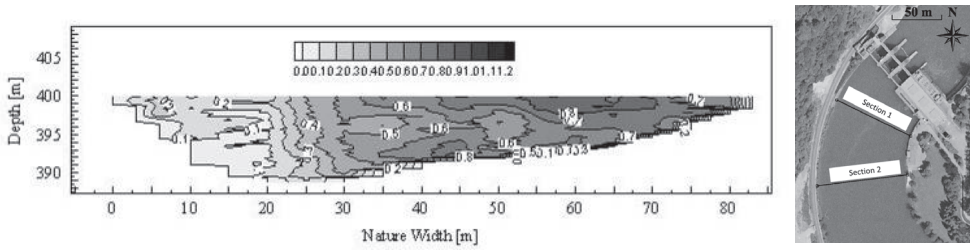

Figure 5 Contour plot of the absolute velocities [m/s], design discharge and turbine operation derived by ADCP measurements in the field in Section 2

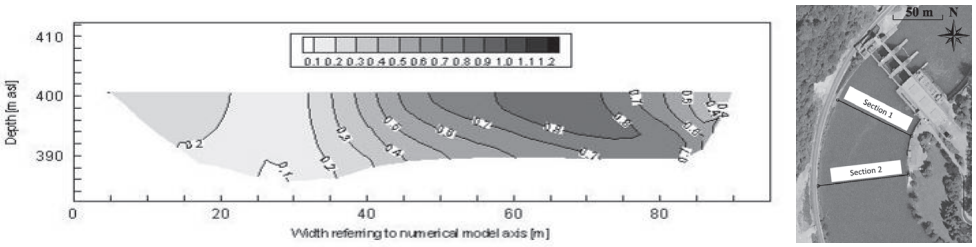

Figure 6 Contour plot of the absolute velocities [m/s], design discharge and turbine operation derived by the numerical model in Section 2

The flow field reproduced by the ADCP measurements and from the numerical model correlate very well. The ADCP measurement profile (Figure 5) show that, because of the complex geometry the highest velocities are at the inner site of the river bend. There is also an explicit separation zone and a backflow area at the left river bank. All these characteristics are reproduced in the numerical flow profile (Figure 6).
The numerical model also reproduces the effects of the secondary currents in the flow field.
The bed levels in the numerical model and in the prototype are slightly different, but this fact has no important influence on the flow field and the velocities as shown in Figure 5 and Figure 6.

The secondary currents were mapped well by the numerical model. Figure 7 illustrates the simulated flow directions at the bed level (light grey) and at the water surface (dark grey) for a 10-year flood without turbine operation.

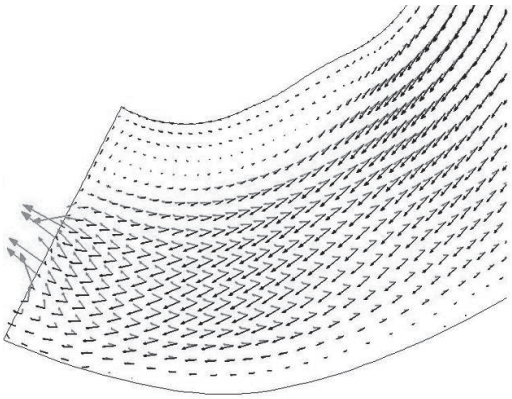

Figure 7 Secondary currents in the river bend – flow direction at the river bed (light gray) and at the water surface (dark grey) without turbine operation

The flow direction at the river bed is pointing towards the turbine inlets and therefore the main part of the sediment is transported to the turbines. In cases without turbine operation a large backflow zone in front of the turbine inlets occur (Figure 7). This backflow zone leads to massive deposition of sediments in this area.

6. RESULTS

6.1. Bed shear stress

Figure 8 shows on the left the "soft-flushing-case" with a discharge of 1,000 m^3/s and a water level of 398 m asl and on the right a discharge of 1,350 m^3/s (10-year-flood) with a water level of 400.5 m asl. The discharge of 1,000 m^3/s was chosen in context of the event probability to enable a frequently soft flushing of the reservoir. In both cases the turbines are not in operation.

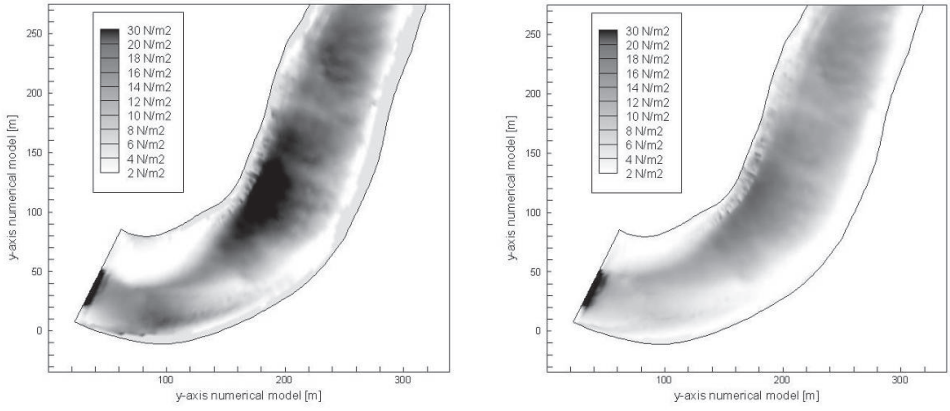

Figure 8 Bed shear stress derived by the numerical model [N/mm^2]
left: soft flushing with 1,000m^3/s and a water level of 398 m asl
right: 10-year-flood with 1,350m^3/s and a water level of 400.5 m asl

The drawdown of the water level increases the flow velocities and the bed shear stresses in the reservoir. Because of the low water depth in the reservoir the bed shear stresses are also increased in the middle of the reservoir. The shutdown of the turbines creates large recirculation zones near the turbine inlets at the inner site of the river bend in the numerical model. These recirculation zones can also be observed in the physical model and in the prototype.

6.2. Sediment transport

Figure 8 shows the comparison of the results obtained from the measured deposits in the physical and the numerical model. The digital elevation model of the sediment deposits in the physical model were carried out by using the measurement data of a three-dimensional laser scanner.

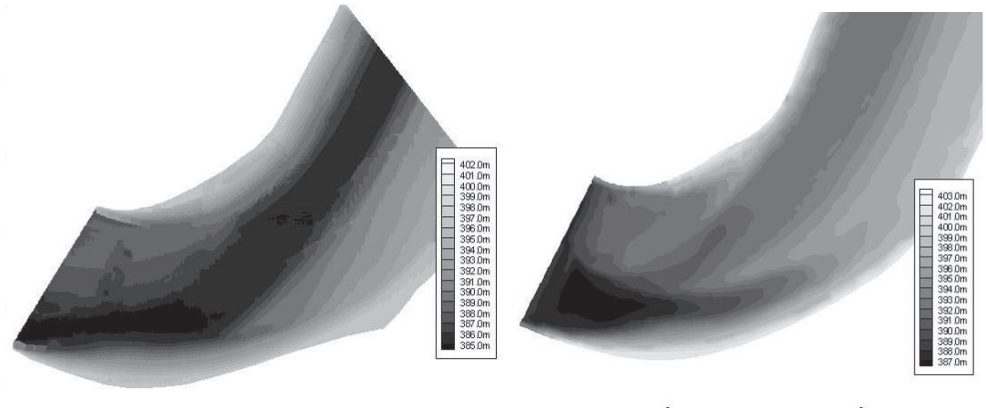

Figure 8 Scanned sediment depositions [m asl] in the physical model (left) and calculated sediment depositions [m asl] derived by the numerical model (right)

In the physical model the flushing channel is deeper than the simulated level in the numerical model. In addition, the numerical model shows more sediment depositions at the outer site of the river bend (Figure 8, right). This deviation may be explained by the fact that due to the very small grain sizes (d_{90}=0.9 mm and d_{50}=0.25 mm) of the deposited sediment in the reservoir, mineral granulates were used to model the sediment transport in the physical model. In consequence the influence of the cohesive sediment behaviour was partly neglected. This could lead to higher erosion rates in the physical model.
However, excluding this deviation, the deposition and the erosion of very fine and cohesive sediments is modeled well compared to the physical model.

7. CONCLUSIONS

In the present study the characteristic flow pattern, bed shear stresses and the sediment transport have been calculated with a three-dimensional numerical model. The results have been compared with ADCP field measurements and ADV measurements in the physical model. The comparisons of the flow velocities in different sections show good agreement. The numerical model predicts the flow characteristics in the river bend very well, but overestimates the high velocities and underestimates the low velocities in the backflow zones. This effect could be caused by slight differences of the reservoir bed geometry, the water level or the non-uniform distribution of the roughness in the reservoir. Also the used turbulence model could cause these slight differences in the flow field.
In the present case the drawdown of the water level increases the bed shear stresses also in the middle of the reservoir and not only close to the weir. The bed shear stresses in the soft flushing case are significantly higher than the bed shear stresses during flood events with higher discharges. Therefore, through soft flushing the sedimentation of particles can be reduced in these sections in relation to a normal “flood-operation”.

The deposition and erosion of very fine and cohesive sediments compare well with the results derived of the physical model, with slight deviations in the channel depth in consequence of the used granulates.
The model tests showed that in case of very fine and cohesive sediments the application of physical models is limited. The calibration of numerical models is also very complicated in this case. More field data and sediment analysis is required to improve the results of the numerical model.

8. ACKNOWLEDGMENTS

This work was conducted in collaboration with DI Lettner and DI Zarfl of the Ennskraft AG, which are gratefully acknowledged.
The second author was funded by the Research Council of Norway, through the RENERGI programme.

9. REFERENCES

Badura, H. (2007), *Feststofftransportprozesse während Spülungen von Flussstauräumen am Beispiel der oberen Mur*, Dissertation, Graz University of Technology, Austria.

Charlton, R. (2008), *Fundamentals of Fluvial Geomorphology*, Routledge, Taylor & Francis Group, London and New York.

Kobus, H. (1984), *Wasserbauliches Versuchswesen*, Schriftenreihe des deutschen Verbandes für Wasserwirtschaft und Kulturbau, 2nd Edition, Parey Verlag, Hamburg.

Morris, G. and Fan J. (1998), *Reservoir Sedimentation Handbook*, McGraw-Hill Publishing Company.

Olsen, N.R.B. (2009), *A Three-dimensional Numerical Model for Simulation of Sediment Movements in Water Intakes with Multiblock Option*, The Norwegian University of Science and Technology, Trondheim.

Patankar, S.V. (1980), *Numerical Heat Transfer and Fluid Flow,* McGraw-Hill Book Company, New York.

Rodi, W. (1980), *Turbulence Models and Their Application in Hydraulics*, A. A. Balkema, Rotterdam.

Schlichting, H. (1979), *Boundary Layer Theory*, McGraw-Hill.

Van Rijn, L.C. (1984a), *Part I: Bed load transport*, Journal of Hydraulic Engineering, 110(10), 1431-1456.

Van Rijn, L.C. (1984b), *Sediment Transport. Part II: Suspended load transport*, Journal of Hydraulic Engineering, 110(11), 1613-1641.

White, R. (2001), *Evacuation of sediments from reservoirs,* Thomas Telford Publishing.

SCHÖNAU - INTERNATIONAL JOURNAL OF SEDIMENT RESEARCH

Available online at www.sciencedirect.com
ScienceDirect
International Journal of Sediment Research 28 (2013) 255-263
INTERNATIONAL JOURNAL OF SEDIMENT RESEARCH
www.elsevier.com/locate/ijsrc

Numerical Analysis of Synthetic Granulate Deposition in a Physical Model Study

Gabriele HARB[1], Stefan HAUN[2], Josef SCHNEIDER[3], and Nils Reidar B. OLSEN[4]

Abstract

The current study focuses on the application of a three-dimensional numerical model for the prediction of morphological bed changes. The sediment deposition in a reservoir during a 10-year-flood was investigated and the results of the simulation were validated with data derived from a physical model study. Because of the small grain sizes in the prototype, synthetic granulate was used in the physical model. The numerical computation domain was a reproduction of the physical model, including the grain sizes and the density of the particles, in order to ensure comparability. The CFD code SSIIM, which solves the RANS-equations in three-dimensions, was used for the simulations. The sediment transport in SSIIM is divided into suspended sediment transport, computed by solving the convection-diffusion equation, and bed-load transport, calculated by an empirical formula. The results of the numerical simulation correspond well to the results of the physical model study. The simulated location and the pattern of the sediment deposition in the reservoir are an accurate representation of the observed distribution in the physical model.

Key Words: Physical modeling, Numerical modeling, RANS-equations, Reservoir management, Sediment

1 Introduction

The construction of dams and reservoirs influences the natural balance of sediment transport processes. The flow velocities, turbulences and bed shear stresses in reservoirs are reduced, and the transported bed and suspended sediment load settles. This leads to the raising of bed levels and to a reduced storage volume by "filling up" the reservoirs. Decreased reservoir volume reduces, and in extreme cases eliminates, the hydropower capacity, water supply and also irrigation and flood control benefits (Morris & Fan, 1998). Reservoirs formed by a dam with less than 20 m height are usually small and the morphological evolution here has a relatively quick development compared to large reservoirs (Wu, 2008). The sedimentation problem increases in cases of low-head hydro power plants such as these.

The investigation of these processes by using physical models in the lab was applied over the past few decades and is still state of the art. Since the 1970s numerical models have been greatly improved and are now widely applied in river engineering. Whereas CFD programs are already used for water flow calculations, the modeling of sediment transport still needs further development. Olsen used in a previous study a two-dimensional numerical model for simulating the flushing process of the Kali Gandaki reservoir in Nepal (Olsen, 1999a). However, two-dimensional depth-averaged approaches are not able to model secondary currents in rivers and reservoirs appropriately. Three-dimensional models are thus now being used ever more frequently. Examples are the simulation of the sediment transport in the Garita reservoir in Costa Rica (Olsen, 1999b), the simulation of the sediment transport in the Three Gorges project (Fang and Rodi, 2003) or the simulation of sediment deposition and erosion in the Angostura reservoir (Haun and Olsen, 2012; Haun et al., 2012).

Physical and numerical models are the major research tools in river engineering with advantages and disadvantages in both cases. Physical models are able to provide directly visible results, but are in most cases expensive and

[1] PhD Student, Institute of Hydraulic Engineering and Water Resources Management, Graz University of Technology, 8010 Graz, Austria. E-mail: gabriele.harb@tugraz.at.
[2] PostDoc, Department of Hydraulic and Environmental Engineering, The Norwegian University of Science and Technology, Trondheim, Norway. E-mail: stefan.haun@ntnu.no.
[3] Project-Senior Scientist, Institute of Hydraulic Engineering and Water Resources Management, Graz University of Technology, 8010 Graz, Austria. E-mail: schneider@tugraz.at.
[4] Professor, Department of Hydraulic and Environmental Engineering, The Norwegian University of Science and Technology, Trondheim, Norway. E-mail: nils.r.olsen@ntnu.no.
Note: The original manuscript of this paper was received in Aug. 2012. The revised version was received in Mar. 2013. Discussion open until June 2014.

time-consuming. The hydrodynamic and morphological processes are very complex in natural rivers, which often make it difficult to ensure the similarity between the physical model and the prototype. Distortions of the model scale (e.g., in roughness or sediment sizes) and variations in the experimental environment may cause errors (Heller, 2011). Numerical modeling is able to give real-scale results without scale distortion and is in most cases more cost and time efficient (Chandler et at., 2003; Gessler and Rasmussen, 2005). However, the reliability of the numerical model depends on the quality of the mathematical implementation of the physical processes. Hence, numerical models need to be verified and validated using analytical solutions and measurement data. Both of the tools mentioned, the physical model and the numerical model, must be calibrated with field measurements, in order to ensure comparability.

The "hybrid modeling approach" – the use of both model types for the same case study – is a method which is used with an increasing frequency in hydraulic engineering (Scheuerlein et al., 2004; Feurich and Rutschmann, 2005). By using this approach the physical model can be applied to analyze a few selected problems in detail, to calibrate the numerical model appropriately, and to validate the numerical results. The calibrated numerical model is normally used to analyze a lot of different scenarios (e.g., the declination of groins in rivers) and to investigate scenarios close to the limitations of the physical model.

In this study the "hybrid modeling approach" was applied. The deposition of synthetic granulates in case of a 10-year flood event was simulated in the numerical model and validated with the results of the physical model. Because of the small grain sizes in the prototype, synthetic granulate was used to model the deposition in the physical model. The numerical model was a reproduction of the physical model. However, there are small differences, such as the partial opening of the weir in the physical model, which could not be reproduced in the numerical model due to the adaptive grid.

2 Experimental Program and Background

The experimental program was carried out at the Hydraulic Laboratory of the Graz University of Technology in the period between 2008 and 2010 (Zenz et al., 2010). The 24 m long and 2.5 m wide model was a representation of the natural riverbed at the geometrical undistorted scale of 1:40. The similarity of the physical model was based on Froude's law. The modelled natural river length of 950 m was divided into a 570 m long part of the hydropower reservoir and a 380 m part of the downstream section. The physical model was built in concrete with a fixed river bed. Figure 1 shows an overview of the reservoir part of the physical model. The power house is located at the inner side of the river bend and the three segment gates with attached flap gates are on the outer side. The prototype was built in the 1970s. In the last years the sediment load transported into the reservoir increased because of more frequently conducted flushing processes in the upstream located reservoirs. Legal restrictions prohibit the lowering of the water level and consequently the flushing of the prototype itself is not possible. Therefore, in case of higher discharges massive sediment depositions occur in the front of the turbine intakes of this hydropower plant, caused by flushing processes at the upstream located reservoirs. Several flood discharges were analysed in the physical model to solve the sedimentation problem. Based on the experience gathered from the prototype the 10-year flood represents the key scenario.

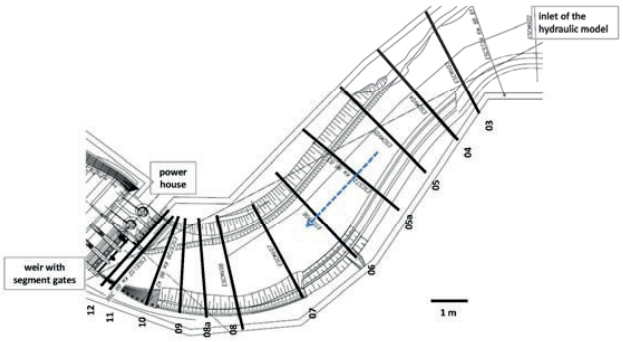

Fig. 1 Plan view of the reservoir part of the physical hydraulic model

The Manning coefficient of the model for the bed roughness was n=0.01667 s $m^{-1/3}$, determined by similarity of the water levels. The grain size distribution of the deposited sediments in the prototype is very fine (d_{90}=0.9 mm and d_{50}=0.25 mm) and has a density of 2.73-2.80 g cm^{-3}. As a consequence of these small grain sizes, synthetic granulate was used to model the sediment transport and the sediment deposition in the physical model. The synthetic granulate had a cylindrical form with a grain size of 2 mm, a density of 1.29 g cm^{-3} and a in the laboratory determined fall

velocity of 0.07 m s^{-1}. The larger but lighter grains are typical for models designed by taking into account the grain Reynolds number (Yalin, 1971; Kobus, 1984).

In this study the flow field and the hydromorphological changes caused by the 10-year-flood in the reservoir were analysed. For the hydrodynamic investigation a steady discharge rate of 133.4 l s^{-1} and a simulation time of 7,200 seconds were applied, which represents 1,350 m^3 s^{-1} and 12 hours in the prototype, respectively. These conditions were pre-specified by the initiator of the model test. In accordance to the operation plan, the turbines were shut down during the flood event. The attached flap gates were fully opened. The left segment gate was shut; the middle and the right one were opened approx. 30 %. During the physical model simulation about 0.11 m^3 of synthetic granulate was added with a continuous rate of approx. 5 g s^{-1} by an upstream located sediment feeding equipment. To derive a digital elevation model of the sediment deposition in the physical model, the depositions were scanned after the experiment by using a three-dimensional laser scanner.

3 Numerical Simulation

For this study the computational fluid dynamics (CFD) code SSIIM 2 was used (Olsen, 2011). The numerical program solves the continuity equation together with the Reynolds-averaged Navier-Stokes (RANS) equations with respect to the mass and momentum conservation in three dimensions (Versteeg and Malalasekera, 1995).

$$\frac{\partial U_i}{\partial x_i} = 0 \tag{1}$$

with i=1, 2, 3

$$\frac{\partial U_i}{\partial t} + U_j \frac{\partial U_i}{\partial x_j} = \frac{1}{\rho} \frac{\partial}{\partial x_j} \left(-P\delta_{ij} - \rho \overline{u_i u_j} \right) \tag{2}$$

where U_j is the averaged velocity, x is the spatial geometrical scale, ρ is the water density, P is the dynamic pressure, δ_{ij} is the Kronecker delta and $-\rho \overline{u_i u_j}$ are the turbulent Reynolds stresses.

The program applies the finite volume method as discretization scheme, where the convective term in the RANS-equations is modeled with a power law scheme (Olsen, 2011). The turbulent stresses were modeled by the standard k-ε model (Launder and Spalding, 1972). The Semi-Implicit Method for Pressure-Linked Equations (SIMPLE) was applied to find the unknown pressure term in the Navier-Stokes equations (Patankar, 1980). A Dirichlet boundary condition was used for the inflow and a zero gradient boundary condition for the outflow. Wall laws by Schlichting (1979) were chosen at the side walls of the numerical model.

$$\frac{U}{u^*} = \frac{1}{K} \left(\frac{30y}{k_s} \right) \tag{3}$$

where u^* is the shear velocity, K is the Karman constant, k_s is the roughness coefficient and y is the water depth.

Changes in the free-water surface were computed in accordance to the pressure gradient between the cell and the neighbour cell (Olsen and Haun, 2010).

$$\frac{\partial p}{\partial x_i} = \rho g \frac{\partial z}{\partial x_i} \tag{4}$$

where p is the pressure, g is the acceleration of gravity and z is the water level elevation.

Depending on the location of the neighbour cell, the flow direction and the Froude number, a weighting coefficient is involved.

$$c_w = \begin{cases} \min(2 - Fr; 1.0) & for \quad w > -0.1 \; and \; Fr < 2.0 \\ w^2 (Fr - 1.0) & for \quad w < -0.5 \; and \; Fr > 2.0 \\ 0.0 \end{cases} \tag{5}$$

with $$w = \frac{\vec{r} \times \vec{u}}{|\vec{r}| \times |\vec{u}|} \tag{6}$$

where c_w is the weighting coefficient for the neighbour cell, Fr is the Froude number, w is the dot product of $\vec{u}$ and $\vec{r}$, $\vec{u}$ is the velocity vector of the cell and $\vec{r}$ is the direction vector pointing to the centre of the neighbour cell.

SSIIM 2 uses an adaptive and non-orthogonal grid, made of tetrahedral and hexahedral cells. The Rhie and Chow (1983) interpolation was applied for the non-staggered grid to calculate the fluxes and velocities at the surface of the cell. The unstructured grid allows a varying number of grid cells in all three spatial directions. A wetting and drying algorithm was used to avoid distorted cells (Olsen, 2011). The algorithm used specifies how many cells are generated in the z-direction, depending on the water depth (y). Two limiting values are required as boundary conditions, where the first value (ζ_1) specifies if a cell is generated or if the water depth is too shallow and the domain dries up and disappears

from the grid ($y < \zeta_1$). If the water depth is sufficient a second value (ζ_2) indicates if one cell is generated and a two-dimensional calculation is made ($\zeta_1 < y < \zeta_2$) or if the number of cells is calculated by equation 7 ($y > \zeta_2$). For this study the pre-specified values are chosen with 0.01 m and 0.02 m for the limiting factors ζ_1 and ζ_2, respectively.

$$n = n_{\max} \times \left(\frac{depth}{depth_{\max}} \right)^{p} \tag{7}$$

where n is the number of grid cells in the vertical direction, n_{max} is the maximum number of grid cells in the vertical direction and p is a parameter for the number of grid cells.

The grid is updated in this study after each time step that changes in the bed and water levels during the computations are taken into account accurately. The computation of the sediment transport is subdivided into suspended and bed load transport. The suspended sediment transport was calculated by solving the transient convection-diffusion equation.

$$\frac{\partial c}{\partial t} + U_j \frac{\partial c}{\partial x_j} + w_f \frac{\partial c}{\partial z} = \frac{\partial}{\partial x_j} \left(\Gamma \frac{\partial c}{\partial x_j} \right) \tag{8}$$

with $\nu_t = S_c \, \Gamma$

where w_f is the fall velocity of the particle, Γ is the turbulent diffusity, c is the sediment concentration over time t and over the spatial geometrical scales x and z, ν_t is the turbulent eddy viscosity and S_c is the Schmidt number (with a default value of 1.0).

A specified sediment concentration in the bed cell was used as the boundary condition for the computations (Van Rijn, 1984b). The bed load was computed by the empirical formula from Van Rijn (1984a).

$$\frac{q_{b,i}}{d_i^{1.5} \sqrt{\frac{(\rho_s - \rho) g}{\rho}}} = 0.053 \frac{\left(\frac{\tau - \tau_{c,i}}{\tau_{c,i}} \right)^{2.1}}{d_i^{0.3} \left(\frac{(\rho_s - \rho) g}{\rho \nu^2} \right)^{0.1}} \tag{9}$$

where $q_{b,i}$ is the transport rate of the fraction of the bed load (per unit width), d_i is the particle diameter, τ is the bed shear stress, $\tau_{c,i}$ is the critical shear stress, ρ_s is the density of the sediment and v is the kinematic viscosity.

The sand slide algorithm used in SSIIM is based on the angle of repose of the bed material. After each update of the mesh the angles of the river banks are checked to see if they are steeper than the pre-specified angle of repose. In such a case the angle of the river banks is corrected to the pre-specified angle of response taking the potential geotechnical failures into account (Olsen, 2001).

In SSIIM an implicit time discretization was used, so a time step size of one second was possible. A sensitivity analysis regarding the time step size was conducted to avoid an influence on the results. However, a decrease of the time step size will not influence the results, so time step independent results were found. In this study the maximum number of cells in the vertical direction was limited to 11. The number of total cells at the be-ginning of the simulation was chosen with about 50,000, representing a cell size of 0.02 m x 0.02 m in the x-and the y-direction, respectively. Due to the changes of the bed and the water levels, 48,600 cells were left after the simulation. The bed roughness was calibrated using the similarity of the water levels in the physical model and the numerical model and set to 0.00862 m in the numerical model. In addition the ADV measurements for design discharge in the physical model were used for the calibration of the numerical model.

The computation was divided into two parts; the computation of the hydrodynamic flow field to obtain a steady flow situation of the flood scenario was made first and followed by the simulation of the morphological bed changes. The hydrodynamic flow field was updated during the simulation of the morphological bed changes after each time step. The real-time computation times were 12 hours and 16 hours, respectively.

4 Results and Discussion

4.1 Hydrodynamic Validation of the Numerical Model and Discussion

The three-dimensional velocity profiles, computed by the numerical model, were validated with the measured ADV-profiles of the flood event in the physical model. The velocity profiles of the ADV measurements are shown in Figure 2a and 3a and the velocity profiles derived by numerical computation are presented in Figure 2b and 3b in section 7 and section 9 in Fig. 1, respectively.

The first measured values in the velocity profiles of the ADV measurements are approx. 5 cm below the surface and approx. 1cm above the bed. This is a constant value due to the distance of the sample volume to the sensors. The section in Figure 2 represents the shallowest section in the physical model with a total water depth of only 20 cm (section 7).

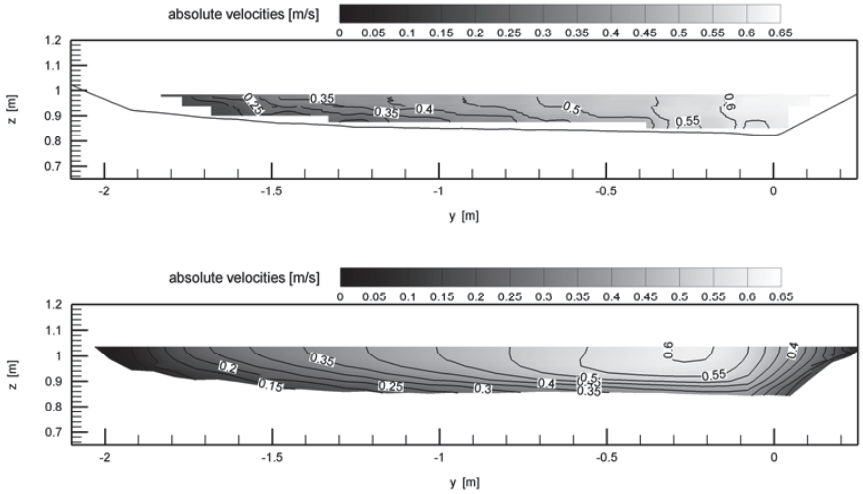

Fig. 2 (a) velocity profile of the ADV measurement and (b) velocity profile derived by the numerical computation in section 7

The comparison of the velocity profiles shows an overall agreement of the flow pattern and the flow distribution for section 7 between the numerical and the physical model. The maximum flow velocity is at the orographic right side (y=0.25 m) in both models with a maximum magnitude of about 0.6 m s^{-1}. The minimum flow velocity is located at the outer side (y=1.5 m) and shows a magnitude of about 0.15-0.2 m s^{-1}. Small differences could be observed, which is most likely caused by differences in the water level calculation and the used turbulence model.

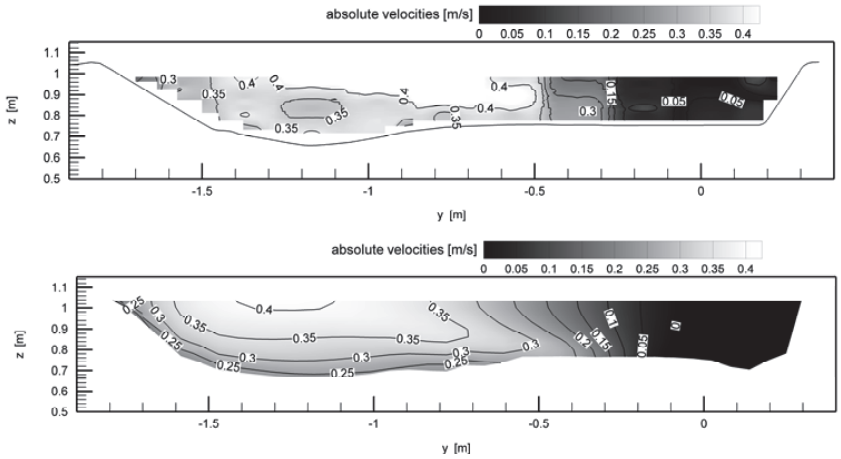

Fig. 3 (a) velocity profile of the ADV measurement and (b) velocity profile derived by the numerical computation in section 9

Section 9, closer to the intakes, presents a more complex flow distribution because of the distinctive secondary currents in this area (Harb et al., 2011). Figure 3b shows that the three-dimensional numerical model predicts a smoother velocity distribution in this section. This effect is caused by the mathematical implementation of the physical processes and the slightly different boundary conditions at the outflow boundary. The complex opening structure of the weirs with overflow and underflow of the segment gates, due to the partial opening, could not be implemented in the numerical model. The physical model as well as the numerical model show a maximum flow velocity at the outer side of the bend (y=1.25 m) with a magnitude of about 0.40 m s^{-1}. However, in the physical model the area of high velocities close to the surface expands more to the inner side of the bend. At the inner side of the river bend an explicit backflow zone with a magnitude of 0.05 m s^{-1} is shown in both models (y=0.2 m).

Figure 4a and 4b show the velocity vectors in front of the intakes computed by the numerical model close to the bed and the surface, respectively.

The velocity vectors at the surface cells are pointing to the open outlets at the outer side of the river bend (Fig. 4 b). Due to the secondary currents at the bed, the bed vectors point directly to the turbine inlets (Fig. 4 a). This influences the sediment transport for the 10-year-flood simulation in a massive way.

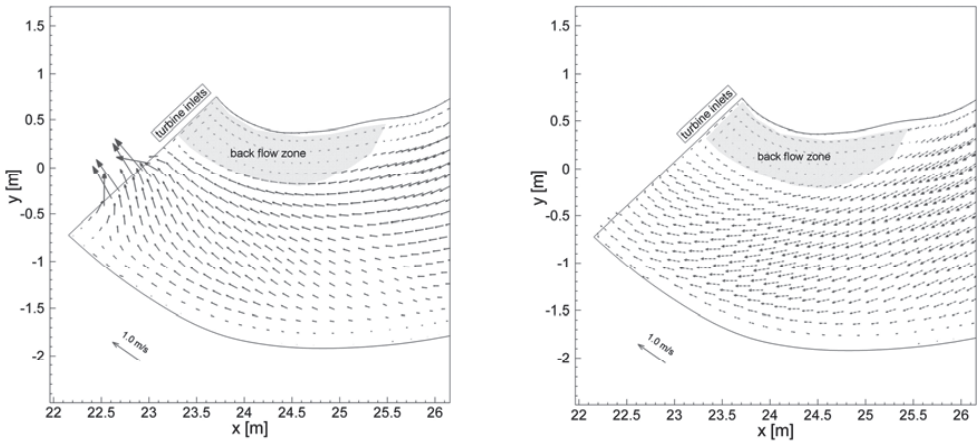

Fig. 4 Velocity vectors at the bed (a) und at the surface (b) in the area of the intakes for the 10-year-flood scenario (plan view)

4.2 Hydromorphological Validation of the Numerical Model and Discussion

In the prototype the power house is located at the inner side of the river bend. Hence, the sediment is transported naturally towards the turbine inlets, which results in sediment deposition in front of the intakes. The results of the hydrodynamic simulation of the 10-year-flood scenario show a distinctive back flow zone in front of the turbine inlets, which increase the sediment flow in this direction (Fig. 4a, b). This leads to huge depositions in front of the intakes. Figure 5 illustrates the deposited synthetic granulates near the turbine inlets after the simulation without turbine operation in the physical model.

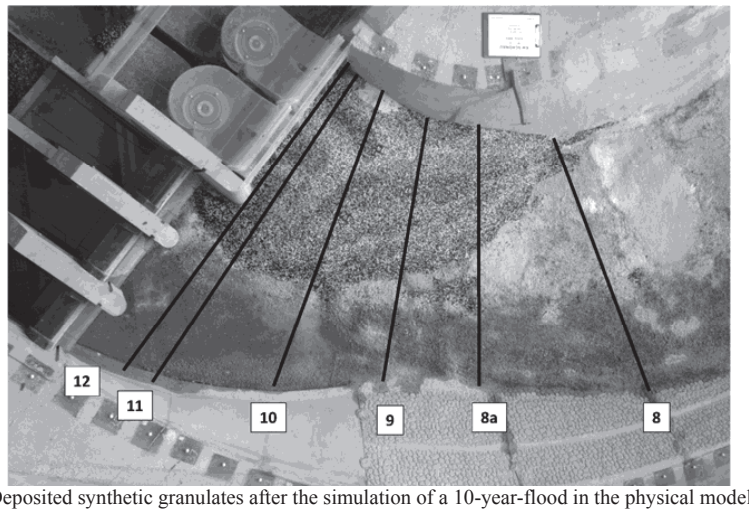

Fig. 5 Deposited synthetic granulates after the simulation of a 10-year-flood in the physical model (plan view)

In the numerical simulation identical parameters for grain size, fall velocity and density of the synthetic granulate were used as in the physical model. The Shields coefficient was, after a sensitivity analysis, chosen with 0.05. The conducted sensitivity analysis showed that the results are very sensitive to changes in this parameter. The Shields parameter was therefore a main calibration parameter for the sediment transport simulation.

Figure 6a – 6e compare the results of the physical and the numerical model. The deposition in the physical model was measured using a three-dimensional laser scanner with a minimum accuracy of +/- 2.0 mm. The data from the laser scan showed a large amount of sediments has deposited in front of the turbines on the orographic right side caused by the secondary currents.

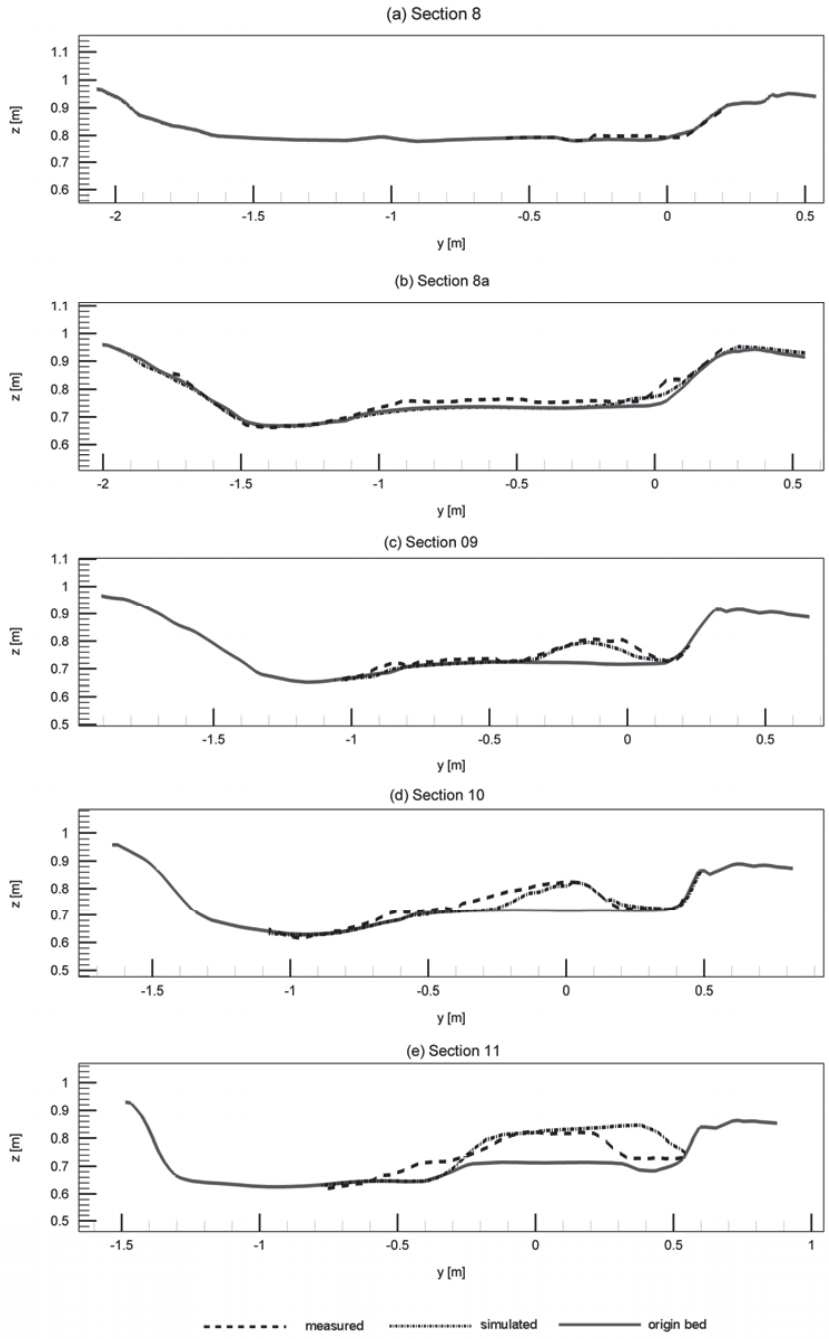

Fig. 6 Comparison of the measured and simulated depositions

Section 7 and 8 show clearly that the deposition in the physical model starts further upstream as in the numerical model. This difference is most likely caused by small differences in the water level calculation and the used turbulence model. In the numerical model also a general drift to the inner side of the bend occurs in section 8, which is most probably a result of an overestimation of the secondary currents in this area. Figure 7 shows the measured velocity vectors in the y-direction and the z-direction indicating the secondary currents in section 9.

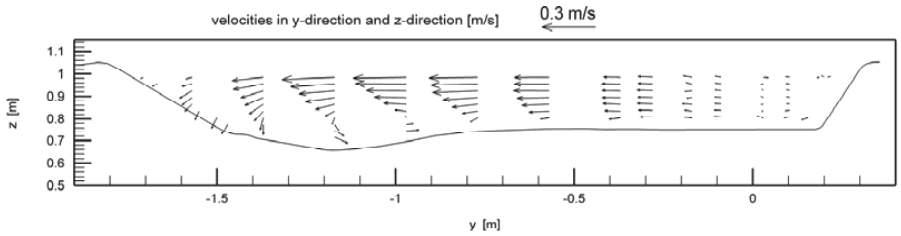

Fig. 7 Measured velocity vectors from the ADV measurements in section 9

The deposition pattern in the physical model is wider than in the numerical model (section 9, 10 and 11). The results showed also that the slopes of the deposited material have a steeper angle in the numerical simulation than in the physical study. This difference can be a result of the implemented sand slide algorithm, which does not take the properties, especially the angle of repose, of the plastic particles completely into account. The result of section 11 shows that the peak piles up in front of the closed intakes at the inner side of the bend in the numerical simulation. This agrees physically very well with the plotted velocity vectors in Figure 4. The numerical model, however, produces a compact deposition structure at the inner side of the bend and deposits too little sediments in the middle of the reservoir. An overestimation of the secondary currents could cause this displacement. For the simulations a first order upwind scheme was used, because the simulation with a second order upwind scheme would increase the overestimated eddies and secondary currents additionally.

4 Conclusions

The current study presents the application of a three-dimensional numerical model for the prediction of morphological bed changes compared with a physical model. In both models the sediment depositions in a reservoir during a 10-year-flood were simulated. Because of the small grain sizes in the prototype, synthetic granulate was used to model the deposition in the physical model. The numerical simulation was a replication of the physical model, including geometry, hydrodynamic boundaries and sediment properties. The hydrodynamic results of the three-dimensional numerical model have been verified with ADV measurements conducted in the physical model. The comparisons of the flow velocities and the characteristic flow pattern show a good accuracy level. The maximum as well as the minimum flow velocities and the flow characteristics upstream of the intakes are predicted well. However, due to the approximations in the numerical model and small assumptions in the model setup (e.g., the complex partial opening of the weir, which could not be reproduced by the numerical model) small differences could be recognized. The bed load transport formula by van Rijn, developed for uniform and non-cohesive sediments, was used in the program to calculate the transport of the synthetic granulates. It is demonstrated, that the computed bed elevation changes are in an overall agreement with the measured depositions. Although minor differences in the deposition pattern could be recognised, the results of the three-dimensional numerical model are consistent with the measured depositions in the physical model. The results support the application of the numerical model as part of a hybrid modelling approach in further sediment studies.

Acknowledgement

The second author was funded by the Research Council of Norway, through the RENERGI programme.

References

Chandler, K., Gill, D., Maher, B., Macnish, S. and Roads, G. 2003, Coping with probable maximum flood – an alliance project delivery for Wivenhoe Dam. Proceedings of the 43rd ANCOLD Conference, Hobart, Tasmania, 332–349.

Fang, H-W. and Rodi W. 2003, Three-dimensional calculations of flow and suspended sediment trans-port in the neighborhood of the dam for the Three Gorges Project (TGP) reservoir in the Yangtze River. J. Hydraulic Res. 41(4), 379–394.

Feurich, R. and Rutschmann, P. 2005, Efficient Design Optimization and Investigation by Combining Numerical and Physical Models. XXXI IAHR Congress Seoul, Theme A, Hydroinformatics, Hydraulic Modelling and Data: Competition or Integration?, 490–500.

Gessler, D. and Rasmussen, B. 2005, Before the flood [online], Desktop Engineering Magazine, Available from: http://www.deskeng.com/articles/aaabhe.htm, [Accessed 17 March 2011].

Haun, S. and Olsen, N.R.B. 2012. Three-dimensional numerical modelling of reservoir flushing in a prototype scale. International Journal of River Basin Management. 10(4) 341-349.

Haun, S., Kjærås, H., Løvfall, S. and Olsen, N.R.B. 2012, Three-dimensional measurements and numerical modelling of suspended sediments in a hydropower reservoir. Journal of Hydrology, 479 180-188.

Harb G., Haun S., Ortner S., Dorfmann C. and Schneider J. 2011, The influence of secondary currents on reservoir sedimentation – experimental and numerical studies. Proceedings of the 34th IAHR World Congress, Engineers Australia, July 2011.

Heller, V. 2011, Scale effects in physical hydraulic engineering models. J. Hydraulic Res. 49 (3), 293-306
Kobus, H. 1984, Wasserbauliches Versuchswesen, Schriftenreihe des deutschen Verbandes für Wasser-wirtschaft und Kulturbau, 2nd Edition. Parey Verlag, Hamburg.
Launder, B.E. and Spalding, D.B. 1972, Lectures in mathematical models of turbulence. Academic Press, London.
Morris G. L. and Fan J., 1998, Reservoir Sediment Handbook. McGraw-Hill Book Co., New York.
Olsen, N.R.B. 1999a, Two-dimensional numerical modelling of flushing processes in water reservoirs. J. Hydraulic Res. 37 (1), 3-16.
Olsen, N.R.B. 1999b, 3D CFD modelling of water and sediment flow in a hydropower reservoir. International Journal of Sediment Research 14 (1), 16- 24.
Olsen, N.R.B. 2001, CFD modelling for hydraulic structures., Department of Hydraulic and Environmental Engineering, The Norwegian University of Science and Technology.
Olsen, N.R.B. and Haun, S. 2010, Free surface algorithms for 3D numerical modelling of reservoir flushing. Dittrich et al. Preprints of the River Flow Conference 2010, Bundesanstalt für Wasserbau, 1105-1110.
Olsen, N.R.B. 2011, A Three-Dimensional Numerical Model For Simulate Of Sediment Movements In Water Intakes With Multiblock Option. Users`s Manual, by Nils Reidar B. Olsen, Department of Hydraulic and Environmental Engineering, The Norwegian University of Science and Technology.
Patankar, S.V. 1980, Numerical Heat Transfer and Fluid Flow. McGraw-Hill Book Company, New York.
Rhie, C. and Chow, W. 1983, Numerical study of the turbulent flow past an airfoil with trailing edge separation. AIAA Journal 21(11), 1525-1532.
Scheuerlein, H., Tritthart, M., Nuñez-Gonzalez, F. 2004, Numerical and physical modeling concerning the removal of sediment deposits from reservoirs. Proc. Conf. Hydraulic of Dams and River Structures, Tehran, Iran, 245–254. Balkema, Leiden, The Netherlands.
Schlichting, H. 1979, Boundary layer theory. McGraw-Hill Book Company, New York.
Van Rijn, L.C. 1984a, Sediment Transport. Part I: Bed load transport. J. Hydraulic Res. 110(10), 1431-1456.
Van Rijn, L.C. 1984b, Sediment Transport. Part II: Suspended load transport. J. Hydraulic Res. 110(11), 1613-1641.
Versteeg, H.K. and Malalasekera W. 1995, An introduction to Computational Fluid Dynamics, The Finite Volume Method. Pearson Education Limited, Edinburgh.
Wu, W. 2008, Computational River Dynamics. Taylor & Francis Group, London, UK.
Yalin, M.S. 1971, Theory of Hydraulic Models. The Macmillan Press LTD, London.
Zenz, G., Schneider, J., Ortner, S., Harb, G., Dorfmann, C., Lazar, F. 2010, KW Schönau - Hydraulischer Modellversuch. Institute of Hydraulic Engineering and Water Resources Management, Graz University of Technology, Austria (unpublished).

LEOBEN - RIVERFLOW 2012

River Flow 2012 – Murillo (Ed.)
© 2012 Taylor & Francis Group, London, ISBN 978-0-415-62129-8

Numerical analysis of sediment transport processes in a reservoir

G. Harb, C. Dorfmann & J. Schneider
Institute of Hydraulic Engineering and Water Resources Management, Graz University of Technology, Austria

S. Haun
Department of Hydraulic and Environmental Engineering, The Norwegian University of Science and Technology, Trondheim, Norway

H. Badura
VERBUND Hydro Power AG, Vienna, Austria

ABSTRACT: Flushing is a possible technique to reduce sediment depositions in reservoirs. The paper presents the application of a numerical model for an Alpine reservoir. An open source numerical model is used to simulate a flushing process. The calibration of the morphological part of the model was complex, because no flushing has been performed in the reservoir so far. Therefore deposition data and freeze core probes have been used to calibrate the sediment transport capacity. The accumulated amount was compared with numerical simulations using different sediment transport formulae. It was found that the Meyer-Peter-Müller bed load equation showed the best agreement with the measured data. In consequence, this bed load formula was used to determine the sediment transport processes in the numerical simulation of the reservoir flushing during a 1-year flood.

1 INTRODUCTION

The construction of dams and reservoirs influence the natural sediment transport processes and affect the sediment connectivity. Due to the increase in water depth in reservoirs, the flow velocities, turbulences and bed shear stresses are reduced variably. This leads to deposition of the transported sediments, increases the bed level and often reduces the storage volume by "filling up" the reservoir. A decreased reservoir volume reduces, and in extreme cases eliminates the capacity of hydropower, water supply, irrigation and flood control benefits (Morris & Fan 1997). Reservoirs formed by dams with less than 20 m height are usually shallow and morphological evolution develops relatively quick compared to large reservoirs (Wu 2008).

The main factors in reservoir sedimentation are the reduced transport capacity of coarse solids as bed load, the transport of fine fractions in a stochastic distribution, and. in some cases the transport of fine fractions in the form of density currents The occurring sedimentation pattern reflects these processes and therefore it is essential to know the processes determining the sedimentation in order to choose the adequate management method (Bechteler 2006).

Three sedimentation zones can be identified along the longitudinal section of a reservoir (Morris & Fan 1997 Figure 1):

a) Upstream portion ("topset bed"): at the head of the reservoir where usually coarser sediments are deposited. However, depending on the morphology of the delta, finer and very fine grain sizes are also possible;
b) Middle portion ("foreset bed"): is characterized by an increasing longitudinal gradient along with decreasing grain sizes;
c) Downstream portion ("bottomset bed"): next to the dam structure where the fine particles are deposited.

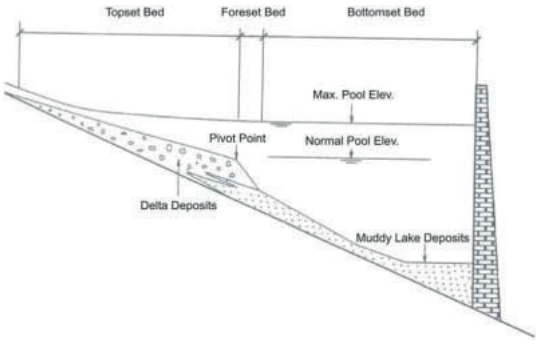

Figure 1. Deposition zones in the longitudinal section through a reservoir (Morris & Fan 1997).

As described in Figure 1, fine sediments are transported to the weir, coarse sediments (gravel and cobbles) deposit mainly at the head of the reservoir.

Hydraulic removal like flushing is one of the most common ways to manage deposition problems in reservoirs. The intention of reservoir flushing is the

remobilization of sediment depositions, accumulated during longer operation periods. In most cases the flushing of reservoirs in the alpine area is a special challenge, because of the deposition of coarse sediment at the head of the reservoir (Scheuerlein 1990). During a flushing event the coarse sediment, eroded from the head of the reservoir, may deposit again further downstream in the reservoir (Atkinson 1996). This effect depends on the reservoir length, the sediment transport capacity and flushing duration.

During short flushing periods the remobilization leads to higher sediment concentrations in the downstream area of the river. This concentration may be harmful to the downstream river ecosystem (e.g. fish). Consequently reservoir flushing programs often require extensive regulations and monitoring programs. An example is the Bodendorf reservoir at the river Mur in Austria (Badura 2007). These constraints may limit the allowable water level drawdown in the reservoir, requiring that the flushing process is performed under pressure and not under free flow conditions. Flushing with partial drawdown of the water level can be performed in reservoirs of run-of-river power plants or in diversion plants. Both mentioned types are characterized by high inflow in relation to the storage volume and shallow reservoirs. Because of the lower water level, the velocities and the bed shear stresses in the reservoir are higher than at maximum operational level and erosion takes place.

Numerical modelling is already used for hydrodynamic calculations; whereas sediment transport modelling still needs further development and research. In a previous study Olsen applied a two-dimensional numerical model for simulating the flushing process of the Kali Gandaki reservoir in Nepal (Olsen 1999a). Examples of three-dimensional modelling are the simulation of the sediment transport in the Three Gorges project performed by Fang & Rodi (2003), the simulation of the sediment transport in the Garita reservoir in Costa Rica (Olsen 1999b) or in the Feistritz reservoir (Dorfmann & Knoblauch 2009).

In this study a numerical analysis is carried out to investigate the sediment transport processes in a reservoir during flushing. Based on the grain-size distribution derived by sediment samples and the total deposited amount of sediments, the sediment transport formulae for the numerical simulation are evaluated.

2 PROJECT AREA AND BACKGROUND

The project area is a reservoir at the river Mur in Styria, Austria (Figure 2). The run-of-river hydropower plant, forming the reservoir, was built in 2006 with an initial storage volume of about 360,000 m^3. Echosoundings performed in 2010 showed that approximately 80,000 m^3 of sediments are already deposited in the small reservoir. This represents an annual sedimentation rate of about 5.5% of the reservoir volume. Due to this fact, the present flushing strategy has to be adapted and optimized.

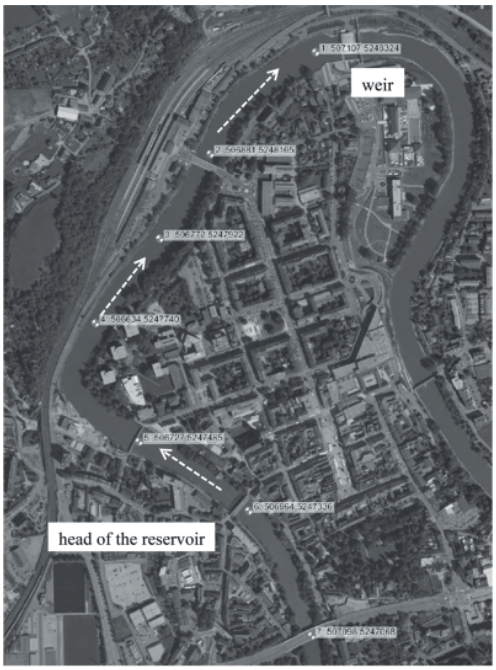

Figure 2. Project area with sediment sampling points.

Table 1. Morphology and hydrology of the project area.

Morphology		Discharge [m^3/s]	
reservoir slope	1.5‰	mean flow	80
reservoir width	80–100 m	design discharge	150
		1-year flood	335
roughness k_{st}	(m$^{1/3}$/s)	5-year flood	510
		10-year flood	580
reservoir bed	~30	30-year flood	750
reservoir banks	15–20	100-year flood	930

The morphological and hydrological conditions of the project area are presented in Table 1.

3 NUMERICAL SIMULATION

The TELEMAC suite has been continuously developed by EDF R&D for over 20 years. One main code within the TELEMAC suite is TELEMAC-2D, which solves the depth-integrated shallow water equations, which can be applied when the horizontal length scale of the flow is much greater than the vertical scale (Hervouet 2007). In the present study the hydrodynamic model TELEMAC-2D, internally coupled with the morphological sediment transport model SISYPHE was used. The package is based on a Finite Element approach (Moulinec et al 2011). TELEMAC uses a triangular and unstructured grid. In general, the space discretization is linear. Several advection schemes are available, e.g. the method of characteristics, the streamline-upwind Petrov-Galerkin (SUPG),

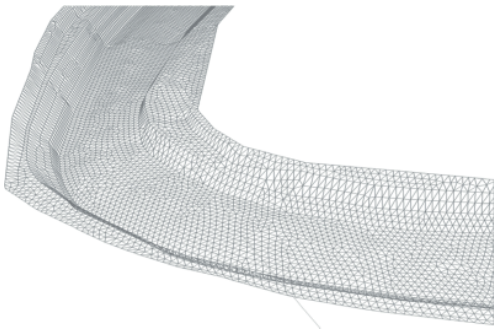

Figure 3. Sketch of the generated mesh with the conserved break lines of the river banks, 3D view superelevated.

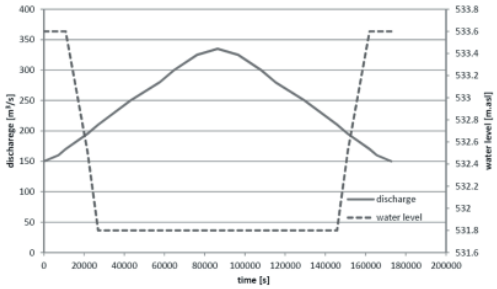

Figure 4. Inflow hydrograph and outlet water level in the numerical simulation.

the Residual Distributive Schemes (N-Scheme and Psi-Scheme). The main results of the hydrodynamic solver are the water depths and the depth-averaged velocities in every node of the computational mesh. In this study for the advection of velocities the method of characteristics and a constant eddy viscosity model were used.

Based on the existing bathymetry data, a three-dimensional digital elevation model was generated. The mesh with approximately 24,000 triangular cells and an average edge length of 2.5 m was mapped on the digital elevation model using the free software BlueKenue (CHC 2010). Figure 3 shows a 3D view of a part of the generated mesh with the conserved break lines of the river banks.

For the numerical simulation a time step of 1.0 seconds was chosen. The flushing event during a 1-year flood was simulated. The stage-discharge function as downstream boundary condition and the inflow hydrograph for the upstream boundary are shown in Figure 4. The bed roughness was set to a constant Mannings value of $n = 0.033$ for the river bed and $n = 0.5$ for the river banks.

In the morphological module SISYPHE the bed load functions of Meyer-Peter-Müller, Einstein-Brown, Engelund-Hansen and Van Rijn are implemented. The evaluation of the sediment transport functions compared with the measured sediment transport in the reservoir is presented later.

Table 2. Characteristic diameters of the sediment samples.

Sediment sample	d_{90}[mm]	d_m[mm]
sample 1	1.2	0.4
sample 2	11.2	1.1
sample 3	22.5	8.4
sample 4	46.0	17.0
sample 5	72.0	22.4
sample 6	91.0	32.8
sample 7	140.0	35.0

3.1 *Required input data and calibration of the numerical model*

The required input data for the numerical simulation were the hydrographs of the last years to determine the hydrological conditions, the stage-discharge curve, the grain size distributions along the reservoir and the sediment transport capacity in the reservoir. The sediment transport capacity of the free flowing zone upstream of the reservoir represents the equilibrium condition. In consequence, the sediment transport capacity of this upstream area was chosen as the boundary condition for the bed load transport into the reservoir.

The calibration of the hydrodynamic model was done using discharge and water level data collected by a gauge of the Government of Styria, which is located near the head of the reservoir. Additional ACDP measurements, performed at the prototype, were used to calibrate the roughness at the river bed and at the banks.

3.2 *Hydrological conditions*

The hydrological conditions in the years since 2006 were analysed. Six flood events with a magnitude of a 1-year flood were identified.

Due to the fact that there was no flood event higher than a 1-year flood in the study area, the amount of deposited sediments could be correlated to these events. Therefore, the average sediment deposition in case of a 1-year flood (approximately 13,000 m^3) was used to evaluate the applicable sediment transport formula.

3.3 *Sediment analysis*

In December 2010 seven representative sediment samples were taken from the reservoir and sieved according to the Austrian Standard ÖNORM B4412. The freeze-core method was used for taking the sediment samples, starting from the weir (sample 1) to the head of the reservoir (sample 7).

Table 2 presents some characteristics diameters of the sediments samples. The mean diameter d_m is defined as

$$d_m = \sum_{i=1}^{n-1} \Delta p_i \cdot \overline{d}_i \quad (1)$$

Where n, Δp_i and $\overline{d}_i$ denote the grain size classes of the sieve analysis, the fraction of the grain size class i and the mean diameter of the size class, respectively.

The samples show big variations in the grain sizes between sample 1 and sample 7.

Based on the measured volume of deposited sediments in different areas of the reservoir and on the sediment samples, a grain size distribution of the incoming sediments in the reservoir was generated.

The grain size classes and the mass-frequency obtained by the sieve analysis were used to calculate the sediment transport capacities using the above mentioned different formulae.

4 EVALUATION OF THE SEDIMENT TRANSPORT CAPACITY

The different sediment transport formulae were developed under different conditions by the analysis of experiments in flumes or in the field. Therefore a wide range in the results from one formula to the other formula can be expected. To determine the sediment transport capacity in the reservoir, the sediment transport formulae by Ackers-White (1973), Engelund-Hansen (1967), Meyer-Peter-Müller (1948), Laursen (Copeland 1989), Toffaleti (1968) and Yang (1973, 1984) were compared. The parameters of developing the different sediment transport formulae are listed in Table 3.

All mentioned sediment transport formulae are total bed formulae except the formula derived by Meyer-Peter-Müller, which is a bed load transport function. The range in the grain sizes of the sediment used in the experiments is given by the overall grain diameter d or the mean diameter d_m. The variable v_m denote the average velocity, h the flow depth and s the energy gradient.

The listed parameters are not limiting factors, and several sediment transport formulae have been applied successfully outside their development range.

None of this sediment transport formulae match exactly with the conditions in the studied area. Due to this fact it is important to verify the accuracy of the predicted sediment transport capacity with the measured amount of transported sediments. For determination of the transported amount of sediments, the investigation of hydrological conditions and the occurred flood events are necessary to correlate the amount of transported sediment with the discharge.

Figure 5 illustrates the calculated sediment transport capacities for the Ackers-White, Engelund-Hansen, Meyer-Peter-Müller and the Toffaleti formula starting from the weir ($x = 0$) to the head of the reservoir ($x = 1800$). The sediment transport capacity derived by the Yang and the Laursen (Copeland) formula were not applicable, because of the very high deviation compared with the measured sediment amount in the reservoir.

The Ackers-White formula gives the highest sediment transport capacity, followed by the Engelund-Hansen formula. The calculated sediment transport capacities of the Toffaleti and the Meyer-Peter-Müller formulae are much smaller. Based on the results shown in Figure 5 the amount of transported sediment for

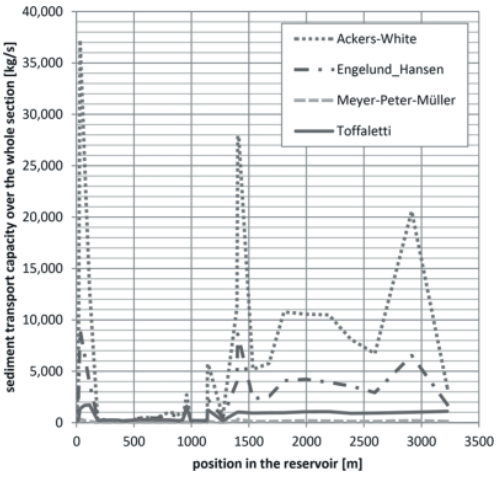

Figure 5. Calculated sediment transport capacities for a 1-year flood in the reservoir from the weir ($x = 0$) to the head of the reservoir ($x = 1800$).

Table 3. Parameters of the sediment transport formulae.

Sediment transport formula	d [mm]	v_m [m/s]	h [m]	s
Ackers-White	0.4–7.0	0.02–2.16	0.003–0.43	0.00006–0.037
Engelund-Hansen (d_m)	0.19–0.93	0.20–1.93	0.06-0.41	0.000055–0.019
Meyer-Peter-Müller	0.4–29	0.37–2.87	0.009–1.19	0.0004–0.02
Laursen (Copeland)				
field (d_m)	0.08–0.7	0.02–2.37	0.20–16.5	0.0000021–0.0018
flume (d_m)	0.011–29	0.21–2.87	0.009–1.10	0.00025–0.025
Toffaleti				
field	0.062–4	0.21–2.37	0.02–17.28	0.000002–0.0011
flume	0.062–4	0.21–1.92	0.02–0.34	0.00014–0.019
Yang				
field sand	0.15–1.7	0.24–1.95	0.01–15.24	0.000043–0.028
field gravel	2.5–7.0	0.43–1.55	0.02–0.22	0.0012–0.029

(Source: U.S. Army Corps of Engineers, Waterway Experiment Station. 1998).

Table 4. Comparison of the calculated and the measured sediment transport rates.

Sediment transport formula	sediment transport capacity [kg/s/m]	transported amount [m^3]
Ackers-White	181.29	591,000
Engelund-Hansen	70.84	230,900
Meyer-Peter-Müller	2.79	9,000
Toffaleti	19.88	64,800
measured	–	13,000

a 1-year flood was calculated and compared to the measured amount (Table 4).

According to the results shown in Table 4 the Meyer-Peter-Müller bed load formula shows the best agreement with the field measurements. The difference between the calculated amount using the Meyer-Peter-Müller formula and the measured value could be explained by the fact that in the calculated value only the six flood events were taken into account. However, also during normal operation with design discharge sedimentation takes place in the reservoir and may causes the difference in the calculation.

5 NUMERICAL MODELLING OF THE RESERVOIR FLUSHING

As mentioned before, no flushing has been performed in the reservoir so far. Therefore no validation data for the reservoir flushing case is available. The reservoir flushing was simulated to assess the sediment transport processes and the possible amount of flushed out sediments.

In the first step the changes in the bed shear stresses for a 1-year flood were evaluated. Figure 6 shows the distribution of the bed shear stresses for the maximum operation level (533.6 m a.sl.).

The highest bed shear stresses are in the free flowing area upstream of the head of the reservoir. In the reservoir the bed shear stresses decrease due to the continuously rising water depth from the head of the reservoir to the weir.

In case of a drawdown of the operation level to 531.8 m asl., the bed shear stresses increase (Figure 7) from the river bend to the weir and facilitate the sediment transport and reaches 80% of shear stress of a free flow at the weir.

In the next step the sediment transport was calculated. The Meyer-Peter-Müller sediment transport formula was chosen according to the evaluation presented before.

Figure 8 shows the derived erosion pattern after the simulation of a flushing event in case of a 1-year flood. The highest erosion rates are in the river bend and at the weir. In these areas up to 1.0 m of deposited sediments was eroded. Depending on reservoir's geometry, parts of the eroded gravel in the river bend deposits

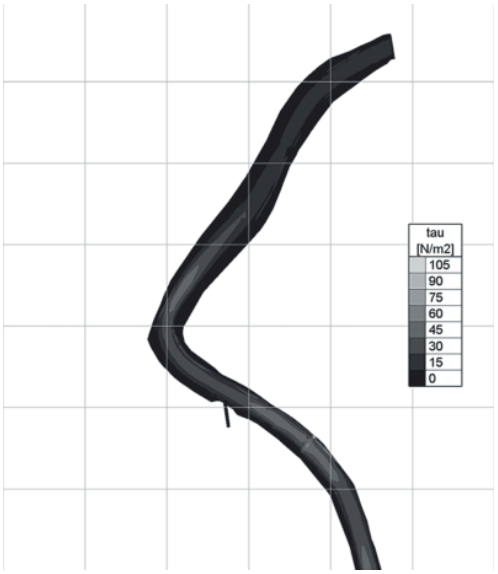

Figure 6. Bed shear stress distribution for the maximum operation level (533.6 m a.sl.) in case of a 1-year flood.

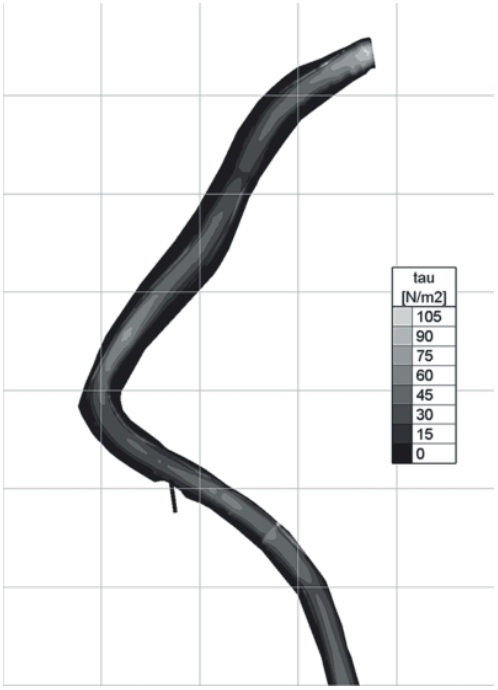

Figure 7. Bed shear stress distribution for the lowering of the water level (531.8 m a.sl.) in case of a 1-year flood.

immediately downstream the river bend. In this case the flushing period with 24 hours was too short to transport these fractions through the reservoir. However, the possible time of water level draw down is coupled with

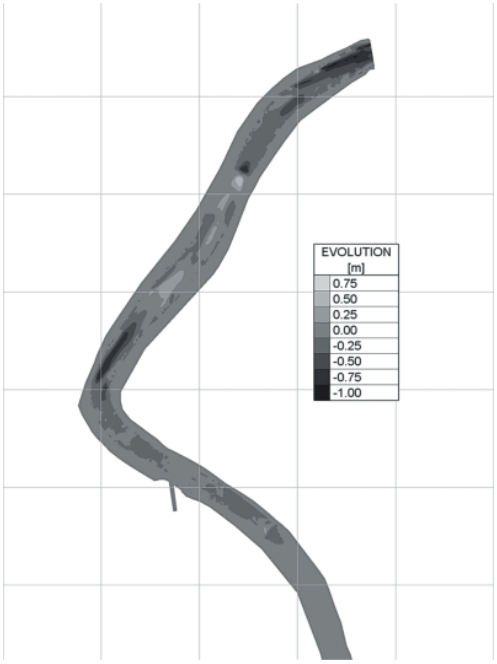

Figure 8. Erosion pattern after flushing (water level 531.8 m a.sl. and 1-year flood).

the natural discharge into the reservoir. If the discharge is higher than a 1-year flood or the flood duration is longer a transport of the gravel fractions through the weir is possible.

In the simulated flushing event most of the sediment transported from upstream of the reservoir passed the weir. In addition approximately 3,100 m^3 of deposited sediments were eroded compared to only 800 m^3 of deposited sediment. In case of a flood operation without drawdown of the water level about 8,000 m^3 of sediments are deposited in the reservoir.

The simulations showed that the main part of the incoming sediment could be transported through the reservoir and in addition deposited sediment can be remobilized.

6 CONCLUSIONS

The paper discussed the application of a numerical model at an alpine reservoir. The open source numerical model TELEMAC-2D combined with the morphological module SISYPHE was used to simulate the flushing process. The sediment transport formula used in the numerical simulation was evaluated based on the grain-size-distribution of the sediment samples and the total deposited amount of sediment in the reservoir. The calculated sediment deposition derived by the Meyer-Peter-Müller bed load formula showed the best agreement with the measured amount. The deviation in the calculated and measured sediment amount could be caused by the by the fact that in the calculated value only the six flood events were taken into account. The sediment depositions during normal operation with design discharge was not taken into account and may causes the difference in the calculation.

Based on the evaluation the sediment transport formula of Meyer-Peter-Müller was used in the numerical simulation of the flushing.

The simulated flushing event showed the possibility of routing sediments from the upstream free flowing area through the reservoir and of remobilization of the deposited sediments. Parts of the eroded sediments in the upstream area of the reservoir resettle in the downstream area due to a widening of the reservoir, but compared with a flood operation without a drawdown of the water level approximately 125 percent more sediment was transported through the reservoir.

The flushing efficiency could be increased in case of higher discharges or longer durations of water level drawdown. However, the possibility of flushing is strictly connected with the hydrological conditions and in the alpine area linked to flood events.

The numerical simulation of sediment transport processes and of flushing events is still a research topic and under development. Further studies and field measurements are required to improve the accuracy of such analyses.

ACKNOWLEDGEMENTS

This work was partly funded by the SEE Hydropower project of the South East Europe Programme of the European Union. The second author was funded by the Research Council of Norway, through the RENERGI programme.

REFERENCES

Ackers, P. and White, W.R., 1973. Sediment Transport: New Approach and Analysis. *Journal of the Hydraulics Division, American Society of Civil Engineers, Vol.99, No HY11.*

Atkinson E. 1996. The Feasibility of Flushing Sediment from Reservoirs. *TDR Project R5839, Report OD 137, HR Wallingford.*

Badura, H. 2007. *Feststofftransportprozesse während Spülungen von Flussstauräumen am Beispiel der oberen Mur*, Dissertation, Graz University of Technology, Austria.

Badura, H, Knoblauch, H. and Schneider J., 2008. *Pilot Action Bodendorf Reservoir (Austria)*. In: ALPRESERV – Pilot Actions and Database, published by the Universität der Bundeswehr München, Volume 5/2008, ISSN 1862–9636

Bechteler, W. 2006. *The purposes of impounding facilities*. In: ALPRESERV – Sediment Management Methods – Technical and legal aspects, published by the Universität der Bundeswehr München, Volume 4/2006, ISSN 1862–9636

Charlton, R. 2008. *Fundamentals of Fluvial Geomorphology*, Routledge, Taylor & Francis Group, London and New York.

CHC – Canadian Hydraulics Centre, National Research Council, 2010. *Blue Kenue, Reference Manual*, August 2010.

Copeland, R.R. and Thomas, W.A., 1989. *Corte Madera Creek Sedimentation Study*. Numerical Model Investigation. US Army Engineers Waterways Experiment Station, Vickingsburg, MS.

Dorfmann, C. & Knoblauch, H. 2009. A Concept for Desilting a Reservoir Using Numerical and Physical Models. Water Engineering for a Sustainable Environment, Proceedings of the 33.IAHR Congress, Vancouver, Canada.

Engelund, F. & Hansen, E. (1967) *A Monograph on Sediment Transport in Alluvial Stream*, 1–63. Teknisk Forlag, Copenhagen V, Denmark.

Fang, H-W. and Rodi W. (2003). Three-dimensional calculations of flow and suspended sediment transport in the neighborhood of the dam for the Three Gorges Project (TGP) reservoir in the Yangtze River. *J. Hydraulic Res*. 41(4), 379–394.

Harb G., Haun S., Ortner S., Dorfmann C. & Schneider J. 2011. The influence of secondary currents on reservoir sedimentation – experimental and numerical studies. *Proceedings of the 34th IAHR World Congress, Engineers Australia, July 2011*.

Hervouet J-M. 2007. *Hydrodynamics of free surface flows: modelling with the finite element method*. Wiley.

Laursen, E. M. 1958. Total Sediment Load of Streams. *Journal of the Hydraulic Division, American Society of Civil Engineers, 84 (HY1)*.

Meyer-Peter, E; Müller, R. (1948). Formulas for bed-load transport. *Proceedings of the 2nd Meeting of the International Association for Hydraulic Structures Research*. pp. 39–64.

Moulinec, C., Denis C. Pham C.-T,. Rougé D,. Hervouet J.-M,. Razafindrakoto E,. Barber a, R.W, 2011. TELEMAC: An efficient hydrodynamics suite for massively parallel architectures. *Computers & Fluids* 51 (2011) 30–34.

Morris, G. and Fan J. 1997. *Reservoir Sedimentation Handbook*, McGraw-Hill Publishing Company.

Olsen, N.R.B. (1999a). Two-dimensional numerical modelling of flushing processes in water reservoirs. *J. Hydraulic Res*. 37 (1), 3–16.

Olsen, N.R.B. (1999b). 3D CFD modelling of water and sediment flow in a hydropower reservoir. *Inte-national Journal of Sediment Research* 14 (1), 16–24.

Patankar, S.V. 1980. *Numerical Heat Transfer and Fluid Flow*, McGraw-Hill Book Company, New York.

Rodi, W. 1980. *Turbulence Models and Their Application in Hydraulics*, A. A. Balkema, Rotterdam.

Scheuerlein, H. 1990. Removal of sediment deposits in reservoirs by means of flushing. *Proceedings International Conference on Water Resources in Mountainous Regions, Symp. 3: Impact of Artificial Reservoirs on Hydrological Equilibrium. Lausanne, Schweiz, 1990*, pp. 99-106.

Schlichting, H. 1979. *Boundary Layer Theory*, McGraw-Hill.

Toffaleti, F.B., 1968. *Technical Report No. 5 – A Procedure for Computation of Total River Sand Discharge and Detailed Distribution, Bed to Surface*. Committee on Channel Stabilization, U.S. Army Corps of Engineers.

U.S. Army Corps of Engineers, Waterway Experiment Station. 1998. *SAM Hydraulic Design Package for Channels User's Manual,* Vicksburg, MS.

Van Rijn, L. C. (1984a). Sediment Transport. Part I: Bed load transport. *Journal of Hydraulic Engineering, 110(10), pp. 1431–1456.*

White, R. 2001. *Evacuation of sediments from reservoirs*, Thomas Telford Publishing.

Wu, W. 2008. *Computational River Dynamics*. Taylor Francis Group, London, UK.

Yang, C.T. 1973. Incipient Motion and Sediment Transport. *Journal of the Hydraulic Division, American Society of Civil Engineers, Vol. 99, HY10.*

Yang, C.T. 1984. Unit Stream Power Equation for Gravel. *Journal of the Hydraulic Division, American Society of Civil Engineers, Vol. 110, HY12.*

BODENDORF - IAHR EUROPE 2012

3D NUMERICAL MODELLING OF THE RESERVOIR FLUSHING OF THE BODENDORF RESERVOIR, AUSTRIA

Stefan Haun[1], Clemens Dorfmann[2], Gabriele Harb[2] & Nils Reidar B. Olsen[1]

[1]Department of Hydraulic and Environmental Engineering, The Norwegian University of Science and Technology, Norway, S. P. Andersens veg 5, 7491 Trondheim

[2]Institute of Hydraulic Engineering and Water Resources Management, Graz University of Technology, Austria, Stremayrgasse 10, 8010 Graz

E-mail: stefan.haun@ntnu.no

Abstract

The Bodendorf reservoir is located in the province of Styria in Austria. The high sedimentation rate of about 4 % per year decreased the reservoir volume from 900.000 m^3 to 300.000 m^3 in only 12 operation years. To reduce the high amount of deposited sediments, a first reservoir flushing was carried out in 1994. Since the first flushing a more or less frequently reservoir flushing was established. Through the Interreg IIIb project ALPRESERV a detailed study of the flushing event in 2004 was conducted. The recorded bathymetry data, water levels, discharge rates and the measured grain size distributions at the bed were used as boundary condition for a flushing simulation. The used numerical model solves the Reynolds-averaged Navier-Stokes equations in three-dimensions. The turbulence is simulated by the standard k-ε model and the pressure is computed accordingly to the SIMPLE method. The program uses an adaptive and unstructured grid which moves during the computation with changes in the bed and water levels. The suspended sediment transport is calculated by solving the convection-diffusion equation and the bed-load transport by the empirical formulas from Meyer-Peter Müller and van Rijn. Bed forms are taken into account in the study by an empirical formula from van Rijn. The presented results of the simulation show agreement in the amount of flushed out sediments. A comparison of the measured and simulated cross sections after the flushing is given in this study. This comparison also shows the sensitivity of the results in relation to different bed-load transport formulas.

Introduction

Reservoir sedimentation is one of the challenges in dam engineering today (Scheuerlein, 1990). Due to the construction of artificial barrages in rivers the alluvial balance is highly affected. Small flow velocities in reservoirs result in depositions and create a sedimentation problem. These accumulations decrease the reservoir volume and so also the available the amount of water for irrigation purposes or producing electricity (Morris and Fan, 1998). Also the lifetime of the reservoir may be reduced by sediment depositions, which represents an economic impact and should be taken into account in early design studies. The severity problem is not uniform distributed over the world. It depends on the hydrology, the geology and the land use in the basin (White and Bettness, 1984). Different approaches, like the use of soil control measure, are in use to minimize the sediment yield from the watershed (Shen, 1999). However, a sediment inflow into the reservoir could never be avoided completely (Scheuerlein, 1990). An often used method for reducing the sediment accumulations in reservoirs is reservoir flushing. During the flushing the water level is drawn down to a level so that free flow conditions occur. The high velocities and an increased bed shear stress initiate the erosion process in the reservoir. The effectiveness of a flushing depends on existing low level outlets and the possibility to ensure the excess runoff from the basin for a period with free flow conditions (White and Bettness, 1984). The performance depends also on the handling of ecological aspects. To avoid impacts on the downstream region, limitations of the minimum oxygen amount and the maximum suspended sediment concentration are most time specified for the flushing.

A special challenge is the flushing of mountain reservoirs, like the Bodendorf reservoir in Austria. This is because of the high amount of coarse material, which settles in the entrance area of the reservoir. During the flushing process this material can erode and settle further downstream in the reservoir (Scheuerlein, 1990).

An accurate prediction of the efficiency of an upcoming flushing is important information for designer and owner of reservoirs. The use of only theoretical approaches is problematic because of the complex mechanisms and the huge amount of involved parameters (Scheuerlein, 1990). An alternative for predictions can be a numerical investigation. Numerical models are more and more

common in river engineering because of a time and cost reduction compared to physical model studies (Gessler and Rasmussen, 2005; Chandler et al., 2003). Previous work in this field was done by Lai and Shen (1996) with a one-dimensional diffusion model for estimating the general trend of the bed evaluation. A two-dimensional model was used for simulating the flushing of the Kali Gandaki reservoir (physical model study) by Olsen (1999). An example for the successful use of a three-dimensional approach is the simulation of the sediment transport in the Three Gorges project by Fang and Rodi (2003).

For this study the Bodendorf reservoir in Austria is chosen. Especially run-of-river power plants, like the Bodendorf reservoir, are highly influenced by sediment deposition (Wu, 2008). A detailed study of the 2004 flushing was carried out in the Interreg IIIb project ALPRESERV for a sustainable sediment management of alpine reservoirs considering ecological and economical aspects. In addition to the analysis of the amount of flushed out sediments, cross section measurements were performed before and after the flushing to get better knowledge about the areas of erosion. Because of this, data with high quality and quantity are available for the computation. Also CFD was involved in this project. Badura (2007) used a commercial two-dimensional approach and presented good agreement between the measured bed level changes and the simulated ones. For the current numerical study bathymetry data, grain sizes, discharge rates and water levels from the 2004 flushing were used. The simulated results were compared with the measured data to show flushing effects, like the erosion pattern in three cross sections. Two different empirical bed-load transport formulas were used to show the dependency of the results related to the used equation.

Site description and Input data

The Bodendorf hydropower plant is located at the river Mur in the province of Styria in Austria. It is designed as run-of-river power plant with a drainage area of about 1,360 km^2 and a capacity of 7.5 MW. The reservoir has a length of about 2.5 km and is due to an average width of only 40 m relatively narrow (Knoblauch et al., 2005). The reservoir had a designed volume of about 900,000 m^3 in 1982. After 12 years of operation about 600,000 m^3 of the reservoir was filled with sediments. So the average deposition is about 35,000 m^3 per year, which represents a sedimentation rate of 4 % of the reservoir volume per year. The amount of flushed out sediments was 47,300 m^3 in 2004, where around 31,500 m^3 were flushed out as bed-load (Badura et al., 2006). This represents a special challenge for the numerical model, where the bed-load transport is simulated by an empirical formula. The grain size distributions show a large variation along the reservoir. The d_{50} at the entrance of the reservoir was 32 mm were in front of the weir the d_{50} showed a value of 1.5 mm. The density for the deposited sediment was 2.55 g/cm^3 (Badura, 2007).

During the flushing a minimum discharge of 80 m^3/s is required to increase the bed shear stress so that the armoring layer breaks up and erosion starts (Knoblauch et al., 2005). The flushing of 2004 showed next to this a flood peak with a discharge of 134 m^3/s during the free flow conditions. The used discharge rates and water level changes at the weir are shown in Figure 1.

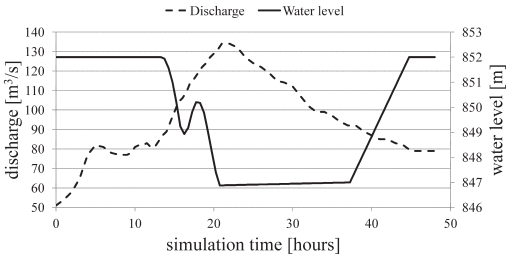

Figure 1: Discharge rates and water levels during the flushing

A detailed bathymetry survey was carried out before and after the flushing. This data is used for setting up the numerical model and for evaluating the amount of flushed out sediments. The bed geometry after the flushing was also used for comparisons of the areas where erosion happens.

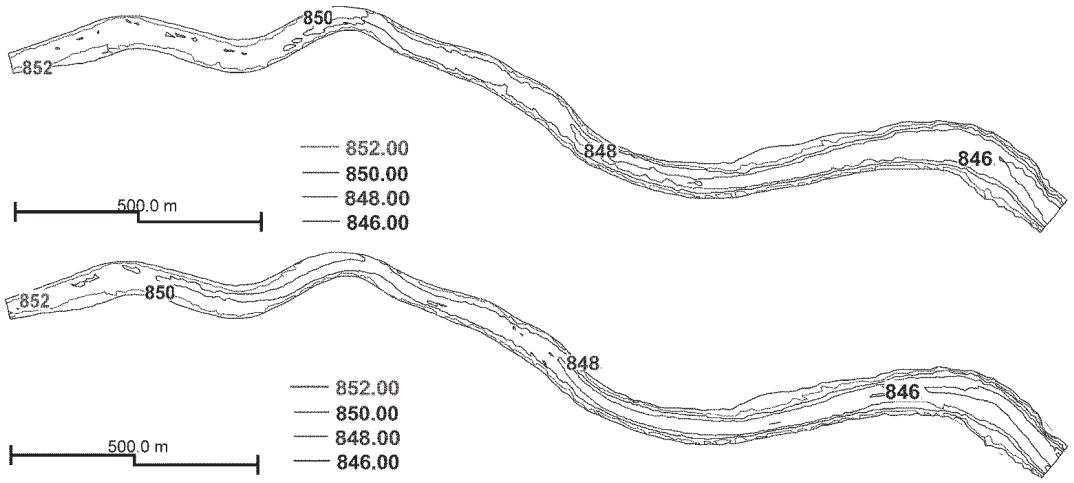

Figure 2: Bed geometry of the Bodendorf reservoir before the flushing (at the top) and after the flushing (below)

Numerical Model

The CFD code SSIIM was used for this study (Olsen, 2012). In SSIIM the RANS-equations are solved in three-dimensions together with the continuity equation to compute the flow field for turbulent flow (Versteeg and Malalasekera, 1995; equation 1 and 2).

$$\frac{\partial U_i}{\partial x_i} = 0 \tag{1}$$

$$\frac{\partial U_i}{\partial t} + U_j \frac{\partial U_i}{\partial x_j} = \frac{1}{\rho} \frac{\partial}{\partial x_j} \left(-P\delta_{ij} - \rho \overline{u_i u_j} \right) \tag{2}$$

with i= 1, 2, 3; where U_j is the averaged velocity, x is the spatial geometrical scale, ρ is the water density, P is the dynamic pressure, δ_{ij} is the Kronecker delta and $-\rho\overline{u_i u_j}$ are the turbulent Reynolds stresses.

As discretication scheme the finite-volume method is used together with a first order upwind scheme (Olsen, 2012). The turbulent Reynolds stresses are calculated by the k-ε model (Launder and Spalding, 1972) and the unknown pressure field is computed by the SIMPLE method (Patankar, 1980). The sediment transport in SSIIM is modelled for multiple sediment sizes, where the suspended sediment transport is modelled by solving the convection-diffusion equation (equation 3).

$$\frac{\partial c}{\partial t} + U_j \frac{\partial c}{\partial x_j} + w \frac{\partial c}{\partial z} = \frac{\partial}{\partial x_j} \left(\Gamma \frac{\partial c}{\partial x_j} \right) \tag{3}$$

where U is the water velocity, w is the fall velocity of the sediment, Γ is the turbulent diffusity and c is the sediment concentration over time t and over the spatial geometrical scales x and z.

For simulating the quantity of the bed-load transport, an empirical formula by van Rijn (1984a) was used as first approach (equation 4).

$$\frac{q_{b,i}}{d_i^{1.5} \sqrt{\frac{(\rho_s - \rho_w) g}{\rho_w}}} = 0.053 \frac{\left(\frac{\tau - \tau_{c,i}}{\tau_{c,i}} \right)^{2.1}}{d_i^{0.3} \left(\frac{(\rho_s - \rho_w) g}{\rho_w \nu^2} \right)^{0.1}} \tag{4}$$

where $q_{b,i}$ is the transport rate of the ith fraction of bed load per unit width, d_i is the diameter of the ith fraction, τ is the shear stress, $\tau_{c,i}$ is the critical shear stress for d_i which was calculated by an analytical form from the Shields curve, ρ_s is the density of the sediment, ρ_w is the density of the water, g is the acceleration of gravity and ν is the kinematic viscosity.

As an alternative bed-load transport formula the Meyer-Peter Müller formula was used (equation 5). This formula is recommended for rivers with steeper slopes and sediment transport mainly at the bed.

$$q_{b,i} = \frac{1}{g}\left[\frac{\rho_w g r I - 0.047 g(\rho_s - \rho_w) d_{50}}{0.25 \rho_w^{\frac{1}{3}} \left(\frac{\rho_s - \rho_w}{\rho_s}\right)^{\frac{2}{3}}}\right]^{\frac{3}{2}} \quad (5)$$

where $q_{b,i}$ is the transport rate of the total bed load per unit width, d_{50} is the characteristic sediment size, I is the slope of the energy line and r is the hydraulic radius.
Because of the influence of bed forms during the flushing, the bed roughness (k_s) was calculated by the numerical program as a combination of the grain-size distribution and the bed-form height (equation 6).

$$k_S = 3.0\, d_{90} + 1.1\Delta\left(1.0 - e^{\left(\frac{-25\Delta}{7.3y}\right)}\right) \quad (6)$$

where d_{90} is the characteristic sediment size, Δ is the bed-form height and y is the water depth.
The bed form height was predicted by an empirical formula (van Rijn, 1984c; equation 7).

$$\frac{\Delta}{y} = 0.11\left(\frac{d_{50}}{y}\right)^{0.3}\left(1 - e^{-0.5\left(\frac{\tau - \tau_{c,i}}{\tau_{c,i}}\right)}\right)\left(25 - \left(\frac{\tau - \tau_{c,i}}{\tau_{c,i}}\right)\right) \quad (7)$$

where d_{50} is the characteristic sediment size, τ is the shear stress and $\tau_{c,i}$ is the critical shear stress for each fraction.
In SSIIM an unstructured and adaptive grid is used. The adaptive grid moves accordingly to changes in the bed and water level. An algorithm for wetting/drying is implemented in the code, which allows a change of number of cells. The used algorithm removes dried up cells from the grid and generates new cells in areas which get wetted during the time depend simulation, so also lateral movements during the computation are possible. For calculating the fluxes and velocities for the non-staggered grid the Rhie and Chow (1983) interpolation is used. The free-water surface is simulated based on the computed pressure field (Olsen and Haun, 2010). An implicit time discretization is used.

Numerical Simulation of the Reservoir Flushing

Based on the existing bathymetry data, grids with a different number of cells were made for the computation domain. The chosen grid had 15,358 cells (Figure 3), and showed grid independent results. In the vertical direction a maximum number of 11 cells were selected. During the computation the number of cells decreases, because of the draw down of the water level, to 5,292. For the simulation a time step of 10.0 seconds was chosen. A zero gradient outflow boundary condition was set for the outflow and a Dirichlet boundary condition for the inflow. At the walls of the domain wall laws by Schlichting (1979) were used. Changes in the water level and discharge rates during the flushing were kept similar to Figure 1.
Due to changes of the grain size distribution along the reservoir a distribution at the weir and at the entrance of the reservoir was specified. Between these areas the grain sizes were linearly interpolated. Table 1 shows the grain sizes chosen at the weir and the entrance area with the corresponding fractions.

Table 1: In the simulation used grain sizes and fractions at the weir and at the entrance area of the reservoir

Grain Size [mm]	Fraction at the weir [%]	Fraction at the entrance of the reservoir [%]
100 - 72	5	25
72 - 52	5	20
52 - 36	10	15
36 - 24	10	15
24 - 11	10	10
11 - 6	20	10
6 - 3	15	3
3 - 1.5	15	1
1.5 - 0.5	10	1

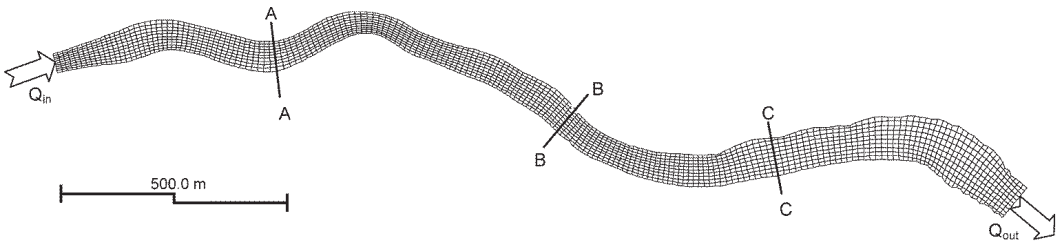

Figure 3: Grid for the flushing simulation with 15,358 cells and the cross sections A – C

Geotechnical failures are in the program taken into account by a sand slide algorithm. The angle of repose, used in this algorithm, was set to φ= 32 ° for this study. During the flushing simulation no sediment inflow was specified. The active sediment thickness was set to be 0.5 m. The roughness at the bed was set to 0.28 m.
The computation time for the flushing on two cores of the CPU (Intel Q9650 3.00GHz) was about 12 hours.

Results

In the presented study the number of flushed out sediments and the bed level changes after the flushing simulation were compared. Three cross sections (A-C; Figure 1) were presented to show the erosion pattern of the simulation (Figure 4 a-c).

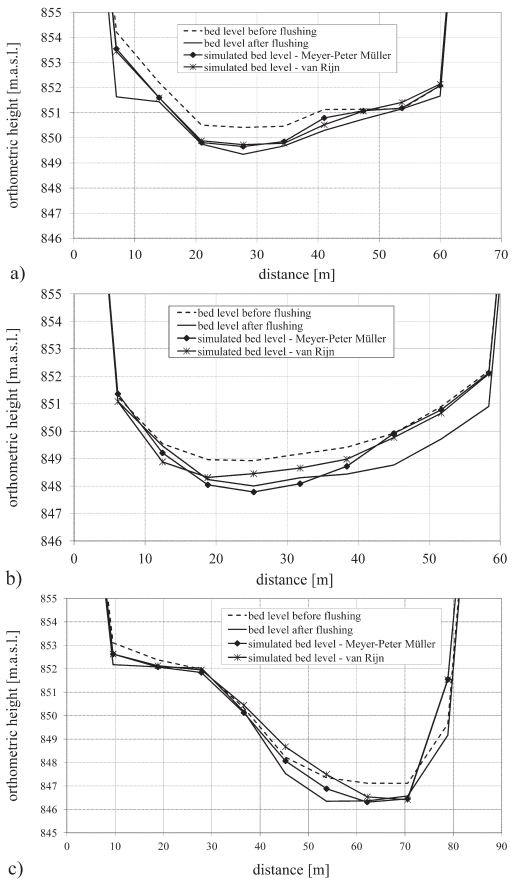

Figure 4: Bed level changes, measured and simulated with van Rijn and Meyer-Peter Müller bed-load transport formulas

The cross sections were chosen in different sections of the reservoir, where varying effects influence the computed erosion. It clearly can be seen that the erosion pattern in cross section A is similar compared with the measurements. However, the erosion is not as deep as measured for both used bed-load transport formulas. Cross section B shows that the erosion in the simulation occurs more at the outer site of the small bend. The measurements show a smaller influence of the secondary currents, and a more uniform erosion patter over the cross section. The results by using the Meyer-Peter Müller formula show better agreement in the shape and depth. Cross section C shows a distinctive channel, which is in the simulation too narrow compared with the measured one. In this cross section the total erosion is much smaller compared with the measurements. The total bed shear stress increases during the free flow condition to a maximum value of 50 N/m^2 in different sections of the reservoir and up to 22 N/m^2 in the area in front of the weir. However, during the simulation the sediment transport capacity in this area is at a maximum value for both formulas. So no additional sediments can be removed from the bed.
The observed bed forms during the flushing were not measured. The bed forms in the simulation show a height of around 1.5 m, which is probably overestimated. This could also influence the estimation of the secondary currents and the erosion pattern in the bends.
The calculated amount of flushed out sediments is in the same range as the measured ones. This is the result of an intensive calibration process. The most important factors are a correct distribution of the sediments and the fraction of compacted sediments in the bed. The difference in the used bed-load transport formulas by van Rijn (23,400 m^3) and the Meyer-Peter Müller formula (31,200 m^3) shows the advantage of using Meyer-Peter Müller for this case.

Conclusion

The numerical simulation of the 2004 reservoir flushing of the Bodendorf reservoir is presented in this study. Bathymetry data and collected field data were used for adjusting the model. The results show that the range of the amount of eroded sediments (47,300 m^3) can be better predicted with the formula from Peter-Meyer Müller (31,200 m^3) compared to the bed-load transport formula from van Rijn (23,400 m^3). However, the erosion pattern shows differences between the simulation and the measurements. Mainly the cross sections located in the downstream region of the reservoir show an irregular erosion pattern in the simulation. Both used empirical bed-load transport formula gave too little transport capacity in the downstream area of the reservoir, which results in too

little erosion in this area. Coarse material, eroded in the inflow area of the reservoir, will in addition settle in the area in front of the weir. In areas where the reservoir shows slight bends, the program overestimates the secondary currents, which results in too deep erosion at the outside of the bend and into too less depth at the inner site of the bend. Field measurements are required to compare the angle of the secondary currents to the results derived by the model. The influence of the bed-load transport formula is also presented in the cross sections. Where the empirical formula by van Rijn is successfully used in previous works with the CFD code SSIIM, the Meyer-Peter Müller formula shows an advantage for this case. The equation is recommended for steeper rivers which transport mainly coarse sediments close to the bed. However, there is no unique formula available at the moment, which can be used for all cases. Further research work is required in allocating of bed-load transport formulas for specific cases.

The observed anti dunes highly influence the erosion rates of the numerical simulation for the flushing. Bed forms are in the numerical program taken into account by an empirical formula. During the flushing no measurements of the bed form heights or a wave length were possible. So it is not possible to compare the results regarding the bed form height of the simulation with field data. However, the numerical model is able to give a range of the amount of erosion for a prediction of an upcoming flushing.

Acknowledgments

The first author is funded from the Norwegian Research Council, through the RENERGI programme.

References

Badura, H., Schneider, J., Knoblauch H., Larsen, O. & Heigerth, G. (2006). Numerische Simulation des Abstauvorganges während Stauraumspülungen am Beispiel des KW Bodendorf / Mur. *Schriftenreihe zur Wasserwirtschaft der Technischen Universität Graz, 46*.

Badura, H. (2007). Feststofftransportprozesse während Spülungen von Flussstauräumen am Beispiel der oberen Mur. *Schriftenreihe zur Wasserwirtschaft der Technischen Universität Graz, 51*.

Chandler, K., Gill, D. Maher, B., Macnish, S. & Roads, G. (2003). Coping with probable maximum flood – an alliance project deliver for Wivenhoe Dam. *Proceedings of the 43rd ANCOLD conference, Hobart, Tasmania.*

Fang, H-W., & Rodi, W. (2003). Three-dimensional calculations of flow and suspended sediment transport in the neighborhood of the dam for the Three Gorges Project (TGP) reservoir in the Yangtze River. *Journal of Hydraulic Research*, 41 (4), pp. 379–394.

Gessler, D., & Rasmussen, B. (2005). Before the flood. *Desktop Engineering Magazine, October*.

Knoblauch, H., Badura, H., Schneider, J., Pichler, W., & Heigerth, G. (2005). Geschiebetransportmodell zur Festlegung der Mindestwassermenge bei Stauraumspülungen. Wasserbaukolloquium 2005: Strömungssimulation im Wasserbau, *Dresdener Wasserbauliche Mitteilungen Heft 32.*

Lai, J.-S., & Shen, H. W. (1996). Flushing sediment through reservoirs. *Journal of Hydraulic Research*, 34 (2), pp. 237-255.

Launder, B. E., & Spalding, D. B. (1972). *Lectures in mathematical models of turbulence*. Academic Press, London.

Morris, G. L., & Fan, J. (1998). *Reservoir Sedimentation Handbook*. McGraw-Hill Book Company, New York.

Olsen, N. R. B. (1999). Two-dimensional numerical modelling of flushing processes in water reservoirs. *Journal of Hydraulic Research*, 37 (1), pp. 3-16.

Olsen, N. R. B. (2012). *A Three-Dimensional Numerical Model For Simulate Of Sediment Movements In Water Intakes With Multiblock Option*. Users`s Manual, by Nils Reidar B. Olsen, Department of Hydraulic and Environmental Engineering, The Norwegian University of Science and Technology.

Olsen, N. R. B., & Haun, S. (2010). Free surface algorithms for 3D numerical modelling of reservoir flushing. *Dittrich et al. Preprints of the River Flow Conference 2010: Bundesanstalt für Wasserbau, Braunschweig, September 8 – September 10*, pp. 1105-1110.

Patankar, S. V. (1980). *Numerical Heat Transfer and Fluid Flow*. McGraw-Hill Book Company, New York.

Rhie, C. & Chow, W. (1983). Numerical study of the turbulent flow past an airfoil with trailing edge separation. *AIAA Journal*, 21(11), pp. 1525-1532.

Shen, H. W. (1999). Flushing sediment through reservoirs. *Journal of Hydraulic Research*, 37 (6), pp. 743-757.

Scheuerlein, H. (1990). Removal of sediment deposits in reservoirs by means of flushing. *Proceedings International Conference on Water Resources in Mountainous Regions, Symp. 3: Impact of Artificial Reservoirs on Hydrological Equilibrium. Lausanne, Schweiz, 1990, pp. 99-106.*

Schlichting, H. (1979). *Boundary layer theory*. McGraw-Hill Book Company, New York.

Van Rijn, L. C. (1984a). Sediment Transport. Part I: Bed load transport. *Journal of Hydraulic Engineering,* 110(10), pp. 1431-1456.

Van Rijn, L. C. (1984c). Sediment Transport. Part III: Bed forms and alluvial roughness. *Journal of Hydraulic Engineering*, 110(12), 1733-1754.

Versteeg, H. K., and Malalasekera, W. (1995). *An introduction to Computational Fluid Dynamics, The Finite Volume Method.* Pearson Education Limited, Edinburgh.

White, W. R. & Bettess, R. (1984). The feasibility of flushing sediments through reservoirs. Challenges in African Hydrology and Water Resources*, Proceedings of the Harare Symposium*, July 1984. IAHS Publ. no. 144.

Wu, W. (2008). Computational River Dynamics. Taylor Francis Group, London, UK.

FISCHING - IAHR 2013

Numerical Analysis of the Flushing Efficiency of an Alpine Reservoir

Gabriele Harb,
PhD-Student, Graz University of Technology, 8010 Graz, Austria. Email: gabriele.harb@tugraz.at

Clemens Dorfmann,
PhD-Student, Graz University of Technology, 8010 Graz, Austria. Email: clemens.dorfmann@tugraz.at

Hannes Badura,
Project Manager, VERBUND Hydro Power AG, 1010 Vienna, Austria, Email: hannes.badura@verbund.at

Josef Schneider,
Assistant Professor, Graz University of Technology, 8010 Graz, Austria. Email: schneider@tugraz.at

ABSTRACT:

In this study a numerical analysis is carried out to investigate the flushing efficiency in an Alpine reservoir. The reservoir is approximately 4.5 km long with an initial storage volume of about 1.4 Mio. m^3. Measurements show that 85,000 m^3 of sediments deposit in the reservoir annually. A small amount of the deposited sediments has been eroded and transported through the reservoir in former flushing events. However, echo-soundings performed in 2009 showed that approximately 860,000 m^3 of sediments are already deposited in the reservoir. This represents an annual sedimentation rate of about 6.1 % of the initial reservoir volume.

Echo-soundings performed before and after the flushing event were used to evaluate the morphological changes. The water levels of the critical flood event (30-year flood) before and after the flushing event were modelled using a three dimensional numerical model to evaluate the changes in the water level at different sections. Additional ADCP measurements performed at the prototype were used to validate the computed velocity fields of the numerical model.

KEY WORDS: Three-dimensional numerical modelling, Reservoir flushing, Reservoir sedimentation, Flood risk, Field measurements,

1 INTRODUCTION

In reservoirs the flow velocities, the turbulence and the bed shear stresses are reduced in case of normal turbine operation. This effect leads to the settlement of sediment particles in the reservoir. In further consequence the bed levels rise and the storage volume is being reduced by “filling up” the reservoir.

Flushing is one of the most common ways to manage sediment depositions in Alpine reservoirs. The intention of reservoir flushing is the erosion of sediment depositions, accumulated during longer operation periods. In case of natural floods or higher discharges the water level is lowered to increase the flow velocities, turbulence and bed shear stress in the reservoir. The increased shear stress facilitates erosion of the sediment depositions in the reservoir and the turbulence keeps sediment particles in suspension.

In most cases the flushing of reservoirs in the alpine area is a special challenge, because of the massive coarsening of the depositions from the weir to the head of the reservoir and the therefore wide grain size distribution. At the head of the reservoir the gravel fractions are deposited, whereas silt and clay particles deposit near the weir.

The application of numerical models for water flow calculations in river engineering can be seen as state of the art technique. Numerical modelling of sediment transport in reservoirs and related flushing modelling is still a complex task and the main aspects of such studies are the evaluation of the sediment transport processes, like in a previous study, where Olsen applied a two-dimensional numerical model for

simulating the flushing process of the Kali Gandaki reservoir in Nepal (Olsen, 1999). Examples of three-dimensional modelling are the simulation of the sediment transport in the Three Gorges project performed by Fang & Rodi (2003), the simulation of the sediment transport in the Feistritz reservoir (Dorfmann & Knoblauch, 2009) or in the Angustura reservoir in Costa Rica (Haun & Olsen, 2012).
In this study a flushing event in an Alpine reservoir is presented and discussed. The deposition of coarse sediment at the head of the reservoir increases the flood risk due to rising bed levels. The investigation focuses on the flushing efficiency and the related decrease of the flood risk due to the lowering of the bed levels. The flood risk was assessed by calculating the water levels of the 20-year flood using the reservoir geometries from before and after the flood event.

2 STUDY AREA AND BACKGROUND

The reservoir is approximately 4.5 km long with an initial storage volume of about 1.4 Mio. m^3. Measurements show that 85,000 m^3 of sediments deposit in the reservoir annually. A small amount of the deposited sediments has been eroded and transported through the reservoir in former flushing events. However, echo-soundings performed in 2009 showed that approximately 860,000 m^3 of sediments are already deposited in the reservoir. This represents an annual sedimentation rate of about 6.1 % of the initial reservoir volume. Figure 1 shows an overview of the meandering reservoir with the sediment sampling points.

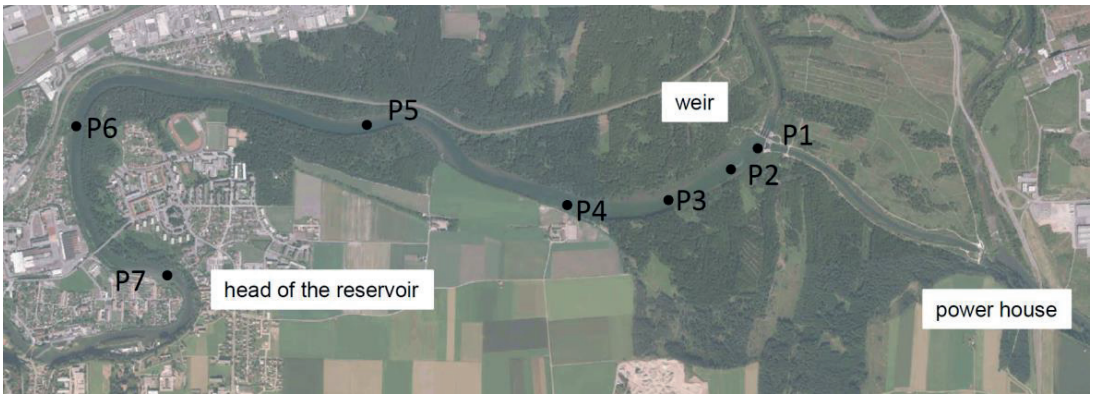

Figure 1 Project area with sediment sampling points

The head of the reservoir is located in an urban area. Hence, the rising of the bed levels in the reservoir and especially in this area creates a problem concerning flood safety in this area. Figure 2 illustrates the rising of the bed levels since the start of operation. The deposition height in front of the weir is about 4-5 m.

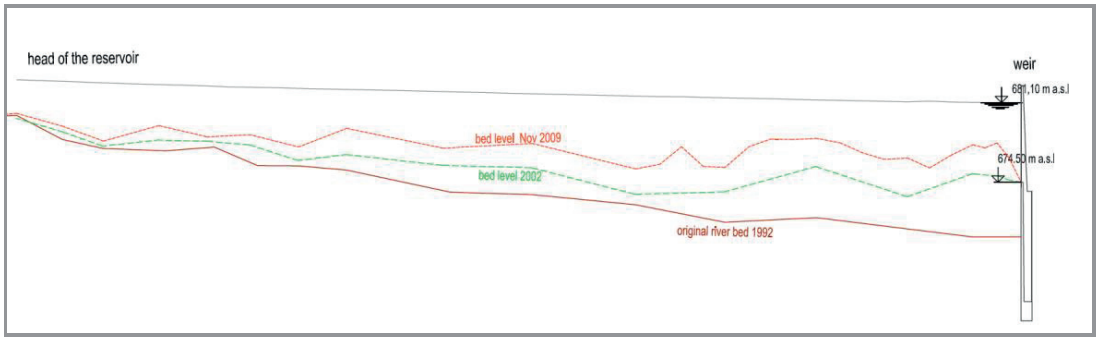

Figure 2 Rising of the bed levels caused by sedimentation in the reservoir, longitudinal section from the head of the reservoir to the weir

In July 2012, two flood events with a probability of approx. 0.2 and 0.05 (~ 5-year flood and ~ 20-year

flood) occurred within 10 days. The water level in the reservoir was lowered according to the operation rules of the hydro power plant and a large amount of sediments were eroded in the reservoir. Figure 2 shows the hydrograph of the flood events in July 2012.

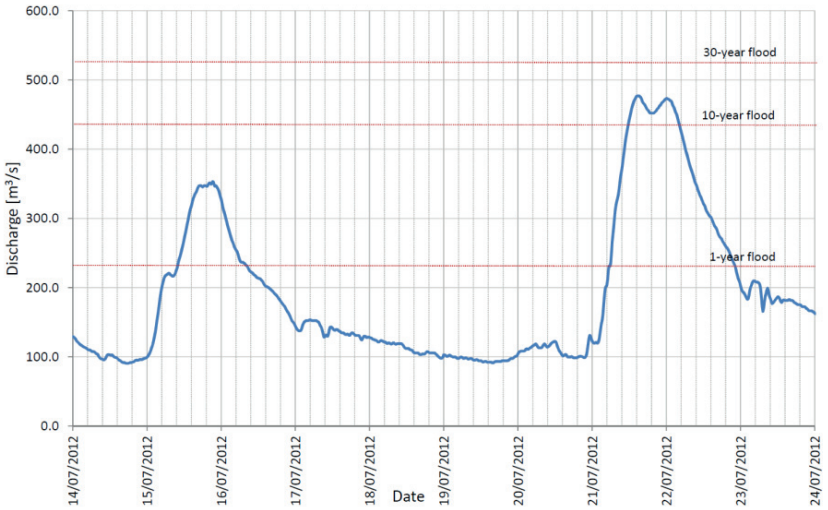

Figure 2 Hydrograph of the flood events in July 2012

3.1 Sediment Sampling

Seven representative sediment samples were taken from the reservoir and sieved according to the Austrian Standard ÖNORM B 4412 in 2010. The freeze-core method was used for taking the sediment samples, starting from the weir (Sample 1) to the head of the reservoir (Sample 7).

Large variations in the grain sizes between Sample 1 and Sample 7 can be observed. The mean diameter d_m of Sample 1 is below 0.1 mm, whereas the d_m of Sample 7 at the head of the reservoir is about 20 mm, which is still relatively small for a reservoir in an Alpine river.

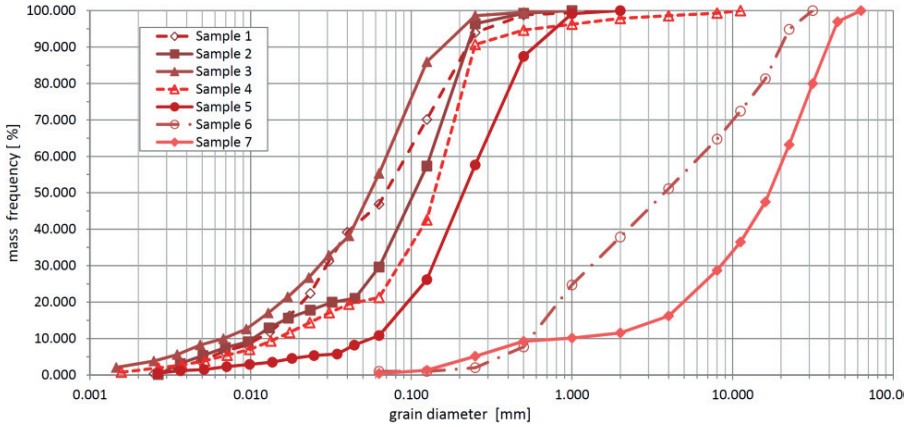

Figure 2 Grain size distributions of the sediment samples taken in the reservoir

3 NUMERICAL SIMULATIONS

3.1 Numerical setup

The numerical simulations were performed with TELEMAC-3D. TELEMAC-3D is a module of the open source TELEMAC-MASCARET suite for the simulations of hydrodynamic flow, contaminant and sediment transport (http://www.opentelemac.org). TELEMAC-3D solves the three-dimensional incompressible Navier-Stokes equations for free surface flow with or without the hydrostatic pressure assumption. A detailed description of the theoretical aspects used in TELEMAC is given in Hervouet (2007). The simulations in this study were performed with hydrostatic pressure assumption, because the sensitivity analysis showed that the use of the non-hydrostatic pressure algorithm did not change the results in this kind of applications significantly. In TELEMAC-3D the two-dimensional triangular mesh is extended to the vertical dimension by the implementation of a number of planes or levels. Different mesh discretizations for the vertical levels are implemented. In this study a homogenous distribution in the vertical direction with five levels was used. The sensitivity analysis using ten levels for the vertical discretization proved made clear that no differences occurred in the computed water surface compared to the use of five levels. The method of characteristics was chosen, however several other schemes are available for the computation of the advection terms. The solver offers a semi-implicit scheme for the time integration. TELEMAC-3D is able to separate the vertical and horizontal turbulence scales for modeling of the turbulence. In this investigation a constant eddy viscosity was applied for the horizontal turbulence and the Prandtl mixing length model was used for the vertical turbulence model. The Prandtl mixing length model expresses the turbulent viscosity as a function of the mean velocity gradient and the mixing length. The Strickler friction law was applied to compute the energy losses caused by bottom friction with a constant Strickler value of 35 $m^{1/3}/s$ for the whole domain. A time step of 1.0 second was chosen for the numerical simulation.
Based on the existing bathymetry data, two three-dimensional digital elevation models were generated; one before and one after the flushing event. The mesh with approximately 211,500 prismatic cells and an average edge length of 4 m was mapped on the digital elevation model using the free software BlueKenue (CHC, 2010).

3.2 Validation of the Numerical model using ADCP measurements

The hydrodynamic model was validated using ADCP measurements performed at the prototype. The ADCP measurements were performed during normal turbine operation. The velocity fields from the measurements were analyzed using the Open Source postprocessing software ADCPtool (Dorfmann & Steidl, 2013). With the ADCPtool 2-D depth averaged flow velocities were calculated and georeferenced. Figure 4 shows the comparison between measured ADCP flow velocities and the computed depth averaged velocities resulting from the 3-D hydrodynamic model. The magnitude and the direction of the calculated velocity vectors compare well with the measured velocity vectors.

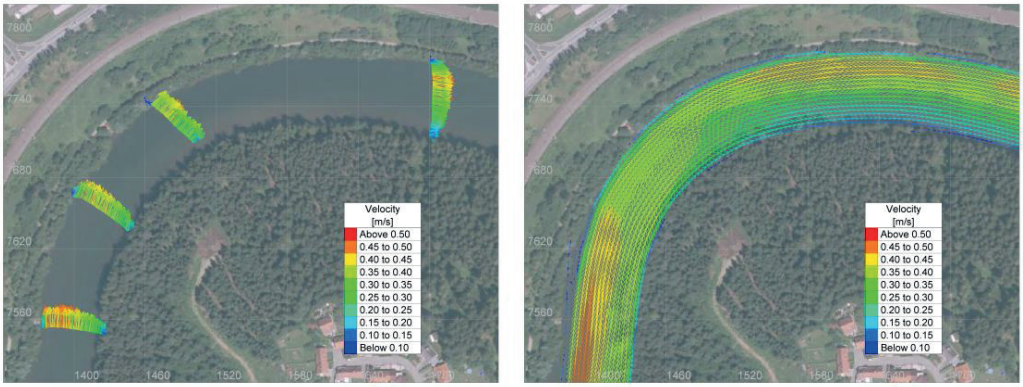

Figure 4 Calculated depth-averaged velocity profiles (left) and measured depth-averaged ADCP profiles (right)

4 RESULTS AND DISCUSSION

4.1 Evaluation of the Bed Changes

Echo-soundings performed before and after the flushing event were used to evaluate the morphological changes caused by the flushing event. Based on these measurements two digital elevation models were developed. The digital elevation model before (Figure 5) and after the flushing event (Figure 6) were used to calculate the differences in the bed levels and the resulting erosion pattern caused by the flushing operation. The measured differences in the bed levels are shown in Figure 7. Massive erosion occurred in the first half of the reservoir upstream of the weir with a lowering of the bed level in the reservoir of up to 2 m. The erosion at the head of the reservoir and in the upper part of the reservoir was limited due to the larger grain sizes and the armored river bed at the head of the reservoir. At the flushing event in July 2012 approx. 240,000 m3 of sediment depositions were removed from the reservoir.

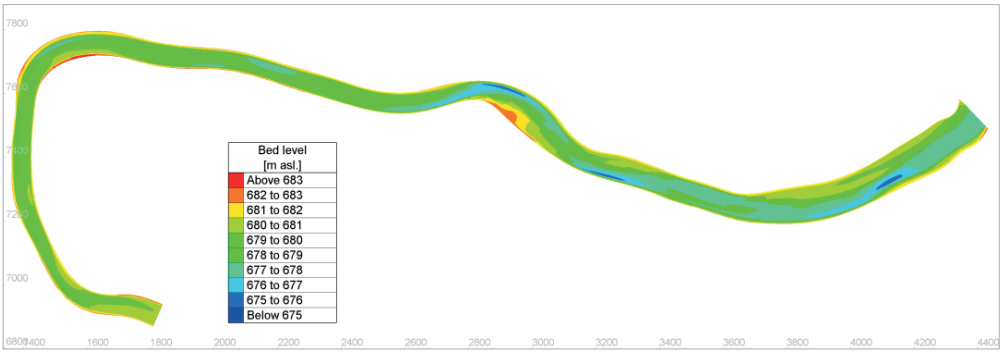

Figure 5 Digital elevation model of the reservoir bed before the flushing event in July 2012

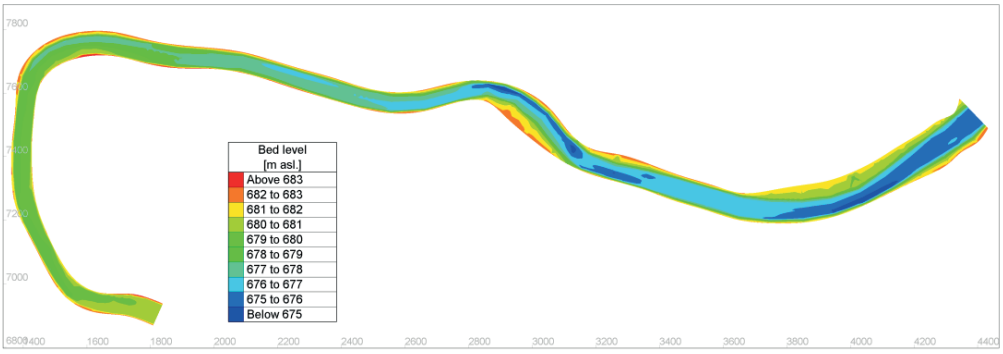

Figure 6 Digital elevation model of the reservoir bed after the flushing event in July 2012

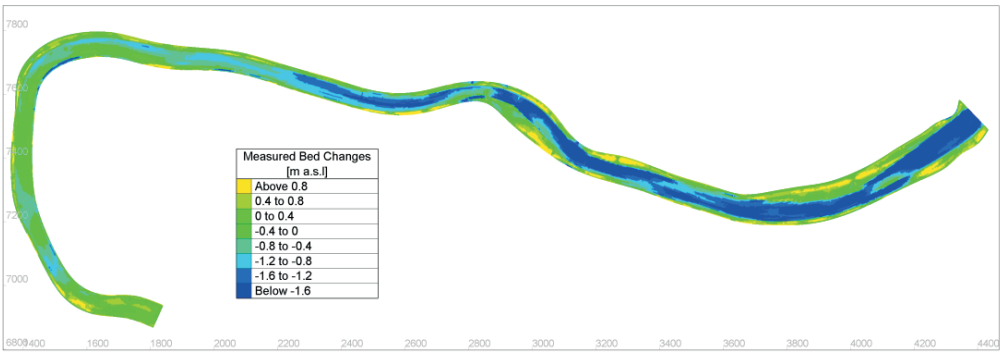

Figure 7 Measured bed changes derived of the digital elevation models, after – before flushing

4.2 Numerical Analysis of the Changes of the Water Level Caused by Flushing

Before the flushing event 2012 the massive sediment depositions in the reservoir increased the flood risk due to the rising bed levels. At the flushing event in July 2012 a large amount of sediment depositions were removed from the reservoir. The average bed slope in the reservoir increased, because of the erosion of these sediment depositions. Hence, in case of free flow conditions the water level at flood events decreases and the bed shear stress increases. The differences in the water levels are shown in Figure 8. The water level decreased in the whole reservoir. The highest differences in the water level are in the first half of the reservoir upstream of the weir. These higher differences are caused by the massive sediment erosion which indicates a good flushing efficiency in the zone upstream of the weir.

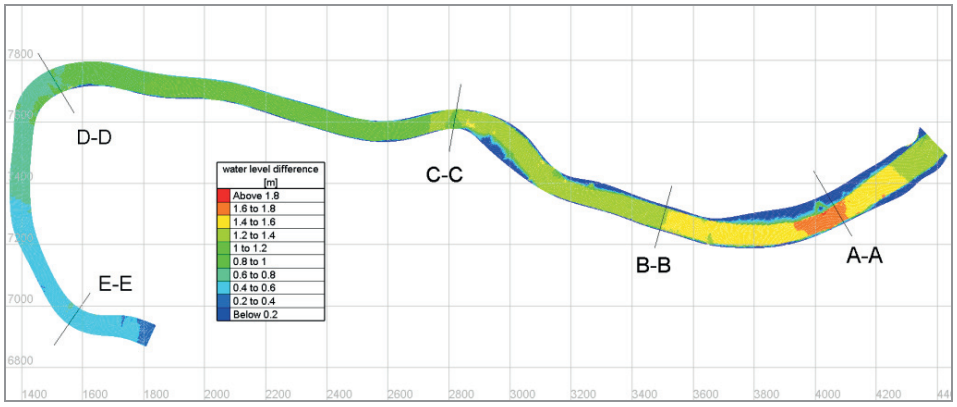

Figure 8 Differences in the water level because of the flushing event and the desilting of the reservoir

Figure 9 illustrates the changes in the bed levels and the caused differences in the water level for the cross sections A-A to E-E. The erosion of the sediment depositions decreases from the weir (cross section A-A) to the head of the reservoir (cross section E-E). Thus, also the lowering of the water level is higher at cross sections A-A and B-B than at cross sections D-D and E-E.
The analysis of the water levels showed that the flushing of the reservoir lowered the flood probability of the urban areas at the head of the reservoir significantly.

4.2 Numerical Analysis of the Bed Shear Stresses in the Reservoir

The bed shear stresses in the reservoir were modelled to provide a better understanding of the sediment transport processes in the reservoir. Figure 10 illustrates the calculated total bed shear stresses for the bed levels before the flushing event in July 2012 in case of a 20-year flood. The highest bed shear stresses occur at the weir. The bed shear stresses at the upper part of the reservoir and at the head of the reservoir are relatively low. This low bed shear stresses and the reduced slope in the reservoir caused by the massive sediment depositions reduces sediment transport capacity in the reservoir in case of flushing events. This effect decreases the possible erosion in the reservoir with continuous progression of the reservoir sedimentation. In the Alpine area flushing events are linked to hydrological boundaries such as flood events. Therefore, large flushing events like the flushing event in July 2012 cannot be planned in advance, but can be used to remove sediment depositions from reservoirs. Caused by the previous mentioned high discharge and the long duration of the flushing event a large amount of deposited sediments could be eroded from the reservoir. Therefore, the bed shear stresses for the bed levels after the flushing event in July 2012 are much higher due to the increased bed slope in the reservoir (Figure 11). The higher bed shear stresses will lead to enhanced sediment erosion in case of future flushing events even at minor flood events.

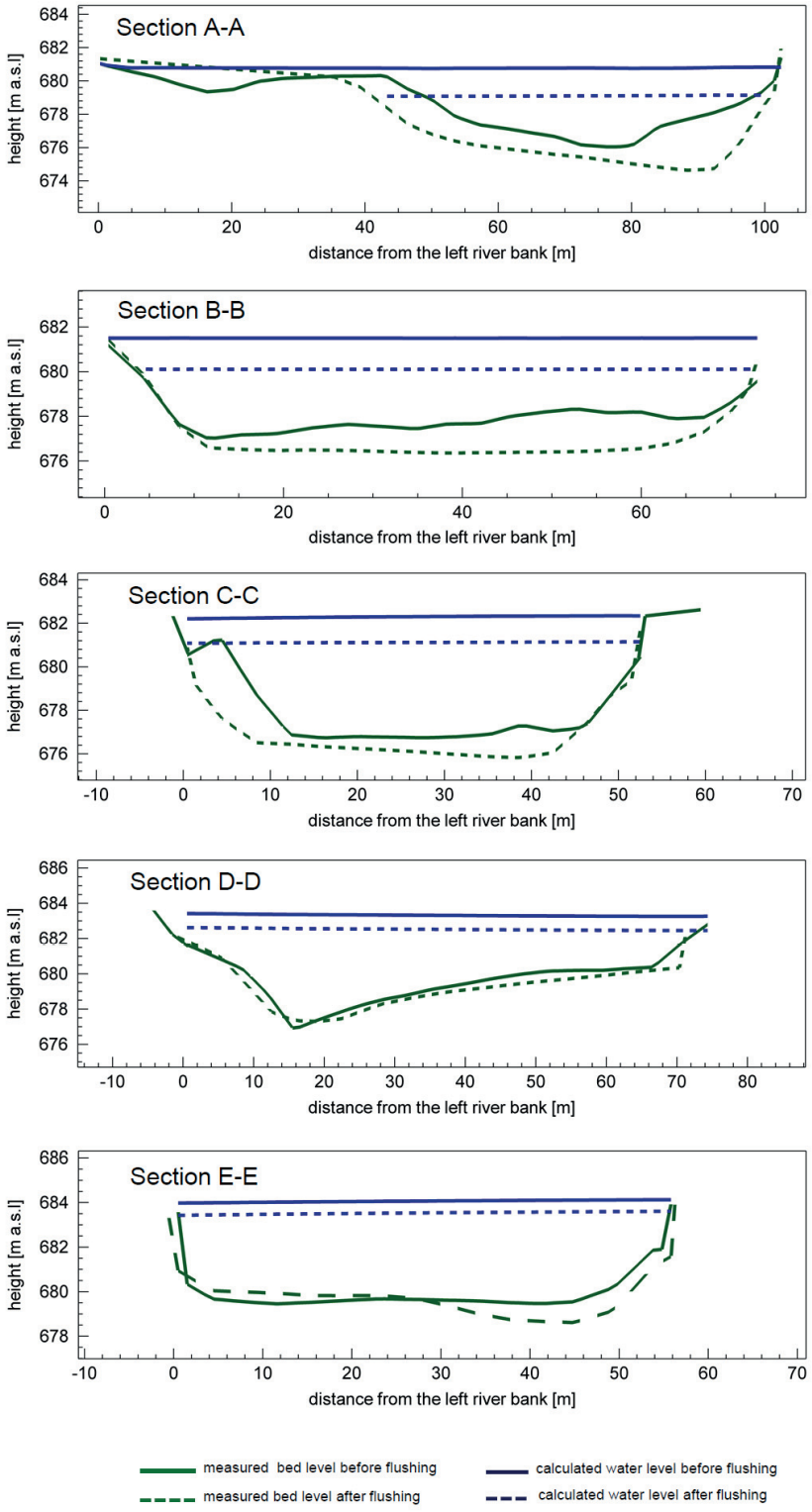

Figure 9 Changes in the bed level and in the water level caused by the flushing event 2012

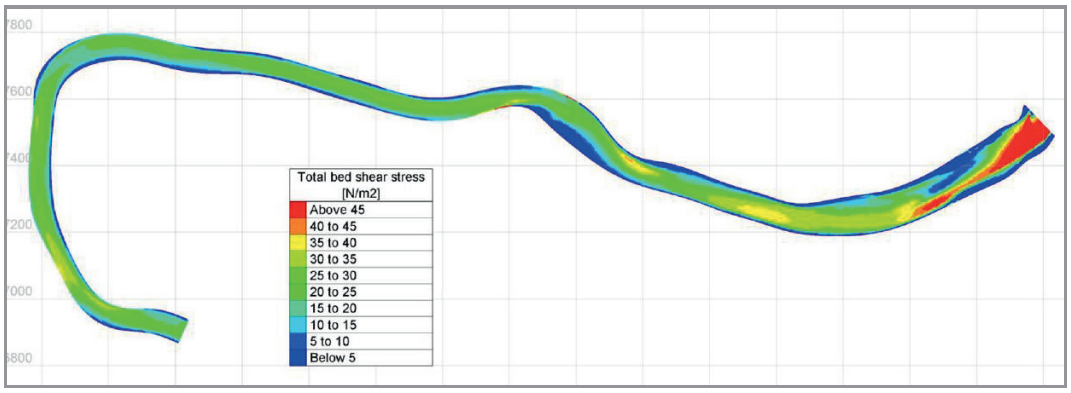

Figure 10 Calculated total bed shear stress before the flushing event in July 2012 for a 20-year flood

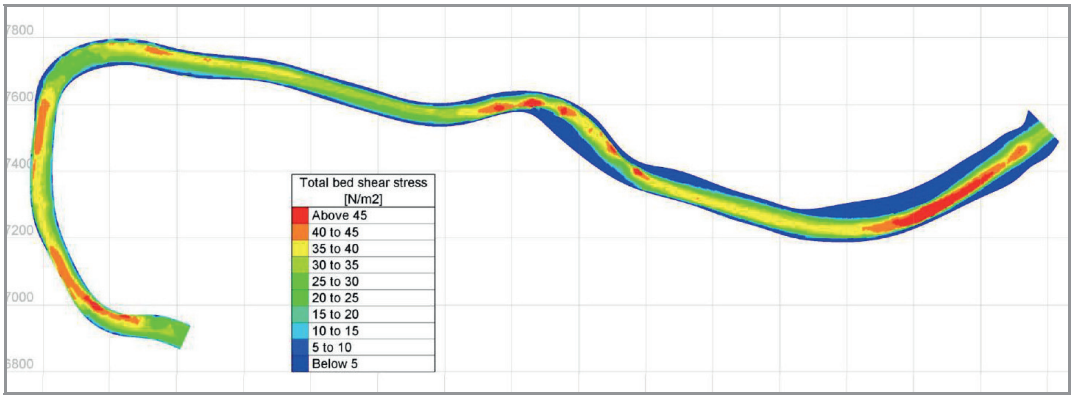

Figure 11 Calculated total bed shear stress after the flushing event in July 2012 for a 20-year flood

5 CONCLUSIONS

The paper discussed the simulation of a flushing event in an Alpine reservoir. The open source numerical model TELEMAC-3D was used to simulate the hydrodynamic processes of a flushing event in 2012. The bed levels in the reservoir were analyzed using echo-soundings of the reservoir before and after the flushing event. A large part of the massive sediment depositions in the reservoir were eroded due to the reservoir flushing. The highest erosion rates occurred in the first half of the reservoir upstream of the weir with a lowering of the bed level in the reservoir of up to 2 m. In this area the mean grain size of the sediment depositions was below 0.1 mm. The erosion at the head of the reservoir and in the upper part of the reservoir was limited due to the larger grain sizes (about 20 mm) and the armored river bed at the head of the reservoir.

The numerical analysis showed that the removal of the sediment depositions increased the bed slope in the reservoir and lead to the lowering of the water level in the reservoir. Hence, the probability of flooding decreased for the urban areas near the head of the reservoir.

The increased bed slope in the reservoir and the lowered water level also enhances the bed shear stresses in the reservoir. These changed conditions could increase the flushing efficiency for performing flushing at minor flood events. However, the possibility of flushing is strictly connected to the hydrological conditions and in the Alpine area consequently linked to flood events.

The next steps in this study will be the numerical modeling of the sediment transport processes at the flushing event in July 2012.

References

CHC - Canadian Hydraulics Centre, National Research Council (2010). Blue Kenue, Reference Manual, August 2010.

Dorfmann, C. & Knoblauch, H. (2009). A Concept for Desilting a Reservoir Using Numerical and Physical Models. Water Engineering for a Sustainable Environment, Proceedings of the 33.IAHR Congress, Vancouver, Canada.

Dorfmann, C. & Steidl, J. (2013). ADCPtool - A postprocessing framework for ADCP measurements, Reference Manual, http://portal.tugraz.at/portal/page/portal/TU_Graz/Einrichtungen/Institute/Homepages/i2130/software/ADCPtool

Fang, H-W. & Rodi W. (2003). Three-dimensional calculations of flow and suspended sediment transport in the neighborhood of the dam for the Three Gorges Project (TGP) reservoir in the Yangtze River. *J. Hydraulic Res*. 41(4), 379–394.

Haun, S. & Olsen, N.R.B 2012, Three-dimensional numerical modelling of reservoir flushing in a prototype scale. International Journal of River Basin Management. 10(4) 341-349.

Hervouet J-M. 2007. Hydrodynamics of free surface flows: modelling with the finite element method. Wiley.

FLUME TESTS - ISRS2013

Evaluation of critical shear stresses of cohesive sediments by using PIV compared with vane strength measurements

G. Harb
Institute of Hydraulic Engineering and Water Resources Management, Graz University of Technology, Austria

S. Haun
Department of Hydraulic and Environmental Engineering, The Norwegian University of Science and Technology, Trondheim, Norway

J. Schneider
Institute of Hydraulic Engineering and Water Resources Management, Graz University of Technology, Austria

ABSTRACT: In reservoirs flow velocities, turbulences and bed shear stresses are reduced, leading into settlements of the transported sediment load. Depositions in reservoirs often contain fine sediments like silt and clay. The occurring cohesive forces increase the critical bed shear stress and the Shield curve is no longer valid. Additional data is required in such cases to estimate the cohesiveness and as consequence the valid critical shear stress. In this study the critical shear stress was evaluated for cohesive sediment samples taken from a reservoir in Austria and from one located in Costa Rica. The sediment samples were placed in a flume and the discharge was varied until mass erosion took place. A 2D PIV device was used to measure the velocity profile and the turbulences at the same time. These values were used to calculate the bed shear stress for the specific discharge where erosion took place. Additional vane strength measurements have been carried out in the reservoirs to test the transferability of the measured vane strength values from the field into useable values for the estimation of erosion rates.

1 INTRODUCTION

In reservoirs flow velocities, turbulences and bed shear stresses are reduced, leading into settlements of the transported bed and suspended sediment load. Depending on the characteristics of the sediment particles and the reservoir operation tasks, sediment particles may deposit in different regions of the reservoir (Morris & Fan, 1998). Hence a spatial and temporal variability of the characteristics of the depositions can be observed.

The bed shear stress is one of the key parameters for sediment transport processes. A large number of options can be found in the literature to predict the bed shear stress (Rowiński et al., 2005). The most used methods are the gravity/bed slope method and the logarithmic wall law method. If a time series of the fluctuating velocity components *u'* and *w'* near the bed is available, e.g. from ADV or PIV measurements in the laboratory or from a numerical model, the Reynolds Stress method may also be used.

The use of the Shield curve is the most used technique to determine the critical bed shear stress for cohesionless depositions. However, depositions in reservoirs often contain fine sediments like silt and clay. Even if it is possible to draw a clear threshold between fine and coarse particles (most times 60 µm is used as threshold), it is not straightforward to use a single number to describe the behavior of the sediments regarding cohesion (Mehta et al., 1989). Occurring cohesive forces increase the critical bed shear stress and the Shield curve is no longer valid. The critical shear stress of the cohesive sediment mixtures may be up to 50 times larger as for cohesionless sediments, having similar arithmetic mean sizes (Kothyari & Jain, 2008). Especially consolidation effects resulting in lower water content, higher shear strength and more stable structural configuration of the deposition layers influence the critical shear stress (Mehta et al., 1989). Kamphuis & Hall (1983) took e.g. the clay content and consolidation pressure in their experimentally studies into account. However, Berlamont et al. (1993) proposed a list of 28 parameters which would be necessary to describe the behaviour of natural cohesive sediments, as a result of physical, chemical and biological processes. Hence additional data is required in such cases to estimate the cohesiveness and the valid critical shear stress. So far there is no standard procedure for the evaluation of the critical shear stresses of cohesive sediments available. In this study the critical shear stress was developed from flume studies, where the discharge rate was increased stepwise till mass erosion took place.

In addition field measurements with a miscellaneous device were conducted (Aberle, 2008). The vane strength measurements have been carried out in the reservoirs to determine the undrained shear strength of the sediments in situ. The results were used to test the transferability of the measured vane strength values from the field into useable values for estimating the erosion rates. In addition a function, devel-

oped with the results of this study and with values from literature, was established which may be used for a further use in these reservoirs.

The sediment samples analysed in this study are taken from the Zlatten reservoir in Austria and the Angostura reservoir in Costa Rica. The depositions in both reservoirs contain a high quantity of fine sediment particles.

2 EVALUATION OF SHEAR STRESSES

The shear stress at the wall is defined by

$$\tau_w = \mu \frac{\delta u}{\delta y}\Big|_w \quad (1)$$

where τ_w is the shear stress at the wall, μ is the dynamic fluid viscosity and $\delta u/\delta y|_w$ is the velocity gradient at the wall.

Hence the shear stress depends on the velocity gradient at the wall, which is at the same time the difficulty in evaluating the shear stress in an accurate way.

For the evaluation of the shear stress both, direct and indirect methods are used. These methods are based on the determination of the shear velocity u_*. The relation of the shear velocity to the shear stress is given by

$$\tau = \rho u_*^2 \quad (2)$$

where ρ is the fluid density.

The shear stress also depends on the wall roughness. The wall roughness is characterized by the shear Reynolds number Re_*, which is defined by

$$\mathrm{Re}_* = \frac{k_s u_*}{\nu} \quad (3)$$

where k_s is the equivalent sand roughness and ν is the kinetic or kinematic viscosity.

Flow conditions with $Re_* < 5$ are called smooth, which means that all roughness elements are inside the viscous sub-layer. If $Re_* > 70$, the flow regime is fully rough (e.g. Yalin, 1977). In this case the viscous sub-layer is so thin that the roughness elements penetrate the logarithmic layer (Graf & Altinakar, 1998). Between $5 < Re_* < 70$ a transitional flow occurs.

2.1 *Methods for the evaluation of bed shear stresses*

2.1.1 *Gravity or bed-slope method*

The gravity method defines the bed shear stress based on the control volume approach and reflects strongly one-dimensional flow conditions. In case of steady, uniform flow the shear velocity can be evaluated by

$$\tau = \gamma R_h I \quad (4)$$

where γ is the specific weight, R_h is the hydraulic radius and I is the energy slope, which is in case of uniform flow equal to the channel slope.

2.1.2 *Logarithmic Law method*

The logarithmic Law method is based on the Kármán-Prantl equation. The shear velocity in the wall region ($y/h < 0.2$) can be evaluated in case of hydraulic rough conditions by fitting measured velocity profiles to the following equation:

$$u^+ = \frac{1}{\kappa} \ln \frac{y}{k_s} + C \quad (5)$$

with

$$u^+ = \frac{u}{u_*} \quad (6)$$

and

$$y^+ = \frac{y u_*}{\nu} \quad (7)$$

where u is the mean velocity, κ is the Kármán constant (usually considered $\kappa = 0.41$), y is the vertical distance and C is considered to be a constant equal to 8.5 (Nezu & Nakagawa, 1993).

2.1.3 *Reynolds Stress method*

The Reynolds Stress method can be used in a fully turbulent two-dimensional flow. For the calculation of the shear stress a time series of the fluctuating velocity components u' and w' near the bed is used. The bed shear stress is then given by

$$\tau = -\rho \overline{u'w'} \quad (8)$$

where u' is the velocity fluctuation in the longitudinal direction and w' is the velocity fluctuation in the vertical direction.

3 SEDIMENT SAMPLING

In August 2010 six representative sediment samples were taken from the Zlatten reservoir in Austria and analysed according to the Austrian Standard ÖNORM B4412. An acrylic cutting cylinder with a diameter of 140 mm was used to obtain nearly undisturbed sediment samples. The cohesive sediment samples were collected at a sediment bank on the orographic left side of the reservoir. The water level at the sediment bank was approx. 0.5 - 0.6 m. The grain size analysis of the sediment samples from the Zlatten reservoir showed a d_{90} of 35 µm and a d_m of 17 µm (Fig. 1). The water content of the samples varied between 30 % and 35 %.

The sediment samples from the Angostura reservoir were taken in July 2012 from a tributary bar which developed at the inflow area of the reservoir during the last years. The water level at the bar was approx. 0.3 - 0.4 m. The used acrylic cutting cylinder had a diameter of 100 mm and the results were also analysed with respect to the same standards. The grain size analysis of the sediment samples showed a d_{90} of 5 µm and a d_m of 3 µm (Fig. 1). The water content of the samples from Costa Rica varied between 30 % and 35 % as well.

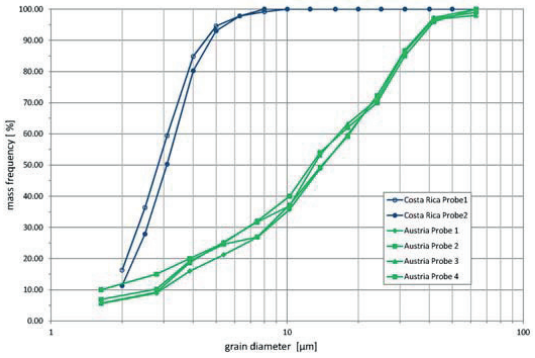

Figure 1. Grain size distribution of the sediment samples gathered in reservoirs in Austria and Costa Rica

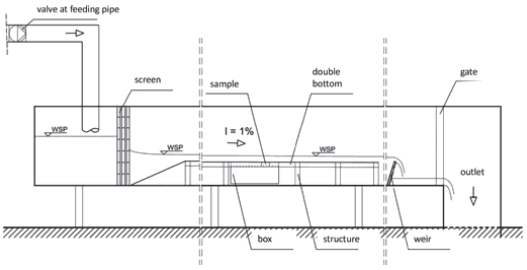

Figure 2. Experimental setup in the flume

4 EXPERIMENTAL SETUP

4.1 *Flume Setup*

The experimental program was carried out at the Hydraulic Laboratory of the Graz University of Technology. The flume is about 14 m long and has a constant rectangular section of 0.8 m width and 0.86 m height (Fig. 2). The glass walls of the channel enable the installation of the PIV-System and allow visual inspection of the test section. The water inflow into the flume is controlled by an upstream located valve in the feeding pipe and measured by an electromagnetic flow meter. The maximum discharge which could be reached with this setup was 150 l/s. The flow depth in the downstream area of the channel was controlled by a gate, located at the outflow area of the flume.

For the experiments a 6 m long double bottom was installed with a declination of 1 % and an open-bottomed test section. So the samples could be easy placed and fitted, with respect to the height, into bottom of the flume. The surface of the double bottom was a smooth acrylic glass plate.

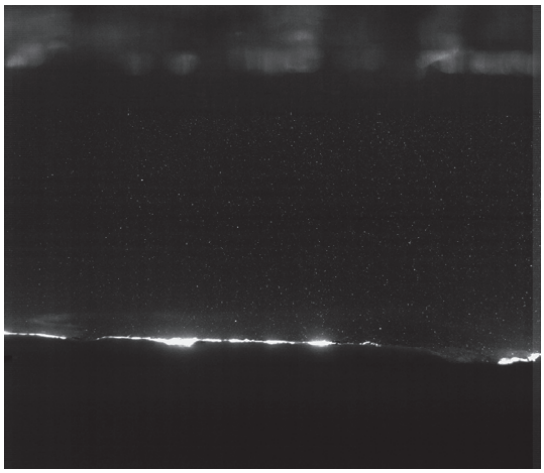

Figure 3. Obtained picture from the PIV measurements

4.2 *Particle Image Velocimetry*

A 2D Particle Image Velocimetry (PIV) system was used for the measurements of the velocity field around the soil sample. The laser used for the PIV-measurement is a Litron Laser – Model (LDY303-PIV) with a repetition rate of 0.2 – 20 kHz, an energy output up to 20 mJ and the defined wave length is 527 nm (green light) (LitronLasers, 2012) The camera is a Photron FASTCAM SA-1 with a frame rate of 5.4 kHz and a resolution of 1024 times 1024 pixel

(Dantek, 2008). For the measurements the laser light sheet was located in the longitudinal axis of the flume directly over the sediment sample.
The camera was oriented normally to the 2D-Laser light sheet. The laser sheet lights the natural particles in the flume and the illuminated particles (seeding) are recorded (Fig. 3). Based on a sensitivity analysis the frame rate was set to 2 kHz.

4.3 *Experimental Conditions*

Two sets of experiments were carried out for different flow conditions and different sediment samples, presented in section 3. The slope of the flume was kept constant (with a declination of 1 %). The flow was supercritical for all discharge rates.

The tested flow conditions are summarized in Table 1. The flow variables used to describe the different flow conditions are the flow rate Q, the mean velocity in longitudinal direction u_m, the flow depth h, the Reynolds number Re and the Froude number Fr. The sediment samples were fitted in the open-bottomed test section in the flume. To avoid an influence due to a sudden increase of the roughness (acrylic glass plate - soil sample) a working area of about 1.2 m x 0.8 m around the undisturbed sediment sample was filled and uniformly pasted with natural disturbed material (compare: Kothyari & Jain, 2008; Roberts et al., 2003). So a similar roughness and surface structure like in the reservoir could be obtained.

However, the use of field sediment samples in a laboratory flume has the disadvantage that the characteristics of the undisturbed samples may change during sampling and transportation (Aberle, 2008). Therefore the sediment samples were stored in the acrylic cutting cylinders in a water basin to retain the natural conditions in the reservoir.

The surface of the disturbed material had to be enforced using cement slurry because of the lower critical shear stress. The experiments started usually with a discharge rate of 20 l/s and was increased stepwise every 10 - 15 minutes and visually inspected at the same time. The discharge was held constant in case that erosion occurred. If no visible erosion was recognized the discharge was increased again (e.g. Aberle et al., 2003).

5 EXPERIMENTAL RESULTS AND DISCUSSION

5.1 *Mean velocity profiles*

The velocity profiles were measured for all flow conditions (Table 1) to determine the bed shear stress. In figure 4 the velocity in the longitudinal axis (u) are shown for the different flow conditions. The velocity values and vertical coordinates have been normalized by the maximum velocity component u_{max} and the corresponding coordinate y_{max}, respectively.

Six u-velocity component profiles are presented in figure 5 for the flow condition V120, measured over different sediment samples. Figure 5 illustrates that the most significant difference among the velocity profiles occur next to the bed, probably due to the not perfectly flat surface of the sediment samples. Depending on the exact height of the surface of the sediment sample, the first measured velocity components are 0.1 mm above the bed.

Table 1. Flow conditions for the experiments

Flow condition	Q [l/s]	u_m [m/s]	h [mm]	Re [-]	Fr [-]
V20	20	0.75	23	$1.3x10^{-4}$	1.57
V25	25	0.84	28	$1.7x10^{-4}$	1.60
V30	30	0.94	33	$2.2x10^{-4}$	1.64
V35	35	1.02	38	$2.7x10^{-4}$	1.67
V40	40	1.07	42	$3.1x10^{-4}$	1.68
V50	50	1.18	49	$3.9x10^{-4}$	1.71
V60	60	1.28	55	$4.8x10^{-4}$	1.73
V70	70	1.36	62	$5.6x10^{-4}$	1.75
V80	80	1.44	68	$6.5x10^{-4}$	1.76
V90	90	1.50	73	$7.3x10^{-4}$	1.77
V100	100	1.57	78	$8.0x10^{-4}$	1.78
V120	120	1.67	89	$9.5x10^{-4}$	1.80

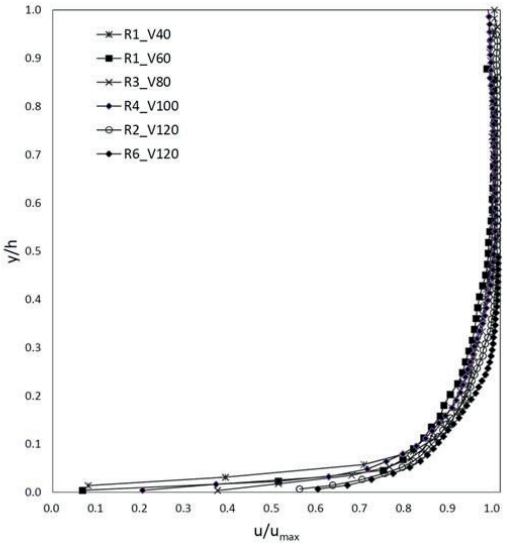

Figure 4. Normalized u-velocity (in the longitudinal direction)

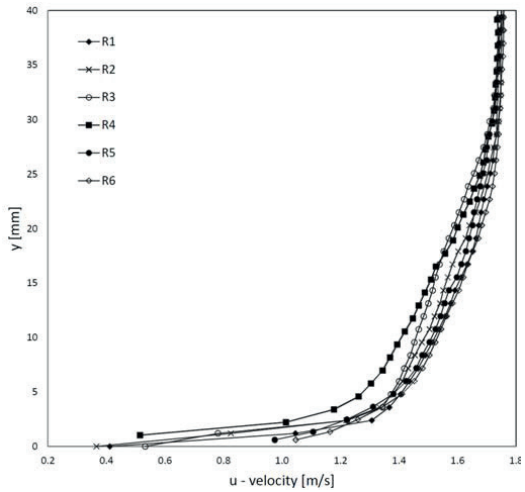

Figure 5. Detail of the measured *u*-velocities for 6 different sediment samples (V120) close to the bed

5.2 *Evaluation of the shear stress*

The evaluation of the shear stresses was performed using the gravity method and the Reynolds stress method, described in section 2. In case of the Reynolds stress method the measured shear stresses were averaged over the measured time and spatial over the sediment sample. The spatial averaging was necessary because slight differences in the height of the probes caused peak values in the obtained shear stresses.

The obtained shear stress values are plotted in figure 6 to show the relationship between the values derived by the gravity method and the Reynolds stress method. Good agreement was found for both methods which indicate that nearly uniform flow conditions occurred in the flume.

In this study six cohesive sediment samples from Austria and two sediment samples from Costa Rica were tested to evaluate the critical shear stresses, as mentioned already. The erosion pattern in this study was identified visually and characterised based on the erosion modes defined by Kothyari & Jain (2008). Whereby the modes of incipient motion (namely: pothole erosion, line erosion and mass erosion) depend strongly on the clay content, the antecedent moisture characteristics and the applied shear stress (Kothyari & Jain, 2008).

Table 2 shows an overview of the measured critical shear stresses for observed mass erosion. In the cases R2, R5, R6 and C2 the failure took place between two natural layers formed by sedimentation in the reservoirs. Figure 7 shows the erosion pattern of the sample C2. The structure of the sediment samples R1, R3, R4 and C1 was also not uniform because of small lenses of fine clay. In these cases mass erosion took place in the more or less compact sediment probe. Layers or small lenses in the depositions develop often if the characteristics of the inflowing sediments change during the deposition period (e.g. coarser sediments during flood events). However, if it is possible to capture such kind of disturbances in a small scale, an observation of the bed for a whole reservoir is almost impossible to conduct.

The obtained critical shear stresses are relatively high compared with previous conducted studies, e.g. Aberle et al. (2006), Debnath et al. (2007), Kothyari & Jain (2008), Tolhurst et al. (2009) and Kothyari & Jain (2010). Only the critical shear stresses given by Kamphuis & Hall (1983) are in the same range as the values derived in this study. The sediment characteristics and critical shear stresses given by Kothyari & Jain (2008 & 2010) and Kamphuis & Hall (1983) are summarised in Table 3.

The reason for the mainly lower critical shear values, found in literature, could be explained by the fact that no consolidation effects were taken into account in the in the laboratory produced sediment depositions. Whereas sediment samples, taken from reservoirs, are influenced by consolidation, leading into higher critical shear stresses.

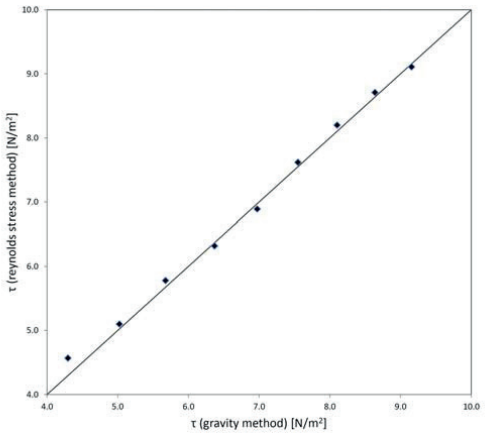

Figure 6. Comparison of the shear stress values (time averaged and space averaged) derived by the gravity method and the Reynolds stress method for different flow conditions

Table 2. Evaluated critical shear stresses

Sediment Sample	Reservoir	Q_{crit} [l/s]	τ_{crit} [N/m^2]	Comment [-]
R1	Austria	120	9.1	line erosion at 80 l/s
R2	Austria	70	6.4	---
R3	Austria	120	9.1	pothole erosion at 80 l/s
R4	Austria	120	9.1	mass erosion at 140 l/s
R5	Austria	60	5.7	---
R6	Austria	40	4.5	---
C1	Costa Rica	120	9.1	---
C2	Costa Rica	25	2.9	---

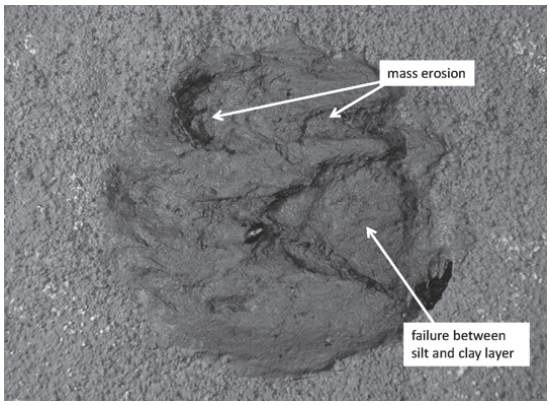

Figure 7. Erosion pattern of the sample C2 after the final run (V 25) with a shear stress of 2.9 N/m^2 with failure between the silt and clay layer

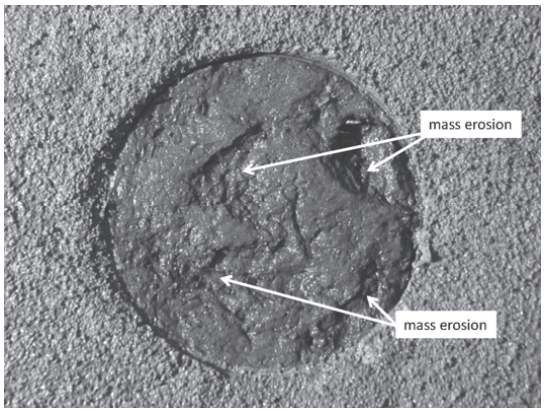

Figure 8. Erosion pattern of the sample C1 after the final run (V 120) with a shear stress of 9.1 N/m^2

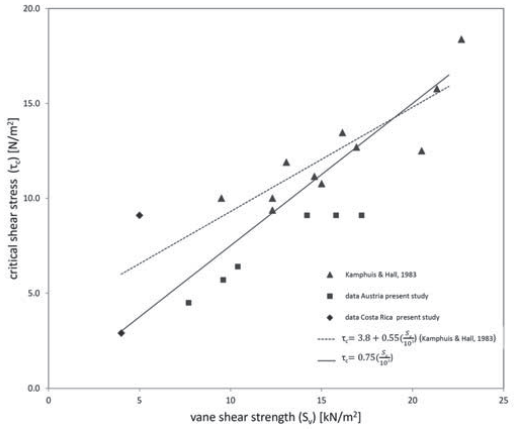

Figure 9. Comparison of the measured critical shear stress values and the measured vane strength values based on data from Kamphuis & Hall (1983) modified with data of the present study

6 VANE STRENGHT MEASUREMENTS

The field vane is one of the most used in situ methods for determining of the undrained shear strength of cohesive sediments (Chandler, 1988). Hence, vane strength measurements have been carried out in the for this study chosen reservoir to test the transferability of the measured vane strength values from the field for the estimation of critical shear stresses of the depositions.

A Geonor H-60 hand-held vane strength tester was used as field equipment for measuring the undrained shear strength (Geonor, 1995). The application range of the device spans from soft to stiff clays in a range of 0 kPa - 200 kPa. The benefits of a hand-held field vane are an easy handling, the repeatability of the results and economical aspects.

The vane strength tests were carried out in the same area where the sediment sampling for the flume test took place. For the measurements the used vane size was 25.4 x 50.8 mm and the used rod had a length of 1 m for both reservoirs. A so called "dummy test" was performed to correct/exclude effects of the skin friction due to the extension rods, when using the equipment under water.

In the Zlatten reservoir the vane strength test was repeated ten times and in the Angostura reservoir the test was repeated twelve times in an area of about 0.5 x 0.5 m for both field sites. Additional vane strength measurements were performed on the sediment samples in the flume after mass erosion took place.

The vane strength measurements were compared with the obtained critical shear stresses from the laboratory study and with the critical shear stresses found in literature (Kamphuis & Hall, 1983; Kothyari & Jain, 2008; Kothyari & Jain, 2010; Table 3). Figure 9 shows the correlation of the data from the present study and the data from Kamphuis & Hall (1983).

In addition, the original function of Kamphuis & Hall (1983) was modified according to the new data.

However, the critical shear stress of cohesive sediments depends on various parameters and therefore this diagram and this function may be used for a rough estimation of the critical shear stress based on measured vane strength values. Further research is necessary for achieving accurate data for studies regarding sediment erosion. Future research tasks include basic research as well as the development of in situ measurement devices which are suitable for a use in large reservoirs.

Table 3. Evaluated critical shear stresses compared with values found in the literature

Sediment Sample/ Literature	Reservoir	d_m [µm]	Water content [%]	Clay[a] [%]	Silt[b] [%]	Sand[c] [%]	τ_{crit} [N/m^2]	S_v [kPa]
R1	Austria	17.8	30.4	10	89	1	9.1	14.2
R2	Austria	17.2	32.9	10	89	1	6.4	10.4
R3	Austria	16.9	31.4	10	89	1	9.1	15.8
R4	Austria	16.5	31.6	10	89	1	9.1	17.2
R5	Austria	17.2	30.9	10	89	1	5.7	9.6
R6	Austria	17.4	32.3	10	89	1	4.5	7.7
C1	Costa Rica	3.1	34.3	15	85	0	9.1	5.0
C2	Costa Rica	3.4	34.0	15	85	0	2.9	4.0
Kamphuis & Hall (1983)		---	24.2 – 37	60	35	5	8.6 – 18.4	9.6 – 22.5
Kamphuis & Hall (1983)		---	35.6	60	38	2	12.2 – 13.4	17.1
Kamphuis & Hall (1983)		---	34.1	62	35	3	---	27.0
Kamphuis & Hall (1983)		---	37.8	60	39	1	9.9 – 10.7	12.2
Kamphuis & Hall (1983)		---	31.8	60	36	4	10.2 – 11.3	15.2
Kamphuis & Hall (1983)		---	35.7	58	40	2	11.3 – 12.5	13.3
Kamphuis & Hall (1983)		---	29.6 – 31.3	48	35	17	4.0 – 8.9	1.9 – 7.6
Kamphuis & Hall (1983)		---	22.6 – 25.8	36	35	29	1.0 – 5.4	3.6 – 11.0
Kamphuis & Hall (1983)		---	20.5	15	35	50	1.5 – 1.8	11.0
Kothyari & Jain (2008)		1500	7.2 – 13.4	10	0	90	0.9 – 1.3	---
Kothyari & Jain (2008)		1330	7.2 – 15.2	20	0	80	1.2 – 1.7	---
Kothyari & Jain (2008)		1170	9.5 – 21.7	30	0	70	1.3 – 1.8	---
Kothyari & Jain (2008)		1000	10.3 – 19.2	40	0	60	1.0 – 1.6	---
Kothyari & Jain (2008)		840	10.0 –20.4	50	0	50	0.9 – 1.5	---
Kothyari & Jain (2010)		1500	---	10	45	45	0.9 – 1.3	---
Kothyari & Jain (2010)		1000	---	40	30	30	0.9 – 1.5	---
Kothyari & Jain (2010)		850	---	50	25	25	0.8 – 1.4	---

[a] $d \leq 2$ µm; [b] 2 µm $< d \leq 64$ µm; [c] $d > 2$ µm

7 CONCLUSIONS

The critical shear stress is a key parameter for predicting erosion rates and effects. In the current paper the evaluation of the critical shear stress of cohesive sediment depositions is presented and discussed. Sediment samples from two reservoirs (Zlatten reservoir, Austria and Angostura reservoir, Costa Rica) were analysed. The samples were placed in a research flume and the discharge was varied stepwise until mass erosion took place. The velocity profiles and the turbulences over the sample were measured with a 2D PIV device and used for calculating the bed shear stress for the specific discharge rate. For the conducted study the gravity method and the Reynolds stress method were used and showed good agreement in the comparison of the values. This indicates that nearly uniform flow conditions occurred in the flume. The results of the critical bed shear stresses, achieved from the conducted flume tests, showed in average similar values as found in the previous conducted study by Kamphuis & Hall (1983).

The results showed that the behaviour of natural cohesive sediments depend on a wide range of parameters (Black et al., 2002; Grabowski et al., 2011). Especially the effects of depositions with a layers structure could be observed and is an important parameter of the deposited sediments. The results of the experiments showed also that the obtained average shear stress was above most of the values found in previous conducted studies (e.g. Kothyari & Jain, 2008). This is most probably due to the natural consolidation effects of the samples taken from the reservoirs, compared to the artificially created depositions made of a mixture of clay, silt and sand, used in other performed studies.

In addition vane strength measurements were performed in the reservoirs to measure the undrained shear strength of the depositions. The obtained vane strength values were set in relation to the critical shear stresses derived by the experimental tests in the flume. This data was also correlated with data derived by Kamphuis & Hall (1983). The original relation function from the critical shear stress to the vane strength values obtained by Kamphuis & Hall (1983) was modified according to the new data. The new function may now be used for a rough estimation of the critical shear stress, based on measured vane strength values. Especially for the Angostura reservoir, where only two samples were available, these rough estimations should be handled with care in further studies.

Future research is necessary for achieving accurate data for studies regarding sediment erosion of

cohesive depositions. These research tasks include basic research as well as the development of in situ measurement devices for a use in large reservoirs.

ACKNOWLEDGEMENTS

This work was partly funded by the SEE Hydropower project of the South East Europe Programme of the European Union.

REFERENCES

Aberle J., Nikora V., McLean S., Doscher C., McEwan I., Green M., Goring D. & Walsh J. (2003): Straight benthic flow-through flume for insitu measurements of cohesive sediment dynamics. *Journal of Hydraulic Engineering, Vol. 129, No. 1, 63-67.*

Aberle J., Nikora V. & Walters R. (2006): Data Interpretation for In Situ Measurements of Cohesive Sediment Erosion. *Journal of Hydraulic Engineering, Vol. 132, No. 6, 581-588.*

Aberle J. (2008): Measurement Techniques for the Estimation of Cohesive Sediment Erosion. *In Hydraulic Methods for Catastrophes: Floods, Droughts, Environmental Disasters, P. Rowinski (ed.),* Publs. Inst. Geophys. Pol. Acad. Sc., E-10 (406), 5 -20.

Berlamont J.E., Ockenden M.C., Toorman E.A. & Winterwerp J.C. (1993): The characterisation of cohesive sediment properties. *Coastal Engineering, 21(1-3)*, 105-128.

Black K.S., Tolhurst T.J., Paterson D.M. & Hagerthey S.E. (2002): Working with Natural Cohesive Sediments. *Journal of Hydraulic Engineering, Vol. 128, No. 2, 1–8.*

Chandler R.J. (1988). *The In-Situ Measurement of the Undrained Shear Strength of Clay Using the Field Vane*. Vane Shear Strength Testing in Soils: Field and Laboratory Studies, ASTM STP 1014, American Society for Testing And Materials, Philadelphia

Debnath K., Nikora V., Aberle J., Westrich B. & M. Muste (2007): Erosion of Cohesive Sediments: Resuspension, Bed Load, and Erosion Pattern from Field Experiments. *Journal of Hydraulic Engineering, Vol. 133, No. 5, 508-520.*

Dantek (2008): DynamicStudio-User's & Installation Guide. Copyright 2008 by Dantec Dynamics A/S, P .O. Box 121, Tonsbakken 18, DK-2740 Skovlunde, Denmark.

Geonor (1995): Instructions for use - Inspection Vane Tester, H-60. User Manual, Geonor AS, Oslo, Norway.

Grabowski R.C., Droppo I.G. & Wharton G. (2011): Erodibility of cohesive sediment: The importance of sediment properties. *Earth-Science Reviews 105 (2011)*, 101–120.

Graf W.H. & Altinakar M.S. (1998): *Fluvial Hydraulics*. Wiley.

Haun S. & Olsen N.R.B. (2012): Three-dimensional numerical modelling of reservoir flushing in a prototype scale. *International Journal of River Basin Management, Vol. 10, No. 4*, 341-349.

Kamphuis J.W. & Hall K.R. (1983): Cohesive material erosion by unidirectoral current. *Journal of Hydraulic Engineering, Vol. 109, No. 1, January, 1983*.

Kothyari U.C. & Jain R.K. (2008): Influence of cohesion on the incipient motion conditions of sediment mixtures. *Water Resources Research, Vol. 44, W04410*.

Kothyari U.C. & Jain R.K. (2010): Erosion characteristics of cohesive sediment mixtures. *Proceedings of the International Conference on Fluvial Hydraulics, Braunschweig, Germany.*

LitronLasers (2012): *The LDY300 PIV Series Dual Head Diode Pumped Q-switched Nd:YLF Lasers*. Datasheet, http://www.litronlasers.com/pdf%20files/LitronLDY300PIV0101_1.pdf, downloaded at the 27th of December 2012.

Mehta A., Hayter E., Parker W., Krone R. & Teeter A. (1989): Cohesive Sediment Transport. I: Process Description. *Journal of Hydraulic Engineering, Vol. 115, No. 8*, 1076–1093.

Morris G.L. & Fan J. (1998): *Reservoir Sediment Handbook*. McGraw-Hill Book Co., New York.

Nezu I. & H. Nakagawa (1993): *Turbulence in open-channel flows*, A.A. Balkema, Rotterdam, Netherlands.

Roberts J.D., Jepsen R.A. & James S.C. (2003): Measurements of sediment erosion and transport with the adjustable shear stress erosion and transport flume. *Journal of Hydraulic Engineering, Vol. 129, No. 11, 862-871*.

Rowiński P., Aberle J. & Mazurczyk A. (2005): Shear velocity estimation in hydraulic research. *Acta Geophysica Polonica, Vol. 53, No. 4, 567-583.*

Tolhurst T.J., Black K.S. & Paterson D.M. (2009): Muddy Sediment Erosion: Insights from Field Studies. *Journal of Hydraulic Engineering, Vol. 134, No. 1, 73-87.*

Yalin S. (1977): *Mechanics of Sediment Transport.* Second Edition, Pergamon Press, New York, USA.

APPENDIX - CURRICULUM VITAE

Graz University of Technology

Institute of Hydraulic Engineering and Water Resources Management

CURRICULUM VITAE

Name	Dipl.-Ing. Gabriele Harb
Date of Birth	26.12.1980
Profession	Civil Engineer
Citizenship	Austria
Position	Researcher

QUALIFICATION

Area of Expertise:	Numerical modeling of hydrodynamic and sediment transport processes, physical hydraulic model tests, field measurements, sediment transport, risk analysis of flood events,
Membership:	IAHR

EDUCATION:

1995 – 2000	Higher Technical Institute Graz Ortweingasse
02/2002 – 04/2008	Diploma Study Civil Engineering at the TU Graz *Master Thesis: Evaluation of the Flood-Damage-Potential and Cost-Benefit-Analysis of Flood-Protection-Buildings at the Case-Study Radkersburg*
Language Skills:	German (mother tongue) English (fluent in spoken and written) Spanish (school level)

PROFESSIONAL EXPERIENCE:

10/2000 – 12/2001	Project Assistant – Architekturbüro Kada, Graz
07/2002 – 04/2008	Technical Assistant and Site Manager – Baufirma Granit, Graz
Since 05/2008	**Researcher – Institute of Hydraulic Engineering and Water Resources Management, Graz**

RESEARCH PROJECTS:

Alp-S	„Quantitative und qualitative Messung des Feststofftransportes mittels berührungsloser Sensortechnik“, innovative sediment transport measurement techniques, field measurements and model tests, 2008-2009
ETS	„Einfluss von Trübeströmen auf die Speicherverlandung – Durchschleusen als Alternative“, turbidity current venting, field measurements, 2006-2008
HPP Schönau	Sediment management in the existing reservoir, physical model test and numerical modeling of sediment transport, 2007-2009
SEE Hydropower	Reservoir management and sediment management, research project, 2009-2012, funded by the South-East-Europe Programme of the European Union,
SHARE	research project, 2009-2012, funded by the Alpine Space Programme of the European Union
HPP Schütt	Analysis of the required minimum-instream flow with field measurements, 2010-2011
HPP Leoben	Sediment management in the existing reservoir and analysis of the flood risk at the head of the hydro power plant using numerical modeling, 2010-2011
HPP Fisching	Sediment management in the existing reservoir and analysis of the flood risk at the head of the hydro power plant using numerical modeling, 2011-2013
HPP Kendlbruck	Sediment management and reservoir flushing for the planned reservoir, 2012-2013
Climcatch	“Impact of climate change on the sediment yield of alpine catchments”, field measurements and analysis of the sediment transport in the project area Oberwölz
HPP Gratkorn	Physical model tests for the planned hydro power plant, 2013-2014

MASTER THESIS:

Stefan Haun	„Parameterstudie zur Berechnung von Druckverlusten beim Düsenstrahlverfahren“, 2009
Thomas Lebesmühlbacher & Madeleine Wilding	„Akzeptanz von Wasserkraftanlagen“, 2010
Gerfried Klammer	„Bestimmung der kritischen Schubspannung bei kohäsiven Sedimenten“, 2011
Teresa Baras	„Geschiebetransport mittels Tracerverfahren in Wildbächen – Naturmessungen und Literaturrecherche“, 2013

Mitteilungen des Institutes für Wasserwirtschaft und Konstruktiven Wasserbau der Technischen Universität Graz

Bisher erschienene Hefte:

Heft	1	(1959)	VEDER, C.: Neue Verfahren zur Herstellung von untertägigen Wänden und Injektionsschirmen in Lockergesteinen und durchlässigem Fels (vergriffen)
Heft	2	(1959)	BEER, O.: Hochwasserentlastungsanlagen österreichischer Talsperren
Heft	3	(1960)	WEHRSCHÜTZ, F.: Wasserentnahme aus alpinen Abflüssen
Heft	4	(1961)	TSCHADA, H.: Die Spiralenauslässe des Kraftwerkes St.Pantaleon
Heft	5	(1962)	GRENGG, H.: Funktion, Ordnung und Gestalt im konstruktiven Wasserbau
Heft	6	(1962)	PIRCHER, W.: Wehreichungen an der Enns
Heft	7	(1962)	WEHRSCHÜTZ, F.: Füll- und Entleerungssysteme von Schiffsschleusen mit großen Fallhöhen
Heft	8	(1962)	REITZ, A.: Das Stauwerk im Bogen
Heft	9	(1963)	PIRCHER, W.: Die Bautypen der Wasserkraft
Heft	10	(1964)	WEHRSCHÜTZ, F.: Kritische Betrachtung der Modellgesetze
Heft	11	(1965)	SIMMLER, H.: Das neue Institut für Wasserbau
Heft	12	(1964)	RADLER, S.: Die Berechnung der Abflüsse im natürlichen Gerinne
Heft	13	(1965)	ALTENBURGER, H.: Der Spiralauslaß als Hochwasserentlastung bei Donaukraftwerken
Heft	14	(1965)	KRESNIK, E.: Kunststoffe im wasserbaulichen Versuchswesen und deren rauhigkeitsmäßige Erfassung
Heft	15	(1970)	SVEE, R.: Untersuchungen über die Stabilität bei Wasserkraftanlagen mit idealer Regelung
Heft	16	(1971)	DROBIR, H.: Die Registrierung eines zeitlich rasch veränderlichen Wasserspiegels mit kapazitiven Meßsonden ROTH, G.: Meßanlage zum Studium instationärer Vorgänge mit Hilfe eines Digitalcomputers
Heft	17	(1971)	DROBIR, H.: Der Ausfluß aus einem Speicher beim Bruch einer Talsperre
Heft	18	(1972)	GRENGG, H.: Wörterbuch der Wasserkraftnutzung; Französisch – Deutsch, Deutsch – Französisch
Heft	19	(1973)	DRAXLER, A.: Mathematisches Modell für die Zuflußprognose als Hilfsmittel zur Optimierung des KW-Betriebes
Heft	20	(1974)	GRENGG, H.: Die Technisierung großer Ströme in Verbindung mit der Wasserkraft
Heft	21	(1975)	GRENGG, H.: Die großen Wasserkraftanlagen des Weltbestandes
Heft	22	(1977)	GRENGG, H.: Die großen Wasserkraftanlagen des Weltbestandes, 2. Teil KRAUSS, H.: Lufteinzug durch den Wasserabfluß in Vertikalrohren

Heft	23	(1979)	LIEBL, A.: Die Lehre aus der Katastrophe beim Aufstau des Tarbela-Dammes in Pakistan aus der Sicht der Stahlwasserbauer
		(1980)	KRÖLL, A.: Die Stabilität von Steinschüttungen bei Sohlen- und Uferbefestigungen in Wasserströmungen
Heft	24	(1981)	TSCHERNUTTER, P.: Grundsatzüberlegungen zur Rentabilität und zum Ausbau von Kleinwasserkraftwerken
Heft	25	(1984)	Helmut Simmler – Zur Vollendung seines 65.Lebensjahres gewidmet von seinen ehemaligen und derzeitigen Mitarbeitern an der TU Graz

Publikation des Institutes für Hydromechanik, Hydraulik und Hydrologie der Technischen Universität Graz

Bisher erschienene Bände:

SACKL, B.	(1987)	Ermittlung von Hochwasser - Bemessungsganglinien in beobachteten und unbeobachteten Einzugsgebieten

Veröffentlichungen des Institutes für Siedlungs- und Industriewasser-wirtschaft, Grundwasserhydraulik, Schutz- und Landwirtschaftlichen Wasserbau der Technischen Universität Graz

Bisher erschienene Bände:

Band	1	(1977)	RENNER, H.: Die Berücksichtigung nichtbindiger überdeckender Schichten bei der Bemessung von Wasserschutzgebieten
Band	2	(1977)	KAUCH, E.P.: Untersuchung des Bewegungsgesetzes für die Filterströmung, im besonderen bei höheren Geschwindigkeiten einschließlich der teilturbulenten Strömung
Band	3	(1977)	PONN, J.: Geschwindigkeitsverteilungen in radial durchströmten Nachklärbecken – Verwendung einer neu entwickelten Thermosonde
Band	4	(1978)	Festschrift zum 60. Geburtstag von E.P. Nemecek
Band	5	(1979)	RENNER, H.: Die Entwicklung einer biologischen Kläranlage für kleinste Verhältnisse
Band	6	(1980)	Forschungsberichte 1979/80
Band	7	(1980)	KAUCH, E.P.: Der Pumpversuch im ungespannten Grundwasserleiter
Band	8	(1982)	DITSIOS, M.: Untersuchungen über die erforderliche Tiefe von horizontal durchströmten rechteckigen Nachklärbecken von Belebungsanlagen
Band	9	(1982)	GEIGER, D.: Einfluß der Schlammräumung im Nachklärbecken auf die erreichbare Feststoffkonzentration im Belebungsbecken
Band	10	(1984)	Forschungsbericht 1983/84, vergriffen
Band	11	(1984)	Beeinträchtigung der Grundwasservorkommen in qualitativer und quantitativer Hinsicht
Band	12	(1986)	KOTOULAS, K.: Natürliche Entwicklung der Längen- und Querprofilform der Flüsse - ein Beitrag zum naturnahen Flußbau
Band	13	(1987)	KAUCH, E.P., M. DITSIOS: Schlammbilanz in Belebungsanlagen - Einfluß der hydraulischen Betriebsparameter für Trockenwetter- und Regenwetterfall

Band	14	(1988)	Festschrift zum 70. Geburtstag von Ernst P. Nemecek
Band	15	(1988)	Vorträge über Siedlungs- und Industriewasserbau
Band	16	(1991)	KAINZ, H.: Auswirkungen von Stoßbelastungen auf den Feststoffhaushalt einer Belebungsanlage
Band	17	(1991)	KLAMBAUER, B.: Grundwasserschutz und Landwirtschaft – Situation in Mitteleuropa

Schriftenreihe zur Wasserwirtschaft Technische Universität Graz

Bisher erschienene Bände:

Band	1	(1992)	Hermann Grengg – zum 100. Geburtstag [1)]
Band	2	(1992)	ZITZ, W.: Die Mitbehandlung angefaulter Sammelgrubenabwässer in einer kommunalen, schwach belasteten Belebungsanlage [2)], vergriffen
Band	3	(1992)	ÜBERWIMMER, F.: Untersuchung der Ressourcen gespannter Grundwassersysteme mit hydraulischen und hydrologischen Modellen[1), 2)]
Band	4	(1992)	Hochwasserrückhaltebecken – Planung, Bau und Betrieb [1), 2)]
Band	5	(1992)	MOLNAR, T.: Rechnerunterstütztes Projektieren von Bewässerungssystemen [1), 2)]
Band	6	(1993)	Klärschlammentsorgung in der Steiermark [2)]
Band	7	(1993)	FRIEDRICH, Ch., WINDER, O.: Lebensraum Grazer Murböschungen – Zoologisch-botanische Untersuchungen einschließlich Planungsvorschläge [2)]
Band	8	(1993)	REICHL, W.: Mehrdimensionale Optimierung quantitativ und qualitativ bewertbarer Zielfunktionen in der Wasserwirtschaft [1)]
Band	9	(1993)	WELLACHER, J.: Instationäre Strömungsvorgänge in Hochwasserrückhaltebecken [1)]
Band	10	(1993)	STUBENVOLL, H. : Analyse der zeitlichen Struktur von Niederschlagsereignissen auf der Grundlage zeitvariabler Datenaufzeichnung; ZEYRINGER, T.: Untersuchung des räumlichen Verhaltens von Niederschlagsereignissen auf zeitvariabler Datengrundlage [1), 2)]
Band	11	(1993)	Ingenieurbiologie im Schutzwasserbau [2)]
Band	12	(1994)	Ländlicher Raum: Abwasserentsorgung in der Sackgasse? [2)], vergriffen
Band	13	(1994)	SACKL, B.: Ermittlung von Hochwasser-Bemessungsganglinien in beobachteten und unbeobachteten Einzugsgebieten [1), 2)]
Band	14	(1995)	Leben mit dem Hochwasser – Gefahr und Anpassung [2)]
Band	15	(1995)	Betrieb, Erhaltung und Erneuerung von Talsperren und Hochdruckanlagen – Symposium [1)]
Band	16	(1995)	RICHTIG, G.: Untersuchungen zur Abflußentstehung bei Hochwasserereignissen in kleinen Einzugsgebieten [2)]
Band	17	(1995)	KNOBLAUCH, H.: Dissipationsvorgänge in Rohrleitungssystemen [1)]
Band	18	(1995)	Fremdwasser in Abwasseranlagen [2)]
Band	19/1	(1996)	XVIII. Konferenz der Donauländer über hydrologische

Band	19/2		Vorhersagen und hydrologisch-wasserwirtschaftliche Grundlagen [1), 2)]
Band	20	(1996)	STRANNER, H.: Schwallwellen im Unterwasser von Spitzenkraftwerken und deren Reduktion durch flußbauliche Maßnahmen [1)]
Band	21	(1996)	DUM, T.: Verifikation eines numerischen Strömungsmodells anhand physikalischer Modelle [1)]
Band	22	(1996)	VASVÁRI, V.: Ein numerisches Modell zur Bewirtschaftung gespannter Grundwasservorkommen am Beispiel des Mittleren Safentales [1), 2)]
Band	23	(1996)	HYDROLOGISCHE MONOGRAPHIE des Einzugsgebietes der Oberen Raab [1), 2)]
Band	24	(1997)	Niederwasser [1), 2)]
Band	25	(1997)	KRALL, E.: Untersuchung der Gesamtwahrscheinlichkeit von Hochwasserereignissen in kleinen, unbeobachteten Einzugsgebieten Österreichs auf der Grundlage von Gebietskennwerten [1), 2)]
Band	26	(1997)	Abwasserentsorgung bei fehlenden Vorflutern [2)]
Band	27	(1997)	Festschrift anläßlich des 60. Geburtstages von Herrn O.Univ.-Prof. Dipl.-Ing. Dr. techn. Günther Heigerth [1)]
Band	28	(1997)	MEDVED, N.: Simulation und systematische Erfassung von Spülvorgängen in verlandeten Flussstauräumen [1)]
Band	29	(1998)	Festschrift anläßlich des 65. Geburtstages von Herrn O.Univ.-Prof. Dipl.-Ing. Dr. techn. Dr.h.c. Heinz Bergmann [1), 2)]
Band	30	(1998)	Festschrift anläßlich des 80. Geburtstages von Herrn em.O.Univ.-Prof. Dipl.-Ing. Dr.h.c. Dr. techn. Ernst P. Nemecek [2)]
Band	31	(1999)	BEUTLE, K.: Untersuchungen zur Schlammstabilisierung bei diskontinuierlich belüfteten Belebungsanlagen [2)]
Band	32	(1999)	REINHOFER, M.: Klärschlammvererdung mit Schilf [2)]
Band	33	(1999)	GRUBER, G.: Der biologisch abbaubare Kohlenstoffgehalt in der Abwassertechnik, BTOC und BDOC als Alternative zum BSB [2)]
Band	34	(2000)	Betrieb und Überwachung wasserbaulicher Anlagen - Symposium [1)]
Band	35	(2001)	FUCHS, D.: Decision Support Systeme für die Rehabilitationsplanung von Wasserrohrnetzen [2)]
Band	36	(2001)	Untersuchungen im Einzugsgebiet der Oberen Raab über hydrologische Folgen einer möglichen Klimaänderung [1), 2)]
Band	37	(2001)	HABLE, O.: Multidimensional probabilistic design concept for the estimation of the overtopping probability of dams [1), 2)]
Band	38	(2001)	VASVÁRI, V.: Geohydraulische und bohrlochgeophysikalische Untersuchungen in geklüfteten Grundwasserleitern [1), 2)]
Band	39	(2002)	SCHATZL, R.: Skalenabhängiger Vergleich zwischen Wetterradardaten und Niederschlagsmessungen [2)]
Band	40	(2002)	GUNDACKER, F.: Untersuchungen zur Schlammstabilisierung bei diskontinuierlich belüfteten Belebungsanlagen bei tiefen Temperaturen [2)]
Band	41	(2003)	Wasserbau neu – Die Wasserbauschule an der Technischen Universität Graz [2)]

Band	42	(2004)	Innovative Messtechnik in der Wasserwirtschaft – Konzeption und Praxiserfahrungen mit einem modularen Monitoringnetzwerk zur universellen Anwendung in der Wasserwirtschaft [2)]
Band	43	(2005)	7. Treffen junger Wissenschaftlerinnen und Wissenschaftler deutschsprachiger Wasserbauinstitute [1)]
Band	44	(2005)	HOCHEDLINGER, M.: Assessment of Combined Sewer Overflow Emissions [2)]
Band	45	(2006)	NEMECEK, E.P., H.HAERTL, H.GERNEDEL und H.NICKL: Horizontalfilterbrunnen [2)]
Band	46	(2006)	WASSERBAUSYMPOSIUM GRAZ 2006 Stauhaltungen und Speicher – Von der Tradition zur Moderne [1)]
Band	47	(2006)	KAN((¦))FUNK – Überprüfung, Bewertung und Sicherstellung der Funktionsfähigkeit von Kanalisationsanlagen in Österreich [2)]
Band	48	(2007)	PATZIGER, M.: Untersuchung der Schlammbilanz in Belebungsstufen aufbauend auf den Prozessen im Nachklärbecken [2)]
Band	49	(2007)	Abwassergebührensplitting, ÖWAV – TU Graz Seminar [2)]
Band	50	(2007)	dex Fachsymposium 2007 – Abwasserableitung, Abwasser- und Klärschlammbehandlung [2)]
Band	51	(2008)	BADURA, H.: Feststofftransportprozesse während Spülungen von Flussstauräumen am Beispiel der oberen Mur [1)]
Band	52	(2008)	ARCH, A.: Luftein- und Austragsprozesse bei Anlagen mit Peltonturbinen im Gegendruckbetrieb [1)]
Band	53	(2008)	GANGL, G.: Rehabilitationsplanung von Trinkwassernetzen [2)]
Band	54	(2008)	Instandhaltung von Trinkwasser- und Abwasserleitungen; ÖWAV – TU Graz Symposium [2)]
Band	55	(2009)	Optimierte Bemessung von Mischwasserentlastungsanlagen, Erfahrungen mit der Anwendung des neuen ÖWAV-Regelblattes 19; ÖWAV – TU Graz Seminar [2)]
Band	56	(2009)	KÖLBL, J.: Process Benchmarking in Water Supply Sector: Management of Physical Water Losses [2)]
Band	57	(2009)	Wasserverluste in Trinkwassernetzen, ÖVGW – TU Graz Symposium [2)]
Band	58	(2009)	MAYR, D.: Hydraulic Studies on Trifurcations[1)]
Band	59	(2009)	MUNALA, G.K.: A Viable Pro-poor Public-Private Partnership Management Model for Water Supply Services; Co-sharing Option for Kisumi, Kenya [2)]
Band	60	(2010)	Management in der Trinkwasserwirtschaft ÖVGW – TU Graz Symposium [2)]
Band	61	(2010)	LARCHER, M.: The Three Chamber Surge Tank – A new way of construction for the tail water area of pumped storage schemes [1)]
Band	62	(2011)	Aqua Urbanica 2011 – Niederschlags- und Mischwasser-bewirtschaftung im urbanen Bereich, D-A-CH Gemeinschaftstagung [2)]
Band	63	(2011)	SINDELAR, C.: Design of a Meandering Ramp [1)]
Band	64	(2011)	GAMERITH, V.: High resolution online data in sewer water quality modelling [2)]

Band	65	(2011)	ZETINIGG, H.: Regeln für den Schutz von Trinkwasserfassungen in Österreich [2)], vergriffen
Band	66	(2013)	VICUINIK, R.: Untersuchungen zur Dynamik der Feststoffsedimentation in Absetzbecken [2)]
Band	67	(2013)	ASLAM, M.T.: Settling of solids in raw wastewater - primary settling tanks and storm water tanks [2)]
Band	68	(2013)	DOBLER, W.: Hydraulic investigations of a y-bifurcator [1)]
Band	69	(2014)	FRIEDL, F.: Vergleich von statistischen und physikalischen Modellen zur Berechnung der Auftrittswahrscheinlichkeit von Schadensarten auf Trinkwasser-Haupt- und Zubringerleitungen [2)]
Band	70	(2013)	ZENZ, G.: 15. JuWi-Treffen, Fachbeiträge zur Tagung vom 31. Juli – 02. August 2013 [1)]
Band	71	(2014)	REGNERI, M.: Modeling and multi-objective optimal control of integrated wastewater collection and treatment systems in rural areas based on fuzzy decision-making [2)]
Band	72	(2015)	GOLDGRUBER, M.: Nonlinear Seismic Modelling of Concrete Dams [1)]
Band	73	(2015)	HARB, G.: Numerical Modeling of Sediment Transport Processes in Alpine Reservoirs [1)]

Die Bände sind zu beziehen bei:

1) Institut für Wasserbau und Wasserwirtschaft
Technische Universität Graz, Stremayrgasse 10/II, 8010 Graz, Österreich
Tel. +43(0)316/873-8361, Fax +43(0)316/873-8357
E-Mail: hydro@tugraz.at

2) Institut für Siedlungswasserwirtschaft und Landschaftswasserbau
Technische Universität Graz, Stremayrgasse 10/I, 8010 Graz, Österreich
Tel. +43(0)316/873-8371, Fax +43(0)316/873-8376
E-Mail: office-sww@tugraz.at

3) Verlag der Technischen Universität Graz
Technische Universität Graz, Technikerstraße 4, 8010 Graz, Österreich
Tel. +43(0)316/873-6157
E-Mail: verlag@tugraz.at